Volume 1

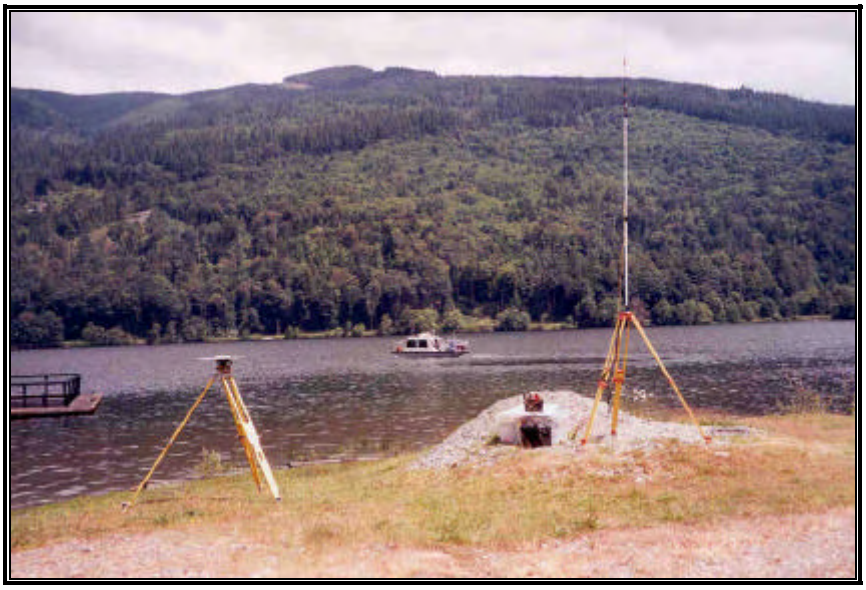

III. Data Collection

III. Data Collection

TABLE OF CONTENTS

	Page
REAL TIME SEDIMENT MONITORING AT RUN-OF-THE-RIVER HYDROPOWER PLANTS: Pravin Karki, Hydro Lab Pvt. Ltd., Katmandu, Nepal; Haakon Støle, Sediment Systems AS, Trondheim, Norway.	III – 1
COMPARISON OF SUSPENDED-SEDIMENT SAMPLERS AND PROCEDURES FOR SAMPLING THE LOWER MISSISSIPPI RIVER: Charles R. Demas and Paul Ensminger, USGS, Baton Rouge, LA; and Nancy Powell, USACE, New Orleans, LA	III – 9
LOADS AND YIELDS OF SUSPENDED SEDIMENT FOR SELECTED WATERSHEDS IN THE LAKE TAHOE BASIN, CALIFORNIA AND NEVADA: Timothy G. Rowe, USGS, Carson City, NV	III – 10
SAMPLING FREQUENCY AND ANNUAL SUSPENDED SEDIMENT LOAD ESTIMATE: Renjie Xia and Misganaw Demissie, Illinois State Water Survey, Champaign, IL	III – 18
PORTABLE BEDLOAD TRAPS WITH HIGH SAMPLING INTENSITY FOR REPRESENTATIVE SAMPLING OF GRAVEL TRANSPORT IN WADABLE MOUNTAIN STREAMS: Kristin I. Bunte and Steven R. Abt, Colorado State U., Fort Collins, CO; John P. Potyondy, USFS, Fort Collins, CO	III – 24
BEDLOAD TRANSPORT RATES AT NEAR-BANKFULL FLOWS IN A STEP-POOL CHANNEL: Daniel A. Marion, USDA-FS, Oxford, MS	III – 32
THE FLUX AND PARTICLE SIZE DISTRIBUTION OF SEDIMENT COLLECTED IN HILLSLOPE TRAPS AFTER A COLORADO WILDFIRE: Deborah A. Martin, USGS, Boulder, CO; John A. Moody, USGS, Lakewood, CO	III – 40
THE INFLUENCE OF SEDIMENT SUPPLY ON RATES OF BEDLOAD TRANSPORT: A CASE STUDY OF THREE STREAMS ON THE SAN JUAN NATIONAL FOREST: Sandra E. Ryan, USDA-FS, Laramie, WY	III – 48
BEDFORM MAPPING IN THE SACRAMENTO RIVER: Randal L. Dinehart, USGS, Sacramento, CA	III – 55
RADIO-TRACKING OF COBBLES IN A MOUNTAIN STREAM IN SOUTHWEST IDAHO: James P. McNamara and J. Carter Borden, Boise State U., Boise, ID; and James Fitzgerald, USEPA, Boise, ID	III – 63
SPECIFIC WEIGHT AND MEDIAN SIZE OF THE BED MATERIAL OF GRAVEL AND COBBLE BED RIVERS: Robert T. Milhous, USGS, Fort Collins, CO	III – 70
THE EVOLUTION OF CLUSTERS IN GRAVEL BED STREAMS: A. N. Papanicolaou, Washington State U., Pullman, WA; A. Schuyler, ENSR, Redmond, WA	III – 78
DENSIMETRIC MONITORING OF SUSPENDED SEDIMENT CONCENTRATIONS, NORTHEASTERN GEORGIA: Daniel L. Calhoun, USGS, Atlanta, GA; and Todd C. Rasmussen, The University of Georgia, Athens, GA	III – 86
CONTINUOUS TURBIDITY MONITORING AND REGRESSION ANALYSIS TO ESTIMATE TOTAL SUSPENDED SOLIDS AND FECAL COLIFORM BACTERIA LOADS IN REAL TIME: Victoria G. Christensen, Andrew C. Ziegler, and Xiaodong Jian, USGS, Lawrence, KS	III – 94

CONTINUOUS AUTOMATED SENSING OF STREAMFLOW DENSITY AS A SURROGATE FOR SUSPENDED-SEDIMENT CONCENTRATION SAMPLING: Matthew C. Larsen, Carlos Figueroa Alamo, USGS, Guaynabo, PR; John R. Gray, USGS, Reston, VA; and William Fletcher, Design Analysis Associates, Inc., Logan, UT III – 102

TURBIDITY THRESHOLD SAMPLING FOR SUSPENDED SEDIMENT LOAD ESTIMATION: Jack Lewis and Rand Eads, USFS, Arcata, CA III – 110

THE PROMISES AND PITFALLS OF ESTIMATING TOTAL SUSPENDED SOLIDS BASED ON BACKSCATTER INTENSITY FROM ACOUSTIC DOPPLER CURRENT PROFILER: Jeffrey W. Gartner and Ralph T. Cheng, USGS, Menlo Park, CA III – 119

ACOUSTIC MEASUREMENT OF SEDIMENT FLUX IN RIVERS AND NEAR-SHORE WATERS: J. M. Land, Dredging Research Ltd., Surrey, England; and P. D. Jones, Environment Agency, Warrington, UK III – 127

FEASIBILITY OF USING ACOUSTIC AND OPTICAL BACKSCATTER INSTRUMENTS FOR ESTIMATING TOTAL SUSPENDED SOLIDS CONCENTRATION IN ESTUARINE ENVIRONMENTS: Michael J. Byrne and Eduardo Patiño, USGS, Ft. Myers, FL III – 135

USE OF ROTATING SIDE-SCAN SONAR TO MEASURE BEDLOAD: David M. Rubin, USGS, Santa Cruz, CA; George Tate, USGS, Menlo Park, CA: David J. Topping, USGS, Reston, VA; and R. A. Anima, USGS, Menlo Park, CA III – 139

LASER SENSORS FOR MONITORING SEDIMENTS: CAPABILITIES AND LIMITATIONS, A SURVEY: Yogesh C. Agrawal and Henry C. Pottsmith, Sequoia Scientific, Inc., Redmond, WA III – 144

AUTOMATED SEDIMENT SIZE DISCRIMINATOR: S.M. Dabney, R.F. Cullum, and S. Smith, USDA-ARS, NSL, Oxford, MS III – 152

CONTINUOUS MONITORING OF SUSPENDED SEDIMENT IN RIVERS BY USE OF OPTICAL SENSORS: David H. Schoellhamer, USGS, Sacramento, CA III – 160

REAL TIME SEDIMENT MONITORING AT RUN-OF-THE-RIVER HYDROPOWER PLANTS

Authors:
Pravin Karki, AMICE Eng., Hydro Lab Pvt. Ltd., Kathmandu, Nepal
Dr. Haakon Støle, Sediment Systems AS, Trondheim, Norway
Authors contact point:
P. Karki: Fax. ++ 977 1 543195, hydrolab@wlink.com.np
H. Støle: Fax: ++ 47 73512856, haakon.stole@bygg.ntnu.no

ABSTRACT

The need for real time data on the sediment contents of water passing the turbines of high head run-of-river hydropower plant is addressed in this paper. Some different methods for observation of sediment concentration are presented. The objectives with the SMOOTH concept (sediment monitoring and operation tool for hydro plants) are outlined and the experience gained through pilot field tests at the Jhimruk hydropower plant in Nepal and laboratory tests at NTNU in Trondheim, Norway are presented in the paper. The paper concludes that the SMOOTH concept requires some further development. SMOOTH is, however, facilitating an operation regime of hydropower plants where the energy production can be optimised and the costs associated with sediment induced wear can be minimized.

INTRODUCTION

SMOOTH is an abbreviation for "sediment monitoring and operation tool for hydro plants." This is the working title for a development program where the objective is to supply an instrumentation package, which will enable the power plant operators to:

- Observe the sediment content in the water supplied to a turbine in real time and thus enable partial or full closedown of the plant when it is more profitable to stop the plant than to generate power.
- Record continuously the actual sediment exposure of the turbines and produce an inventory of sediment exposure of each unit of the plant.
- Optimise the power plant operation and the maintenance work with respect to sediment-induced wear.
- Facilitate continued research on sediment induced wear of turbines and cost effective design and operation of sediment handling facilities at run-of- river hydropower plants.

There is most probably a level at each high head run-of-river hydropower plant where the costs are higher than the benefits of continued generation due to excessive sediment induced wear and the resulting maintenance needs and costs. Real time data on sediment content in the water supplied to the power plant is necessary in order to enable a cost effective operation of the plant with respect to sediment induced wear. The main challenge in this respect has been to find a system capable of observing the sediment concentration in the water passing through the turbines

in real time. It is also necessary to observe the flow through the turbines in order to obtain an inventory of sediment exposure of each turbine.

Dr. Haakon Støle, principal of Sediment Systems has developed the SMOOTH concept in cooperation with Department of Hydraulics and Environmental Engineering at Norwegian University of Science and Technology where Mr. Pravin Karki completed his MSc. studies in 1998. The title of his thesis is "The SMOOTH concept real time sediment monitoring." The main components of the SMOOTH concept have also been tested through two field studies at the Jhimruk hydropower plant in Nepal in cooperation with Butwal Power Company Ltd. (BPC).

THE SMOOTH CONCEPT

The content of suspended sediments in a water flow is normally observed through water sampling followed by analysis of the water in a sediment laboratory. The concentration of sediments is described as the dry weight of the suspended solids in relation to the total weight of the water and sediment mixture and the unit PPM (parts per million) or mg/kg. As water flow is normally measured by volume per time unit and not by weight per time unit, the unit milligram per litre (mg/1) is often used to describe sediment concentration in river hydraulics.

Concentration analysis takes time. If the sediment content shall be observed continually and in real time, another approach must be used in order to measure sediment concentration. There are two main approaches to concentration measurements in real time.

Turbidity:
Suspended sediments have an impact on the visibility of a fluid. This effect is used to measure sediment content by use of turbidity meters. Turbidity measurements are mainly applicable for fine sediments. Suspended and grains will not easily be detected through turbidity observations.

Density:
Suspended sediments with a density different from the density of water will have an impact on the density of the fluid. The density of the sediment and water mixture is also dependent on the temperature. The sediment concentration observations based on density measurements must therefore involve temperature measurements. The two main technologies applied for density measurements in the processing industry are Coriolis flow meters and gamma radiation density meters. If both density and the temperature are known, it should be possible to determine the sediment concentration.

Different instruments have different working ranges. Density meters are not very accurate for low concentrations, say below 500 PPM, while turbidity meters for water quality studies etc. has the normal working range and high accuracy in the range below 1000 PPM.

The basic principles of the SMOOTH concept is to measure continuously the following parameters of the flow:

- Density and temperature are converted into concentration, based on long-term simultaneous observations and water sampling. The sediment content in the samples is analysed in a sediment laboratory through the well-proven filtration method.
- Volume-flow through the sensor, which is converted to pipe flow in the penstock where the sampler is installed.

The main components of the SMOOTH rig are:

a) The SMOOTH sampler, which is installed in a 5/4" threaded hole in the penstock upstream of the turbine (the dismantling pipe unit is used for this in Jhimruk). The sampler abstracts a branch flow from the penstock flow, which is conveyed through the sensor before it is returned to the penstock or tapped for manual sampling and filtration analysis for calibration purposes.
b) The sensor is a Coriolis flow meter where the density, the temperature and the volume flow of the branch flow is measured.
c) The transmitter is linked to the sensor and is upgrading the signals from the sensor so it can be transmitted over a simple line to the control room where the computer is located. The transmitter can also display the process variables directly.
d) A personal computer with the required software continuously converts the observed parameters to sediment concentration and turbine flow. The inventory of the sediment load is maintained and all data are stored on files, which can be processed further in a worksheet program. Several units can be connected to one computer.

The main objectives with the next phase of the SMOOTH development program are to include the following additional parameters in the package:

- Differential pressure over the turbine, i.e. the net working head of the turbine
- The output from the generator for each unit

This is expected to facilitate an indirect monitoring of the relative efficiency of each unit over time. The time series of flow, concentration, head and production are expected to be useful in connection with studies of sediment induced wear of turbines and optimum operation of hydropower plants.

SMOOTH AT JHIMRUK HYDROPOWER PLANT

General

The sediment transport observed in Jhimruk River during the first years of operation had been far more severe than expected during the planning and design process of Jhimruk hydropower plant. This includes the content of hard minerals (quartz) and the concentration of suspended sediments which both are much higher than expected. The owner, BPC, has experienced unexpected high rates of sediment-induced wear of the hydraulic machinery. The sediment induced wear is so high that an overhaul frequency of once per year is not sufficient in order to avoid irreparable damages if the plant is operated at full load throughout the monsoon season.

BPC and Sediment Systems have worked on various approaches to the sediment-related problems at Jhimruk as shown below.

a) Improved sediment trapping in the existing settling basins.
b) Develop structures with additional sediment exclusion capacity.
c) Obtain improved resistance to sediment induced wear of the hydraulic machinery.
d) Improved operation of the plant aiming at reducing sediment exposure by real time monitoring of the sediment content in the turbine flow combined with a modified operation strategy which allows for reduced production or close down of the plant during periods of high sediment exposure.

Monitoring in the Powerhouse - The 1996 Program

The SMOOTH sampling rig was installed at unit no 3 in Jhimruk hydropower plant during the 1996 monsoon season. The main objective with this arrangement was to obtain experience with the concept and the various components. The rig was not used for minute-to-minute operation of the plant during this first test. Data for calibration of the density sensor was the most important issue.

The density and concentration data applied for calibration of the sensor is shown in Figure 1. The following conclusions were drawn from this field-test program.

- The concentration recorded by the SMOOTH sampler meets the required accuracy for real time assessment of the concentration in connection with power plant operation purposes. The recorded sediment data will also be of a sufficient standard for sediment exposure documentation purposes with respect to the turbines.
- Further development is needed both on the hardware as well as the software side.

Monitoring at the Headworks – The 1998 Program

The SMOOTH rig was installed at the tunnel portal downstream of the settling basin in 1998. This arrangement facilitated an earlier warning in the case of influx of water with high content of suspended sediments compared with the 1996 location in the powerhouse. The sampling arrangement is shown in Figure 2.

LABORATORY TESTS OF THE SMOOTH SAMPLER

Laboratory Set Up

A laboratory test rig was constructed at the SINTEF/NTNU hydraulic laboratory in Trondheim to verify the proper functioning of the SMOOTH concept. Concentration and density calibration was performed in the early stages of SMOOTH development, especially during the Jhimruk 1996 study. However flow calibration was never performed and in this respect, the laboratory set up is seen as a very important step in the development of SMOOTH. Figure 3 shows the laboratory set up of the SMOOTH test rig in the laboratory. The pipe delivering water to the turbine in a prototype was represented by one of the main supply pipes in the laboratory. A sediment feeding system was constructed in order to simulate transport of both fine and coarse particles.

Flow Calibration

In a series of five tests, 216 observations were taken and viewed as one population with two variables. Since the flow was highly turbulent, a large number of observations were necessary in order to even out small differences. The observations and the resulting rating equation are shown in Figure 4. The rating curve is acceptable and the predictions for the main pipe flow, Qp based on the sensor flow, Qs is satisfactory.

Density and Concentration Calibration

The main objective of the density and concentration calibration was to establish a relationship between density and concentration. Figure 5 shows the plot of concentration vs. density, which is based on 100 samples.

CONCLUSIONS

The SMOOTH concept is promising. The pilot tests and the laboratory tests have proven that it is possible to observe pipe flow as well as sediment concentrations in the water flowing through the turbines with an acceptable level of accuracy. There is, however, scope for improvements and further development of the concept.

The SMOOTH concept will produce real time data on sediment content in the water and may therefore be used to adopt an operation strategy where the power production can be optimised and the costs associated with sediment induced wear can be minimized at run-of-river hydropower projects. The concentration in the water flow to the turbines of Jhimruk hydropower plant varies very rapidly. High frequent sampling is therefore needed in order to obtain a reliable sediment load inventory for the turbines.

REFERENCES

Bishwakarma, Meg B., 1998, Sediment Exclusion Optimisation Study - Jhimruk Hydropower Plant, Nepal. MSc. thesis IVB-NTNU, Trondheim, Norway.

Karki, Pravin, 1998, The SMOOTH Concept - Real-time Sediment Monitoring. MSc. thesis IVB-NTNU, Trondheim, Norway.

Støle, Haakon, 1997, The SMOOTH Test Programme 1996 - Jhimruk Hydropower Plant. SEDIMENT SYSTEMS - Dr. ing. H. Støle AS, Trondheim, Norway.

Støle, Haakon, 1998, SMOOTH 1998, Jhimruk Hydropower Plant. Real Time Sediment Monitoring, Progress Report and Instruction Manual. SEDIMENT SYSTEMS - Dr. ing. H. Støle AS, Trondheim, Norway.

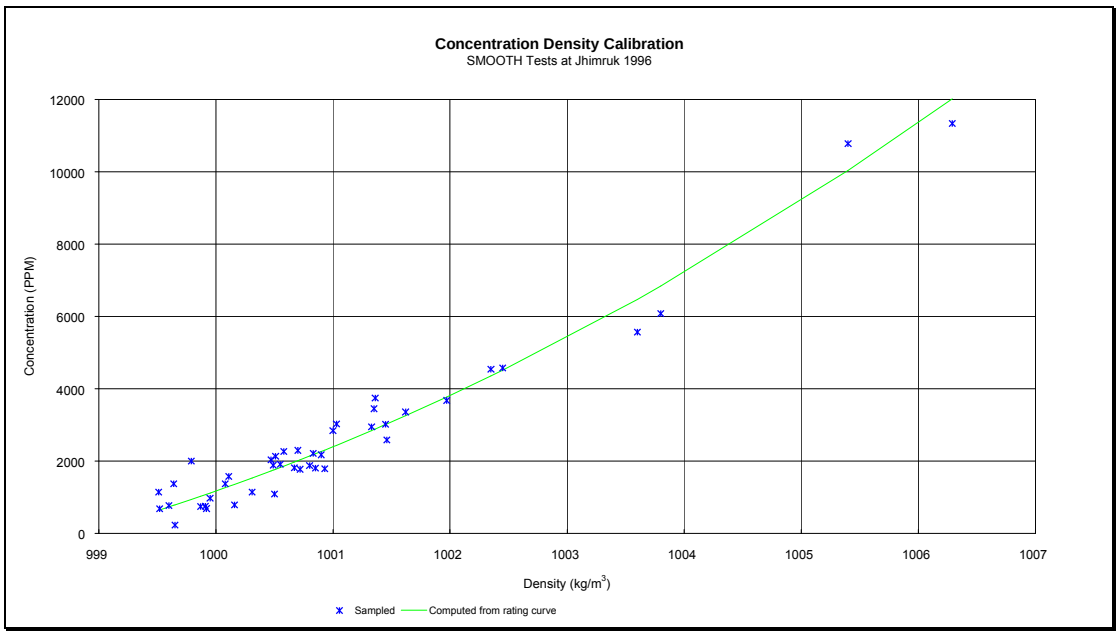

Figure 1 Concentration and density calibration at Jhimruk 1996.

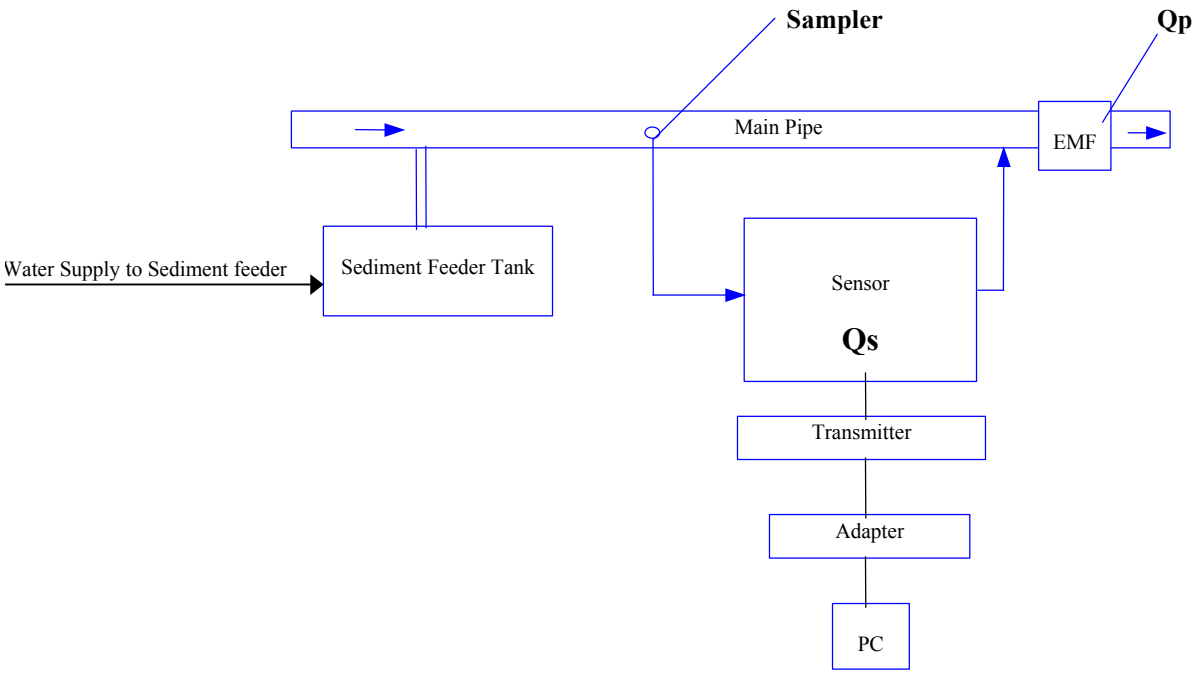

Figure 2 Laboratory setup of SMOOTH

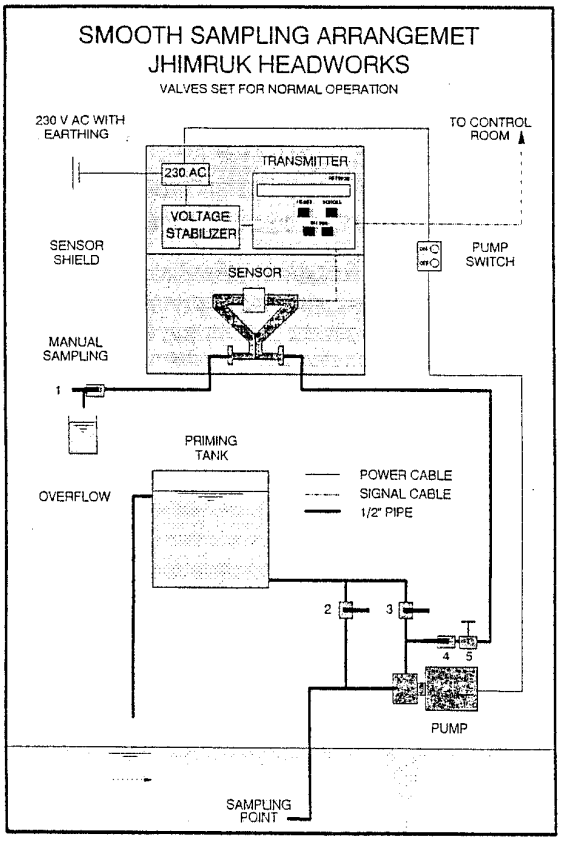

Figure 3 SMOOTH Sampling Arrangement Jhimruk Headworks

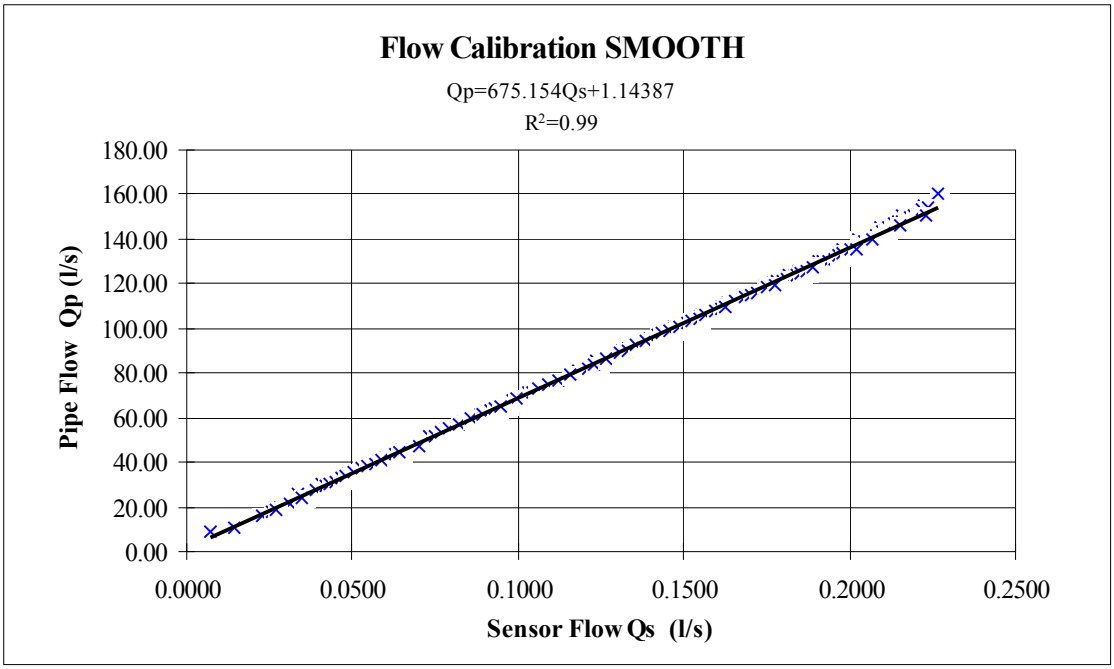

Figure 4 Flow calibration - sensor flow and pipe flow rating

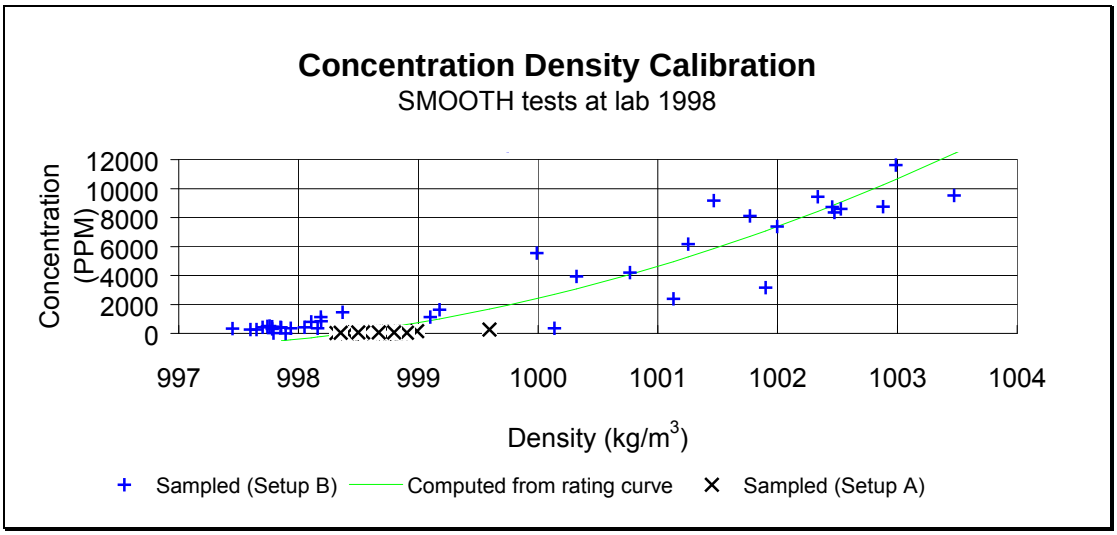

Figure 5 Concentration and density calibration

COMPARISON OF SUSPENDED-SEDIMENT SAMPLERS AND PROCEDURES FOR SAMPLING THE LOWER MISSISSIPPI RIVER

By [1]Charles R. Demas, District Chief, U.S. Geological Survey, Water Resources Division, Baton Rouge, Louisiana; [2]Paul A. Ensminger, Supervisory Hydrologist, U.S. Geological Survey, Water Resources Division, Baton Rouge, Louisiana; [3]Nancy J. Powell, Chief, Hydrologic Engineering Section, USACE, New Orleans District, New Orleans, Louisiana

[1]U.S. Geological Survey, Water Resources Division, 3535 S. Sherwood Forest Blvd, Suite 120, Baton Rouge, LA 70816, crdemas@usgs.gov
[2]U.S. Geological Survey, Water Resources Division, 3535 S. Sherwood Forest Blvd, Suite 120, Baton Rouge, LA 70816, paensmin@usgs.gov
[3]U.S. Army Corps of Engineers, CEMVN-ED-HH, P.O. Box 60267, New Orleans, LA 70160, 504-862-449, nancy.j.powell@mvn02.usace.army.mil

Abstract: The U.S. Army Corps of Engineers (USACE) primary sediment-sampling station for the Mississippi River in the New Orleans District is at Tarbert Landing, Mississippi. Suspended-sediment and bed-material sediment samples have been collected at this location since the 1960s. Similarly, the U.S. Geological Survey (USGS) has operated a long-term sampling station 40 miles downstream near St. Francisville, Louisiana, since 1973, as part of the National Stream-Quality Accounting Network (NASQAN). Since 1997, different methods have been used to collect suspended-sediment samples. Both agencies use the same P-series samplers (P-63 and P-61). However, each agency uses a different sample-collection procedure: the USACE collects 20 point samples, which consists of 5 samples at 4 verticals across the river; the USGS collects depth-integrated samples at 3 verticals across the river; the number of depth-integrated samples in a vertical depends on the depth of the river at that vertical.

In 1994, the USGS began using the D-77 Teflon bag sampler to collect water samples for trace metal analyses, to avoid potential chemical contamination by trace metals from the brass P-series samplers. This bag sampler has a lower nozzle efficiency rating than the P-series samplers; therefore, both samplers are used when trace-metal and suspended-sediment samples are collected. In 1996, the Federal Interagency Sedimentation Project (FISP) undertook development of a new Teflon bag sampler, the D-96, with similar or better nozzle efficiencies than the P-series samplers and as inert chemically as the D-77 sampler.

In May 2000, the USGS and the USACE performed a series of tests to compare the D-96 to the P-series suspended-sediment samplers and to compare the resulting data from suspended-sediment samples that were collected using the same P-series sampler but different sample-collection procedures (point and depth-integrated). Results indicated that the D-96 samples were statistically similarly to P-63 samples when the P-63 was used for point sampling but not when used for depth-integrated sampling. Further, point samples and depth-integrated samples collected using the P-63 sampler were not statistically similar. The Teflon bags used in the D-96 sampler were very "sticky" when first used and retained measurable amounts of sediment after being rinsed. The amount of retained sediment decreased substantially when the Teflon bags were pre-rinsed several times with filtered de-ionized water.

LOADS AND YIELDS OF SUSPENDED SEDIMENT FOR SELECTED WATERSHEDS IN THE LAKE TAHOE BASIN, CALIFORNIA AND NEVADA

By Timothy G. Rowe, Hydrologist, U.S. Geological Survey, Carson City, Nevada

Abstract:The U.S. Geological Survey, in cooperation with the Tahoe Regional Planning Agency, has monitored tributaries in the Lake Tahoe Basin since 1988 to determine streamflow and concentrations of sediment and nutrients contributing to loss of clarity in Lake Tahoe. Loads and yields of suspended sediment for 10 selected watersheds totaling nearly half the area tributary to Lake Tahoe (152 square miles [mi^2]) are described. The size of the watersheds ranges from 2.15 mi^2 (Logan House Creek) to 56.5 mi^2 (Upper Truckee River).

The Upper Truckee River had the largest median loads of sediment (7.2 tons per day [ton/d]), Logan House Creek had the smallest loads of sediment (<0.01 ton/d). Third Creek had the largest yield for sediment (0.32 (ton/d)/mi^2), Logan House Creek had the smallest yield for sediment (<0.01 ton/d/mi^2).

INTRODUCTION

Lake Tahoe is an outstanding natural resource and famous for its alpine setting and deep, clear waters. Protection of this renowned clarity has become very important in the past half century, as the clarity has been decreasing by about 1 foot per year (Goldman and Byron 1986). This decrease is due mainly to human activities, which have increased dramatically in the Lake Tahoe Basin since 1960.

Increased nutrient concentrations within Lake Tahoe are considered the primary cause of algal growth, and thereby loss of clarity, in the lake. Suspended sediment also is of concern, because nutrients attach to and are transported by sediment particles. Within the Lake Tahoe Basin, stream discharge is suspected of being one of the major pathways for nutrient and sediment transport to the lake. Increased development has accelerated this transport through urbanization of wetland areas, added erosion from development of steep mountain sides, and discharge by septic and sewage systems within the basin.

Public concern for the clarity of Lake Tahoe also has increased over the years. As an example, voters in Nevada passed bond acts in 1986 and 1996 to fund construction projects in Nevada to reduce erosion and the transport of nutrients and sediments to Lake Tahoe.

The Tahoe Regional Planning Agency (TRPA), the U.S. Geological Survey (USGS), the Tahoe Research Group of the University of California, Davis (TRG), and State and local agencies have been monitoring the Lake Tahoe Basin for nutrients and sediments since the 1970's. One cooperative program, a tributary-monitoring study by the USGS and TRPA, began in the 1988 water year. The primary purpose of the study was to provide a long-term data base for monitoring local water-quality thresholds and estimating the loads of nutrients and sediment from selected Lake Tahoe tributaries. This study initially included four Lake Tahoe Basin watersheds and has expanded over the years. The current network includes 32 stream sites in 14 of the 63 Lake Tahoe watersheds where sediment, nutrient, and streamflow data are collected (fig. 1 and Boughton et al 1997).

This paper presents findings from the cooperative study for 10 near-mouth sampling sites in 10 watersheds of the Lake Tahoe Basin during water years 1988-96. For this report, the period of record for four sites is 1988-96, and for six sites is 1993-96, although the data-collection effort is ongoing. All years referred to are water years—October 1 through September 30.

Suspended-sediment used in this report are from instantaneous samples collected during the day throughout the entire water year.

DESCRIPTION OF STUDY AREA

Lake Tahoe, the highest lake of its size in the United States, with an average lake-surface altitude of about 6,225 ft above sea level, is about 22 miles (mi) long and 12 mi wide. The average depth of the lake is about 1,000 ft and the deepest part is about 1,636 ft. The basin area is 506 square miles (mi^2), consisting of 192 mi^2 in lake-surface area and 314 mi^2 in surrounding watershed area (Crippen and Pavelka 1972). The highest altitude in the watershed is in the Trout Creek Basin (10,881 ft).

The 10 watersheds sampled for this study compose nearly half (152 mi^2) the watershed area. The size of the selected watersheds ranges from 2.15 mi^2 (Logan House Creek) to 56.5 mi^2 (Upper Truckee River). The main stream channel lengths range from 3.30 mi (Logan House Creek) to 21.4 mi (Upper Truckee River).

Precipitation, which falls mostly as snow from November into June, varies across the basin, from 30-40 inches per year (in/yr) on the eastern side to 70-90 in/yr on the western side (Crippen and Pavelka 1972). Annual precipitation in the basin was below normal for 6 years (1988-92 and 1994) and above normal during the remaining 3 years (1993, 1995, and 1996) of the study (Dan Greenlee, Natural Resources Conservation Service, oral commun., 1996).

METHODS

Streamflow was measured and gaging stations were operated according to USGS guidelines (Buchanan and Somers 1969; Kennedy 1983). All streamflow data are available in USGS electronic data bases and USGS published annual Water Resources Data Reports for Nevada and California.

Drainage areas for sampling sites and total watershed areas (table 1) were reported by Cartier et al (1995), and channel lengths were reported by Jorgensen et al (1978).

Suspended sediment samples were collected using USGS guidelines (Edwards and Glysson 1988). The samples were analyzed by the USGS California Sediment Laboratory in Salinas, Calif., using USGS guidelines (Guy 1969). All suspended sediments data are available in USGS data bases and in published annual Water Resources Data Reports for Nevada and California .

Daily loads of suspended sediment were calculated by multiplying the instantaneous suspended-sediment concentration values by the instantaneous streamflow value and converting the product to tons per day.

For each watershed, summary statistics were calculated for loads of suspended sediment using methods described by Helsel and Hirsch (1992); median daily loads are presented in table 3. Median values were chosen as preferable summary values because they are not strongly influenced by a few extreme values.

Median loads were normalized to a common unit (square miles), and the resulting yields were ranked for each of the 10 sampled watersheds, with a rank of 1 assigned to the highest median yield and 10 to the lowest.

RESULTS

Instantaneous streamflow at the time of sample-collection visits ranged from 0 cubic feet per second (ft^3/s), at two sites during low base-flow periods in July 1988 and August 1994, to 1,750 ft^3/s at Upper Truckee River during a rain storm at the spring snowmelt-runoff peak in May 1996. The highest median streamflow value for sampling visits was 158 ft^3/s at Upper Truckee River. The lowest median streamflow value was 0.20 ft^3/s at Logan House Creek (table 2).

For periods of record discussed herein, the Upper Truckee River had the highest average annual daily mean streamflow, 123 ft^3/s, and highest average annual runoff, 89,000 acre feet (acre-ft), and Logan House Creek had the lowest at 0.30 ft^3/s and 221 acre-ft, respectively. The highest average annual unit runoff, 2,860 acre-ft/mi^2, was in Blackwood Creek and the lowest, 106 acre-ft/mi^2, was in Logan House Creek.

The hydrograph of daily mean streamflow for Incline Creek (fig. 2*A*) for 1996 shows a seasonal pattern that is typical of streams in the Lake Tahoe Basin. Most runoff is during the April-through-June snowmelt period. Sharp peaks represent fall and early winter rains (December), rain-on-snow storms (February), and summer thunderstorms (May and July).

The longer term hydrograph (fig. 2*B*) for Incline Creek for the 9-year period of record discussed herein clearly shows the effects of drought (water years 1988-92 and 1994), as compared to years in which runoff was above normal (1993, 1995, and 1996). The average annual daily mean streamflow for the 9 years is 6.26 ft^3/s.

Instantaneous measurements of suspended-sediment concentrations from the 10 stream sites ranged from <1 milligrams per liter (mg/L) at many sites during the summer to 3,930 (mg/L) at Third Creek during a rainstorm on snowpack in March 1993 (table 3). Median values ranged from 3.0 mg/L at Logan House Creek, to 80 mg/L in Third Creek.

Median suspended sediment loads ranged from <0.01 ton per day (ton/d) for Logan House Creek to 7.2 ton/d in the Upper Truckee River. Median yields of sediment showed different results—from 0.01 ton per day per square mile ($ton/d/mi^2$) for Logan House Creek to 0.32 $ton/d/mi^2$ for Third Creek (fig. 3). When yields were ranked, Third Creek had the highest rank (1) and Logan House Creek had the lowest (10; table 3).

DISCUSSION

Concentrations of suspended sediment varied widely in the sampled watersheds of the Lake Tahoe Basin. This variation is largely due to differences in weather patterns, precipitation amounts, and natural conditions across the basin. For example, more precipitation falls on the western side of Lake Tahoe, and the streamflow runoff and sediment loads reflect that. The years of drought conditions also reduced sediment loads in the watersheds.

When the concentrations are flow-weighted and loads are calculated, the largest loads are in the Upper Truckee River watershed. This is solely because the Upper Truckee River is the largest watershed and delivers the greatest annual runoff to Lake Tahoe. The smallest loads are from Logan House Creek, which is the smallest of the 10 sampled watersheds and delivers the least annual runoff to the lake.

Third Creek has the highest sediment yield, which is due to the exposed soil caused by the large snow and rock avalanche of February 17, 1986, in the upper reach (Bill Quesnel, Incline Village General Improvement District, oral commun., 1992). The next largest yields of sediment were in Blackwood Creek, followed by Ward Creek, Upper Truckee River, and Incline Creek. The watersheds with the smallest yields are Glenbrook and Logan House Creeks. This ranking agrees with a suspended-sediment study on nine Lake Tahoe Basin watersheds (eight of which are included here) between 1981-85 by Hill and Nolan (1988). They found that the highest annual suspended-sediment yields were from Blackwood Creek, Ward Creek, Upper Truckee River, and Third Creek.

For the 10 selected watersheds, the higher yields were from six watersheds on Lake Tahoe's western, southern, and northern sides, all of which receive greater precipitation and are more developed and affected by human activities. The lower yields were from four watersheds on the eastern side, which receive less precipitation and are somewhat less developed.

REFERENCES

Boughton, C.J., T.G. Rowe, K.K. Allander, and A. R. Robledo. 1997. Stream and ground-water monitoring program, Lake Tahoe Basin, Nevada and California. U.S. Geological Survey Fact Sheet FS-100-97.

Buchanan T.J., and W.P. Somers. 1969. Discharge measurements at gaging stations. U.S. Geological Survey Techniques of Water-Resources Investigations, book 3, chap. A8.

Cartier, K.D., L.A. Peltz, and Katie Long. 1995. Hydrologic basins and hydrologic-monitoring sites of Lake Tahoe Basin, California and Nevada. U.S. Geological Survey Open-File Report 95-316.

Crippen J. R., and B.R. Pavelka. 1972. The Lake Tahoe Basin, California-Nevada. U.S. Geological Survey Water-Supply Paper 1972.

Edwards, T.K., and G.D. Glysson. 1988. Field Methods for measurement of fluvial sediment. U.S. Geological Survey Open-File Report 86-531.

Goldman, C.R., and E.R. Byron. 1986. Changing water quality at Lake Tahoe—The first five years of the Lake Tahoe Interagency Monitoring Program. Tahoe Research Group, Institute of Ecology, University of California, Davis.

Guy, H.P., 1969. Laboratory theory and methods for sediment analysis: U.S. Geological Survey Techniques of Water Resources Investigations, book 5, chap. C1.

Helsel, D.R., and R.M. Hirsch. 1992. Statistical methods in water resources. Studies in Environmental Science 49. Amsterdam, Elsevier.

Hill, B.R., and K.M. Nolan. 1988. Suspended-sediment factors, Lake Tahoe Basin, California-Nevada, *in* I.G. Poppoff, C.R. Goldman, S.L. Loeb, and L.B. Leopold, eds. International Mountain Watershed Symposium Proceedings, Lake Tahoe, June 8-10, 1988. South Lake Tahoe, Calif., Tahoe Resource Conservation District.

Jorgensen, A.L., A.L. Seacer, and S.J. Kaus. 1978. Hydrologic basins contributing to outflow from Lake Tahoe, California-Nevada. U.S. Geological Survey Hydrologic Investigations Atlas HA -587.

Kennedy, E.J., 1983, Computation of continuous records of streamflow. U. S. Geological Survey Techniques of Water- Resources Investigations, book 3, chap. A13.

Rowe, T.G., and J.C. Stone. 1997. Selected hydrologic features of the Lake Tahoe Basin, California and Nevada. U.S. Geological Survey Open-File Report 97-384.

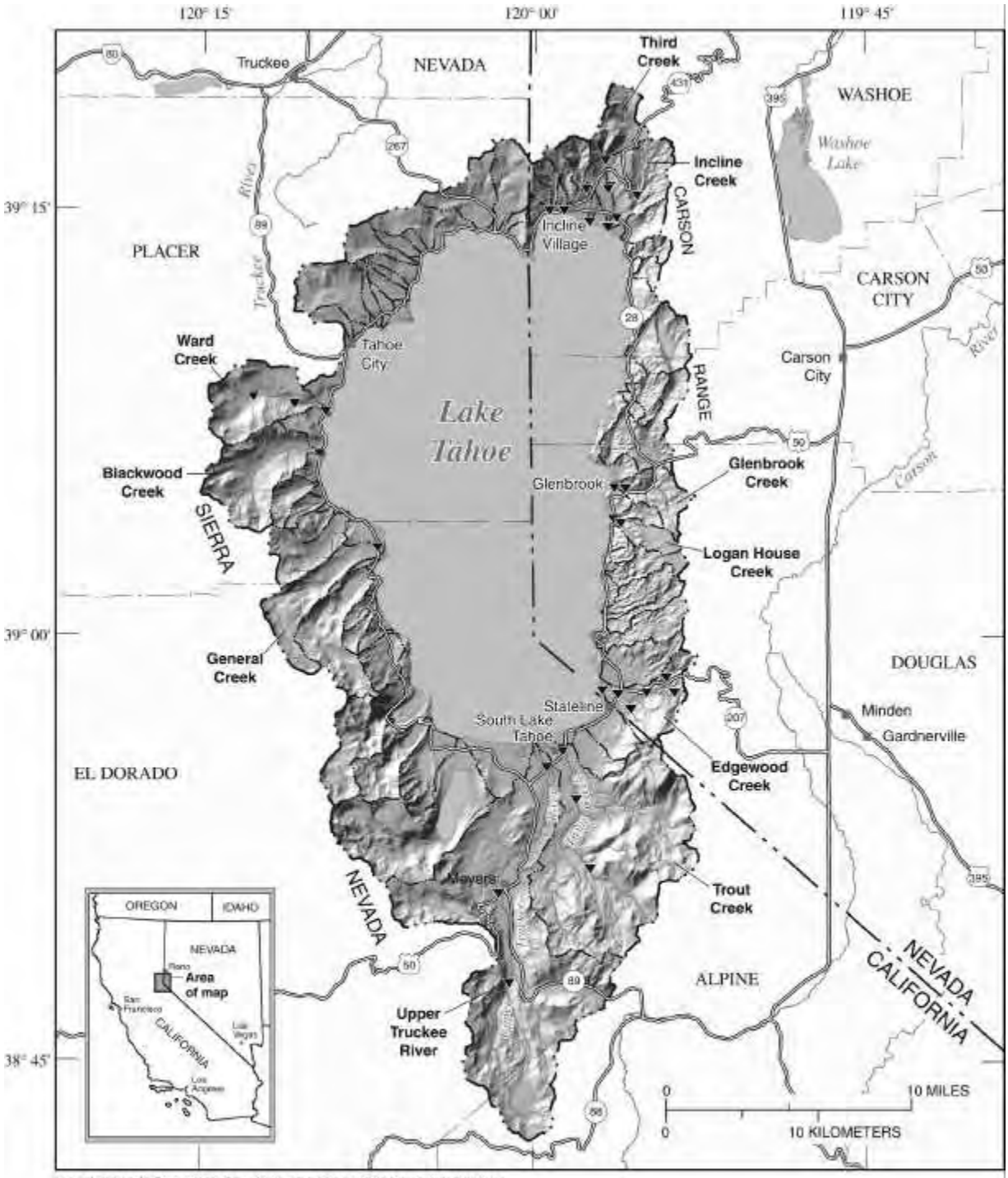

Base from U.S. Geological Survey digital data, 1:24,000 and 1:100,000, 1969-85. Universal Transverse Mercator projection, Zone 11

EXPLANATION

- **Boundary of Lake Tahoe Basin**
- **Boundary of subbasin**—Name of subbasin is indicated
- **Surface-water site**

Figure 1. Geographic setting, hydrologic basins, bathymetry, surface-water sampling sites, and selected watersheds in the Lake Tahoe Basin (modified from Rowe and Stone 1997).

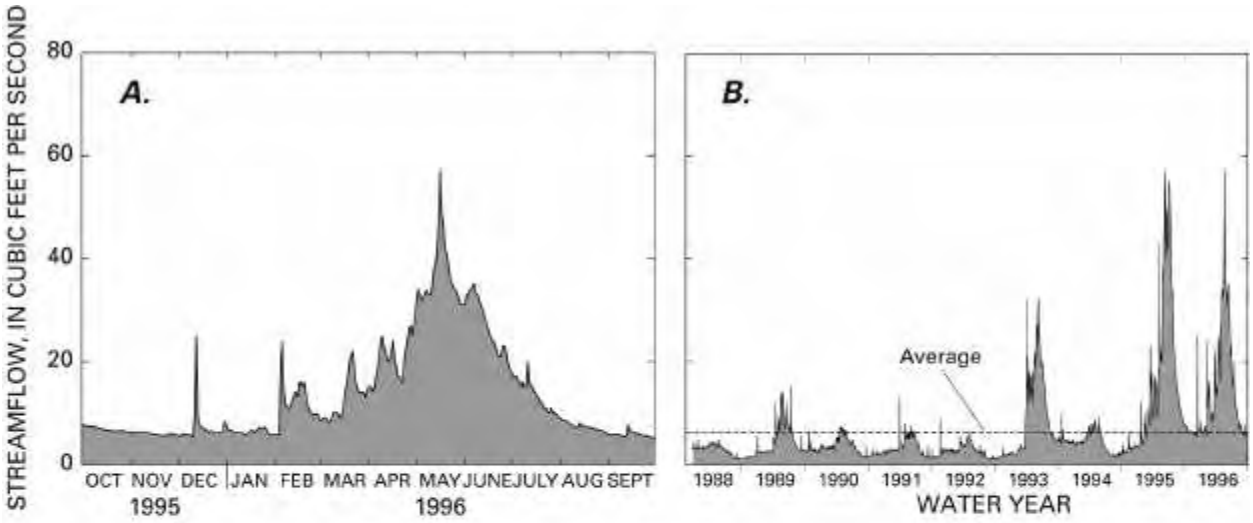

Figure 2. (***A***) Daily mean streamflow for Incline Creek during 1996 water year, a representative stream in the Lake Tahoe Basin, and (***B***) daily mean streamflow for Incline Creek, 1988-96 water years, representing years of drought and above-normal runoff.

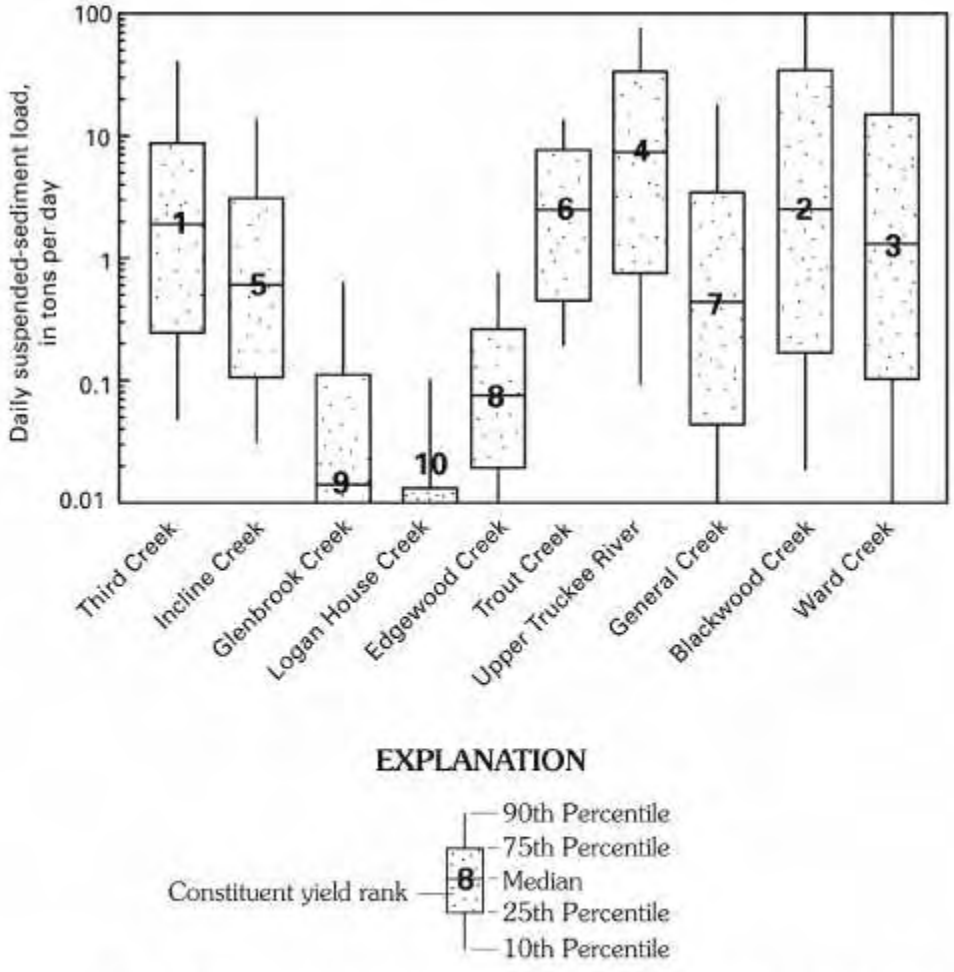

Figure 3. Suspended-sediment loads depicted by box plots and yelid ranks for selected surface-water sampling sites in the Lake Tahoe Basin, 1988-96.

Table 1. Sampling-site information for selected Lake Tahoe watersheds

Sampling site (figure 1)	Total watershed drainage area (square miles)[a]	Sampling-site drainage area (square miles)	Main channel length (miles)[b]
Third Creek near Crystal Bay, Nev.	6.05	6.02	7.05
Incline Creek near Crystal Bay, Nev.	6.70	6.69	4.66
Glenbrook Creek at Glenbrook, Nev.	4.11	4.10	3.92
Logan House Creek near Glenbrook, Nev.	2.15	2.09	3.30
Edgewood Creek at Stateline, Nev.	6.64	5.61	5.53
Trout Creek at South Lake Tahoe, Calif.	41.2	40.4	10.7
Upper Truckee River at South Lake Tahoe, Calif.	56.5	54.0	21.4
General Creek near Meeks Bay, Calif.	7.63	7.39	9.17
Blackwood Creek near Tahoe City, Calif.	11.2	11.1	6.20
Ward Creek near Tahoe Pines, Calif.	9.75	9.73	5.90

[a] From Cartier et al 1995
[b] From Jorgensen et al 1978

Table 2. Streamflow information for selected Lake Tahoe Basin watersheds

[Abbreviations: acre-ft, acre-feet; ft^3/s, cubic feet per second; ft, feet; mi^2, square miles]

Sampling site	Range and median of sampled streamflow[a] (ft^3/s)	Period of record (water years)	Average annual mean daily streamflow (ft^3/s)	Average annual runoff (acre-ft)	Average annual yield[b] (acre-ft/mi^2)
Third Creek	0.93 - 118 (6.0)	1988-96	6.68	4,830	802
Incline Creek	.56 - 71 (5.7)	1988-96	6.26	5,040	753
Glenbrook Creek	0 - 35 (0.88)	1988-96	1.30	943	230
Logan House Creek	0 - 7.9 (0.20)	1988-96	.30	221	106
Edgewood Creek	1.1 - 25 (3.6)	1993-96	3.72	2,690	480
Trout Creek	3.2 - 305 (49.5)	1993-96	44.8	32,400	802
Upper Truckee River	.70 - **1,750**[c] **(158)**	1993-96	**123**[c]	**89,000**[c]	1,650
General Creek	.41 - 559 (30.5)	1993-96	20.2	14,700	1,990
Blackwood Creek	1.1 - 936 (60.0)	1993-96	44.0	31,800	**2,860**[c]
Ward Creek	.22 - 950 (47.5)	1993-96	32.1	23,200	2,380

[a] Median, in parentheses, equals 50-percent value.
[b] Yield is annual runoff divided by sampling-site drainage area.
[c] **Bold** indicates highest value.

Table 3. Suspended-sediment and nutrient information for selected Lake Tahoe Basin watersheds

[Abbreviations: mg/L, milligrams per liter; ton/d, tons per day; ton/d/mi^2, tons per day per square mile]

Sampling site	Concentration range (mg/L)	Median concentration[a] (mg/L)	Median load[b] (ton/d)	Median yield[c] (ton/d/mi^2)	Yield rank[d]
Third Creek	1 - **3,930**[e]	**80**[e]	1.9	**0.32**[e]	**1**[e]
Incline Creek	1 - 1,840	26	.62	.09	5
Glenbrook Creek	1 - 606	6.0	.02	.01	9
Logan House Creek	<1 - 388	3.0	<.01	.01	10
Edgewood Creek	1 - 130	5.0	.08	.01	8
Trout Creek	2 - 335	14	2.5	0.06	6
Upper Truckee River	1 - 458	15	**7.2**[e]	.13	4
General Creek	<1 - 404	7.0	.43	.06	7
Blackwood Creek	1 - 1,080	16	2.6	.23	2
Ward Creek	<1 - 3,000	10	1.3	.14	3

[a] Median equals 50-percent value.
[b] Median load equals 50-percent value. Load = concentration x streamflow x load factor (0.0027 for ton/d).
[c] Median yield is median load divided by sampling-site drainage area.
[d] Rank from 1 to 10: 1 indicates highest contribution of constitutent and 10 Lowest contribution.
[e] **Bold** indicates highest value.

SAMPLING FREQUENCY AND ANNUAL SUSPENDED SEDIMENT LOAD ESTIMATE

By Renjie Xia, Associate Professional Scientist; Misganaw Demissie, Principal Scientist, both from Illinois State Water Survey, Champaign, IL

ABSTRACT: Because it is expensive to collect suspended sediment samples on a daily basis, the samples are collected at various sampling frequencies. Typically, the annual suspended sediment load is estimated based on a suspended sediment rating curve. This study selected one Illinois gaging station in the Kankakee River basin where suspended sediment concentrations were collected on a daily basis by the U. S. Geological Survey during Water Year 1993. To investigate the effects of sampling frequency on the annual suspended sediment load estimate, it is assumed that the U.S. Geological Survey collected water discharge and suspended sediment concentration data on a weekly basis during Water Year 1993. The estimated annual sediment load based on the weekly sampling frequency did not correspond well with the annual sediment load measured. When additional suspended sediment samples collected during high flow periods were incorporated into the data analysis, the accuracy of the estimation of the annual sediment load was improved. Conclusions presented in this paper are preliminary since only one case was studied.

INTRODUCTION

Suspended sediment in rivers has become a concern in recent years, not only because the suspended sediment causes siltation in streams, reservoirs, lakes, and estuaries, but also because the sediment is a potential carrier of pollutants and conveys the pollutants into various environments. To predict the extent of siltation in water bodies or the amount of pollutants carried by suspended sediment, accurate estimation of suspended sediment load has become important.

Suspended sediment load is commonly expressed as metric tons per day (metric system of units) or as tons per day (English system of units). Thus, the daily suspended sediment load refers to the number of tons of sediment a river transports on a daily basis, while the annual suspended sediment load refers to the number of tons of sediment a river transports during an entire year.

Calculating the annual suspended sediment load is simple if the suspended sediment concentration is measured every day. The daily mean suspended sediment load is computed by multiplying the daily mean water discharge by the daily mean concentration and applying a proper coefficient, i.e., 0.0864 in the metric system of units or 0.0027 in the English system of units (Porterfield 1972). The daily mean water discharge is computed from continuous measurement while the daily mean concentration is time-integrated based on instantaneous suspended sediment concentrations measured during the day. The annual suspended sediment load is simply the sum of all the daily loads. However, frequently the suspended sediment concentration is not measured every day, but rather at different sampling frequencies, such as every other day or once a week. Therefore, a standard procedure used to calculate the annual suspended sediment load is: (1) a suspended sediment rating curve expressing the relation between the water discharge and sediment load is first developed by using continuous water

discharge data and sediment load data computed from days on which the daily mean concentration is known; (2) sediment loads for days on which the concentration is unknown are estimated by using this rating curve (e.g., Vanoni 1975; Mimikou 1982; and Williams 1989); and (3) finally, the annual suspended sediment load is calculated as the sum of the measured and estimated daily sediment loads.

Since the number of sediment load data entries corresponding to each sampling frequency varies (for example, 183 data points for a sampling frequency of every other day and only 52 data points for a sampling frequency of once a week for an entire year), the rating curves analyzed from these different data groups are also different. Thus, the annual sediment loads estimated from rating curves corresponding to different sampling frequencies vary. Assuming the annual suspended sediment load computed from the daily sampling frequency is a "true" value, investigating the difference between the true value and other annual sediment loads estimated from rating curves based on other sampling frequencies will be an interesting subject.

Weber et al. (1979) demonstrated that sampling frequency has significant effects on the accuracy of mass discharge estimates. Dickinson (1981) studied the effects of four sampling frequencies on the accuracy and precision of annual suspended sediment load estimates and stated that infrequent sampling of suspended sediment concentrations can lead to gross underprediction. Richards and Holloway (1987) indicated that infrequent sampling (less than about 50 samples per year) will generally provide load estimates that are strongly biased and very imprecise. Based on field data collected from one Illinois gaging station in the Kankakee River basin, this paper compared the annual sediment loads estimated from daily and weekly sampling frequencies, and investigated the effects of sampling frequency on the annual suspended sediment load estimate.

SELECTION AND COMPARISON OF SUSPENDED SEDIMENT DATA

The selected gaging station near Wilmington, Illinois, in the Kankakee River basin, has a drainage area of 14,265 km^2 (5,510 mi^2). This station has monitored by the U.S. Geological Survey (USGS) since 1978. The suspended sediment data in Water Year 1993 was used in this study. The USGS collected data of continuous water discharge and instantaneous suspended sediment concentration on a daily basis during Water Year 1993 from January 1 to September 30. For the period of nine months (or 273 days), the USGS provided 273 data entries for the daily mean water discharge and daily mean suspended sediment load.

To investigate the effects of sampling frequency on the annual suspended sediment load estimate, it is assumed that the USGS collected data of water discharge and suspended sediment concentration on a weekly basis during Water Year 1993. Thus, 39 water discharges and suspended sediment loads were picked out from the total 273 data entries. These water discharge and sediment load data, i.e., 273 data entries collected on a daily basis and 39 data entries collected on a weekly basis, are shown in Fig. 1. Figure 1 shows that weekly sampling did not detect two of the highest suspended sediment loads.

Table 1 lists the maximum, minimum, and mean values of daily mean suspended sediment load, Q_s, sorted from the 273 data entries and the 39 data entries, respectively. These differences of

maximum, minimum, and mean values for the two data groups indicate that the suspended sediment load data collected at a weekly sampling frequency cannot faithfully represent data collected on a daily basis.

Table 1. Maximum, Minimum, and Mean Daily Suspended Sediment Loads

Sampling frequency	Q_s (metric tons/day) collected in 1993		
	Maximum	Mean	Minimum
Daily	50,894	3,400	96
Weekly	36,651	3,749	133

ANNUAL SUSPENDED SEDIMENT LOAD

The sum of the 273 mean daily sediment loads (928,262 metric tons) measured by the USGS from January 1, 1993 to September 30, 1993 is assumed to be the true annual sediment load for that period. For the weekly sampling frequency, the sediment loads were measured on 39 days but not on 234 days. The 39 measurements of sediment loads and water discharges were used to create a suspended sediment rating curve, which was further used to estimate the 234 daily sediment loads not measured. Thus, the annual sediment load for the weekly sampling frequency is the sum of 39 measured daily sediment loads and 234 estimated daily sediment loads. In this paper, the following linear logarithmic regression equation (the most commonly used relationship between water discharge and sediment load) is used as the suspended sediment rating curve

$$\log Q_s = a + b \log Q_w \qquad (1)$$

where Q_s is the daily suspended sediment load, Q_w is the daily water discharge, and a and b are coefficients. Conventionally, a and b can be determined by least-squares regression analysis.

Using the standard procedure mentioned above, the sediment rating curve and annual suspended sediment load corresponding to the weekly sampling frequency were calculated for the gaging station investigated. Table 2 summarizes the values of a and b and the annual suspended sediment load for the weekly sampling frequency.

A relative difference in percentage between the true annual sediment load and the load estimated from weekly sampling frequency is further calculated by using the following equation:

$$D = \frac{Y_T - Y_{weekly}}{Y_T} \qquad (2)$$

where D is the relative difference of annual sediment load in percentage, Y_T is the true annual sediment load, and Y_{weekly} is the annual sediment load estimated from weekly sampling frequency. The Y_T and Y_{weekly} values are equal to 928,262 and 690,774 metric tons, respectively; thus, the value of D is as large as 25.58 %. This indicates that the annual suspended sediment load is underestimated when weekly sampling frequency is used.

Table 2. Results Based on Suspended Sediment Load Data
Collected at Weekly Sampling Frequency

Sampling frequency	a	b	Annual sediment load (metric tons)	Relative difference D (%)
weekly	-1.79	2.01	690,774	25.58

ANNUAL SUSPENDED SEDIMENT LOAD CONSIDERING PEAK SEDIMENT DISCHARGES

In practice, except for suspended sediment samples collected using a certain sampling frequency, additional samples are often collected during high flow periods. If additional samples collected during periods of the two highest sediment discharges in Water Year 1993 are added to the data group corresponding to the weekly sampling frequency, the annual sediment load changes. These additional samples increase the number of sediment load data corresponding to the weekly sampling frequency. Consequently, the equation of suspended sediment rating curve changes; thus, the annual sediment load estimated from the rating curve must vary too.

Data for six additional sediment loads collected from periods of the two highest sediment discharges were added to the data group formed from the weekly sampling frequency. Using the calculation procedure mentioned above, the rating curve and the annual sediment load corresponding to the weekly sampling frequency were recalculated. The number of days for which the sediment loads are measured increases from 39 to 45 days while the number of days for which the sediment loads are not measured decreases from 234 to 228 days. The 45 measurements of sediment loads and water discharges were used to create a rating curve that was used to estimate the 228 daily sediment loads not measured. The annual sediment load for the weekly sampling frequency is the sum of 45 measured daily sediment loads and 228 estimated daily sediment loads. Furthermore, the relative difference in percentage between the true annual sediment load and the load estimated from the weekly sampling frequency plus the six additional sediment loads was also recalculated. These results are shown in Table 3.

Table 3. Results Based on Suspended Sediment Load Data from Weekly Sampling Frequency
and Additional Data Collected during Two Highest Sediment Discharges

Sampling frequency	a	b	Annual sediment load (metric tons)	Relative difference D (%)
weekly	-0.61	1.59	912,232	1.73

Table 3 shows that the difference between the true annual sediment load and the annual sediment load computed from data based on the weekly sampling frequency plus six additional data points is still existed, but the D value becomes very small (1.73 %). Therefore, the annual sediment load computed from data based on the weekly sampling frequency plus the additional data approximates the true annual sediment load very well. This indicates that when using a lower

sampling frequency (for example weekly) plus collecting additional samples during high flow periods, the estimate of the annual sediment load could be satisfactory.

Comparing Table 3 and Table 2 shows that accuracy improves after adding additional samples collected from the periods of the two highest sediment discharges to the sediment load data originally provided by the weekly sampling frequency. The annual sediment load computed from the weekly sampling frequency plus additional sediment load data approximates the true annual sediment load. This means that collecting additional samples during high flow periods is important. It may be economical to estimate the annual sediment load by using a lower sampling frequency in normal flow periods and collecting additional suspended sediment samples during high flow periods.

CONCLUSIONS

Because it is expensive to collect suspended sediment samples on a daily basis, the samples are collected at various sampling frequencies. Thus, the annual suspended sediment load is estimated based on known measured data. This study investigated the effects of sampling frequency on the annual suspended sediment load estimate for one Illinois gaging station in the Kankakee River basin, monitored by the USGS during Water Year 1993. Based on this analysis, the following conclusions can be made:

(1) This study confirms the previous investigations that sampling frequency affects the estimation of the annual suspended sediment load.

(2) The annual suspended sediment load estimated from a weekly sampling frequency does not correspond to the sediment load estimate based on a daily sampling frequency. Incorporating additional suspended sediment data collected during high flow periods to the data analysis improves the accuracy of the estimation of the annual sediment load.

(3) It may be more economical to estimate the annual sediment load by using a lower sampling frequency during normal flow periods and collecting additional suspended sediment samples during high flow periods.

REFERENCES

Dickinson, W.T., 1981. *Accuracy and Precision of Suspended Sediment Loads*. Erosion and Sediment Transport Measurement, Proceedings of the Florence Symposium, June 1981, 195-202.

Mimikou, M., 1982. *An Investigation of Suspended Sediment Rating Curves in Western and Northern Greece*. Journal of Hydrological Sciences, Vol. 27, 3, 369-383.

Porterfield, G.,1972. *Computation of Fluvial Sediment Discharge*. U.S. Geol. Survey Tech. of Water Resources Investigations, Book 3, Chap. C3.

Richards, R.P. and Holloway, J., 1987. *Monte Carlo Studies of Sampling Strategies for Estimating Tributary Loads*. Water Resources Research, Vol. 23, 10, 1939-1948.

Vanoni, V.A., 1975. *Sedimentation Engineering*. Manuals and reports on engineering practice, ASCE, Vol. 54, 215-230.

Weber, H., Cluis, D., and Bobée, B., 1979. *Accuracy Evaluation in the Calculation of Mass Discharges*. Journal of Hydrology, Vol. 40, 175-184.

Williams, G.P., 1989. *Sediment Concentration Versus Water Discharge during Single Hydrologic Events in Rivers*. Journal of Hydrology, Vol. 111, 89-106.

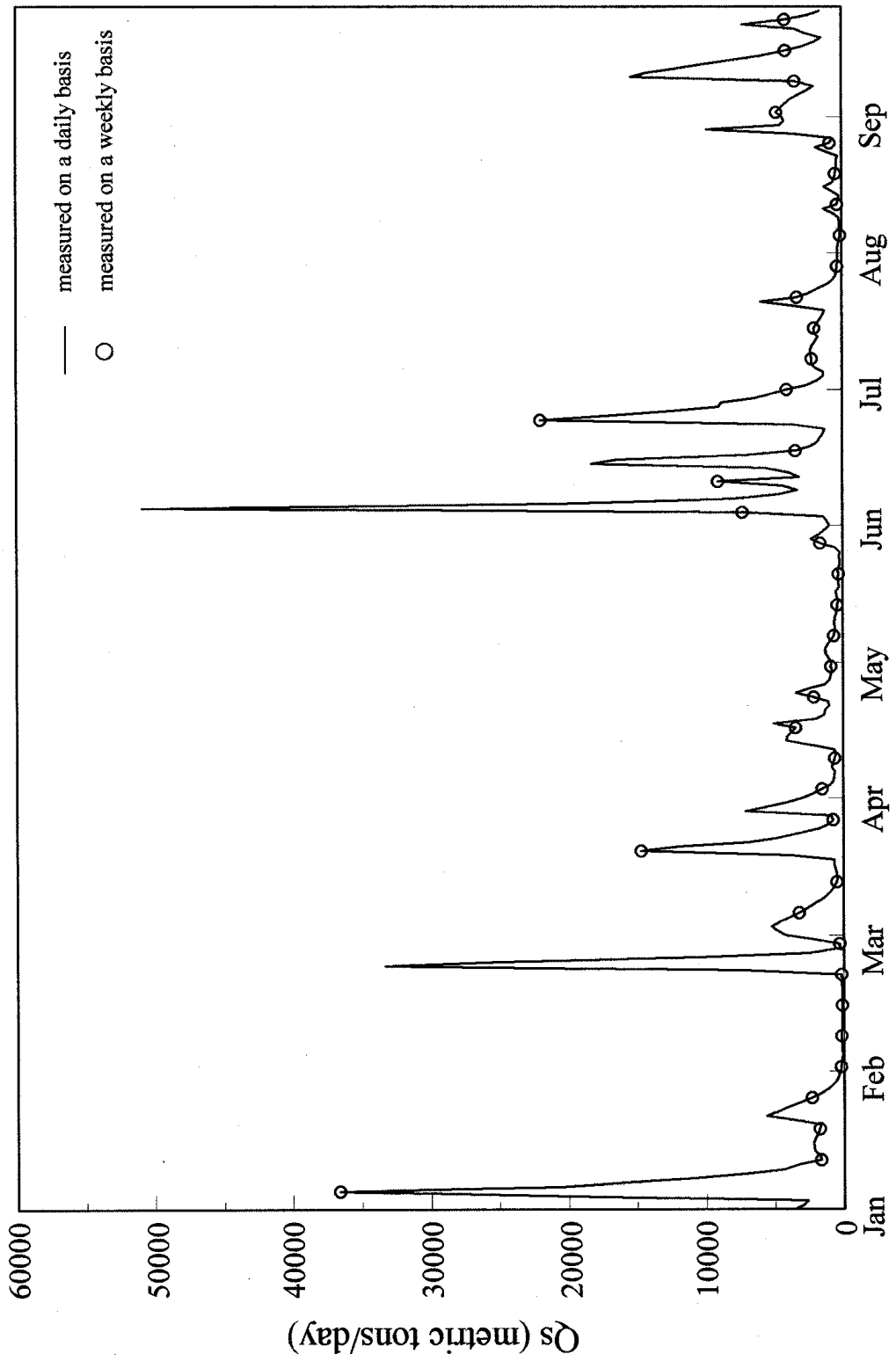

Fig. 1 Suspended sediment load measured by USGS during Water Year 1993

PORTABLE BEDLOAD TRAPS WITH HIGH SAMPLING INTENSITY FOR REPRESENTATIVE SAMPLING OF GRAVEL TRANSPORT IN WADABLE MOUNTAIN STREAMS

Kristin I. Bunte, Fluvial Geomorphologist, Colorado State University, Fort Collins, Colorado;
Steven R. Abt, Professor, Civil Engineering, Colorado State University, Fort Collins, Colorado;
John P. Potyondy, Hydrologist, USDA Forest Service, Rocky Mountain Research Station, Fort Collins, Colorado.

Engineering Research Center, Colorado State University, Fort Collins, CO 80523; Bunte: phone (970) 491-3980, kbunte@engr.colostate.edu; Abt: phone (970) 491-8203, sabt@engr.colostate.edu; Potyondy: phone: (970) 295-5986, jpotyondy@fs.fed.us.

Abstract A portable bedload trap was developed for representative sampling initiation of gravel motion and coarse bedload transport rates in wadable gravel- and cobble-bed mountain streams. The trap is 0.3 m wide, 0.2 m high and has a 0.9 m long trailing net with a 3.5 mm mesh width. The trap can be quickly installed on a stream bottom with little disturbance of the bed and can be operated by 1-3 persons over a wide range of flow. For sampling, the trap is temporarily fastened onto ground plates anchored into the stream bottom. Sets of 5 to 6 traps were installed on riffles or runs of three mountain gravel-bed streams. Sampling time was usually one hour and facilitated representative samples of a wide range of transport rates (up to 7 orders of magnitude) and bedload particle sizes (4-90 mm). This capability for representative sampling provided valuable bedload data-sets suitable for performing initial motion computations.

INTRODUCTION

Knowledge of the conditions of flow required for incipient motion of gravel and cobble particles in mountain streams is important for channel maintenance analyses as well as for the general understanding of stream processes. Computational methods used to predict critical flow for incipient gravel motion include the dimensionless critical shear stress value t^*_c of ≈ 0.06 (Shields 1936), the critical dimensionless transport rate W^*=0.002 (Parker et al. 1982; Wilcock and McArdell 1993), Lane's (1955) diagram of critical shear stress versus particle sizes required for stable channels, and empirical equations relating critical flow velocity, shear stress, unit discharge, or unit stream power to the largest transportable sediment size (Williams 1983). However, none of these equations can provide a reliable prediction of critical flows in mountain streams because local hydraulic conditions, the stability of the bed pavement, and sediment supply may vary over a wide range.

Measurements of incipient gravel motion are problematic in mountain streams because bedload transport comprises a wide range of particle sizes and transport rates that extend over several orders of magnitude. For example, at the beginning of gravel motion, only one small gravel particle may be transported per unit width and unit time, resulting in a very small computed transport rate. In contrast, cobbles mobile during high flows are accompanied by a large mass of smaller gravel particles, and the resulting transport rate is very large. Another characteristic of bedload transport is that gravel and cobble particles move infrequently at the onset of motion (the rate of motion to be exceeded to qualify for mobility is still to be determined). Thus, sampling periods must be sufficiently long to collect infrequently moving particles. Dietrich and Whiting (1989) suggested that the sampling time $t_{s(i)}$ should be long enough to ensure that the mass of one particle of the *i*th size class does not exceed the proportion by mass of that size class in the actual bedload particle-size distribution. Sampling time $t_{s(i)}$ is defined as $m_i / q_b \cdot f_i \cdot w_s$ where m_i is the mass of a particle of the *i*th size class, q_b is the sampled bedload transport rate per unit width, f_i is the percent frequency of the *i*th size class in the bedload sample, and w_s is the sampler width.

A variety of different technologies have been used for sampling gravel and cobble bedload. Vortex samplers (Milhous 1973; Hayward and Sutherland 1974; Tacconi and Billi 1987) and conveyor belt samplers (Klingeman and Emmett 1992) collect all bedload passing a cross-section for a specified time (e.g., 1 minute or 1 hour) and can produce representative bedload samples under a wide range of transport conditions, but installation and maintenance of these samplers is too costly and time consuming to be available at every site. Basket samplers 0.3 m wide or greater have been used to sample coarse bedload since the 1930's (Hubbell 1964; Nansen 1974; Engel and Lau 1981). However, the practicality of these samplers is hampered by their heavy weight (iron frame and wire mesh) which requires using a crane, and the relatively small sampler volume (~15,000 - 30,000 cm^3) which limits the sampling duration. Pressure-difference bedload samplers (Helley and Smith 1971; Emmett 1984) are the most

commonly used samplers for coarse bedload. The handheld version, operable in wadable flows, has a small entrance (0.076 by 0.076 m) and a small sampler capacity (3,000 cm^3), and is therefore poorly suited for sampling coarse gravel bedload. Samplers with larger openings (0.15 by 0.15 m, or 0.3 by 0.15 m) and large capacities are better suited for sampling gravel bedload, but are difficult to operate during high flows.

Small non-recording bedload traps (Church et al. 1991; Lepp et al. 1993; Wathen et al. 1995; Bunte 1997) are relatively easy to install and may be left to sample for long periods. However, traps installed in the bed are difficult to empty during high flows, and if emptied after a flood event, the collected D_{max} particle size or the total transport mass can only be related to peak flood conditions. Similarly, the post-flood recovery of passive tracer particles integrates particle movement over the entire flood (Church and Hassan 1992; Schmidt and Gintz 1995; Ferguson and Wathen 1998). Active radio tracers that provide real-time information about their location and state of motion (Ergenzinger et al. 1989; Busskamp 1994; Chacho et al. 1996) can be used to monitor particle mobility in a specified flow, but costs and logistics make it difficult to monitor more than a few tracer particles at a time. Large bedload traps with openings 0.6 to 1.5 m wide and large attached nets have been used to measure gravel and cobble transport rates (Bunte 1996; Whitaker and Potts 1996) in mountain streams. In spite of their satisfactory sampling properties, large bedload traps are unwieldy, spatially fixed to one location, and require a sturdy bridge, some stream construction, and a 2-4 person team depending on sampler size, force of flow, and sampled sediment mass.

Since a simple device for representative samples of coarse bedload transport is not available, it was the objective of this study to develop a set of portable bedload traps operable without elaborate stream construction. The traps should be operational in wadable gravel- and cobble-bed streams and provide representative samples of coarse bedload transport over a wide range of transport rates commonly encountered at flows between 30 and 150% of bankfull discharge. The data should be suitable for reliable computation of incipient motion of gravel and cobble particles.

METHODS

Construction and Operation of the Bedload Traps A bedload trap was developed and constructed with an opening 0.3 m wide, 0.2 m high, and 0.1 m deep. The opening frame is fabricated of 6.4 mm thick (1/4 inch) aluminum. The opening is unflared, and sufficiently large to accommodate cobble-size particles (Fig. 1). Bedload collected in the trap is retained in a 0.9 m long trailing, knotless nylon net. A 3.5 mm mesh-width combines the advantages of relatively unobstructed water flow with the ability to retain small gravel particles (4 mm). The traps' light weight (2.2 kg) goes hand in hand with a non-mechanized trap operation: the lightness facilitates manual operation, whereas easy handling allows lightweight construction.

During the sampling process, the bedload traps are fastened onto ground plates that are anchored in the stream bottom. Their presence prevents the inclusion of unwanted particles while the sampler is placed onto or removed from the bed. Ground plates are 0.4 m wide, 0.25 m long, and comprised of 6.4 or 3.2 mm thick aluminum sheets. To install a ground plate on the stream bottom, large surface particles are cleared from the area below the ground plate to allow a positioning flush with the average height of the bed. The front edge of the ground plates is slightly bent (10º) and penetrates the bottom sediment to provide a smooth entrance for bedload particles. The ground plate is anchored into the stream bed with stakes that are driven through a hole on both sides of the plate. The stakes are 12.7 mm (1/2 inch) in diameter, 0.9 m long, and should be driven about 0.3 m deep into the stream bottom in a near-vertical position. A piece of brightly colored garden hose was placed onto the top of the stakes to ensure that the plate position remained visible even in the highest flow. Slits near the bottom and the top of the frame hold two adjustable webbing loops. Webbing loops hold the frame in place after it is checked for contact with the ground plate. The webbing loops are pulled tight around the stakes, pushed down, and fastened with shaft collars that have a fitted thumb screw. Once installed, stakes and ground plates may remain in place during the entire sampling season, unless local scour or deposition in a mobile bed necessitates reinstallation.

Several traps should be installed across the stream width at a riffle or "crossing", the most wadable part of a stream, to ensure that all traps can be reached during high flow. Trap spacing should be approximately even over the cross-section. The combined width of all traps should cover 10-50% of the active stream width, depending on the desired sampling intensity or the extent of spatial variability of bedload transport. If trap spacing is uneven, the computation of transport rates should be adjusted to reflect irregular spacing.

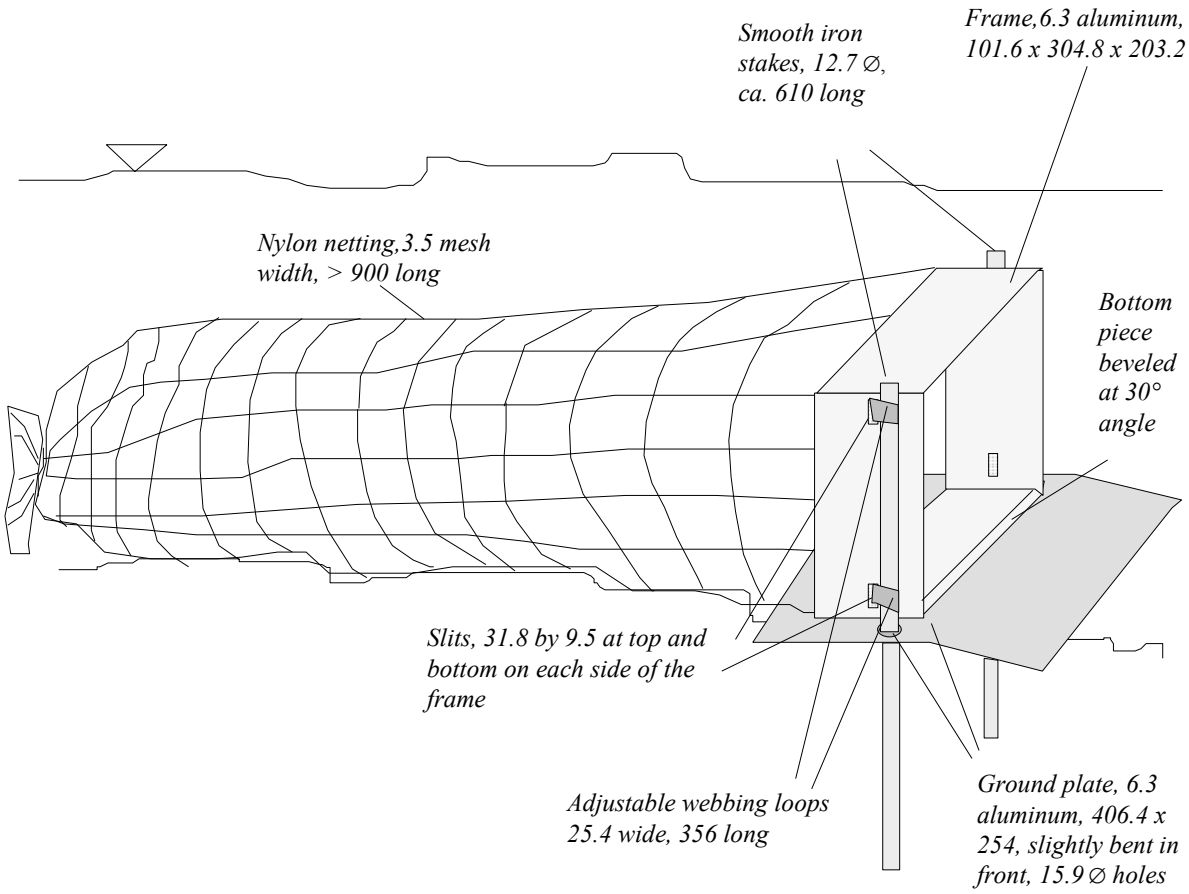

Fig. 1: Schematic diagram of a bedload trap. All measurements in mm (from Bunte 1998).

During the sampling process, the downstream end of the net is tied closed with a cord. To empty the traps after sampling, the traps may be disconnected from the ground plates and moved to the stream bank. A more efficient way to empty the traps at lower flows is to leave the traps on the ground plates and untie the cord at the end of the net. The contents of the net is then shaken into a plastic bag or a bucket, and the net is again closed for the next sampling period. The time for closing and opening the net is recorded for each trap. Closing and emptying the nets in the stream requires only 2-3 minutes per net, and allows consecutive bedload samples to be taken over the course of a day. Traps can be operated by a single person at low flows, but require 2-3 persons and safety procedures at high flows. Bedload samples taken with the traps may contain large amounts of organic debris. Samples rich in organic debris should be carefully inspected in order not to overlook individual bedload particles. The organic debris may provide useful information for fisheries biologists or stream ecologists.

Field studies The bedload traps were tested in three mountain streams with coarse gravel and cobble beds (Table 1) (Bunte 1998, 1999 a and b). Five to 6 traps where installed across riffles or runs with a spacing of 1-2 m between traps. Using 5 or 6 traps simultaneously in streams 6-10 m wide samples a large portion (about 20%) of the stream width. Fastening the traps to the stream bed allows sampling over a long duration. Sampling duration is limited only by the time over which flow can be considered constant and the capacity of the traps which is approximately 50,000 cm^3 or 20 kg of bedload. Sampling over a one hour period makes it possible to sample infrequently moving particles that pass the site with an average frequency of once per hour, and the large trap capacity accommodates cobble bedload which is accompanied by a large mass of gravel particles.

The sampling efficiency of the bedload traps could not be tested during field experiments because transport rates were temporary and spatially variable. However, sampling efficiency of the bedload traps is not expected to decrease over time if only a small amount of bedload accumulates near the end of the net. Gravel and cobble particles move by rolling and sliding, and the inertia of their movement is likely to advance particles that have

Table 1: Field site and measurement characteristics

Stream	Location	Drainage Area (km^2)	Surface D_{16}, D_{50}, D_{84} (mm)	Subsurf. D_{50} (mm)	Q_{bkf} (cfs)	Slope (m/m)	Bkf. width (m)	Active width (m)	No. of traps	No. of data	Meas. flows (%Q_{bkf})
St. Louis Cr.	Williams Mts., CO	34	17, 53, 120	41	141	0.017	6.5	6.0	5	41	16- 67
Ltl. Granite Cr.	Gros Ventre R.,WY	55	23, 59, 133	42	200	0.017	14.3	12.4	6	58	19-130
Cherry Cr.	East Cascades, OR	41	4, 49, 152	30	109	0.025*	9.5	6.1	6	21	36-145

* general stream gradient; local gradient at riffle below pool exit slope estimated at 0.015.

arrived at the entrance of a bedload trap into the net, even if the hydraulic efficiency inside the net was decreased. Hydraulic efficiency may decrease if organic debris accumulates in the net. Therefore, organic debris should be flushed and extracted from the net between samples. Sampling efficiency is reduced if individual particles are allowed to fill the traps during high transport rates. The net capacity for cobbles can be extended by using a larger mesh size that allows small particles to pass. Sampling efficiency is not expected to decrease while migrating bedload sheets push gravel into the traps. The force exerted by the moving gravel sheet exceeds the forces acting to impede gravel collection in the net.

RESULTS

High Intensity Sampling, Representative Transport Rates and Steep Rating Curves The design and operation of the bedload trap produces a high sampling intensity. If, for example, all of the bedload passing a site within one hour is considered 100%, then using 6 traps simultaneously, each 0.3 m wide, for 1 hour at a time in a stream 10 m wide collects 18% of the bedload. By contrast, a 1-hour sampling effort with a handheld sampler 0.076 m wide (20 locations spaced 0.5 m apart, 1.5 minutes per location, 2 traverses) collects 0.8% of the bedload. The sampling intensity obtained with the bedload traps reaches the minimum sampling time suggested by Dietrich and Whiting (1989) for all but the lowest transport rates.

The combined effects of long sampling duration and large trap capacity made it possible to sample transport rates that ranged over 7 orders of magnitude. Very small transport rates of about 0.0001 g/s accrued from collecting one particle of 4 mm in one of the traps over the 1-hour period. High transport rates of up to 1000 g/s accrued when migrating bedload sheets filled some of the traps with 20 kg of sediment in 5 minutes. This wide span of transport rates (Q_b) sampled over a 2-3 fold range of flow (Q) resulted in steep rating curves with power function exponents b ($Q_b = aQ^b$) of up to 10 or more (Fig. 2) for all three sites. Rating curves obtained from Helley-Smith samplers in gravel beds typically have exponents of 1.5 to 5. The scatter about the rating curves is relatively small for samples from the bedload traps and is attributed to the representative sampling facilitated by the long sampling duration and the avoidance of unwanted particle pick-up from the bed.

Initial Motion Based on Fractional Rating Curves The wide range of particle sizes and a relatively small rating curve scatter featured by the samples from the bedload traps provide a foundation for computing fractional bedload transport rating-curves that may be used for various methods of initial motion computation. Fractional bedload rating curves for 0.5 f size classes for Little Granite Creek are parallel to each other, and exceed each other for consecutively larger size classes by a factor of about 1.2 (Fig. 3a). This indicates a stable ratio of transport rates for different size classes and similar transport rates for particles of neighboring size classes and provides a relation for estimating fractional transport rates of unmeasured flows and size classes. Initial motion may be computed from the intercept of fractional rating curves with a preset marginal transport rate, e.g., 0.0001 g/m·s, or the dimensionless transport rate of W^*=0.002 (Wilcock and McArdell 1993). The intercept of the rating curves for numbers of particles moving per size class (Fig. 3c) with a preset number transport rate (e.g., 1, or 10 particles/m·hour) could likewise be used as an initial motion criterion for gravel and cobble particles. Samples from the bedload traps (low rating-curve scatter and steeply increasing transport rates) are also suitable for the computation of the onset of Phase II transport as the abrupt increase of gravel transport rates in a linear plot of fractional transport data over discharge (Emmett 1999) (Fig. 3b).

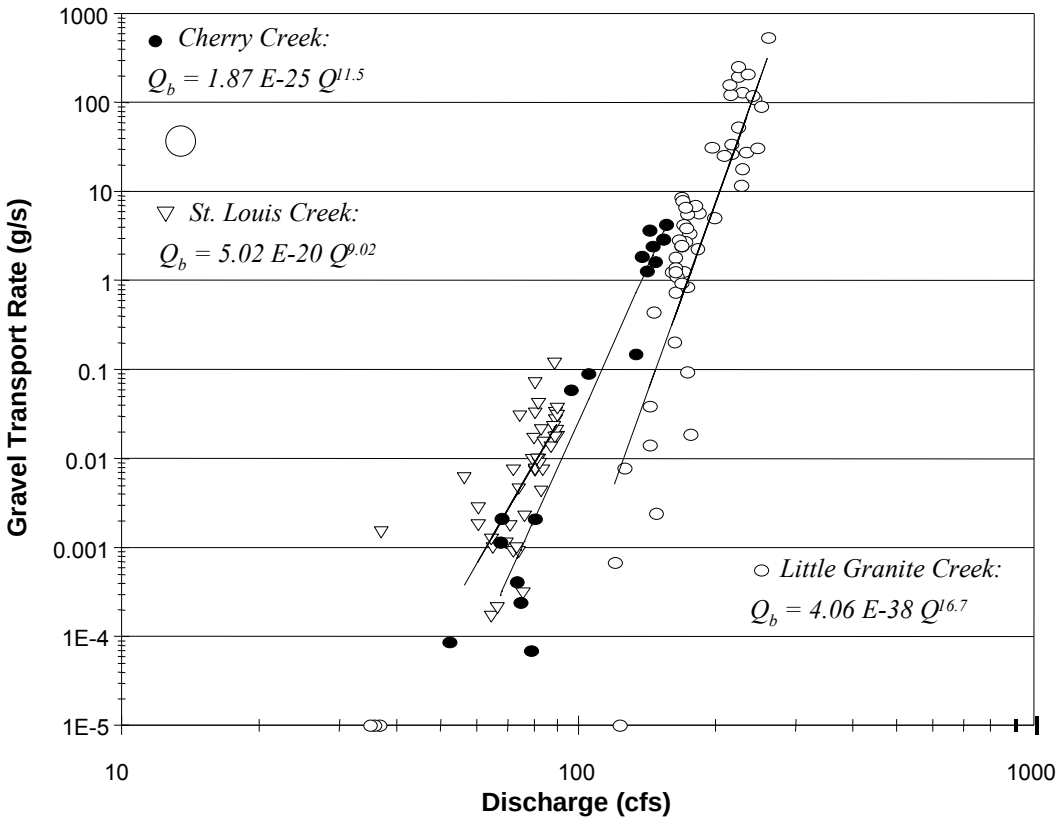

Fig. 2: Bedload transport rates collected with the bedload traps at three streams and their rating curves

Initial Motion Based on Flow Competence Initial motion can also be computed from a flow-competence analysis which refers to the largest particle size, or size class, D_{max}, that is transported (or sampled) at a specified flow. Flow competence has an implicit, but unstated component of time and space (the time period and stream width within which motion must be observed). Since no formal agreements exist, this study computed flow competence based on the collection of at least one particle per size class in one of the bedload traps during a one-hour sampling interval.

The ability of the traps to representatively sample the largest mobile particles which move infrequently produces well-defined flow-competence curves. At Little Granite Creek, the sampled D_{max} particle size increased from 4 to 90 mm over a two-fold increase in flow from 120 to 260 cfs (Fig. 3d). Infrequently moving D_{max} particles would not be reliably sampled if sampling times were short (1-2 minutes). The absence of a potential D_{max} particle in several samples leads to a higher critical discharge and a larger variability of flow-competence curves.

Flow conditions for incipient motion are often expressed in terms of critical dimensionless shear stress $t^*_c = r \cdot g \cdot d \cdot S / (r_s - r) \cdot g \cdot D_{50}$, where r and r_s are the water and sediment density, g is gravitational acceleration, d is mean depth of flow, S is stream gradient and D_{50} is taken as the surface sediment size. If critical discharge in Fig. 3d is expressed in terms of t^*_c, the computed values for t^*_{c50} (Table 2) are considerably higher than the commonly assumed values of 0.03-0.07 and might indicate a relative high threshold for gravel movement in armored mountain streams.

SUMMARY AND CONCLUSION

Bedload traps overcome many of the sampling problems experienced with other bedload sampling devices. The lightweight traps are portable and operable by several individuals, without the need for stream construction or a crane. The trap opening and the net capacity are sufficient for large gravel particles and cobbles, while the mesh width is fine enough to retain small gravel particles. The simultaneous use of 5-6 (or more) traps across the stream

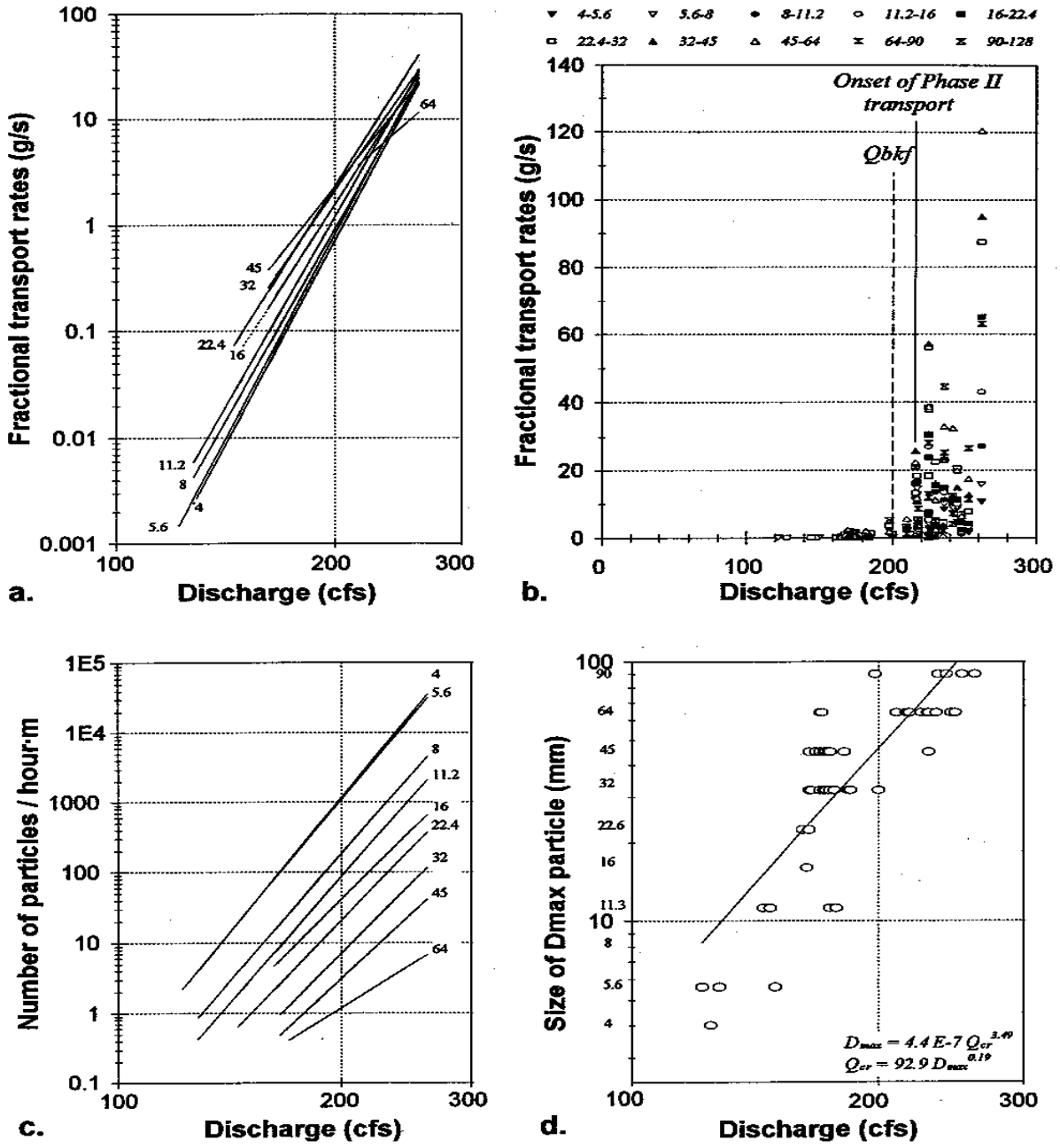

Fig. 3: Data form the bedload traps at Little Granite Creek: (a.) Rating curves for fractional transport rates of 0.5 *f* gravel size classes; (b.) Fractional transport rates plotted in linear scale for determining the onset of Phase II transport ("bedload explosion"); (c.) Rating curves of transport rates of numbers of particles per 0.5 *f* size class moving per hour; (d.) Sampled D_{max} particle size and flow competence curve.

Table 2: t^*_c and t^*_{c50} for five particle sizes computed from samples of the bedload traps.

	4 mm	16 mm	64 mm	D_{50surf}	D_{50sub}
Little Granite Creek	0.065	0.080	0.102	0.100	0.095
St. Louis Creek	0.072	0.086	0.107	0.104	0.100
Cherry Creek	0.100*	0.128*	0.160*	0.148*	0.138*

* The high threshold of motion for Cherry Creek is not so much attributed to bed material properties as to the local stream morphology that causes somewhat odd flow hydraulics at the site.

and the long sampling periods (1 hour) produce a high sampling intensity that allows sampling bedload particles that move infrequently. These attributes are important when studying initial motion for which infrequent motion is typical. The bedload traps are also capable of collecting a wide range of transport rates and particle sizes during a one-hour period, ranging from samples with one small gravel particle to 20 kg of sediment comprising a few cobble particles plus a large mass of smaller gravel sizes.

This study found the traps to be a suitable device for sampling coarse bedload in wadable gravel and cobble bed streams. The bedload rating and flow competence curves are well-defined due to the large measured range of transport rates and particles sizes and provide good data for various methods of initial motion computations.

Acknowledgements Sean McCoy, Kurt Swingle, Dan Armstrong, Rhett Travis, Dan Mastburgen and Brian Smith (all CSU) helped with field and lab work in Colorado and Wyoming. Paul Bakke, Tim Sullivan, Mike McNamara, Walt Lucas, Scott Richards, Richard Ford, Missy Shuey and Terry Smith from the Water Resources Team of the Winema National Forest in Klamath Falls helped with the fieldwork in Oregon. The Bridger-Teton National Forest in Jackson Hole, WY supported the study in Wyoming, and Wes Smith helped with the fieldwork. Sandra Ryan, Rocky Mountain Research Station, allowed us to use her study sites on the Fraser Experimental Forest. The shop of the Engineering Research Center, Colorado State University, constructed the metal parts of the sampler. Trap development was funded by the Stream Systems Technology Center, USDA Forest Service, Rocky Mountain Research Station, Fort Collins, CO. We thank everyone involved for their assistance.

REFERENCES

Bunte, K., 1996. Analyses of the temporal variation of coarse bedload transport and its grain size distribution (Squaw Creek, Montana, USA). U.S.D.A., Forest Service, Rocky Mountain Forest and Range Experiment Station, *General Technical Report* RM-GTR-288, 123 pp.

Bunte, K., 1997. Development and field testing of a bedload trap for sand and fine grovels in mountain gravel-bed streams (South Fork Cache la Poudre Creek, CO), Report prepared for the Stream Systems Technology Center, USDA Forest Service, Rocky Mountain Research Station, Fort Collins, CO, 53 pp.

Bunte, K., 1998. Development and field testing of a stationary net-frame bedload sampler for measuring entrainment of pebble and cobble particles, Report prepared for the Stream Systems Technology Center, USDA Forest Service, Rocky Mountain Research Station, Fort Collins, CO, 74 pp.

Bunte, K., 1999a. Field testing of bedload traps for measuring entrainment of pebbles and cobbles at Little Granite Creek, WY. Report prepared for the Stream Systems Technology Center, USDA Forest Service, Rocky Mountain Research Station, Fort Collins, CO, 78 pp.

Bunte, K., 1999b. Field testing of bedload traps for measuring entrainment of pebbles and cobbles at Cherry Creek, OR. Report prepared for the Stream Systems Technology Center, USDA Forest Service, Rocky Mountain Research Station, Fort Collins, CO, 75 pp.

Busskamp, R., 1994. The influence of channel steps on coarse bed load transport in mountain torrents: Case study using the radio tracer technique 'PETSY'. In:. *Dynamics and Geomorphology of Mountain Rivers*. P. Ergenzinger and K.-H. Schmidt (eds.). Lecture Notes in Earth Sciences, Springer Verlag, Berlin, 129-139.

Chacho, E.F., R.L. Burrows and W.W. Emmett, 1996. Motion characteristics of coarse sediment in a gravel-bed river. In: *Proceedings of the Sixth Federal Interagency Sedimentation Conference*, Las Vegas, Nevada, March 10-14, 1996, p. V-1 to V-8.

Church, M. and Hassan, M.A., 1992. Size and distance of travel of unconstrained clasts on a streambed. *Water Resources Research* 28(1): 299-303.

Church, M., Wolcott, J.F., Fletcher, W.K., 1991. A test of equal mobility in fluvial sediment transport: behavior of the sand fraction. *Water Resources Research* 27(11): 2941-2951.

Dietrich, W.E, Whiting, P., 1989. Boundary shear stress and sediment transport in river meanders of sand and gravels. In: *River Meandering.* S. Ikeda and G. Parker (eds.), Water Resources Monograph 12, American Geophysical Union, Washington, DC, p. 1-50.

Emmett, W.W., 1984. Measurement of bedload in rivers. In: *Erosion and Sediment Yield: Some Methods of Measurement and Modelling.* R.F. Hadley and D.E. Walling (eds.), Geo Books, Norwich, Great Britain, p. 91-109.

Emmett, W.W., 1999. Quantification of channel maintenance flows for gravel-bed rivers. D.S. Olsen and J.P. Potyondy (eds.), *Wildland Hydrology.* American Water Resources Assoc., Herndon VA, TPS-99-3, p. 77-84.

Engel, P. and Y.L. Lau, 1981. The efficiency of basket type bed load samplers. In: *Erosion and Sediment Transport Measurement.* IAHS Publ. no. 133: 27-34.

Ergenzinger, P., K. -H. Schmidt, and R. Busskamp, 1989. The pebble transmitter system (pets): first results of a technique for studying coarse material erosion, transport and deposition. *Zeitschrift für Geomorphologie N.F.* 33(4): 503-508.

Ferguson, R.I and S.J. Wathen, 1998. Tracer-pebble movement along a concave river profile: virtual velocity in relation to grain size and shear stress. *Water Resources Research* 34 (8): 2031-2038.

Hayward, J.A., Sutherland, A.J., 1974. The Torlesse stream vortex-tube sediment trap. *Journal of Hydrology* (N.Z.) 13(1): 41-53.

Helley, E.J. and W. Smith, 1971. Development and calibration of a pressure -difference bedload sampler. USDI, Geological Survey, Water Resources Division, Open File Report, Menlo Park, California, 18pp.

Hubbell, D.W., 1964. Apparatus and techniques for measuring bedload. *Geological Survey Water Supply Paper* 1748, 74p.

Klingeman, P.C. and Emmett, W.W., 1982. Gravel bedload transport processes. In: *Gravel-bed Rivers. Fluvial Processes, Engineering and Management.* R.D. Hey; J.C. Bathurst and C.R. Thorne (eds.), John Wiley and Sons, Chichester, p. 141-179.

Lane, E.W., 1955. Design of stable channels. *Transactions, American Society of Civil Engineers*, 120:1234-1279.

Lepp, L.R., Koger, C.J., Wheeler, J.A., 1993. Channel erosion in steep gradients, gravel-paved streams. *Bulletin of the Association of Engineering Geologists*, 30 (4): 443-454.

Milhous, R., 1973. Sediment transport in a gravel-bottomed stream. Ph.D. thesis, Oregon State University, Corvallis, USA.

Nanson, G.C., 1974. Bedload and suspended-load transport in a small, steep, mountain stream. *American Journal of Science* 274: 471-486.

Parker, G., Klingeman, P.C., McLean, D.G., 1982. Bedload and the size distribution of paved gravel-bed streams. *Journal of the Hydraulics Division*, ASCE, 108 (HY4): 544-571.

Schmidt, K.-H. and D. Gintz, 1995. Results of bedload tracer experiments in a mountain river. In: *River Geomorphology.* E.J. Hickins (ed.), John Wiley and Sons, Chichester, p. 37-54.

Shields, A., 1936. Application of similarity principles and turbulence research to bed-load movement. Translated from: "Anwendung der Ähnlichkeitsmechanik und der Turbulenz-forschung auf die Geschiebebewegung" by W.P. Ott and J.C. Uchelen. Soil Conservation Service Cooperative Laboratory, California Institute of Technology, Pasadena, California.

Tacconi, P., Billi, P. 1987. Bed load transport measurement by a vortex-tube trap on Virginio Creek, Italy. In: *Sediment Transport in Gravel-Bed Rivers.* C.R. Thorne, J.C. Bathurst, and R.D. Hey (eds.), John Wiley, Chichester, p. 583-615.

Wathen, S.J., Hoey, T.B., Werritty, A., 1995. Unequal mobility of gravel and sand in weakly bimodal river sediments. *Water Resources Research* 31 (8): 2087-2096.

Whitaker, A.C., Potts, D.F., 1996. Validation of two threshold models for bedload initiation in an upland gravel-bed stream. In: *Watershed Restoration Management - Physical, Chemical, and Biological Considerations.* American Water Resources Association, Proceedings of the Annual Symposium 1996, p. 85-94.

Wilcock, P.R., McArdell, B.W., 1993. Surface-based fractional transport rates: mobilization thresholds and partial transport of a sand-gravel sediment. *Water Resources Research* 29 (4): 1297-1312.

Williams, G.P., 1983. Paleohydrological methods and some examples from Swedish fluvial environments. *Geografiska Annaler* 65 A (3/4): 227-243.

BEDLOAD TRANSPORT RATES AT NEAR-BANKFULL FLOWS IN A STEP-POOL CHANNEL

Daniel A. Marion, Research Hydrologist, USDA Forest Service, Oxford, MS
Forest Hydrology Laboratory, Oxford, MS 38655-4915; phone 662-234-2744 ext 36, fax 662-234-8318;, fsmarion@olemiss.edu

Abstract: This paper examines unit bedload transport rates (BTRs) at near-bankfull flows within a small step-pool channel in the Ouachita Mountains of central Arkansas. For this study, five runoff events with peak discharges between 0.25 and 1.34 cms (1.0- to 1.6-yr recurrence intervals) were produced in a natural channel using a streamflow simulation system. BTRs range from $3.5x10^{-6}$ to $3.3x10^{-2}$ kg/sec/m during these events and are somewhat lower in magnitude than those reported previously for step-pool channels. BTR behavior is best modeled using discharge, but the relationship differs significantly between events with peak flows less than 0.61 cms (1.1 yr) and those greater than 0.88 cms, (1.2 yr). The smaller events exhibit higher BTRs than the larger events at flows from 0.11 to 0.35 cms, but similar rates at higher discharges. Slope coefficients are within the range Ryan and Troendle (1996) determined for two step-pool sites in Colorado. BTRs show similar positive relationships to both shear stress and stream power, but these relationships are weaker than the one with discharge. These results support the idea that sediment availability limits BTRs in step-pool channels.

INTRODUCTION

Bedload transport rates (BTRs) have received only limited study in step-pool channels. Reported maximum rates are highly variable, ranging from 0.30 (Ryan 1994) to 1.67 kg/sec/m (Hayward 1980), and often appearing to be controlled as much by local conditions as hydraulic factors. The relationship of BTR to discharge has been examined most often (e.g., Nanson 1974, Hayward 1980, Ashida and others 1981, Ketcheson 1986, Ryan and Troendle 1996), but results are often confounded by differences in antecedent conditions (e.g., sediment supply or the magnitude and number of previous events). Its relationship to other hydraulic forces has only been assessed in a few studies (Warburton 1992, Blizard and Wohl 1998).

This paper examines BTRs in a step-pool channel during simulated, near-bankfull streamflow events and controlled antecedent conditions. It documents BTR ranges and how these compare with previously reported values. It also examines relationships between BTRs and discharge, shear stress, and stream power, and discusses factors that can explain observed BTR characteristics.

METHODS

A typical step-pool reach located within the Ouachita Mountains near Hollis, Arkansas was used for this study. This reach is located on an unnamed tributary of Little Bear Cr and is hereafter referred to as Toots Cr. Annual precipitation averages 130 cm, occurring almost entirely as rain, and streamflows are ephemeral to intermittent. The catchment area above the study reach is 39 ha with an overall relief of 140 m and hillslopes ranging from 15 to 30%. Vegetation is predominantly composed of a shortleaf pine (*Pinus echinata Mill.*) overstory and a mixed

hardwood understory including white oak (*Quercus alba L.*), red oak (*Q. rubra L.*), and various hickories (*Carya* spp.) (Marion and Malanson in press). Within the 100-m study reach, the channel has a weighted (by channel length) mean gradient of 8.8%. Banks are composed of mixed colluvial and alluvial deposits while surface bed material ranges from silts to boulders with an overall D_{50} of 56 mm. Bankfull widths average 4.2 m.

Five individual flow events with peak discharges ranging from 0.25 to 1.34 m^3/sec (1.0- to 1.6-yr recurrence intervals) were simulated. Bankfull discharge was estimated to be 1.11 m^3/sec (1.4-yr recurrence interval) from channel features and computed hydraulic values. All flow events were created using controlled releases from a storage tank (see Marion and Weirich 1997 for details on system operation). Events were produced on five consecutive days and sequenced so that Event 1 had the smallest peak flow while Event 5 had the largest (Figure 1).

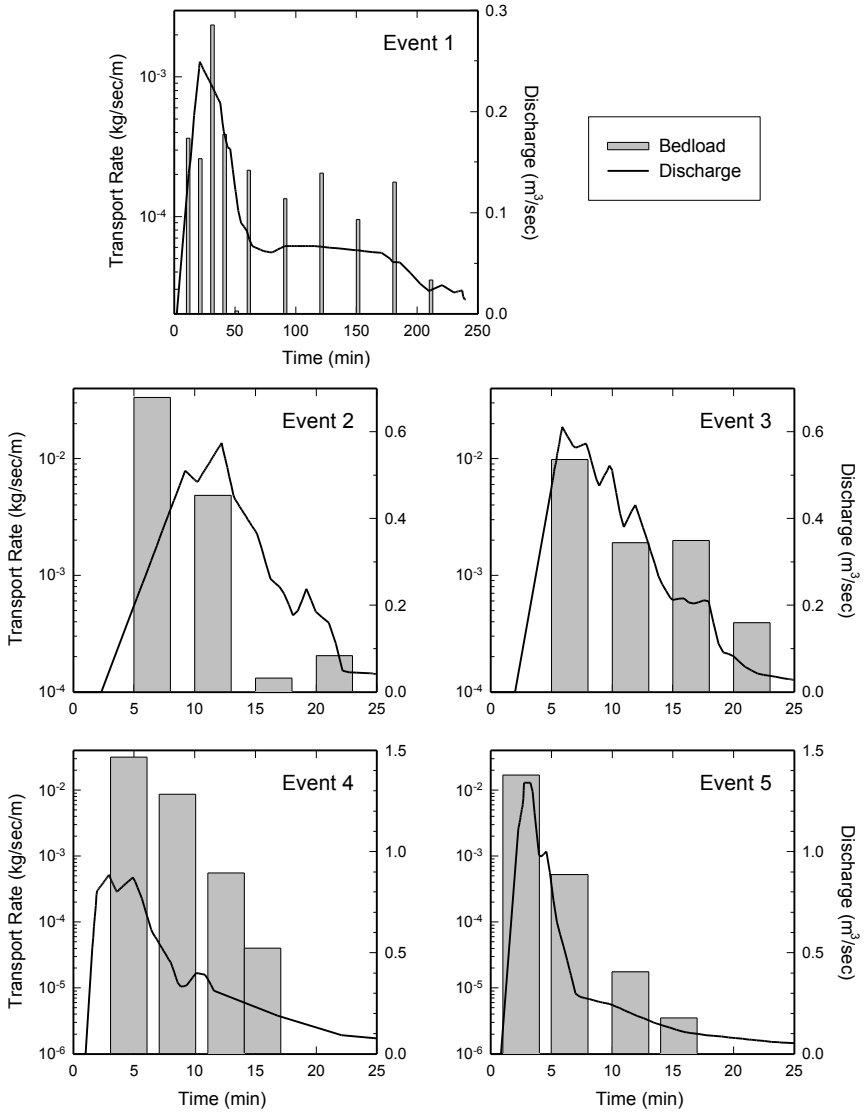

Figure 1. Bedload transport rates and discharges during Toots Cr events. Bar width equivalent to 3-minute sampling interval.

BTRs were measured using a standard 76-mm Helley-Smith sampler (Helley and Smith 1971). Throughout each event, samples were taken for 1-min intervals at three fixed locations across a sampling bridge to produce a composite sample for each measurement time. Bedload was also measured for each event using a pit trap installed at the downstream end of the study reach. Samples were oven dried and passed through a one-f sieve series from 0.062 to 16.0 mm. Larger grains were measured individually.

Bedload tracers, channel cross-sections, and bed erosion pins were also used to assess bed material entrainment, scour, and fill. Seventy-three bed clasts between 16 and 256 mm were randomly selected, marked, and re-installed within the study reach. Cross-sections were monitored at three channel locations and erosion pins were installed in all fine-sediment bed patches (Marion and Weirich 1999). All devices were measured prior to Event 1 and after each subsequent event. The channel was also visually inspected at the same times to identify any localized changes in erosion or storage.

RESULTS

BTRs from Helley-Smith samples are shown in Figure 1. BTRs range from 3.5×10^{-6} to 3.3×10^{-2} kg/sec/m during the five events. Maximum BTRs do not do not vary consistently with event magnitude. Events 2 and 4 exhibit the largest maximum BTRs. In both cases, the events that immediately followed had either equivalent (Event 3) or somewhat greater (Event 5) flows, but had markedly lower maximum BTRs.

Overall, Toots Cr BTRs are somewhat lower in magnitude than those that have been reported previously for step-pool channels. Their range is shown in Figure 2 along with BTR and corresponding discharge ranges for several small mountain streams. Toots Cr BTRs span the lower to middle portion of the overall range defined by the five step-pool sites. Differences from other sites may be partially due to hydraulic differences and measurement methods. Larger BTRs generally occur at sites having greater discharges. Also, the studies with the two largest BTRs both measured bedload using traps, whereas the other studies used Helley-Smith samplers.

BTRs determined at Toots Cr using the 73-mm Helley-Smith sampler may be low. Maxima for the coarsest Helley-Smith samples are consistently smaller than those measured with both the bedload trap and tracers (see Table 1). These differences are most likely due to the limitations of the Helley-Smith sampler which excludes grains approaching or greater than its orifice size and has less opportunity to catch larger grains due to the limited time it is deployed in any given spot.

Table 1. Maximum bedload sizes by measurement method and percent of tracers displaced for Toots Cr events. The coarsest Helley-Smith samples are used for each event and measured to the nearest f -size class.

Event	Maximum Size Displaced (mm)			Percent of Tracers
	Helley-Smith	Bedload Trap	Tracers	Displaced
1	16-32	67	123	16
2	64-128	156	170	7
3	16-32	74	38	2
4	32-64	132	130	10
5	32-64	75	180	15

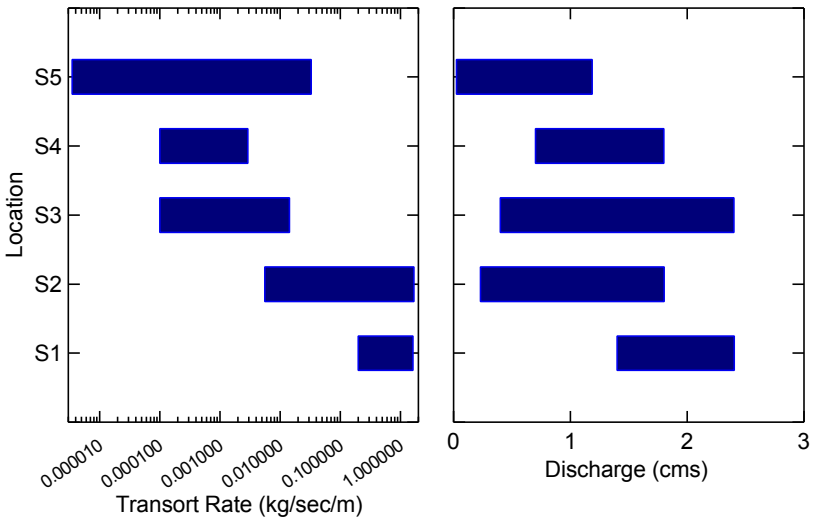

Figure 2. Bedload transport ranges and corresponding discharges for step-pool channels. Sources: S1 = Takahashi and Sawada, S2 = Hayward 1980, S3–S4 = Ryan 1994, S5 = this study.

Any bedload exclusion would reduce the computed BTR, but this is especially true for the largest sizes in which a small number of grains account for much of the total sample mass.

BTRs generally increase with increasing discharge. However, as evident from Figure 3, the relationships between BTR and discharge are different for events with peak discharges less than 0.71 cms (Events 1–3) and those with higher values (Events 4–5). Results using a General Linear Model and the Bonferroni multiple comparison test (Milliken and Johnson 1984) clearly indicate that BTR response to increased discharge is similar in Events 1–3 or Events 4–5, but that there are significant differences ($P = 0.04$) between these event groups. Model statistics are listed in Table 2. According to these results, BTRs during Events 1–3 at low to moderate discharges (0.11–0.35 cms) are much higher than during Events 4 and 5. Plots of the two models (Figure 3) suggest that the apparent differences may disappear at discharges greater than 0.35 cms (~ 1.05-yr event).

Several authors have noted significant relationships between BTR and discharge in step-pool channels (Nanson 1974, Ketcheson 1986, Blizard and Wohl 1998), however only Ryan and Troendle (1996) report their results in units that allow comparison to the Toots Cr findings. Using the same model form as here, Ryan and Troendle obtained exponents of 2.13 and 2.24 for two sites during two snowmelt seasons. These fall between the exponents obtained for Toots Cr (see Table 2). Their b_0 values (5.5×10^{-4} and 3.4×10^{-4}, respectively) are smaller than those for Toots Cr. Their model R^2 values were also comparable (0.79 and 0.44).

Neither bed shear stress nor cross-sectional stream power explain BTR change better than discharge for the five events. Both were analyzed using the same methods as for discharge and both were found to show clear differences between the same event groups as does discharge (all $P < 0.02$). The resulting models for shear stress and stream power are listed in Table 2.

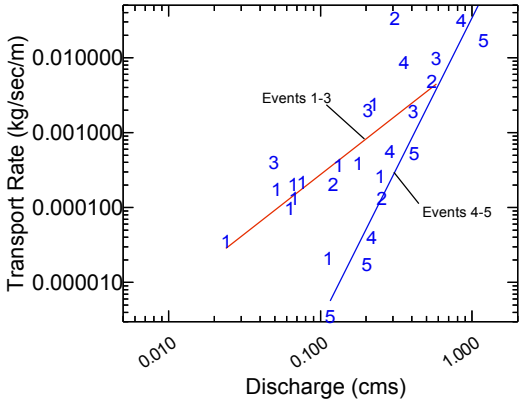

Figure 3. Relationship between bedload transport rates and discharge for Toots Cr events. Symbols indicate event numbers.

Blizard and Wohl (1998) found significant relationships (a = 0.05) between BTR and both shear stress and stream power at two of three sites on East St. Louis Cr in the Colorado Rocky Mountains. Their data were taken throughout one snowmelt season, not individual events like at Toots Cr. They used mean stream power (after Rhoads 1987) rather than cross-sectional stream power. They analyzed these relationships using both at-a-point data and data averaged over entire cross-sections, the latter being the same as done for Toots Cr. Blizard and Wohl found mean cross-section values for both shear stress and stream power to be somewhat more successful than at-a-point values at modeling BTR change, but did not report model R^2 values.

Table 2. Model statistics for predicting bedload transport rate (kg/sec/m) during Toots Cr events. Sample sizes are 19 for Events 1–3 and 8 for Events 4–5. Model form: $y = b_0 \cdot x^{b1}$.

Independent Variable	Event Group	b_0	b_1	R^2
Discharge (cms)	1–3	1.05×10^{-2}	1.58	0.54
	4–5	3.43×10^{-2}	4.04	0.84
Shear stress (N/m^2)	1–3	1.38×10^{-1}	1.22	0.27
	4–5	9.82×10^{-4}	5.59	0.79
Stream power (W/m)	1–3	1.26×10^{-4}	0.80	0.32
	4–5	2.11×10^{-9}	3.46	0.84

DISCUSSION

Two aspects of the results seem problematic. The first is that BTR relationships with hydraulic factors vary between Events 1–3 and Events 4–5. The second is that maximum BTRs varied markedly between events that are equivalent (Events 2 and 3) or similar (Event 4 and 5). The magnitude of BTRs is controlled by (1) the competency of the flow that occurs, (2) the amount of sediment in the bed that the flow is competent to transport, and (3) any restrictions on the exposure of these grains to the tractive forces inherent in the flow. Differences in BTRs between events can be ascribed to differences in one or more of these factors.

Flow competency differences between equivalent or similar events do not appear to be sufficient to explain the patterns noted above. As evident from Table 1, all events were capable of transporting up to small-cobble (64–128 mm) grains. Competency may have decreased during Event 3 relative to Event 2, which might explain the difference in maximum BTRs, but certainly did not in Event 5. In general all events transported D_{max} sizes that are roughly equivalent.

A reduction in the amount of smaller bed material between Events 1–3 and 4–5 could explain the difference in BTRs at low to moderate flows, however such a reduction does not seem likely. During Events 1–3, the majority of bedload that moved at discharges up to 0.35 cms was less than 7 mm. While overall bed size composition was not remeasured after each event, fine-sediment patches in the bed and channel cross-sections were remeasured. Previously, Marion and Weirich (1999) reported that patches exhibited net filling during all events including Events 4 and 5, while cross-sections exhibited little change. Not reported, but relevant here is that through all five events the bed material at both patches and cross-sections showed no signs of coarsening and grains less than 7 mm remained abundant. These findings and observations suggest that sediment less than 7 mm did not decrease in amount during Events 4 and 5.

The most probable explanation of BTR differences is that bed conditions evolve during each event that restrict how much sediment, especially the smaller grains, is available to be entrained. Laronne and Carson (1976) observed that smaller grains had infilled gaps within larger-grain particle clusters (e.g., steps) after peak flows within a step-pool channel. Such infilling can tighten grain packing and reduce the fine-sediment exposure to tractive forces. This bed restructuring probably occurred during all events. In this way, the amount of finer sediment would not change in the bed, but its availability during a given flow event might vary depending on the size of previous events.

The sporadic nature of bed material entrainment in coarse, heterogeneous substrates provides the mechanism by which flow competency can remain unchanged yet BTRs can vary greatly. Parker and others (1982) observed that only a very small number of the larger grains actually move in any given event. Small- to large-cobble grains (< 256 mm) were transported during all events at Toots Cr (Table 1). However, the low percentage of tracer displacements (Tables 1) and lack of pronounced cross-section changes (Marion and Weirich 1999) suggest that such entrainment occurred discontinuously throughout the reach. If finer sediment is not exposed when larger grains move, then BTRs might actually decrease even though flow competency (as represented by bedload D_{max}) remains the same.

Thus, changes in finer-sediment availability during the five events can explain both the BTR variation between Events 1–3 and 4–5, and the difference in maximum BTRs between similar events. In the case of the former, at peak Event 4 and 5 discharges, BTRs were relatively high (Figure 1) as larger grains were mobilized. However, subsequent flows at moderate to low hydraulic force levels encountered a better-organized bed with less finer sediment available than during Events 1–3, and lower BTRs resulted. In the case of the latter, differences in peak BTRs are possible if both larger bedload were entrained *and* new finer-sediment sources were briefly exposed during peak discharge for Events 2 and 4, but both conditions did not occur during Event 3 and 5 peak discharges. The sediment sources that produced Event 2 and 4 peak BTRs may have occurred at locations that were not replenished during recession flows. If so, then Events 3 and 5 would have to either displace more or larger particles, or exploit new finer-sediment sources to produce equivalent BTRs.

Others have concluded that limits on sediment supply are the most likely cause for reduced BTRs during constant or increasing flows in step-pool channels. Nanson (1974) found restricted sediment supply the best explanation for declining BTRs during high discharges after the snowmelt peak flow. Ashida and others (1976) also reasoned that limited sediment storage explained numerous observations of declining BTRs despite discharges remaining constant or even increasing. Blizard and Wohl (1998) note that random events such as tree fall into the channel can also explain BTR variation, however such events did not occur during the Toots Cr experiments.

CONCLUSIONS

Unit BTRs range from 3.5×10^{-6} to 3.3×10^{-2} kg/sec/m during the five events and are highly variable. BTR behavior is best modeled using discharge magnitude, but this relationship differs significantly between Events 1–3 and the larger Events 4 and 5. BTRs also show positive relationships to both shear stress and stream power, but these relationships are much weaker than the one with discharge.

Variation in BTRs between events at low to moderate hydraulic ranges and the marked differences in peak BTRs between similar events (2 v. 3 and 4 v. 5) are best explained by the evolution and disruption of bed material organization during the events and the influence this has on sediment availability. Neither reductions in finer-sediment amounts in the bed between events, nor flow competency differences appear sufficient to explain these results. Rather it is reasoned that bed restructuring through infilling and tightening (Laronne and Carson 1976) of cobble or boulder clusters during each event reduces BTR response during subsequent events until higher forces levels occur and new, entrainable sediment is exposed.

ACKNOWLEDGEMENTS

I thank Roger A. Kuhnle, Sandra E. Ryan, and Howard G. Halverson for their constructive reviews of this paper, and the many Forest Service and University of Iowa personnel who provided assistance. The following organizations provided funding for this research: the USDA Forest Service, Southern and Rocky Mountain Research Stations; the Ouachita National Forest; the National Council of the Paper Industry for Air and Stream Improvement; and the University of Iowa.

REFERENCES

Ashida, K., Takahashi, T., Sawada, T., 1976, Sediment Yield and Transport on a Mountainous Small Watershed. Bulletin of the Disaster Prevention Research Institute, 26(240), 119-144.

Ashida, K., Takahashi, T., Sawada, T., 1981, Processes of Sediment Transport in Mountain Stream Channels. In: Davies, T. R. H., Pearce, A. J., eds, Erosion and Sediment Transport in Pacific Rim Steeplands. International Association of Hydrological Sciences Publication No. 132, 166-178.

Blizard, C. R., Wohl, E. E., 1998, Relationships Between Hydraulic Variables and Bedload Transport in a Subalpine Channel, Colorado Rocky Mountains, U.S.A. Geomorphology, 22, 359-371.

Hayward, J. A., 1980, Hydrology and Stream Sediments in a Mountain Catchment. Canterbury, New Zealand, Tussock Grasslands and Mountain Lands Institute Special Publication 17, 236 p.

Helley, E. J., Smith, W., 1971, Development and Calibration of a Pressure Difference Bedload Sampler. USGS Water Resources Division Open-file report. 18 p.

Ketcheson, G. L., 1986, Sediment Rating Equations: an Evaluation for Streams in the Idaho Batholith. General Technical Report INT-213, USDA Forest Service, Intermountain Research Station, 12 p.

Laronne, J. B., Carson, M. A., 1976, Interrelationships between Bed Morphology and Bed-Material Transport for a Small, Gravel-Bed Channel. Sedimentology, 23, 67-85.

Marion, D., Malanson, G., [in press], Ordination of Wood Vegetation in a Ouachita National Forest Watershed. In: Guldin, J. M., ed, Proceedings of the Symposium on Ecosystem Management Research in the Ouachita and Ozark Mountains, 1999 October 26-28, Hot Springs, AR. USDA Forest Service, Southern Research Station.

Marion, D. A., Weirich, F., 1997, Simulating Storm Events. Environmental Testing & Analysis, 6(4), 15-16.

Marion, D. A., Weirich, F., 1999, Fine-Grained Bed Patch Response to Near-Bankfull Flows in a Step-Pool Channel. In: Olsen, D. S., Potyondy, J. P., eds, Wildland hydrology, Proceedings of the Specialty Conference; 1999 June 30-July 2; Bozeman, MT. American Water Resources Association, 93-100.

Milliken, G. A., Johnson, D. E., 1984, Analysis of Messy Data. Lifetime Learning Publications, 473 p.

Nanson, G. C., 1974, Bedload and Suspended Load Transport in a Small, Steep, Mountain Stream. American Journal of Science, 274(5), 471-486.

Parker, G., Klingeman, P. C., McLean, D. G., 1982, Bedload and Size Distribution in Paved Gravel-Bed Streams. Journal of the Hydraulics Division, Proceedings of the American Society of Civil Engineers, 108(HY4), 544-571.

Rhoads, B. L., 1987, Stream Power Terminology. Professional Geographer, 39(2), 189-195.

Ryan, S. E., 1994, Effects of Transbasin Diversion on Flow Regime, Bedload Transport, and Channel Morphology in Colorado Mountain Streams. University of Colorado, 236 p, Ph.D. Dissertation.

Ryan, S.E., Troendle, C.A., 1996, Bedload Transport Patterns in Coarse-Grained Channels Under Varying Conditions of Flow. In: Proceedings of the Sixth Federal Interagency Sedimentation Conference, 1996 March 10-14, Las Vegas, NV. [Publisher unknown], VI-22 to VI-27b.

Takahashi, T., Sawada, T., 1994, Bed Load Prediction in Steep Mountain Rivers. In: Cotroneo, G. V.; Rumer, R. R., eds., Hydraulic Engineering '94; Proceedings of the 1994 conference; 1994 August 1-5; Buffalo, New York. American Society of Civil Engineers, 810-814.

Warburton, J., 1992, Observations of Bed Load Transport and Channel Bed Changes in a Proglacial Mountain Stream. Arctic and Alpine Research, 24(3), 195-203.

THE FLUX AND PARTICLE SIZE DISTRIBUTION OF SEDIMENT COLLECTED IN HILLSLOPE TRAPS AFTER A COLORADO WILDFIRE

Deborah A. Martin[1], Hydrologist, U.S. Geological Survey, Boulder, Colorado; John A. Moody [2], Hydrologist, U.S. Geological Survey, Lakewood, Colorado

[1] 3215 Marine Street, Suite E-127, Boulder, Colorado, 80303-1066, (303) 541-3024, fax (303) 447-2505, damartin@usgs.gov, [2] Box 25046, Denver Federal Center, Mail Stop 413, Lakewood, Colorado, 80225-0046, (303) 236-0606, fax (303) 236-5034, jamoody@usgs.gov

INTRODUCTION

Flooding and erosion following wildfires are well-recognized phenomena in montane areas of the western United States (e.g., Connaughton, 1935; Buck et al., 1948; Sartz, 1953; Cleveland, 1977; Swanson, 1981; White and Wells, 1984; Wells, 1986; Morris and Moses, 1987; McNabb and Swanson, 1990; Booker et al., 1993) and internationally (e.g., Atkinson, 1984; Ballais and Magagnosc, 1993; Andreu et al., 1994; Soler et al., 1994; Soto et al., 1994; Inbar et al., 1998; Prosser and Williams, 1998). The removal of duff, litter and the forest canopy along with the physical and chemical alteration of soil by fire change the erosional threshold of burned watersheds (McNabb and Swanson, 1990; Meyer and Wells, 1997; Moody and Martin, unpublished data). Hillslope erosion and transport processes include rainsplash (Foster, 1982; Moss and Green, 1983), sheetwash (Foster, 1982), rilling (Young and Wiersma, 1973; Mosley, 1974; Foster and Meyer, 1975), dry ravel (the transport of surface material by gravity and wind, not by flowing water; Krammes, 1960, 1965), and freeze-thaw action. The rates of these processes are altered when watersheds burn (Miller, 1994).

In this paper we report the results of hillslope erosion monitoring in the Spring Creek watershed southwest of Denver, Colorado following a wildfire in 1996. The hillslope sediment-flux measurements and particle-size analyses were part of a larger study to determine the storage and transport of sediment in two adjacent burned watersheds (Buffalo Creek and Spring Creek) that in a year contributed more than 30 times the average annual pre-fire flux of sediment to Strontia Springs Reservoir (Moody and Martin, unpublished data), a water supply reservoir serving Denver and Aurora, Colorado. The data provided by this study will contribute to a more detailed understanding of the movement and particle-size distribution of sediment in burned areas, which will help land mangers in their post-fire rehabilitation planning and implementation.

BACKGROUND

The Buffalo Creek Fire burned 4690 hectares of mainly ponderosa pine and Douglas-fir forest in May 1996 (Figure 1). Approximately 62% of the area burned was classified as high-intensity burn (Bruggink et al., 1998), based on the complete combustion of needles on burned trees and the consumption of litter and duff. On 12 July 1996, a rainstorm with an estimated intensity of 99 mm h^{-1} (Jarrett and Browning, unpublished data) followed by other less intense storms produced dramatic erosion and deposition in the Buffalo Creek and Spring Creek watersheds. Soils in the watersheds are decomposed granite derived from the Pike's Peak batholith and are classified as easily erodible due to the shallow depth to bedrock and hence the high runoff potential when thoroughly wet (Moore, 1992). The burned area is in mountainous terrain dominated by short-duration, high-intensity summer rainfall. Snow pack and spring snowmelt are minimal.

We evaluated hillslope erosion in Spring Creek watershed. The hillslopes in the Spring Creek watershed are steep, typically 30 º or greater. Spring Creek flows generally west to east, creating predominantly north- and south-facing hillslopes. The vegetation on the south-facing hillslopes is mostly ponderosa pine (*Pinus ponderosa*) with a small proportion of Rocky Mountain juniper (*Juniperus scopulorum*) and widely dispersed bunch grasses in the understory, whereas the vegetation on the north-facing slopes is generally Douglas-fir (*Pseudotsuga medezii*) with very little understory vegetation. Like much of the Colorado Front Range, both extensive grazing and active fire suppression for over 100 years have allowed tree densities to increase over historic densities in the pre-fire suppression era (Brown et al., 1999; Kaufmann et al., 2000a, 2000b). The increase in vegetation density affects fire behavior, the production of volatile organic compounds that may contribute to the water repellency of the soil, and the heat impulse to the soil (Miller, 1994). While pre-fire hillslope erosion rates are unknown for the Spring Creek watershed, typical annual fluxes for adjacent areas are 0.0-0.1 kg m^{-1} (Bovis, 1974; Morris and Moses, 1987; Welter, 1995).

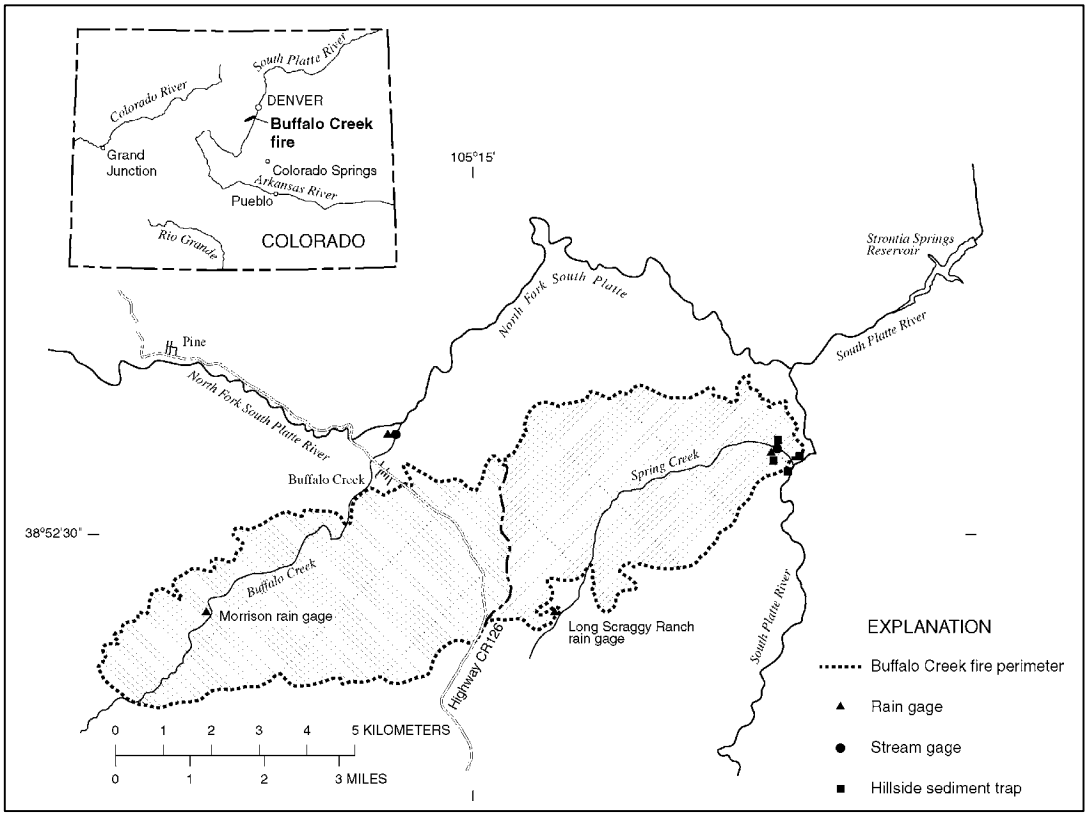

Figure 1 The Buffalo Creek Fire perimeter and the location of the hillslope sediment traps.

METHODS

We deployed sediment traps in interrill areas of severely burned and unburned hillslopes of the Spring Creek watershed. Traps were installed in the burned area on north-facing and south-facing hillslopes in 1997, one year after the wildfire, and in an unburned area on a north-facing and a south-facing hillslope in the second year after the wildfire. Four replicate traps were installed on each hillslope (south-facing, severely burned; north-facing, severely burned; south-facing, unburned; and north-facing, unburned). A sediment trap consisted of a trough constructed of PVC pipe with a 1-m x 0.1-m collection slot (Gerlach, 1967; Fitzhugh, 1992; Moody and Martin, unpublished data). Traps were installed perpendicular to the slope. A bucket collected sediment and water from the trough and additional buckets collected the water overflow from the trough. Metal edging enclosed the area of hillslope that contributed sediment to the trough. In 1997, the enclosures were of variable size averaging 10 m^2. Starting in 1998, the enclosures were reconfigured and standardized to 5 m^2 (1 m wide x 5 m long).

We collected sediment and water from the four replicate traps either after major storm events or as frequently as possible during the summer at all sites. Sediment from traps on the south-facing severely burned hillslope was also collected during the early spring and late fall to correspond to when rill-erosion measurements were made on the same hillslope. On the other hillslopes, sediment was allowed to accumulate throughout the winter until the first collection of the following summer. The four replicate samples collected at the end of each accumulation period constitute a group. Group averages for the median particle diameter, dispersion, and flux were computed using the four replicate samples. Seasonal means were computed as the means of the group averages and confidence limits were determined assuming that the group averages were statistically independent samples (Table 1). In addition, we took 5-cm diameter x 10-cm deep soil cores from the unburned, north- and south-facing hillslopes to characterize the particle-size distribution of the source of sediment collected in the hillslope traps.

Table 1: Seasonal median particle diameter, dispersion, and flux of sediment collected in traps on hillslopes in the Spring Creek watershed

[A group consists of four replicate samples; dispersion is dimensionless; NA= not applicable; numbers following ± sign are 95 % confidence limits; [a] summer consists of 122 days in June, July, August, and September and includes 31 August 1997, [b] The flux of sediment overtopped the traps and so the summer 1997 total flux and the 31 August 1997 flux are minimum estimates; [c] winter consists of 243 days]

Location	Number of groups	D_{50} mm	Dispersion	Flux kg m^{-1}
North-facing, unburned, 12 cores, 10-cm deep	1	2.9	4.2	NA
South-facing, unburned, 12 cores, 10-cm deep	1	2.6	4.9	NA
North-facing, burned, hillslope traps:				
Summer[a,b] 1997	7	2.0 ± 0.7	5.9 ± 1.6	>5.9
31 August[b] 1997	1	3.3	3.9	>3.3
Winter[c] 1997-1998	1	1.3	NA	0.90
Summer 1998	4	3.4 ± 1.2	3.1 ± 0.9	0.30 ± 0.38
Winter 1998-1999	1	3.6	3.9	0.05
Summer 1999	2	4.1 ± 2.6	2.6 ± 1.9	0.10 ± 0.68
South-facing, burned, hillslope traps:				
Summer 1997	7	4.6 ± 1.2	4.1 ± 1.7	0.85 ± 0.18
31 August 1997	1	6.2	2.3	0.52
Winter 1997-1998	1	7.6	4.8	0.24
Summer 1998	4	6.0 ± 3.5	2.8 ± 0.8	0.15 ± 0.16
Winter 1998-1999	3	9.5 ± 7.3	1.9 ± 0.8	0.08 ± 0.10
Summer 1999	2	9.4 ± 6.4	2.0 ± 0.6	0.11 ± 0.43
North-facing, unburned, hillslope traps:				
Summer 1998	4	3.3 ± 0.9	2.8 ± 0.7	0.15 ± 0.10
Winter 1998-1999	1	4.6	2.6	0.06
Summer 1999	2	4.4 ± 6.4	2.5 ± 1.3	0.08 ± 0.29
South-facing, unburned, hillslope traps:				
Summer 1998	4	3.8 ± 0.4	2.2 ± 0.4	0.20 ± 0.18
Winter 1998-1999	1	3.9	2.4	0.05
Summer 1999	2	4.1 ± 3.2	2.1 ± 0.6	0.13 ± 0.22

Particle-Size Distribution: All of the sediment collected in the traps was processed in the laboratory. In the field, the total volume of water in the buckets was measured and recorded. If the water contained suspended sediment, the water was churned in a churn splitter (Meade and Stevens, 1990) and a 1-L water subsample taken to the laboratory. The sediment was dried at 105° C and weighed to determine mass. To determine the particle-size distribution, we sieved the dry sediment by whole phi (F) intervals (F = $-\log_2$ of the particle size diameter in mm; Krumbein, 1934). In addition, when sufficient dry sediment existed, a 1-gram subsample of the <0.063 mm particle size class was settled following the methods described by Guy (1969) to determine the silt (0.004-0.063 mm) and the clay (<0.004 mm) particle-size fractions. Also, we settled the water subsample and added the mass of the silt and clay to the mass of those particle-size classes determined from the settling of the dry sediment. We calculated the median particle diameter (D_{50}) and the dispersion (s) to characterize the particle-size distribution of the eroded sediment (Table 1). The dispersion is a dimensionless number (geometric standard deviation, $s = \sqrt{D_{84}/D_{16}}$, where D_{84} and D_{16} are the diameters at which 84 percent and 16 percent of the sediment are finer than the specified diameter; Inman, 1952) that measures the spread of the particle-size distribution and is equal to 1.0 for a distribution with only one particle-size class. Curves of the particle-size distribution were fit to the data using a cubic-spline program (R.F. Stallard, USGS, written communication) for the particle size data, and 95% confidence limits (Table 1) were computed using the Student-t distribution. Figures 2A and 2B show the curves for the three summer seasons during the study period.

Sediment Flux: Sediment fluxes are reported for both the summer months (June-September) and for the winter months (October-May), based on the mass of sediment collected from the hillslope traps. Because we did not collect sediment after each storm, the data from each collection date represent the sediment moved by a variety of hillslope-

transport processes. Even though we used bounded plots, we think that it is impossible to define the true contributing area from which sediment is eroded and later deposited in our hillslope sediment traps. Therefore, we chose to express our data as sediment flux rates, which we calculated as the mass of sediment transported across a unit contour (1 meter) per unit time (1 day). We multiplied the mass per bounded area by the length of the enclosure to yield mass per unit contour width and divided the result by the number of days in the accumulation period. Because sediment in the traps was not collected for the same time intervals each year, the sediment flux rate was multiplied by the number of days in the appropriate season (122 days for the summer season, 243 days for the winter season) to yield comparable seasonal fluxes (Table 1).

The 31 August 1997 storm: The storm of 31 August 1997 was notable for its greater rainfall intensity and sediment flux than any other storm during the study period. The storm lasted for about an hour, produced 48 mm of rain and had a 30-minute maximum intensity of 88 mm h^{-1}. We have reported the data separately for this date in Table 1 to highlight the episodic nature of hillslope erosion and because the rainfall intensities more closely match the intensity of the 12 July 1996 storm that produced the initial post-fire erosion in Spring Creek. The mass of sediment from the 31 August 1997 storm filled up and spilled over the hillslope traps on the north-facing, burned hillslope. Therefore, sediment fluxes for this date and for the whole 1997 summer season for the north-facing, burned hillslope can only be considered as minimum amounts.

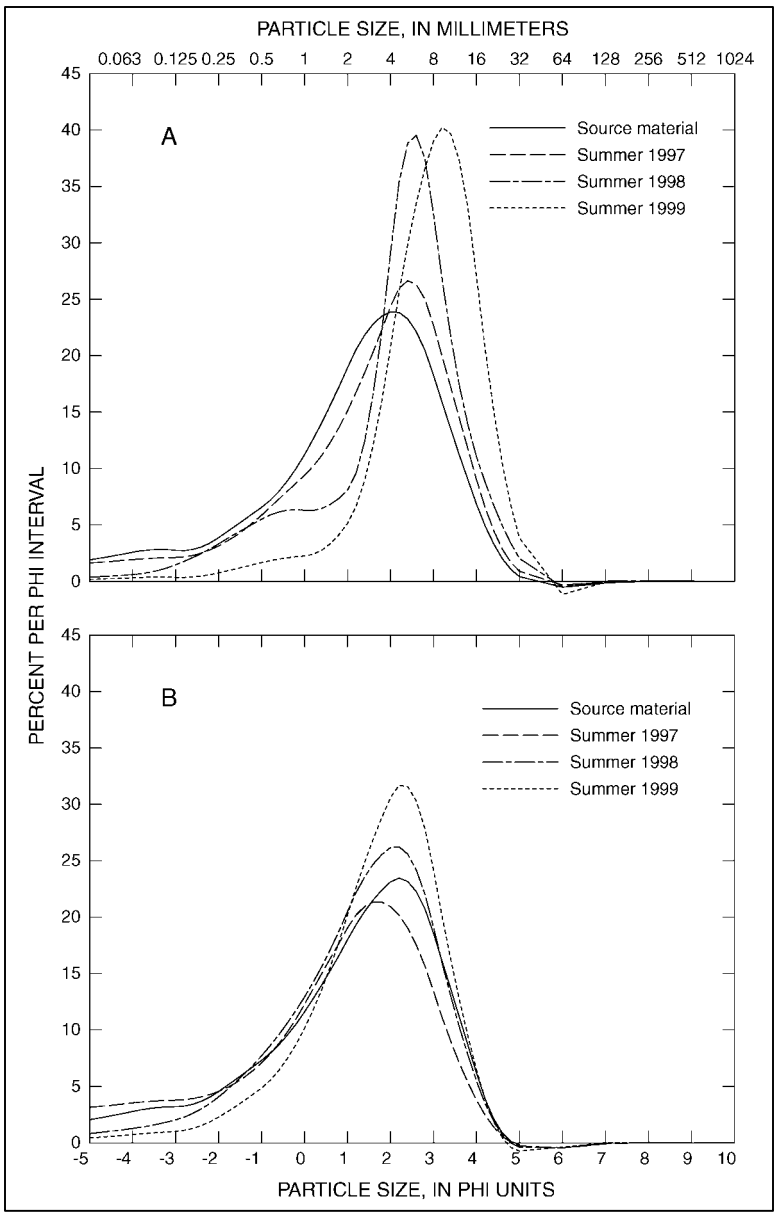

Figure 2.Particle-size distributions (summer only and source material) A. South-facing burned hillslope B. North-facing burned hillslope

RESULTS AND DISCUSSION

The Particle-Size Distribution: For samples collected from the burned hillslopes, we measured coarser particle sizes in the summer of 1999 (D_{50}=4.1 mm for north-facing, D_{50}=9.4 mm for south-facing) than in the summer of 1997 or 1998 (Table 1), even though the maximum rainfall intensities decreased during the study period. We have two hypotheses to explain the shift to coarser particle sizes. The coarsening (Figure 3A) may be the result of a diminished supply of the finer-grained material. Some of the finer material was eroded from the watershed during the 1996 storms after the wildfire, as evidenced by post-flood deposits of ash and fine-grained sediment in Strontia Springs Reservoir and downstream of the Strontia Springs Reservoir dam, and during 1997 as evidenced by sediment collected in the hillslope traps (see 1997 dashed curve in Figure 2A). Alternatively, there may be a

preferential transport of coarser material with time after the fire, possibly by the dry ravel process. The decrease in the dispersion with time (Table 1) on both the north-facing and south-facing burned hillslopes during the summer seasons may be an indication of the increase in importance of the dry ravel. In this climate, dry ravel is mainly triggered by wind and disturbance by fauna (lizards, snakes, crickets, grasshoppers, and mice, all of which we inadvertently caught in our hillslope erosion traps). We observed that as the surface of both the unburned hillslopes and burned hillslopes became dry, it became increasingly difficult to walk on the surface. Coarse-grained material (>4 mm diameter) acted as ball bearings while the fine-grained material was more cohesive and had hardened. In agricultural areas, Young and Onstad (1976) also found that sand-sized material was enriched in eroded material in interrill areas, but this result differs from the findings of Meyer et al. (1975), Monke et al. (1977), and Alberts et al. (1980).

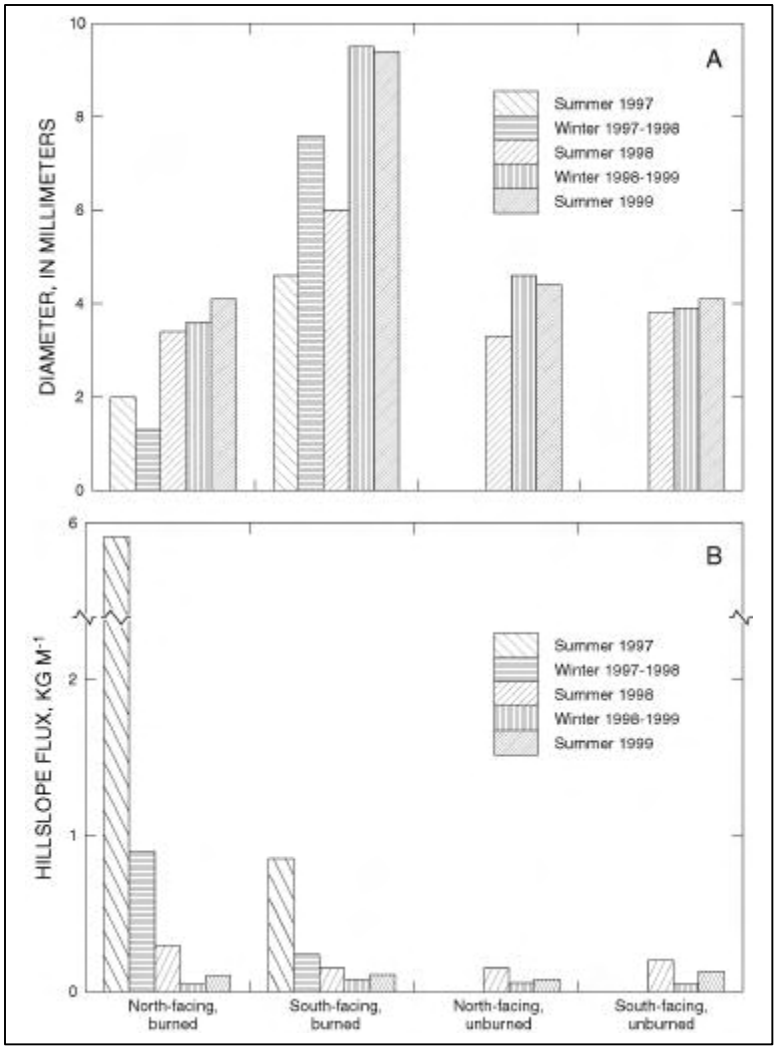

Figure 3. Seasonal change in median particle diameter and hillslope sediment flux in the Spring Creek watershed. A. Median particle diameter of eroded sediment collected in hillslope traps during summer (June-September, 122 days) and winter (October-May, 243 days) seasons. B. Hillslope flux for summer (June-September, 122 days) and winter (October-May, 243 days) seasons. Hillslope traps were not deployed in the unburned area until 1998.

The eroded sediment from the south-facing, burned hillslope was coarser during each season than the sediment from the north-facing burned slope (Table 1 and Figure 3A). The relative coarseness of the eroded sediment from the burned south-facing hillslope compared to the north-facing burned hillslopes and the unburned hillslopes may be a reflection of both the hillslope vegetation cover and the prior removal of fine-grained sediment discussed above. As the south-facing, burned slope is recovering, there has been a regrowth of the bunch grasses that existed before the wildfire. Even under unburned conditions, bare hillslopes are exposed between the bunch grasses. Field observations suggest that these bare spots are more susceptible to dry ravel and disturbance than are vegetated hillslopes. The previous loss of the fine-grained material would reduce the soil cohesion and allow more coarse-grained material to erode. In contrast, the north-facing, burned hillslopes have developed a dense cover of herbaceous vegetation (including creeping dogbane, *Apocynum androsaemifolium*, sugarbowl, *Clematis hirsutissima*, and leafy spurge, *Euphorbia esula*) as they have recovered during the three years of our study. Based on observations of the north-facing, unburned hillslopes, it is clear that before the fire the north-facing hillslopes had very little understory vegetation because of competition for light and nutrients under the closed, mainly Douglas-fir canopy. The thick vegetation cover on the recovering north-facing, burned hillslopes may be stabilizing the coarser-grained material.

Sediment flux: The pattern of sediment flux was similar on burned and unburned hillslopes beginning in the summer of 1998 (Figure 3B). By the summer of 1999, all four hillslopes have similar sediment fluxes. The flux of sediment from the north-facing, burned hillslope was greater than from the south-facing, burned hillslope through

the summer of 1998. We hypothesize that the pre-fire vegetation density on the north-facing slope may account for this behavior. The fuel loading on the north-facing hillslopes (mainly densely spaced Douglas-fir with a thick duff layer) was greater than the south-facing hillslope and the burned north-facing soils were more water-repellent (Jeff Bruggink, USFS, written communication; for a more complete discussion of fire-induced water repellency see DeBano, 1969; Debano et al., 1977; Giovannini et al., 1983). The greater water repellency on the north-facing burned hillslopes probably created greater runoff that, in turn, caused greater erosion. Also, the thick litter and duff layer on the north-facing hillslopes could have held sediment that is easily mobilized once the litter and duff were burned off (P.M. Wohlgemuth, USFS, written communication). As herbaceous groundcover grows, the sediment is increasingly stabilized.

CONCLUSIONS

We found that the flux of sediment decreased and the median diameter of eroded sediment increased from burned hillslopes in Spring Creek watershed during the three years following the Buffalo Creek Fire. It took three years for fluxes of sediment from burned hillslopes to return to rates of unburned hillslopes, which and is within the range (3-9 years) of other studies of burned areas in other soils and terrains (Rowe et al., 1949, 1954; Doehring, 1968; Brown, 1972; Wells et al., 1979; Laird and Harvey, 1986; Wells, 1986; Potyondy and Hardy, 1994). In addition, the sediment fluxes that we have documented during the first three years after the wildfire are comparable to values, 2.9-4.0 kg m^{-1}, measured by Morris and Moses (1987) for another Colorado Front Range wildfire. Although fluxes from the burned hillslopes appear to have returned to rates in unburned areas, as of August 2000 considerable sediment was stored in tributaries and in the main channel of Spring Creek. This stored sediment may be a long-term supply of sediment to the downstream water-supply reservoir or it may be stabilized by riparian vegetation until another erosional cycle is initiated by wildfire or another disturbance (Moody and Martin, unpublished data). We are continuing to monitor hillslope fluxes and stored channel sediment to provide data to support land management decisions.

ACKNOWLEDGEMENTS

The Denver Water Board, the National Research Program of the U.S. Geological Survey, and the U.S. Forest Service provided funding for this study. We particularly wish to thank Bob Weir (retired), Denver Water Department, for his support, enthusiasm and vision, and Jeff Bruggink, U.S. Forest Service, for his support and cooperation. Several people collected and processed samples, surveyed, or provided other support. We extend our heartfelt thanks to Craig Allen, Greg Alexander, Tanya Ariowitsch, Brent Barkett, Jeff Blossom, Régis Braucher, Terry Brinton, Allen Gellis, Eleanor Griffith, David Kinner, Bob Meade, Lisa Pine, Mark Richards, Pete Robichaud, Bob Stallard, Howard Taylor, and Peter Wohlgemuth. We thank Sue Cannon, Allen Gellis, and Peter Wohlgemuth for their detailed reviews of this manuscript.

REFERENCES

Alberts, E. E., Moldenhauer, W. C., and Foster, G. R., 1980, Soil aggregates and primary particles transported in rill and interrill flow. Soil Science Society of America Journal, 44, 590-595.

Andreu, V., Rubio, J. L., Forteza, J., and Cerni, R., 1994, Long Term Effects of Forest Fires on Soil Erosion and Nutrient Losses. in: Sala, M. and Rubio, J. L., editors, Soil Erosion and Degradation as a Consequence of Forest Fires, Barcelona/Valencia. Logroño: Geoforma Ediciones, 79-89.

Atkinson, G., 1984, Erosion damage following bushfires. Journal of Soil Conservation, New South Wales, 40(1), 4-9.

Ballais, J. L. and Magagnosc, J. S. editors, 1993, L'Erosion consecutive a l'incendie d'Aout 1989 sur la montagne Sainte-Victoire; trois annees d'observations (1989-1992). dans Les Facteurs anthropiques de l'erosion dans les domaines tropicaux et mediterraneens, Journees de travail, Association de Geographes Francais, Paris, France, 423-437.

Booker, F. A., Dietrich, W. E., and Collins, L. M., 1993, Runoff and erosion after the Oakland firestorm. California Geology, 46(6):159-173.

Bovis, M. J., 1974, Rates of soil movement in the Front Range, Boulder County, Colorado. Unpublished Ph. D. Dissertation, Dept. of Geography, University of Colorado, Boulder, 235 p.

Brown, J. A. H., 1972, Hydrologic effects of a brushfire in a catchment in southeastern New South Wales. Journal of Hydrology, 15, 77-96.

Brown, P. M., Kaufmann, M. R., and Shepperd, W. D., 1999, Long-term, landscape patterns of past fire events in a montane ponderosa pine forest of central Colorado, 14, 513-532.

Bruggink, J., Bohon, D., Clapsaddle, C., Lovato, D., and Hill, J., 1998, Buffalo Creek Burned Area Emergency Rehabilitation Final Report. 22 p.

Buck, C. C., Fons, W. L., and Countryman, C. M., 1948, Fire Damage From Increased Run-Off and Erosion San Bernardino National Forest. United States Dept. of Agriculture Forest Service California Forest and Range Experiment Station.

Cleveland, G. B., 1977, Marble Cone fire; effect on erosion. California Geology, 30(12), 267-271.

Connaughton, C. A., 1935, Forest fires and accelerated erosion. Journal of Forestry, 33,751-752.

DeBano, L. F., 1969, Observations on water-repellent soils in western United States. in DeBano, L. F. and Letey, J. (eds.), Water-repellent Soils, Proceedings of the Symposium of Water-repellent Soils, May 6-10, 1968, University of California, Riverside, 17-29.

DeBano, L.F., Dunn, P. H., and Conrad, C. E., 1977, Fire's effect on physical and chemical properties of chaparral soils. U. S. Dept. of Agriculture, Forest Service General Technical Report WO-3, 65-74.

Doehring, D. O., 1968, The effect of fire on geomorphic processes in the San Gabriel Mountains, California. in Parker, R. B., editor, Contributions to Geology. Laramie, Wyoming: University of Wyoming, 43-65.

Fitzhugh, R., 1992, Construction of simple surface runoff sampler. WRD Instrument News (Dept. of Interior, U.S. Geological Survey, Water Resources Division), 58, p. 1,4.

Foster, G. R., 1982, Modeling the Erosion Process. in Haan, C. T., Johnson, H. P., and Brakensiek, D. L., editors, Hydrologic modeling of small watersheds, St. Joseph, Michigan: The American Society of Agricultural Engineers, 297-380.

Foster, G. R. and Meyer, L. D., 1975, Mathematical simulation of upland erosion by fundamental erosion mechanics. in Present and Prospective Technology for Predicting Sediment Yields and Sources, Proceedings of the Sediment-Yield Workshop, U.S. Dept. of Agriculture Sedimentation Laboratory, Oxford, Mississippi, Nov. 28-30, 1972, U.S. Dept. of Agriculture, Agricultural Research Service, Publication ARS-S-40, 190-207.

Gerlach, T., 1967, Hillslope troughs for measuring sediment movement. Revue Geomorphologie Dynamique, 17(4), 173-174.

Giovannini, G., Lucchesi, S. and Cervelli, S., 1983, Water repellent substances and aggregate stability in hydrophobic soil. Soil Sci., 135(2), 110-113.

Guy, H. P., 1969, Laboratory theory and methods for sediment analysis. U.S. Geological Survey Techniques Water-Resources Investigation, Book 5, Chapter C1, 58 p.

Inbar, M., Tamir, M., and Wittenberg, L., 1998, Runoff and erosion processes after a forest fire in Mount Carmel, a Mediterranean area: Mediterranean erosion. Geomorphology, 24(1), 17-33.

Inman, D. L., 1952, Measures for describing the size distribution of sediments. Journal of Sedimentary Petrology, 22(3), 125-145.

Kaufmann, M. R., Regan, C. M., and Brown, P. M., 2000a, Heterogeneity in ponderosa pine/Douglas-fir forests: age and stucture in unlogged and logged landscapes of Central Colorado. Canadian Journal of Forest Research.

Kaufmann, M. R., Huckaby, L., and Gleason, P., 2000b, Ponderosa pine in the Colorado Front Range: Long historical fire and tree recruitment intervals and a case for landscape heterogeneity. in Crossing the Millennium: Integrating Spacial Technologies and Ecological Principles for a New Age in Fire Management, Proceedings from the Joint Fire Science Conference and Workshop, Boise, Idaho, June 15-17, 1999, 153-160.

Krammes, J. S., 1960, Erosion from Mountain Side Slopes after Fire in Southern California. Berkeley, California, United States Dept. of Agriculture, Forest Service, Pacific Southwest Forest and Range Experiment Station Research Note, 171, 7 p.

Krammes, J. S., 1965, Seasonal debris movement from steep mountainside slopes in Southern California. in Federal Interagency Sedimentation Conference: United States Dept. of Agriculture, United States Dept. of Agriculture Miscellaneous Publications, 970, 85-89.

Krumbein, W. C., 1934, Size frequency distributions of sediments. Journal of Sedimentary Petrology, 4, 65-77.

Laird, J. R. and Harvey, M. D., 1986, Complex-response of a chaparral drainage basin to fire. in Hadley, Richard F., editor, Drainage Basin Sediment Delivery, Albuquerque, New Mexico, International Association of Hydrological Sciences, Publication 159, 165-183.

McNabb, D. H. and Swanson, F. J., 1990, Effects of Fire on Soil Erosion. in Walstad, J. D., Radosenvich, S. L., and Sandberg, D. V., editors. Natural and Prescribed Fire in the Pacific Northwest Forests. Corvallis, Oregon: Oregon State University Press, 159-176.

Meade, R. H., and Stevens, H. H., Jr., 1990, Strategies and equipment for sampling suspended sediment and associated toxic chemicals in large rivers—with emphasis on the Mississippi River. Science of the Total Environment, 97/97, p. 125-135.

Meyer, G. A. and Wells, S. G., 1997, Fire-related sedimentation events on alluvial fans, Yellowstone National Park, U.S.A. Journal of Sedimentary Research, 67, no. 5, p. 776-791.

Meyer, L. D., Foster, G. R., and Romkens, M. J. M., 1975, Mathematical simulation of upland erosion using fundamental erosion mechanics. Proceedings of the Sediment Yield Workshop, U.S. Dept. of Agriculture Sedimentation Laboratory, Oxford, Mississippi, 177-189.

Miller, M., editor,1994, Fire Effects Guide. National Wildfire Coordinating Group, National Interagency Fire Center NFES #2394, PMS 481.

Moore, R., 1992, Soil Survey of Pike National Forest, Eastern Part, Colorado, Parts of Douglas, El Paso, Jefferson and Teller Counties. U. S. Dept. of Agriculture, Forest Service and Soil Conservation Service, 106 p.

Monke, E. J., Marelli, H. J., Meyer, L. D., and DeJong, J. F., 1977, Runoff, erosion, and nutrient movement from interrill areas. Transactions of the American Society of Agricultural Engineers, 20, 58-61.

Morris, S. E. and Moses, T. A., 1987, Forest fire and the natural soil erosion regime in the Colorado Front Range. Annals of the Association of American Geographers,77(2), 245-254.

Mosley, M. P., 1974, Experimental study of rill erosion. Transactions of the American Society of Agricultural Engineers, 17(5), 909-916.

Moss, A. J. and Green, Patricia, 1983, Movement of solids in air and water by raindrop impact. Effects of drop-size and water-depth variations. Australian Journal of Soil Research, 21, 257-269.

Potyondy, J. P. and Hardy, T., 1994, Use of pebble counts to evaluate fine sediment increase in stream channels. Water Resources Bulletin, 30(3), 509-520.

Prosser, I. P. and Williams, Lisa, 1998, The effect of wildfire on runoff and erosion in native Eucalyptus forest. Hydrological Processes, 12(2):251-265.

Rowe, P. B., Countryman, C. M., and Storey, H. C., 1949, Probable Peak Discharges and Erosion Rates From Southern California Watersheds as Influenced by Fire. U. S. Dept. of Agricuture Forest Service, California Forest and Range Experiment Station, Unpublished Report.

Rowe, P. B., Countryman, C. M., and Storey, H. C., 1954, Hydrologic analysis used to determine effects of fire on peak discharge and erosion rates in Southern California watersheds. U. S. Dept. of Agricuture Forest Service, California Forest and Range Experiment Station, Unpublished Report. 49 p.

Sartz, R. S., 1953, Soil erosion on a fire denuded area in the Douglas Fir region. Journal of Soil and Water Conservation, 8, 279-281.

Soler, M., Sala, M., and Gallart, F., 1994, Post fire evolution of runoff and erosion during an eighteen month period. in Sala, M. and Rubio, J. L., editors, Soil Erosion and Degradation as a Consequence of Forest Fires, Barcelona/Valencia. Logroño: Geoforma Ediciones, 149-161.

Soto, B., Basanta, R., Benito, E., Perez, R., and Diaz-Fierros, F., 1994, Runoff and erosoin from burnt soils in northwest Spain. in Sala, M. and Rubio, J. L., editors, Soil Erosion and Degradation as a Consequence of Forest Fires, Barcelona/Valencia. Logroño: Geoforma Ediciones, 91-98.

Swanson, F. J., 1981, Fires and Geomorphic Processes. in Mooney, H. A., Bonnicksen, T. M., Christensen, N. L., Lotan, J. E., and Reiners, W. A., editors, Proceedings, Fire and Ecosystem Processes, Honolulu, Hawaii, U. S. Dept. of Agriculture, Forest Service General Technical Report WO-26, 401-420.

White, W. D. and Wells, S. G., 1984, Geomorphic Effects of La Mesa Fire. in Foxx, T. S., compiler, La Mesa Fire Symposium, Los Alamos, New Mexico, Los Alamos, New Mexico: Los Alamos National Laboratory, 73-90.

Wells, C. G., Campbell, R. E., Debano, L. F., Lewis, C. E., Fredriksen, R. L., Franklin, E. C., Froelich, R. C., and Dunn, P. H., 1979, Effects of Fire on Soil: State-Of-Knowledge Review. US Dept. of Agriculture, Forest Service Report WO-7. 34 p.

Wells, W. G., II, 1986, The influence of fire on erosion rates in California chaparral. in Proceedings of the Chaparral Ecosystems Research Conference, Santa Barbara, California. California Water Resources Center, University of California, Davis, Report Number 62, 57-62.

Welter, S. P., 1995, Topographic influences on erosion and soil development in hollows of the Rampart Range, Colorado. Ph. D. Dissertation, Dept. of Geography, University of Colorado, Boulder, 263 p.

Young, R. A. and Onstad, C. A., 1976, Predicting particle size composition of eroded soil. Transactions of the American Society of Agricultural Engineers, 19, 1071-1075.

Young, R. A. and Wiersma, J. L., 1973, The role of rainfall impact in soil detachment and transport. Water Resources Research, 9(6), 1629-1636.

THE INFLUENCE OF SEDIMENT SUPPLY ON RATES OF BEDLOAD TRANSPORT: A CASE STUDY OF THREE STREAMS ON THE SAN JUAN NATIONAL FOREST

Sandra E. Ryan, Research Hydrologist, USDA Forest Service, Forestry Sciences Laboratory, Laramie, WY.

Abstract: This paper compares and contrasts differences in the rate and size of bedload moved over a range of flows in 3 streams on the San Juan National Forest that have different modes and supplies of sediment. The East Fork of the San Juan (EFSJ) drains an area with unstable volcanic bedrock and active mass wasting. The bed material is primarily loosely bound sand, gravel, and small cobbles that are readily mobilized, producing high rates of bedload transport; the estimate of the mean rate of bedload transport per basin area at the 1.5-year return interval flow is 0.029 kg s^{-1} km^{-2}. The grain size distribution of bedload observed at high flows approaches that of the bed, suggesting transport at EFSJ approximates an "equal mobility" mode. Silver Creek, a tributary to EFSJ, likewise has an abundant source of sediment from active avalanche chutes and debris slides that deliver material directly to the channel. This material is readily entrained, producing high rates of transport as it moves through the system Consequently, transport rates were much lower on the recessional limb of the seasonal hydrograph due to diminishing sediment supply; mean rate of transport per basin area on the rising limb was approximately 0.031 kg s^{-1} km^{-2} and 0.002 kg s^{-1} km^{-2} on the falling limb, about an order of magnitude difference. Irregular transport rates in this channel reflect the episodic nature of the sediment supply. By contrast, observed rates of sediment transport at Florida River above Lemon Reservoir were very low, which is indicative of the stability of the landscape and lack of sediment supplied from upstream. The mean rate of transport per unit basin area measured at the 1.5-year return interval flow was 0.0003 kg s^{-1} km^{-2}. Sediment most likely originated from more mobile patches located between larger boulders and cobbles and does not reflect widespread entrainment over the channel surface. The presence of larger particles in the samples at increasingly greater discharge suggests that sediment is more selectively entrained.
Key Words: Gravel-bed channels, transport processes, sediment supply, Elwha bedload sampler.

INTRODUCTION

Observed rates of bedload transport in steep mountain channels are influenced by a number of factors, including the amount of sediment available for transport. When sediment supply is abundant, the relative rates of bedload transport are greater than when sediment is limited. There may also be differences in the mode of transport, with streams having substantial supplies of sand and gravel being more equally mobile: that is, the majority of grain sizes are entrained at approximately the same flow and in proportion to that found in the channel bed (e.g. Parker and Klingeman, 1982). Channels with low supplies of sediment tend to exhibit selective transport, with sand and small gravel moving at low flow and more coarse grains transported with increasing discharge (e.g. Lisle, 1995). The morphology and grain size distribution of the channel also reflects, in part, the size and amount of sediment supplied to the system (Buffington and Montgomery, 1999). Streams with significant sediment supplies are typically finer grained, have pool-riffle or, possibly, plane-bed morphology, and transport material over a considerable portion of the channel surface. By contrast, channels with restricted sediment supplies are coarser, may exhibit stepped morphology or particle clusters, and have widespread inactive zones where rates of transport are minimal (Dietrich, et al.,1989). Observed relationships are sensitive to differences in the underlying lithology of the basin because modes of sediment supply are linked to the stability of the landscape.

OBJECTIVE

The objective of this paper is to compare and contrast rates of bedload transport in 3 streams on the San Juan National Forest with substantially different supplies of sediment and channel morphology. Sediment supply is linked, in a general way, to differences in the timing and rate of materials supplied from mass wasting and fluvial processes.

SITE DESCRIPTION

The ***East Fork of the San Juan River*** (EFSJ) near Pagosa Springs, Colorado, drains a 166 km^2 basin underlain by unstable volcanic bedrock formations, consisting primarily of Tertiary-aged andesitic lavas, breccias, tuffs, and

conglomerates (Steven, et al., 1974). The wetted width of the channel at the $Q_{1.5}$ year flow is 17.2 m, mean depth is 0.53 m, mean velocity is 1.73 m s^{-1}, and water surface slope is 0.008 m/m. The study reach is plane bed in nature, with no clear pool-riffle pattern. The reach immediately upstream, however, is braided, providing an abundant source of sediment. The bed material is primarily gravel and small cobbles (D_{50} is 32 mm) and is relatively well-sorted for a gravel bed channel; the bed is fairly loose and easily overturned, reflecting low embeddedness. ***Silver Creek***, a tributary to EFSJ, drains a 15.7 km^2 southwest facing basin. The area is likewise underlain by unstable volcanic bedrock, with secondary exposures of sandstone, shale, and conglomerate of Tertiary and Cretaceous age (Steven, et al., 1974). The wetted width at the $Q_{1.5}$ year flow is 4.2 m, mean depth is 0.30 m, mean velocity is 1.03 m s^{-1}, and water surface slope is 0.045 m/m. The channel bed consists of low-rise steps composed of large cobbles and pools with sand and gravel substrate (D_{50} is 23 mm); many steps are formed of large woody debris. The area upstream of the cross-section is confined by steep, unstable bedrock walls with active chutes that deliver a substantial amount of sediment directly to the channel. Materials are delivered episodically with the release of avalanches and debris falls during winter and spring and more consistently as ravel during summer months. The ***Florida River*** above Lemon Reservoir near Durango, Colorado drains a 115 km^2 basin underlain primarily by Precambrian-aged granitic bedrock. The sediment supply to the Florida site is considerably less than that observed at the East Fork and Silver Creek sites, owing to the stability of the underlying lithology. The channel' s wetted width at the cross-section during the $Q_{1.5}$ year flow is 16.4 m, mean depth is 0.77 m, mean velocity is 1.34 m s^{-1}, and water surface slope is 0.013 m/m. The channel surface has broadly spaced step-pool topography composed of large cobbles and boulders with some patches of sand and gravel; D_{50} is 88 mm. The channel becomes constrained by bedrock about 100 meters above the sampling site, though the valley bottom at the study site is wider and more unconfined.

Sustained high flows from melting snow occur between mid-May to early-July at all 3 sites. Additionally, the Arizona monsoon can produce secondary high flows associated with intense rainfall in August and September. The annual peak discharge occurred in late summer or early fall in a few years of record, though the duration of these events was short-lived. Large floods caused by rain-on-snow are infrequent because of the separation between the timing of the monsoon relative to that of snowmelt runoff.

METHODS

Rates of flow and bedload transport were measured during snowmelt runoff in May-June, 1999. Bedload was collected using a hand-held version of an Elwha sampler, developed by Hydrologists at the USGS Volcano Observatory in Washington, USA. The sampler is a scaled-down version of the Toutle River sampler (Childers, 2000) and both the Toutle River and Elwha samplers are intended to sample bedload in streams with very high rates of transport. The opening (4 x 8") is larger than a traditional Helley-Smith sampler (Helley and Smith, 1971) and so it is capable of trapping larger grains, should they be in motion. The Elwha sampler has a 1.40 expansion ratio and a large catch bag (approximately 3.5 ft^3) with 0.5 mm mesh size. Data on bedload were collected at discharges up to about the 1.5-year return interval flow ($Q_{1.5}$). Rates of sediment transport were computed from the total weight of inorganic material collected at about 10-20 equidistant positions on the cross-section. Streamflow was estimated for each bedload sample using the mean discharge during the sampling period determined from a stage-discharge relationship developed for the site. Mean velocity was measured with Price AA or pygmy current meters. Discharge was calculated from the average velocity, interval width, and total depth measurements for channel subsections, using standard methods (Buchanan and Somers, 1965). Bedload samples were dried and sieved using standard sedimentological methods (Folk, 1968). One-half phi interval sieves, ranging from 0.50 to 64 mm, were used to separate sediment into grain size classes. The grain size distribution of the channel surface was determined from pebble counts using about 100 grains in the vicinity of the sampling site.

RESULTS

Discharge observations: The East Fork of the San Juan has been gauged by the US Geological Survey since 1957 and so there are more than 40 years of record for flow frequency calculations. The gage (09339900) is located approximately 100 m downstream of our bedload sampling site and there was good correspondence between the USGS gauged flows and flows measured by our crews using current meters. The 1.5-year return interval flow is 15.7 m^3 s^{-1}, based on Log Pearson III analysis (Benson, 1968). The highest discharge at which bedload was sampled was

13.8 $m^3 s^{-1}$ or 88% of the $Q_{1.5}$ flow. At Silver Creek an *Aquarod* (Sequoia Scientific) was installed in May 1999 to measure stage at 15 minute intervals over the duration of the flow season. Because there is no long-term flow record for this site, $Q_{1.5}$ was estimated using field parameters. The best estimate of $Q_{1.5}$ was 1.3 $m^3 s^{-1}$, based on flows measured at field identified bankfull (assuming bankfull as the surrogate for the 1.5-year flow). Moreover, Silver Creek is about 9% of the basin area above the gage on the East Fork San Juan and so should contribute about 9% of the 1.5-year flow at the gage on the main stem; 9% of $Q_{1.5}$ at EFSJ is 1.4 $m^3 s^{-1}$, which is slightly larger than the field estimate of 1.3 $m^3 s^{-1}$, but indicates that the estimate is reasonable. The highest flow at which bedload was measured on Silver Creek was 1.39 $m^3 s^{-1}$, which is 107% of the $Q_{1.5}$ estimate. The State of Colorado maintains a gage on the Florida River with 28 years of record from which flow frequency estimates were determined. This gage is located approximately 3 km downstream of the sampling site, above Lemon Reservoir; $Q_{1.5}$ at the gage is 17.0 $m^3 s^{-1}$. A regression analysis using flow measured at the sampling site during bedload collection and the flow record at the gage indicated that the correspondence between the 2 records was strong ($R^2 = 0.99$). The $Q_{1.5}$ estimate for the study site was 14.5 $m^3 s^{-1}$, based on the regression relationship between our measurements and flows observed at the state gage. Bedload was sampled at flows up to 15.3 $m^3 s^{-1}$ which is 106% of $Q_{1.5}$.

Rates of total transport in 1999: Rates of flow and total transport were normalized by dividing values by the basin area so that comparisons between basins of different sizes could be made. All plots depict the period between May 8 and June 26, the period of high runoff from snowmelt in 1999. The EFSJ site (Figure 1) has very high rates of transport that are at least an order of magnitude greater than that observed for other gravel bed channels on Forests in the Rocky Mountain Region (typically between 0.001-0.002 kg s^{-1} km^{-2} at $Q_{1.5}$) (USDA Forest Service, unpublished data). The estimate of the mean rate of bedload transport per basin area at the 1.5-year flow for the EFSJ site was 0.029 kg s^{-1} km^{-2}. Likewise, Silver Creek has very high, though irregular, rates of bedload transport on the rising limb of the seasonal hydrograph, due largely to an abundant supply of sediment and debris from upslope (Figure 2). This loosely bound material is readily entrained, resulting in high transport rates (0.02 to 0.05 kg s^{-1} km^{-2}) as it is "flushed" from the system. Transport rates at comparable discharges on the recessional limb of the hydrograph were about an order of magnitude lower (0.002 kg s^{-1} km^{-2}), reflecting a diminishing sediment supply. By contrast, transport rates measured at the Florida site are among the lowest observed in the Rocky Mountain Region (USDA Forest Service, unpublished data), which is likely due to a very low supply of sediment from bedrock reaches upstream. The mean rate of transport per unit basin area observed at $Q_{1.5}$ was 0.0003 kg s^{-1} km^{-2} (Figure 3).

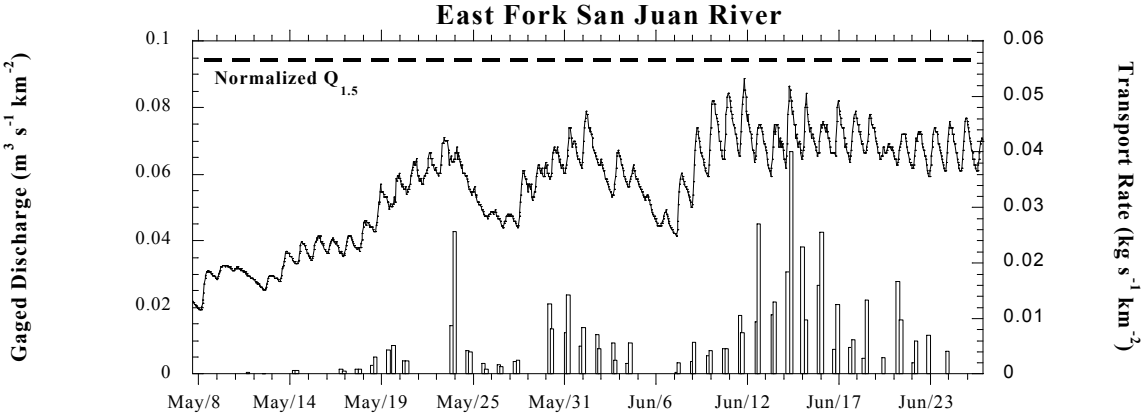

Figure 1. Flow (solid line) and bedload transport (bars) observed at East Fork San Juan River near Pagosa Springs, Colorado between May 8 and June 26, 1999. Dashed line indicates relative discharge at the 1.5-year return interval flow.

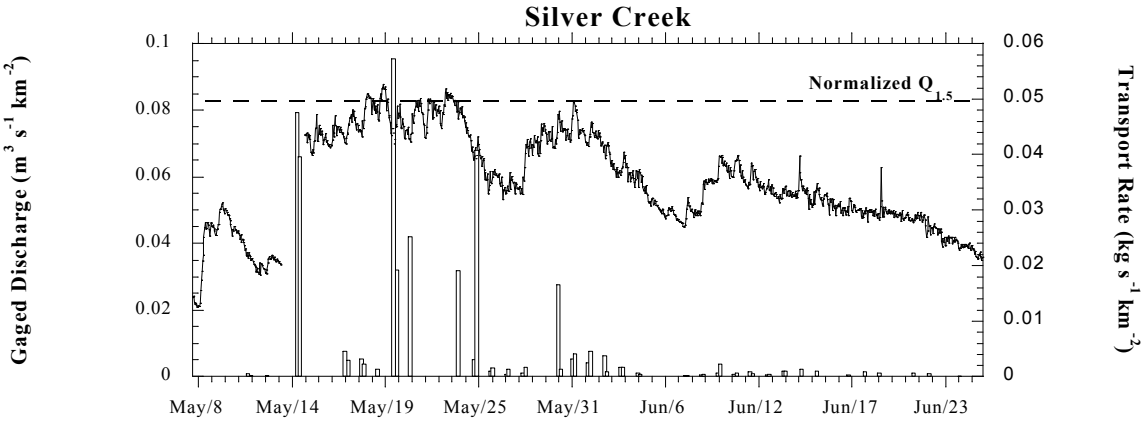

Figure 2. Flow (solid line) and bedload transport (bars) observed at Silver Creek near Pagosa Springs, Colorado between May 8 and June 26, 1999. Dashed line indicates relative discharge at the 1.5-year return interval flow. Missing flow record reflects a period when the gage was affected by a small debris jam that produced error in stage readings.

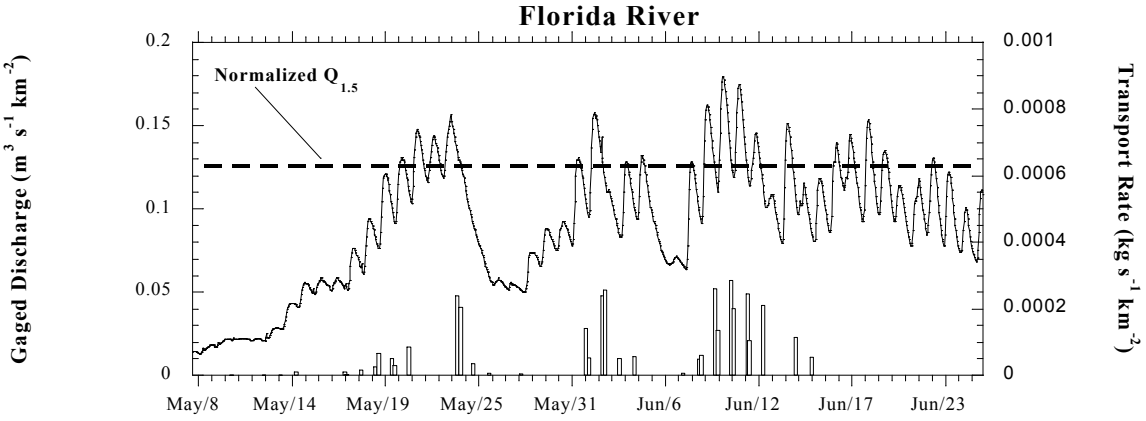

Figure 3. Flow (solid line) and bedload transport (bars) observed at Florida River above Lemon Reservoir near Durango, Colorado between May 8 and June 26, 1999. Dashed line indicates relative discharge at the 1.5-year return interval flow. Note that there is a substantial difference in scale for the rate of transport on this plot compared to Figures 1 and 2.

Fractional rates of transport: Fractional transport rates are shown on a series of log-linear plots so that the data may be more easily discerned; values of zero were removed for plotting purposes. Samples collected at the EFSJ site consisted primarily of sand and gravel less than 16 mm over a wide range of flows (Figure 4a). Grains larger then 32 mm (D_{50} of the channel surface) were trapped beginning at about 50% of $Q_{1.5}$ and grains larger than 64 mm (D_{77} of the channel surface) were trapped consistently beginning at 66% of the bankfull discharge. Though no bedload measurements were taken at $Q_{1.5}$, it is likely that the bedload further coarsens and the grain size distribution approaches that of the bed at flows near bankfull. Hence, patterns of sediment transport on EFSJ suggest near "equal mobility" (e.g. Parker and Klingeman, 1982) at flows approaching bankfull because nearly all grain sizes on the bed are represented in the bedload.

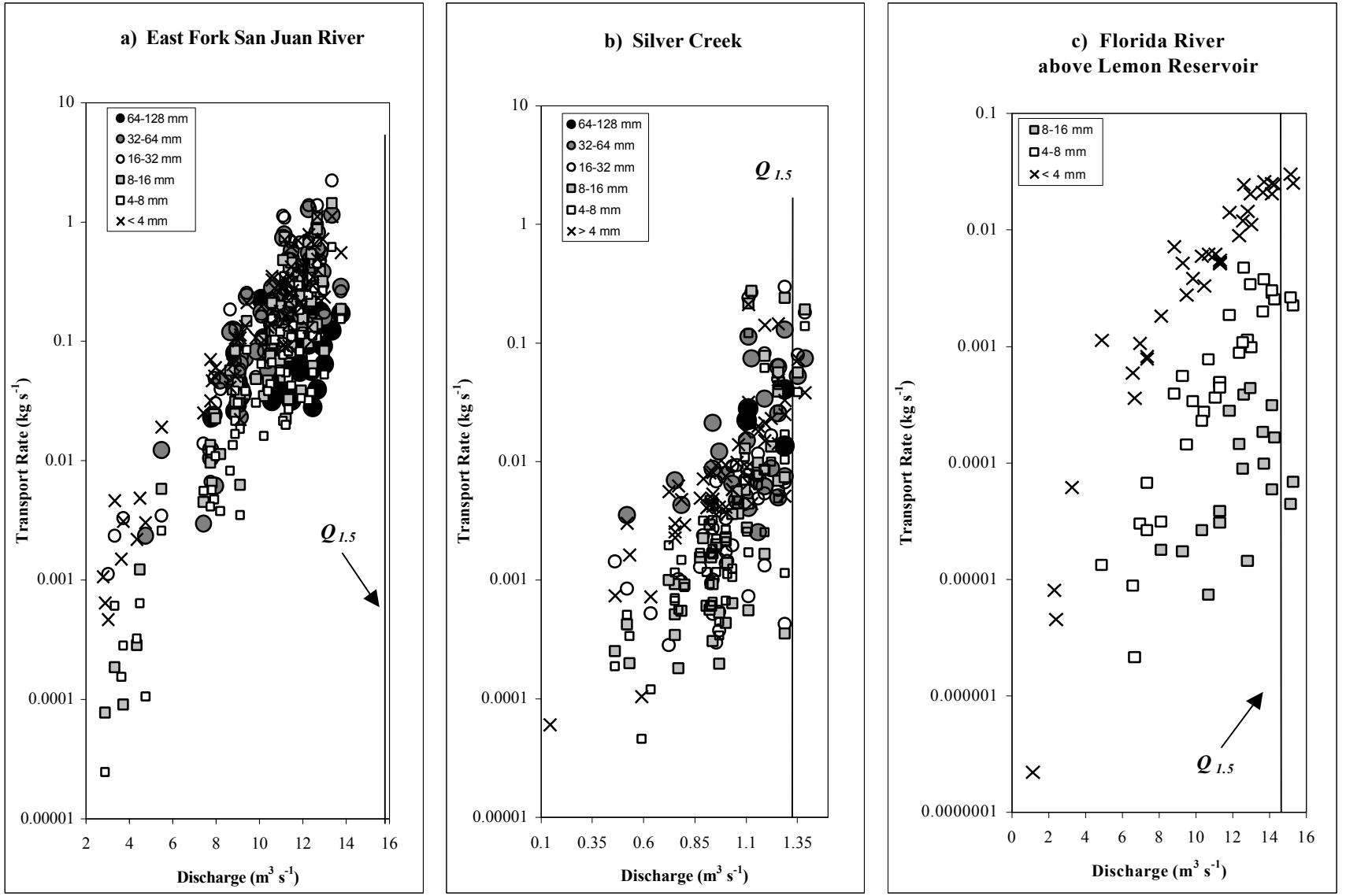

Figure 4. Fractional transport rates measured at a) East Fork San Juan River, b) Silver Creek, and c) Florida River, all sites on the San Juan National Forest.

Similar to the results from EFSJ, samples from Silver Creek consisted primarily of sand and gravel over a range of flows (Figure 4b). Gravel larger than 32 mm (D_{61} of the channel surface) was trapped beginning at about 77% of the $Q_{1.5}$ discharge; only 4 samples contained cobbles larger than 64 mm (D_{83} of the channel surface). Most noticeably, the relative proportion of coarse gravel (> 32 mm) varied considerably in samples collected at high flows. For instance, the 8 large samples from the rising limb of the hydrograph consisted primarily of 4–32 mm gravel (65% $\pm$ sd 14%), most of which was trapped at one or two positions in the cross-section; only 15% ($\pm$ sd 6%) of the sample was larger than 32 mm, on average. By contrast, samples from the recessional limb, though smaller, frequently contained a higher percentage of coarse gravel: an average of 33% of the sample (range between 5 and 80%) was larger than 32 mm. Some samples contained a large amount of sand while others were cleaner; proportionally, between 1 and 75% of the high flow samples (> 1.0 $m^3 s^{-1}$) contained grains < 4 mm. Samples collected at lower flows (< 1 $m^3 s^{-1}$) consisted primarily of sand and pea gravel, though more than half contained 16 –32 mm sized pebbles. In short, there was no well-defined relationship between the composition of the samples and flows at which they were captured. Transport patterns on Silver Creek appear to be strongly controlled by large and varied sediment sources supplied from upslope. The channel becomes a highly effective conduit for moving the sediment supplied from the hillslope once flows are about 75% of the bankfull discharge.

Patterns of fractional transport rates at Florida River were quite different than described for the other sites. Here, sand and pea gravel were the predominant grain sizes and typically 90% or more of the sample was < 4 mm (Figure 4c). Medium gravel (8-16 mm) was trapped beginning at about 10 $m^3 s^{-1}$ (70% of $Q_{1.5}$) though the rates remained quite low. Low transport rates consisting primarily of sand are indicative of a system with low sediment supply. Additionally, no sample contained grain sizes larger than 16 mm which is likely due to the absence of this size gravel from the channel surface. In all likelihood, the bedload originated from finer-grained, relatively well-sorted patches of sediment contained between larger boulders and cobbles. The presence of larger particles in the samples at increasingly greater discharges suggests that even the more mobile patches of sediment are moved by selective entrainment. Given the predominance of large cobbles and boulders, the Florida River site is unlikely to exhibit widespread entrainment over a majority of the channel surface.

DISCUSSION AND CONCLUSIONS

Rates and sizes of sediment transported in gravel bed streams reflect many factors, including the characteristics of materials supplied from hillslope and channel sources. This paper describes differences and similarities in patterns and grain sizes moved in 3 channels on the San Juan National Forest. The sites have distinctive modes of sediment supply that are linked, in a general way, to the stability of the landscape. Observed rates of transport were relatively high in streams draining a basin underlain by readily eroded volcanic bedrock (East Fork basin). The unstable hillslopes directly impinge on steep tributary channels that become effective conduits for transporting materials from active debris chutes and ravel (Silver Creek). Transport rates are, at times, high, though irregular in this system (0.002 - 0.031 kg s^{-1} km^{-2} at $Q_{1.5}$), reflecting the episodic nature of the sediment supply. Materials moved by the tributaries are deposited downstream in a wide valley bottom with a braided to plane-bed channel (EFSJ) that also has very high, though comparatively more regular, rates of transport (about 0.029 kg s^{-1} km^{-2} at bankfull). The grain size distribution of the bedload approaches that of the bed at near bankfull discharges, reflecting further the relaxation of supply limitations.

By contrast, observed rates of sediment transport are quite low (0.0003 kg s^{-1} km^{-2}) in the Florida River basin which is underlain by stable granitic bedrock, signifying a relatively low supply of sediment. The primary source of material in this system is from the channel beds and banks, as there are few external sources, such as active landslides, upstream. Sand and fine gravel, originating from finer-grained patches interspersed between large particles, are transported over a largely stable boulder and cobble bed; widespread entrainment is unlikely to occur over a majority of the channel surface. As a result, the particle size distribution of the bedload is considerably finer than that of the bed over a wide range of discharges. Coarser grains are entrained at increasingly greater flows indicating that sediment is selectively entrained which is likely due the limitations on the supply of sediment in this stable landscape.

REFERENCES

Benson, M.A. 1968. Uniform flood-frequency estimating methods for federal agencies. Water Resources Research 4(5):891-908.

Buchanan, T.J. and Somers, W.P. 1965. Discharge measurements at gaging stations. USGS Techniques of Water Resources Investigations, Book 3, Chapter A8. 65 p.

Buffington, J.M. and Montgomery, D.R. 1999. Effects of sediment supply on surface textures of gravel-bed rivers. Water Resources Research 35(11):3523-3530.

Childers, D. 2000. Field comparisons of six pressure-difference bedload samplers in high-energy flow. USGS Water Resources Investigations Report 92-4068. 59 p.

Dietrich, W.E., Kirchner, J.W., Ikeda, H., and Iseya, F. 1989. Sediment supply and the development of the coarse surface layer in gravel-bedded rivers. Nature 340:215-217.

Folk, R.L. 1968. Petrology of Sedimentary Rocks. Hemphill, Austin, TX. 170 p.

Helley, E.J. and Smith, W. 1971. Development and calibration of a pressure difference bedload sampler. USGS Water Resources Division Open-file report, 18 pp.

Lisle, T.E. 1995. Particle size variations between bed load and bed material in natural gravel bed channels. Water Resources Research 31(4):1107-1118.

Parker, G. and Klingeman, P.C. 1982. On why gravel bed streams are paved. Water Resources Research 18:1409-1423.

Sequoia Scientific' s*Aquarod* website: http://www.sequoiasci.com/aquarod.html

Steven, T.A., Lipman, P.W., Hail, W.J., Jr., Barker, F. and Luedke, R.G. 1974. Geologic map of the Durango quadrangle, southwestern Colorado. USGS Miscellaneous Investigations Map I-629 (compiled on the USGS Geologic Map of Colorado by O. Tweto, 1979).

The use of trade or firm names in this publication is for reader information and does not imply endorsement by the U.S. Department of Agriculture for any product or service.

Author contact point – 222 S. 22nd St., Laramie, WY 82070. Phone: (307) 745-2005 Fax: (307) 745-2397 e-mail: sryanburkett@fs.fed.us

BEDFORM MAPPING IN THE SACRAMENTO RIVER

Randal L. Dinehart, Research Hydrologist, U.S.Geological Survey, Sacramento, California

rldine@usgs.gov

Abstract Detailed bedform mapping in reaches of large rivers has become practical with the wide availability of differential Global Positioning System receivers and digital sonar. The spatial variations in bedload transport throughout a surveyed reach can be effectively assessed with bedform mapping at a lower cost than bedload sampling. Bedform transport is calculable from bedform maps that are produced on a routine basis. Bedform mapping also shows changes in bedform regime related to bedload movement at high discharges. During 1998 through 2000, a reach of the Sacramento River was repeatedly mapped for bedform configuration. Field and computational methods were refined for efficient measurement of bedform height and celerity to apply the bedform-transport equation. For two-dimensional dunes at low velocities, the bedform-transport method yielded reasonable estimates of bedload transport. Bedform-transport rates through the reach were correlated with time-averaged stream velocity at a nearby gaging station. The relation was significant and consistent for lower discharges, but the bedform-transport method is believed to neglect a measurable fraction of bedload sediment at higher discharges. The variations in bedform configuration at the study reach correspond to discharge-related episodes of sand transport in the lower Sacramento River.

INTRODUCTION

Sand bedload is transported in the lower Sacramento River as dune bedforms. To evaluate sediment transport in the lower Sacramento River, bedform regimes have been mapped by the U.S. Geological Survey for various flow conditions. Rates of bedform transport can be calculated from the change in bedform position over a few days. To support flow modeling and studies of river sedimentation, detailed mapping of bed configuration also can provide useful diagnostic data. The primary obstacle to bedform mapping is the belief that hardware costs are prohibitive and the technology is complex. However, inexpensive differential Global Positioning System (GPS) receivers, sonar hardware, and commercial software can be used with relative ease for bedform mapping, as described in this paper.

Except during high discharges, sand in the lower Sacramento River usually is transported very near the bed, and depth-integrating samplers will not collect sand closer than 0.1 meter (m) from the bed. Therefore, sand transported as bedload during most of the year must be quantified by methods other than depth-integrated sampling. The usual approach is to determine bedload-transport rates using a bedload sampler (Helley and Smith, 1971) in a scheme that derives a distribution from multiple sampling points across the stream (Emmett, 1980; Hubbell and others, 1987; Gomez and Troutman, 1997). However, deep, dune-covered channels are difficult to sample for bedload because the transport rate varies widely at a point and across the channel during the period of measurement.

For the present study, one beneficial use of bedform mapping in the Sacramento River has been to compute bedload transport by applying a one-dimensional bedform-transport equation (Simons and others, 1965). Transport rates calculated from bedform migration have long been recognized as reasonable and defensible, but the bedform-transport method has been used far less than bedload sampling. Bedform transport is measured by surveying bedforms repeatedly along a gridded reach and computing transport for the intervening periods. For a deep, sand-bedded river with substantial bedload transported in bedforms, the bedform-transport method has been found, with this study, to yield reasonable transport estimates without the high costs of bedload sampling.

The bedform transport quantity Q_{bf} (volume transport/unit time/unit width) for triangular bedforms is approximated as

$$Q_{bf} = cH/2\ (1-\lambda_p) \qquad (1)$$

where c is bedform celerity, H is bedform crest height, and λ_p is the porosity of the bedform sediment, from (volume of voids)/(volume of total sample) (Simons and others, 1965). For well-sorted sand, the porosity value ranges from 0.3 to 0.4. To obtain a weight rate, the bulk density of bedform sand replaces $(1-\lambda_p)$. To measure bedform transport, the crest height H of bedforms is obtained from surveyed bedform profiles. Bedform celerity c is derived from two profiles measured at times separated by a period sufficient for a migration distance of low error relative to the positional accuracy.

EQUIPMENT

Data for the production of bedform maps were collected by combining GPS navigational positions and bed elevation from sonar. Sonar transducers and all surveying hardware were portable and mounted on an open aluminum boat (fig. 1). The sonar device for depth measurement was a Datasonics PSA-902, with a transducer frequency of 200 Kilohertz, a resolution of 0.01 m at a maximum range of 14 m, and a conical beam of 10^o. The differential GPS receiver (Trimble Pathfinder ProXR) has a second-by-second resolution of 0.70 m (detailed specifications available from Trimble Inc.).

Figure 1. A small boat fitted with framework to suspend multiple sonar transducers and acquire depths and differential GPS data simultaneously.

Corrections for compass bearing and boat pitch and roll were not necessary on the calm waters of the lower Sacramento River for reliable bedform profiles. The most common disturbances to surveying were occasional wakes from passing boats, which were edited from final data sets. A portable personal computer was used for GPS navigation and data acquisition. The GPS and sonar data were logged into a Microsoft Excel spreadsheet during surveys. The GPS navigation program, Fugawi Moving Map Software (Northport Systems), was selected to guide channel surveys because of the ability to import custom digital maps.

BEDFORM MAPPING

A reconnaissance survey along the lower Sacramento River located a straight reach below Garcia Bend (approximately 15 kilometers south of downtown Sacramento) with two-dimensional dunes having

continuous crests for over half the channel width. This location was chosen for the relative uniformity of bedforms and the minimal effect of bar-scale features on bedform migration. The river channel is 180 m wide between leveed banks, with nearly 30 m at each bank considered inactive for bedform transport. Bed material is medium sand (0.25-0.5 millimeters). For the study reach, a porosity of 30 percent for fine-to-medium sand (Larcombe and Ridd, 1995) applied to a solid density of 2,650 kilograms per cubic meter (kg/m^3) gives about 1,900 kg/m^3.

Longitudinal profiles of bedforms were surveyed along grid lines that were 0.5 km long. To guide surveys with the GPS navigation software, grid lines were added to scanned segments of topographic maps with an image-editing program. Distance between grid lines was determined by the two-dimensional scale of the bedforms to be measured. Preliminary surveys during 1998 with two transducers mounted 3 m apart on the survey boat showed that sand dunes were continuous across that distance. Using aluminum extension ladders for support, a lateral array of four transducers was deployed on the survey boat. The four lines of bed elevation measured in a single direction is called a track. The bedform dimensions were adequately resolved by the array spacing, with 2-3 m between adjacent tracks (fig. 2a). Bedform maps, which were registered to state plane coordinates and local gaging-station datum, were derived by triangulating the adjacent survey profiles to a contoured surface (fig. 2b).

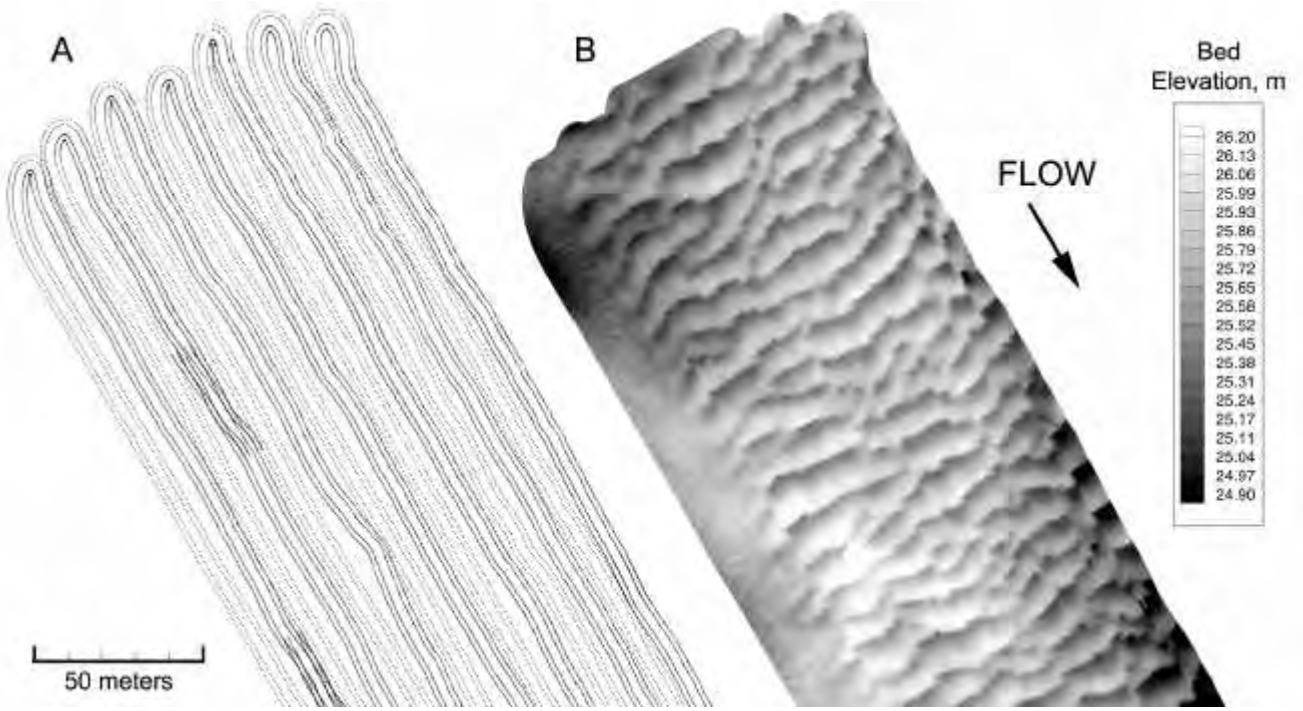

Figure 2. Survey tracks (A) and corresponding contour map (B) from longitudinal profiles of bedforms in Sacramento River, April 14, 2000. The range of bed elevation shown is 1.3 meters.

In the streamwise direction, at least two depth points per meter were acquired by motoring at 1 meter per second while sampling depth at 2 Hertz. The streamwise intervals assured that bedform fronts were well located because the horizontal distance from crest to trough on steep faces is of the same order as the specified resolution of 0.7 m for GPS positions. The GPS data acquired by the portable PC include the latitude, longitude, and time. Within the Excel spreadsheet, a running average for five horizontal positions was applied to smooth irregularities induced by the changing accuracy of differential corrections. Positions

for times of known depths were then interpolated using smoothed positions. The interpolated decimal locations were subsequently converted to state plane coordinates, in meters.

Orientation of the transducer array in the horizontal plane was determined from the trajectory of the GPS antenna. The trajectory, in radians, was applied at the smoothed GPS location to determine the perpendicular line of the transducer array. Sequential positions of transducers mounted away from the GPS antenna were determined by reference to the boat trajectory for the preceding and subsequent interpolated positions. The distance from the antenna to a transducer was taken as the hypotenuse of a right triangle with the sides equal to the x and y distances from the logged GPS position. A positive distance from the GPS antenna gave the starboard transducer positions and a negative distance gave the port positions, in state plane coordinates in meters.

BEDFORM-TRANSPORT CALCULATION

Bedform height and celerity are required for a volumetric calculation of bedform-transport rate. In the bedform-transport equation, the mean bedform height h often has been derived from the crest-to-trough distance H, divided by two, on the assumption that the bedform shape is triangular. With digital profile data, the area under dune surfaces in the bedform profile can be found directly by numerical integration if the data points are spaced regularly. Inevitably, the original survey data will not be spaced regularly. Survey tracks deviate from grid lines and are subject to changes in velocity while traversing the reach. However, when the surface-contour maps were created with Tecplot (Amtec Engineering, Inc.), profile grids could be extracted at regular intervals along straight lines superimposed near the original survey tracks. Then, lines connecting the sequential minima at troughs can be calculated to provide a base elevation to subtract from the bed elevation during the integration. The integrated area, divided by the corresponding profile length, yields a mean height h for the bedform-transport equation.

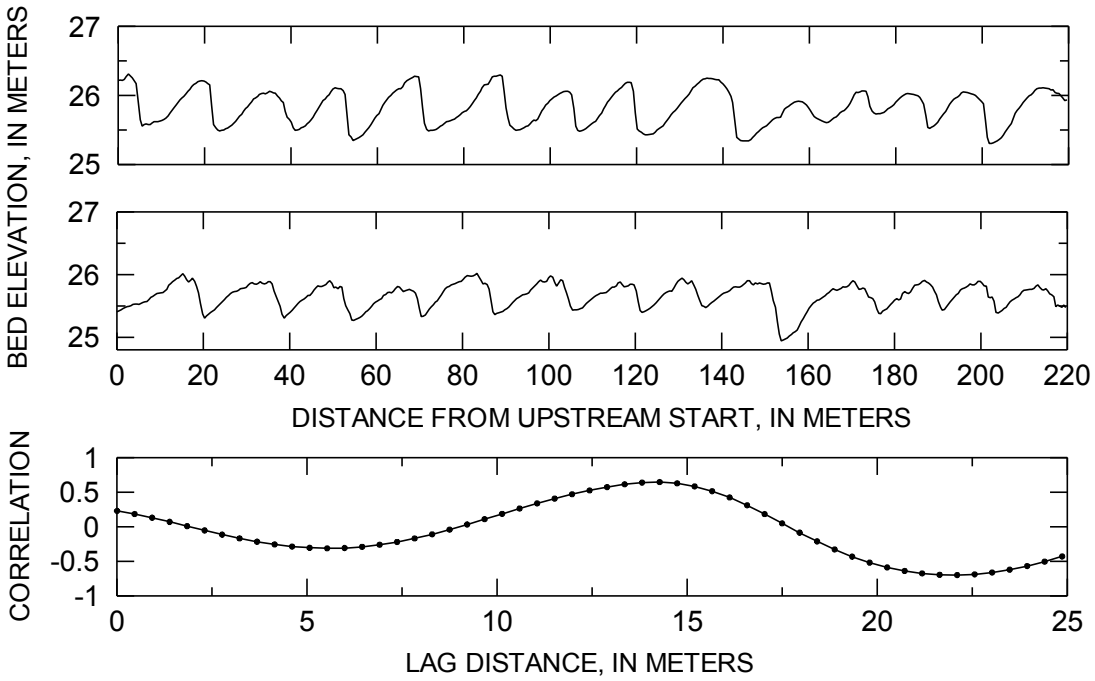

Figure 3. A cross correlation of two successive bedform profiles at a central grid line, January 18 and 25, 2000. For the 7-day period, the lag distance of 14.3 meters is produced by a bedform celerity of 2.04 meters per day.

For bedform celerity, profiles are measured at the same line of two surveys where the intervening period is short enough that unique sequences of bedforms have not lost significant correlation. At celerities around 1 meter per day, this period could be as long as a week. For a transport rating, the intervening period preferably will have flow conditions that are stationary or change slowly. The resampled profiles are cross-correlated to obtain an overall lag, in meters. Two successive bedform profiles and their cross-correlation function are shown in figure 3. The corresponding bedform celerity is obtained by dividing the lag distance at peak correlation by the time between surveys.

Lines for cross correlation were chosen perpendicular to the bedform fronts by inspection of the bedform maps. Cross-sectional bedform-transport rates were obtained by calculating celerity and mean height at 4-6 equally spaced profiles. The greatest celerities were measured in areas of small dunes or along the high-velocity core of the channel.

TRANSPORT RELATION WITH STREAM VELOCITY

To explore a method to reduce the frequency of bedform surveys, the applicability of a transport relation with stream velocity was investigated. In this study, all field efforts were directed at developing bedform-mapping techniques, so that no measurements of flow conditions were made at the study site. Because bedload transport is a function of boundary shear stress to the 3/2 power, and shear stress is a function of mean velocity squared, bedload transport can be expressed as a cubic function of mean velocity (V^3).

Mean velocity and stage for the Sacramento River is measured continuously at USGS gaging stations located 15 km upstream (Sacramento) and 6.4 km downstream (Freeport) from Garcia Bend. An ultrasonic velocity meter is operated at Sacramento River at Freeport to provide stream discharge. The mean velocity recorded hourly at Freeport was cubed and then averaged for the interval between bedform surveys. Although the measured velocity includes tidal effects, the mean velocity for most intervals between bedform surveys was stationary or slowly changing.

Dates of survey	Average celerity, m/day	Average bedform height, m	Bedform transport rate, tonnes/day	Average stream velocity, $(m/s)^3$
July 31-August 4,1998	2.01	0.22	51.2	0.18
April 29-May 6, 1999	1.15	0.29	38.2	0.19
July 16-20, 1999	0.95	0.33	34.6	0.16
July 20-27, 1999	1.12	0.33	42.3	0.17
July 27-August 6, 1999	1.00	0.33	37.2	0.16
August 6-12, 1999	0.43	0.32	15.6	0.10
January 18-25, 2000	1.70	0.39	72.8	0.23
April 6-14, 2000	1.49	0.21	35.8	0.18

Table 1. Summary of data extracted from bedform surveys at Sacramento River at Garcia Bend, 1998-2000. Transport rates were calculated from 4 to 6 subdivided intervals of a 60-meter width.

The bedform-transport rates versus V^3 for eight periods during 1998-2000 are shown in figure 4 and listed in table 1. The rates are given for a constant active width of 60 m to avoid comparison of irregular features at the margins. Bedform-transport rates at Garcia Bend were measured over a range of V^3 from 0.10 to 0.23 $(m/s)^3$ (table 1).

BEDFORMS, BEDLOAD AND HIGH DISCHARGES

Transformations in bedform regimes indicate modes of bedload movement at high discharges. During most of the year, sand bedforms at the study site are two dimensional and move about 1 m/day with crest heights near 1 m. At lower discharges, measured bedform-transport rates ranged from 15.6 to 51.2 tonnes/day; mean bedform heights ranged from 0.2 to 0.4 m; and average bedform celerity ranged from 0.4 to 2 m/day (table 1). Bedform wavelengths, measured trough to trough, ranged from 12 to 17 m.

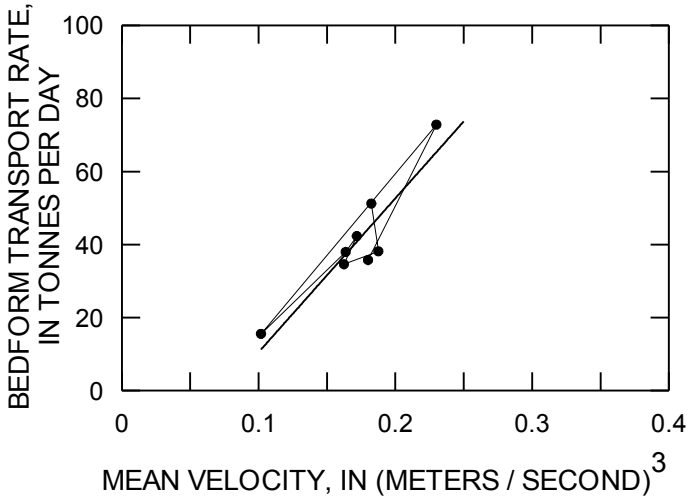

Figure 4. Bedform-transport rates and stream velocity for eight periods during 1998-2000.

During high discharge, much of the bedload sand is depleted from the reach, as indicated by the changes in bedform regime from January 18 to April 14, 2000 (fig. 5). Longer distances from trough to stoss, increased exposure at the trough level, and overall bed degradation all indicate depletion of bed material from the reach. The January surveys showed the lengthening and flattening of dunes and their superposition by smaller bedforms during sustained discharge increase. During high discharges in the Sacramento River in March 2000, V^3 was about 1.4 $(m/s)^3$ for a month, an order of magnitude greater than velocity at lower discharges. Bedform surveys during that period showed that mean bedform heights, at 0.3 m, were similar to those measured at lower discharges, but wavelengths averaged 6 m, being reduced from a range of 12 to 17 m.

Because the shortened, three-dimensional bedforms deformed rapidly at high discharges in March 2000, celerity was not measurable accurately from surveys made only 4 days apart. Visual overlays of the two surveys indicated an offset of 40-60 m for the two surveys. Using the existing data set of celerities and V^3, a bedform celerity of 12 m/day was extrapolated to correspond with the 1.4 $(m/s)^3$ value of V^3 for the period, which is consistent with the apparent offset. Using the measured bedform height of 0.3 m and an extrapolated celerity of 12 m/day yields a bedform-transport rate of 410 tonnes/day. For comparison, a linear extension of the bedform-transport rating to 1.4 $(m/s)^3$ indicates a rate greater than 550 tonnes/day. This disparity between rates extrapolated by various methods should be expected. Although bedforms migrate more rapidly at higher discharges, increased celerity is not accompanied by increased bedform volume, causing the bedform-transport rates to deviate from bedload-transport rates at higher discharges. Following several weeks of maximum stream discharge, mean bedform height was diminished from 0.3 m to less than 0.1 m in late March 2000, and the featureless reach remained eroded to the approximate level of previous bedform troughs. As flow receded in April 2000, bedform surveys indicated the reappearance of dune bedforms with smaller heights and wavelengths than those measured at similar discharge in January 2000.

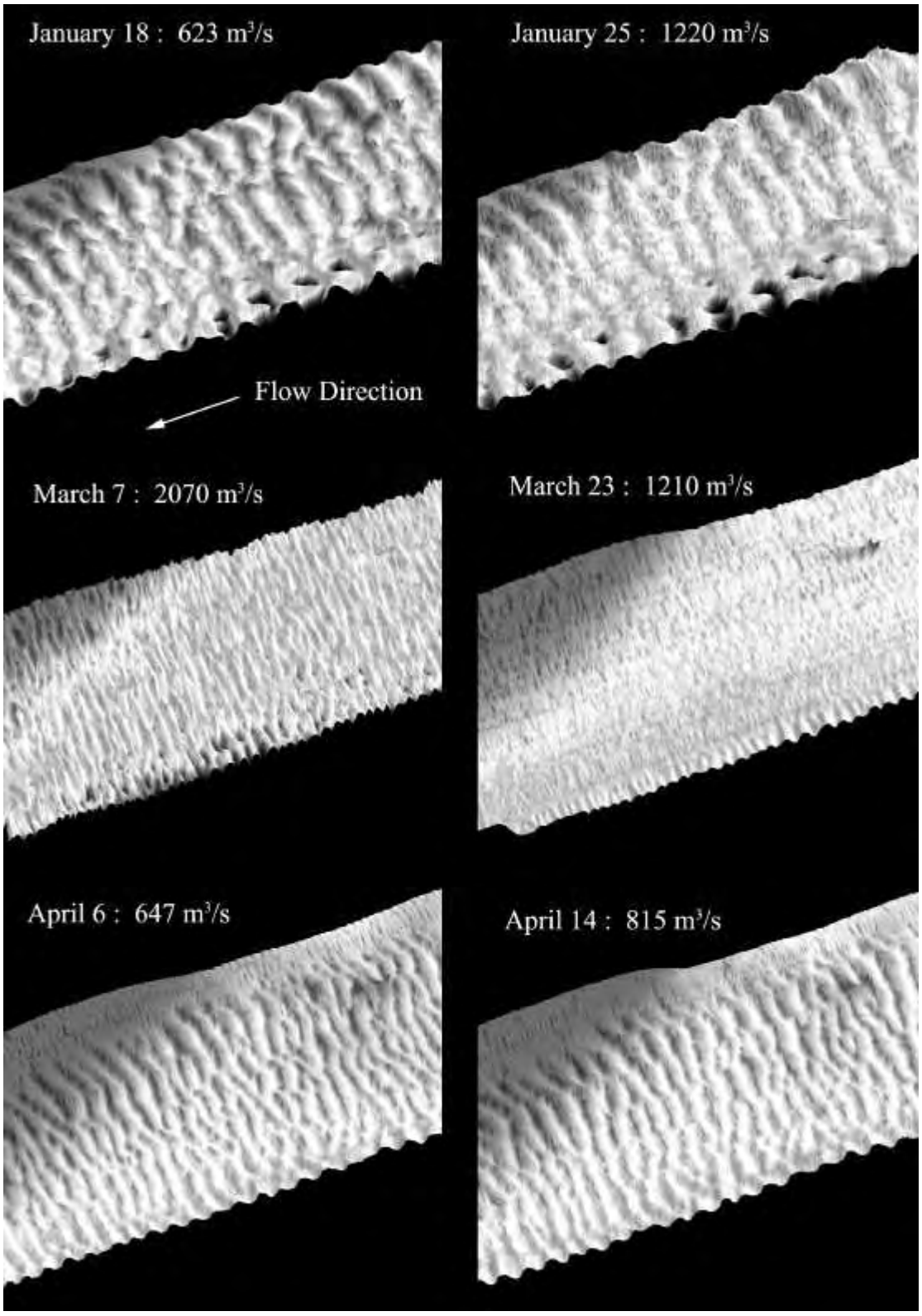

Figure 5. Bedform regime from January 18 to April 14, 2000, at gridded reach. Distance shown is 200 meters; survey width is about 100 meters. Stream discharge during survey is given in cubic meters per second (m^3/s).

Suspended-sediment samples have been collected and analyzed by the USGS for the Sacramento River at Freeport since the late 1970s. Using the sand divisions of samples, one finds that the discharge of suspended sand can range from 1,000 to 10,000 tonnes/day during the same periods that bedform-transport rates consistently exceed 500 tonnes/day. Therefore, bedload discharge during high discharges may equal from 5 to 50 percent of the suspended-sand discharge and, thus, require accounting as a significant component of sediment transport. Total sand discharge would be measurable by more frequent bedform surveys at high flow and increased suspended-sediment sampling. A well-known technique is to extrapolate the total sand discharge from bed-material samples, suspended-sediment samples, and hydraulic conditions (e.g., Colby and Hembree, 1956). Bedform mapping is valuable for such computations because the bed regime at higher discharges is not a single-valued function of hydraulic conditions, as seen in figure 5. Bedload sampling could verify the order of magnitude of bedform-transport estimates. However, the real benefit of bedform mapping is that the spatial variations in bedload transport throughout the surveyed reach are more effectively assessed than with bedload sampling.

SUMMARY

During 1998 through 2000, bedform configuration was repeatedly mapped in a reach of the Sacramento River. Methods have been refined for efficient measurement of bedform height and celerity to apply the bedform-transport equation. Bedform-transport rates were correlated with time-averaged stream velocity at a nearby gaging station. The relation was significant and consistent during lower discharges, but the likely departure between bedform- and bedload-transport rates at higher discharges requires additional sampling methods. For a deep, sand-bedded river with substantial bedload transported as bedforms, the bedform-transport method has yielded reasonable transport estimates without the high costs of bedload sampling. The variations in bedform configuration at the study reach correspond to discharge-related episodes of sand transport in the lower Sacramento River.

REFERENCES

Colby, B.R., and Hembree, C.H., 1955, Computations of total sediment discharge, Niobrara River near Cody, Nebraska. U.S. Geological Survey Water-Supply Paper 1357, 187 p.

Emmett, W.W., 1980, A field calibration of the sediment-trapping characteristics of the Helley-Smith bedload sampler. U.S. Geological Survey Professional Paper 1139, 44 p.

Gomez, B., and Troutman, B.M., 1997, Evaluation of process errors in bed load sampling using a dune model. Water Resources Research, 33, pp. 2387-2398.

Helley, E.J., and Smith, Winchell, 1971, Development and calibration of a pressure-difference bedload sampler. U.S. Geological Survey Open-File Report, 18 p.

Hubbell, D.W., Stevens, H.H., Skinner, J.V., and Beverage, J.P., 1987, Laboratory data on coarse-sediment transport for bedload-sampler calibrations. U.S. Geological Survey Water-Supply Paper 2299, 31 pp.

Larcombe, P. and Ridd, P.V., 1995, Megaripple dynamics and sediment transport in a mesotidal mangrove creek: Implications for palaeoflow reconstructions. Sedimentology, 42, pp. 593-606.

Simons, D.B., Richardson, E.V., and Nordin, C.F. Jr., 1965, Bedload equation for ripples and dunes. U.S. Geological Survey Professional Paper 462H, 9 pp.

RADIO-TRACKING OF COBBLES IN A MOUNTAIN STREAM IN SOUTHWEST IDAHO

James P. McNamara[1], Boise State University, Boise, Idaho; J. Carter Borden[2], Boise State University, Boise, Idaho; James Fitzgerald[3], Environmental Protection Agency, Boise, Idaho

1. Department of Geosciences, Boise State University, Boise, Idaho. Phone: (208) 426-1354, Email: jmcnamar@boisestate.edu

2. Department of Geosciences, Boise State University, Boise, Idaho. Phone: (208) 426-2220, Email: cborden@trex.boisestate.edu

3. Currently at United States Forest Service, Shasta Trinity Forest, Hayfork, California, 96041. Phone: (530) 628-5227, Email: JamesK@fs.fed.us

INTRODUCTION

Einstein (1950) suggested that the motion of individual particles in bedload is a stochastic process that occurs in a series of motion and rest periods. There have been few studies to verify this concept in field conditions. Chacho et al. (1989) and Ergenzinger et al. (1989) simultaneously and independently performed the first field studies to investigate individual particle movement using radio-tracking techniques. Subsequent papers by both groups provided valuable information on the behavior of individual bedload particles. (Ergenzinger and Schmidt, 1990; Schmidt and Ergenzinger, 1992; Chacho et al., 1994; Chacho et al., 1996). These studies reported similarities in some factors such as transport velocities and step lengths, but large discrepancies in other factors such as length of rest periods. A general conclusion shared by both groups is a confirmation of Einstein's ideas that particle behavior is largely a stochastic process. Both groups urged continued field investigations to further characterize the stochastic nature of particle movement in streams.

The purpose of this project is to determine the feasibility of using radio-tracking techniques to investigate bedload dynamics in Reynolds Creek, a coarse-gravel, cobble bed stream in the Owyhee Mountains of Southwest Idaho. We placed five rocks equipped with motion sensing transmitters in the stream and monitored their behavior through the snowmelt period in 1999. Here, we report on the motion characteristics, incipient motion (critical flow rate required to induce motion), and particle hysteresis (higher rate of bedload transport on one limb of a hydrograph than for the same flows on the other limb). Many observations presented here can not be generalized because of the small sample size and data quality issues associated with learning the techniques. However, these observations serve as examples of potential applications of radio-tracking in studies of fluvial sediment transport.

STUDY AREA

The Northwest Watershed Research Center (NWRC) is a research facility of the USDA Agricultural Research Service that maintains the Reynolds Creek Experimental Watershed (RCEW) in the Owyhee Mountains, Southwest Idaho as a field laboratory for the development and assessment land management practices on western rangelands. The watershed hosts scientists conducting experiments on hydrology, meteorology, engineering, soil physics, and range science. The watershed has complete geologic, vegetation, and soil surveys and 30 years of climate, streamflow, snow budgeting, soil moisture, groundwater recharge, water quality, and temperature monitoring data. Though extensive research has been conducted in many scientific disciplines within RCEW, bedload transport has received little attention. In 1974 and 1975, Johnson conducted studies evaluating the performance of the Helley-Smith sampler, and on bedload transport rates in Reynolds Creek (Johnson and Hanson, 1976; Johnson et al., 1977). Johnson (1977) concluded that *20*% of the sediment leaving the basin was in the form of bedload. Nearly all of the bedload movement occurs during the snowmelt period when streamflows are highest for the year. The study reach begins approximately two hundred meters above a weir, called the Tollgate Weir, which drains 5448 ha. The stream is approximately 10 m wide, has a slope of 0.026, and d_{50} surface grain size of 87 mm.

METHODS

Field Methods:

Five cobbles (Table 1) were implanted with Telonics IMP/210/L transmitters of dimensions 8.1x2.3 cm by boring the rock with a diamond bit and a drill press then placed in the study reach at the beginning of the snowmelt period. This timing had two benefits. First, the snowmelt period is the time when the stream is most likely to have the competence to move bedload. Second, the daily fluctuations in streamflow provide a predictable set of "storms". The rocks were painted bright yellow and placed randomly with 100 additional painted tracer rocks in a cross-section at the beginning of a relatively straight reach. Each transmitter sends a pulse on a unique frequency at one preset pulse rate if the rock is at rest, and another pulse rate if the rock is in motion. The transmissions are picked up by a receiver located on the right bank about half way between the location of emplacement and the Tollgate Weir. The receiver station consists of a Telonics omni-directional RA-6B antenna, a TR-2 programmable receiver, a TS-1 scanner, and a Campbell Scientific CR10X datalogger. The datalogger triggers the scanner to switch frequencies on the receiver every 5 seconds. With 5 motion sensing transmitters and one beacon transmitter it takes 30 seconds to cycle through the transmitters. When a rock moves, the pulse rate switches from the resting pulse rate to the motion pulse rate and remains at the motion pulse rate for 30 seconds. The receiver sends the pulse rate information in an audio signal to the signal processor, which then sends a current proportional to the audio signal to the CR10X. Current passes through a 100 OHM resistor and is converted to a voltage, which is sampled twice in a 5 second period by the datalogger. Because the signal processor does not send frequency information to the datalogger, it is necessary to have a beacon transmitter with a clearly identifiable pulse rate sampled along with the transmitters, and that the order that the transmitters are sampled be known so that the transmitters can be identified in the output file. Every 30 seconds the datalogger stores 12 voltage measurements for the 6 transmitters that reveal if each rock moved in that 30 second period. A Campbell SM716 storage module filled and had to be exchanged every 7 days. A 12 volt deep cycle battery that is maintained by a 10 amp solar panel powers the system. The radio-rocks were located occasionally to measure the distance of transport by tracking them with a portable directional antenna, receiver, and signal strength meter. Four cross-sections were surveyed between the starting location and the weir to obtain reach-averaged cross-section geometry for hydraulic calculations. The NWRC provided discharge data at the Tollgate Weir.

Table 1. Properties of radio-rocks.

Rock	858	863	867	903	947
a axis (mm)	144	142	120	144	116
b axis (mm)	88	76	92	88	88
c axis (mm)	84	62	64	68	64
Post-drill Density g/cm^3	2.34	2.29	2.51	2.55	2.7

Analysis Methods:

Motion Characteristics and Hysteresis: The motion characteristics of the tagged rocks were analyzed by counting the number of 30-second motion and rest periods on rising and falling limbs and comparing the counts to the durations of rising and falling stages. Particle hysteresis over the duration of the study was evaluated by determining the probability of motion for each particle on rising and falling limbs. Particle hysteresis during individual streamflow events was evaluated by determining the discharges at the initiation and cessation of motion for two rocks that moved the farthest during the period of study. If the rock moved sporadically through the entire event and into the next without clear breaks in motion, the event was not evaluated. We defined hysteresis as occurring when a 5% difference in discharge between initiation and cessation of motion occurred. Positive hysteresis exists when discharge of motion is lower than discharge of cessation.

Incipient Motion: The shear stress required to initiate motion of each radio-tagged rock was evaluated using Shield's equation

$$t_c = q_c(d_s - d)d \qquad (1)$$

where τ_c is the critical shear stress required to move a particle of diameter d, d is the specific weight of the particle, d is the specific weight of water, and q_c is the dimensionless critical Shield's parameter. The difficulty in applying this technique to estimate shear stress of incipient motion is to obtain an appropriate value for q_c. A common approach is to assume that q_c = 0.06. However, reported values have ranged from 0.03 to 0.086 (Buffington and Montgomery, 1997). The radio-tracking techniques presented here allow observation of incipient motion and calculation of q_c.

The times of initial motion for each storm and each rock were noted, and critical discharges at those times, Q_{ci}, were obtained from the hydrograph at the Tollgate Weir where the subscript *i* denotes the storm event. Discharges were converted to shear stresses first by obtaining the hydraulic radius through Manning's equation

$$Q_{ci} = (1.49/n)\, R_i^{2/3} S^{1/2} A_i \qquad (2)$$

where n is Manning's Roughness coefficient, S is the water surface slope, and A_i and R_i are the channel cross-section area in feet-squared and the hydraulic radius in feet for event i.

Manning's Roughness was obtained using Jarrett's equation (Jarrett, 1984)

$$n = 0.39 S^{0.38} R_i^{-0.16} \qquad (3)$$

where R is the hydraulic radius in feet. Substitution of Equation 3 into Equation 2 yields

$$Q_{ci} = 3.82 R_i^{0.83} S^{0.12} A_i \qquad (4)$$

Equation 4 was solved by iteration for R_i in a given cross-section by assuming a stage, calculating A_i and R_i from the cross-section, calculating a discharge, Q_{ci}, and comparing Q_{ci} to the actual Q_{ci}.

The shear stress at Q_{ci} was then calculated by

$$t_{ci} = dR_i\, S$$

Equation 1 was then solved for the critical Shields parameter for each event.

RESULTS

Four of the rocks moved between 6 and 55 meters in motion periods associated with nearly every daily peak (Figure 1). Rock 863 only moved a few meters in the first couple days of the experiment then never moved again, and is excluded from these analyses. The upper rows in Table 2 contain the number of motion periods, no-data periods, and rest periods for the four active rocks. For example, rock 947 was in motion during 8025 30-second periods on rising limbs and 7150 periods on falling limbs for a total of 15175 periods.

The second set of rows contains the distribution of motion, no-data, and rest periods. For example, for rock 947, 53% of motion periods occurred on rising limbs and 47% of motion periods occurred on falling limbs. Forty-one percent of no-data periods occurred on rising limbs and 59% of no-data periods occurred on falling limbs. Twenty-eight percent of rest periods occurred on rising limbs and 72% of rest periods occurred on falling limbs. Thirty-two percent of all periods occurred on rising limbs and 68% of all periods occurred on falling limbs. This is equivalent to saying that 32% of the time the stream is in a rising limb of a hydrograph.

The third set of rows describes the duration of each motion property. Rock 947 was in motion during 20% of all periods on rising limbs, 8% of all periods on falling limbs, and 12% of all periods. It was at rest during 74% of all periods on rising limbs, 88% of all periods on falling limbs, and 84% of all periods. These percentages are also probabilities. For any period on a rising limb there is a 0.2 probability that rock 947 was in motion, and a 0.08 probability that it was in motion during any falling limb period.

The fourth set of rows contain the joint probabilities of each combination of rising or falling limb and motion property. For example, each 30-second period has a 0.32 probability of occurring on a rising limb and then a 0.2 probability that the rock was in motion during that period. The joint probability that the stream was rising and that the rock was in motion is therefore 0.32 * 0.20 = 0.06.

The average step lengths for the entire period of study were calculated by dividing the number of motion periods into the total distance of movement. A better approach that will be used in future is to calculate step lengths for each storm.

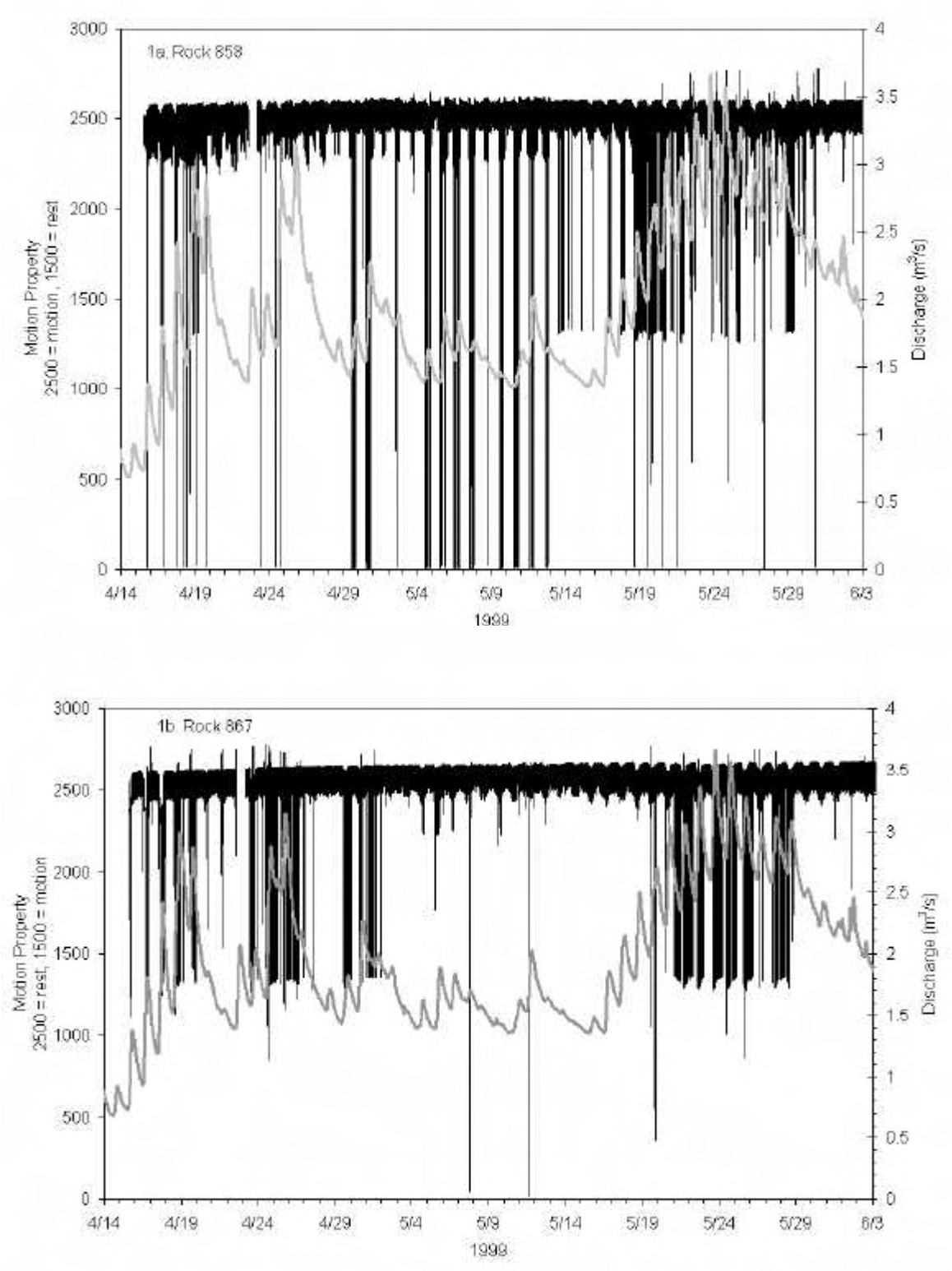

Figure 1. Motion properties of rock a) 858, and b) 868. The magnitude of the left axis is related to the pulse rate of the transmitter where approximately 2500 indicates no motion and approximately 1500 indicates motion.

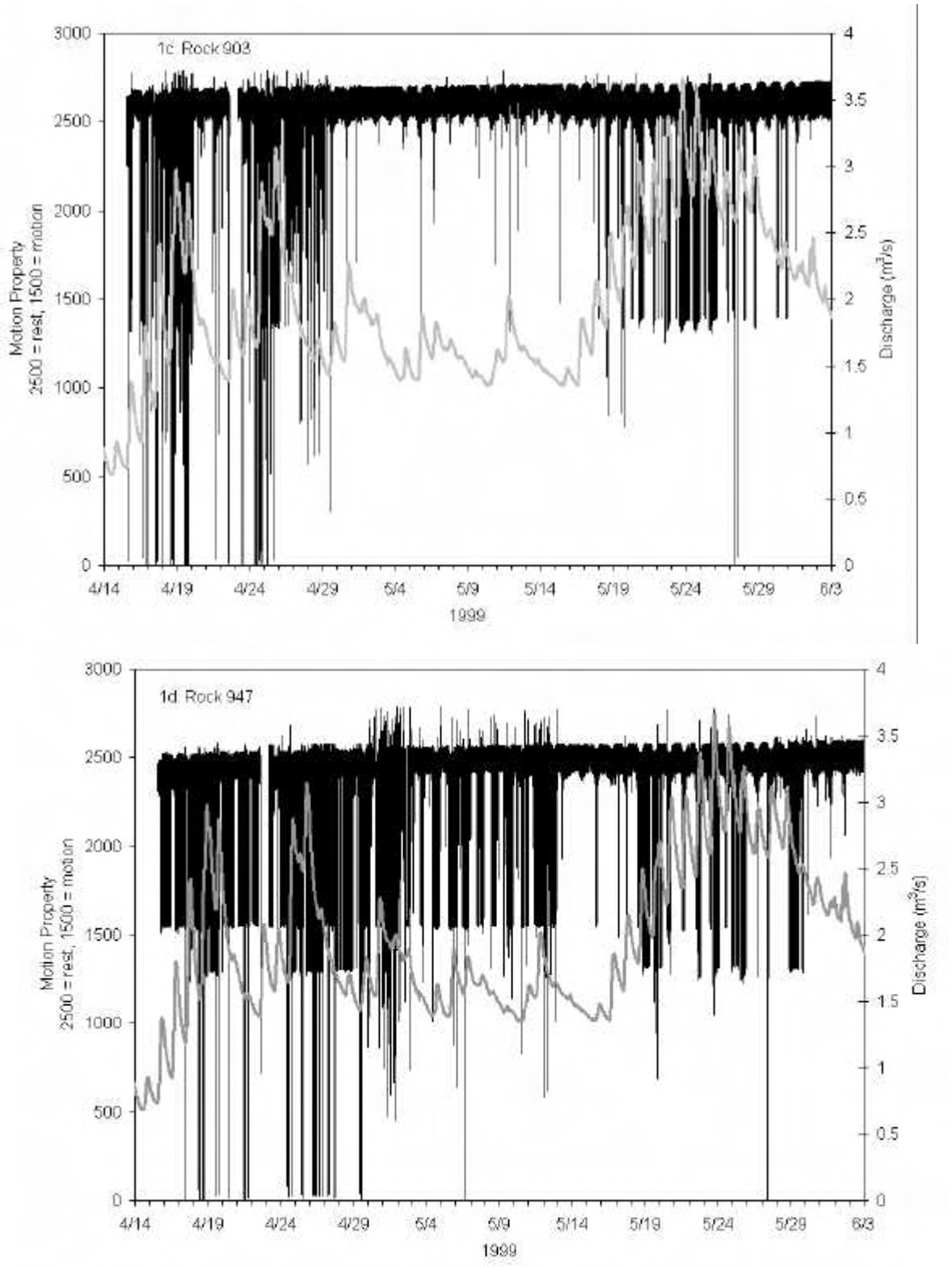

Figure 1 (continued). Motion properties of rock c) 903, and d) 947. The magnitude of the left axis is related to the pulse rate of the transmitter where approximately 2500 indicates no motion and approximately 1500 indicates motion.

Table 2. Motion characteristics of radio-rocks.

		Rock 858			Rock 867			Rock 903			Rock 947		
		Rising Limbs	Falling Limbs	Total	Rising Limbs	Falling Limbs	Total	Rising Limbs	Falling Limbs	Total	Rising Limbs	Falling Limbs	Total
Data	Motion Periods	478	536	1014	2929	2688	5617	611	660	1271	8025	7150	15175
	No Data Periods	2160	3840	6020	1086	1533	2717	2268	4250	6518	2144	3033	5177
	Rest Periods	36774	82006	117780	17097	52661	69925	35502	81648	117150	29601	74737	104338
	total	39432	86382	124814	21122	56864	93259	38381	86558	124939	39770	84920	124690
Distribution of Events	Motion Periods	0.47	0.53	1.00	0.52	0.48	1.00	0.48	0.52	1.00	0.53	0.47	1.00
	No Data Periods	0.36	0.64	1.00	0.40	0.56	1.00	0.35	0.65	1.00	0.41	0.59	1.00
	Rest Periods	0.30	0.70	1.00	0.20	0.62	1.00	0.30	0.70	1.00	0.28	0.72	1.00
	total	0.31	0.69	1.00	0.23	0.61	1.00	0.31	0.69	1.00	0.32	0.68	1.00
Duration of Occurence	Motion Periods	0.01	0.01	0.01	0.14	0.05	0.06	0.02	0.01	0.01	0.20	0.08	0.12
	No Data Periods	0.06	0.04	0.05	0.05	0.03	0.03	0.06	0.05	0.05	0.05	0.04	0.04
	Rest Periods	0.93	0.95	0.94	0.81	0.93	0.91	0.92	0.94	0.94	0.74	0.88	0.84
	total	1.00	1.00	1.00	1.00	1.00	1.00	1.00	1.00	1.00	1.00	1.00	1.00
Joint Probability	Motion Periods	0.00	0.00	0.01	0.03	0.03	0.06	0.00	0.01	0.01	0.06	0.06	0.12
	No Data Periods	0.02	0.03	0.05	0.01	0.02	0.03	0.02	0.03	0.05	0.02	0.02	0.04
	Rest Periods	0.29	0.66	0.94	0.18	0.56	0.91	0.28	0.65	0.94	0.24	0.60	0.84
	Total	0.31	0.69	1.00	0.23	0.61	1.00	0.31	0.69	1.00	0.32	0.68	1.00

The average discharge at the time of initial motion for rocks 867, 903, and 947 are 1.65, 2.23, and 1.73 m^3/s (Table 3). These flows were exceeded 59, 31 and 51 percent of the time between days 106 and 149. The rocks were in motion only 6, 1, and 12 percent of that same time period. The critical Shields parameter for each rock is 0.057, 0.068, and 0.061 with an average of 0.062.

Rock 867 exhibited positive hysteresis during at least 6 events and negative hysteresis during 2 events. Rock 947 exhibited positive hysteresis during 6 events and negative hysteresis during 1 event. Hysteresis was not detectable during all other events.

Table 3. Travel distances and critical hydraulics.

	Rock 858	Rock 867	Rock 903	Rock 947
Distance Traveled (m)	6.85	50.5	21.52	55.1
Average Step Length (mm)	12.78	18.84	32.61	7.71
Average Critical Discharge (m^3/s)	xx	1.69	2.23	1.73
Average Critical Shear Stress (N/m^2)	xx	84.69	96.17	86.34
Average Critical Shield's Parameter	xx	0.057	0.067	0.061
Duration of Q>Qc (%)	xx	59	31	51

DISCUSSION AND CONCLUSIONS

The motion periods are nearly evenly distributed between rising and falling limbs for all rocks. However, the time that the creek spent in rising limbs was much less than it spent in falling limbs. Rock 947 was in motion 20% of all time on rising limbs, 8% of all time on falling limbs, and 12% of the total time. This is equivalent to saying that if the stream was rising there is a 20% chance that the rock was in motion, while if the was falling there is an 8% chance that it was in motion. The rock is therefore more likely to move during rising flows than during falling flows. The distributions of hourly discharges for rising and falling limbs are nearly identical to each other. We can therefore say that any given flow rate is more likely to move the rock if it occurs on a rising limb than if it occurs on a falling limb. Hence, there is hysteresis of motion for rock 947. This is also true for rock 867, which along with rock 947 are the two rocks that moved the farthest. This is not true for rocks 858 and 903, which are the two rocks with shorter travel distances. Hysteresis in 2 of 4 samples is not enough to conclusively say that individual particles experience hysteresis. However, it does demonstrate that radio-tracking can be used to study the relationships between individual particle motion and bedload hysteresis. The critical flow rates for motion of each rock occurred much more frequently than the rocks actually moved. This is likely due to the intermittent nature of movement once a rock is entrained, and possibly to hysteresis with a higher likelihood of motion on rising limbs than falling limbs.

There are three primary issues concerning data quality. First, the number no-data periods is disturbing. We assume that this arises from radio interference that alters the frequency of the signal transmitted so that the receiver does not pick up the pulse rate. Second, although each transmitter pulses at a precise rate depending on if it is in motion or not, that pulse rate is somewhat modified by receiver and digital signal processor so that the output that the datalogger records is not exactly what the transmitters send. It is therefore somewhat subjective at times determining if a pulse rate is the motion or rest rate. Most of the time, however, the differences were clear. Third, we are uncertain what magnitude of motion is required to trigger the motion sensor. It may be that rocks simply jiggle in place. Future studies will include careful observation of the rocks while in the stream.

REFERENCES

Buffington, J. M. and D. R. Montgomery (1997). A systematic analysis of eight decades of incipient motion studies, with spatial reference to gravel-bedded rivers. Water Recourses Research 33(8): 1993-2029.

Chacho, E. F., R. L. Burrows and W. W. Emmett (1989). Detection of coarse sediment movement using radio transmitters. XXIII Congress of the International Association for Hydraulic Research, The National Research Council of Canada.

Chacho, E. F., Jr., R. L. Burrows and W. W. Emmett (1994). Monitoring gravel movement using radio transmitters. Hydraulic Engineering '94, Proceedings of the 1994 ASCE National Conference on Hydraulic Engineering., Buffalo, New York.

Chacho, E. F. J., R. L. Burrows and W. W. Emmett (1996). Motion characteristics of coarse sediment in a gravel bed river. Sixth Federal Interagency Sedimentation Conference, Las Vegas, Nevada.

Ergenzinger, P. and K. Schmidt, -H. (1990). Stochastic elements of bedload transport in a step-pool mountain river. IAHS Publication(194): 39-46.

Ergenzinger, P., K. H. Schmidt and R. Busskamp (1989). the pebble transmitter system (PETS): first results of a technique for studying coarse material erosion, transport and deposition. Zeitschrift fur Geomorphologie 4(33): 503-508.

Jarrett (1984). Hydraulics of high-gradient streams. Journal of the Hydraulics Division, Am. Soc. Civil. Engr. 110(11): 1519-1539.

Johnson, C. W., R. L. Engleman, J. P. Smith and C. L. Hanson (1977). Helley-Smith bed load samplers. Journal of the Hydraulics Division, Proceedings of the American Society of Civil Engineers 103(10): 1217-1221.

Johnson, C. W. and C. L. Hanson (1976). Sediment sources and yields from sage-brush rangeland watershed. Third Federal Inter-agency Sedimentation Conference, Denver, Colorado.

Schmidt, K. H. and P. Ergenzinger (1992). Bedload Entrainment, Travel Lengths, Step Lengths, Rest Periods-Studied with Passive (Iron, Magnetic) and Active (Radio) Tracer Techniques. Earth Surface Processes and Landforms. L. John Wiley & Sons. 17**:** 147-165.

SPECIFIC WEIGHT AND MEDIAN SIZE OF THE BED MATERIAL OF GRAVEL AND COBBLE BED RIVERS

Robert T. Milhous, Hydrologist, Midcontinent Ecological Science Center, U.S. Geological Survey, Fort Collins, Colorado

Address: 4512 McMurry Ave. Fort Collins, CO 80525-3400; phone: 970 226 9322; email: robert_milhous@usgs.gov.

INTRODUCTION

Two characteristics of the bed material of gravel and cobble bed rivers are considered herein. The first is the measurement of the specific weight (bulk unit weight) of the river substrate, and the second is a review of alternative ways of characterizing the median size (or grain size distribution curve) of the stream bed armour.

There are two reasons for this paper. The first is a need to understand each characteristic in order to characterize the relation between physical habitat for aquatic animals and the sediment of a gravel and cobble bed river. The second is that each characteristic may have an impact on the calculation of sediment transport in the river.

There are three components of the bed-material of gravel and cobble bed rivers: 1) the fines and sand on the surface, 2) the stream bed armour (surface layer), and 3) the substrate below the armour. In some rivers the first component (fines and sand) may be missing. For many sediment transport and physical habitat studies it is important to know the characteristics of the three components.

An example of the three bed components at one site along the Boulder River in Montana are presented in Figure 1. The fines and sand component is not a topic of this paper. The other two components are considered.

The characteristic related to the substrate is the weight per unit volume of the bed sediment (i.e. the specific weight) and the ratio of the volume of voids to the total volume (porosity). The reason for the interest in specific weight and porosity is that the nature of the biota using the substrate and the ability of the stream to move the stream bed may be related to these factors. Two examples of where the specific weight and porosity of the bed material can be important for environmental reason are 1) determining the quantity of metals stored in the stream bed, and 2) determining the void space available for aquatic animals. The technique for obtaining the specific weights is relatively simple and is derived from geotechnical techniques used in the control of embankment construction.

The characteristic related to the armour is the determination of the median size (d50) of the armour. The median size of the armour, as presented in Figure 1, is 152 mm. Other median sizes calculated from the same data are 62 mm and 27 mm. This difference is significant and important. The correct distribution to use in any riverine analysis depends on the type of analysis being made and the source of the empiricisms used in the analysis. For instance, size

distributions for Oak Creek (Western Oregon) were determined using a process similar to the procedure used to determine the curve presented in Figure 1 (d50 of 152 mm). The Oak Creek data have been compared with data from other streams where the d50 was determined using procedures similar to the analysis of the Boulder River that resulted in a d50 of 62 mm. This would not seem to be a good idea.

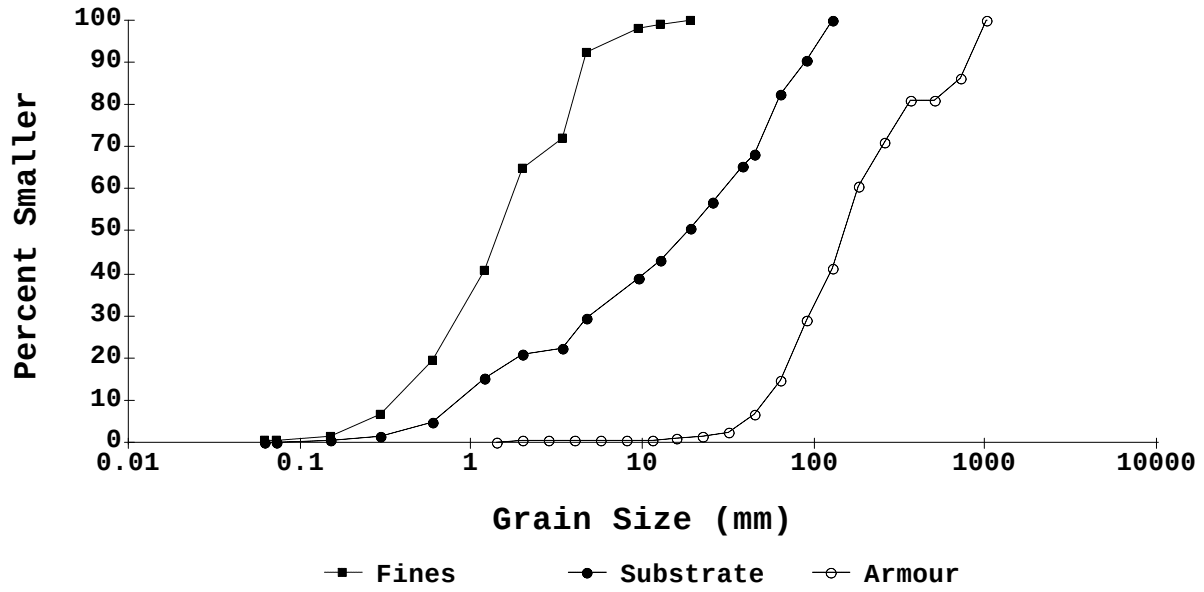

Figure 1. The three components of the bed of the Boulder River below Galena Gulch downstream of Basin, Montana.

SUBSTRATE SPECIFIC WEIGHT

The specific weights and porosity of the substrate at three locations along the Boulder River in Montana are presented in Table 1. The data in Table 1 are in downstream order.

The substrate specific unit weights have been measured in a number of other gravel and cobble of rivers. The range in specific weights measured is from 105 to 151 lbs/cubic foot and porosity from 0.04 to 0.41.

Table 1. The bulk unit weight and porosity of the substrate at three locations along the Boulder River in Montana. The specific gravity of the particles is 2.65.

Bulk Unit weight (lbs/ft^3)	Porosity	Median Size (mm)	%<2mm	Location
117	0.29	16.8	24.1	above Basin
109	0.34	18.3	20.8	below Basin
137	0.17	25.4	20.0	below Boulder

Estimates of the specific weight as a function of the median size were developed by the California Department of Water Resources, CA-DWR, (Vanoni, 1975). Komura (1963) developed an equation relating the specific weight and median size. The Komura relation is W = 125 - (7 * (d50^0.21)) where d50 is the median size of the substrate in feet and W the specific weight of the substrate in lbs/cubic foot. The two relations are shown on Figure 2 along with the three specific weights from the Boulder River given in Table 1 and data from five other rivers (some rivers have more than one sample location). At best, the California Department of Water Resources relation and Komura equation give an estimate of the median specific weight of a gravel substrate; in many situations that may be all that is needed.

In some cases the typical specific weight may not be adequate. One of these is where the interest is in the habitat for animals using the substrate and the second when there is interest in the movement of metals and water through the substrate and the storage of metals in the substrate. In such situations, the two relations shown in Figure 2 are not adequate and the specific weight should be measured. The reason the average specific weight is not adequate from a physical habitat viewpoint is because the species of aquatic animals found in the substrate is related to the size and quantity of the voids. The exchange rate between the surface water and pore water of the substrate is also related to the size of the voids.

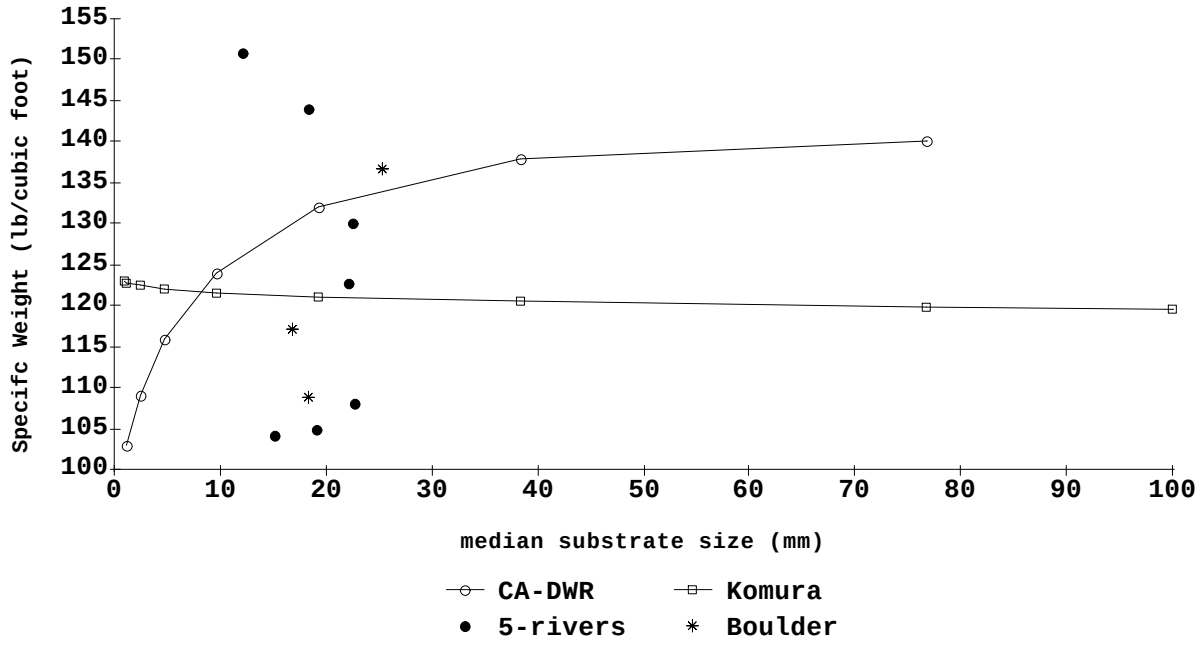

Figure 2. The relation between median substrate size and the specific weight of the bed material based on two approaches to calculating the specific weight from median size and measure results.

Two observations: 1) more data on the variation of the specific weight is needed for gravel and cobble rivers, and 2) the two relations shown on Figure 2 are not adequate to use in estimating the specify weight in any given river.

The technique used to make the specific weight measurements presented above for the Boulder River and for the other five rivers starts by constructing a frame of either wood or metal large enough to allow a hole to be dug in the substrate large enough for the required sample size. The required sample size is not well defined; in practice, the best results have been obtained when the sample size is been between 0.5 and 0.75 cubic feet. The steps to follow in obtaining a sample are:

Step 1: Position the frame in the area where the substrate density is to be measured.

2: Remove the armour from the stream bed where the substrate sample is to be obtained.

3: Set the frame on the stream bed where the armour has been removed. Make sure the edges are such that a plastic sheet will fit the frame well and can be expected to fit the same for both the without hole and with hole measurements.

4: Place a plastic sheet in the frame and fill the frame with water measuring either the weight or volume placed in the frame to where the water is just ready to flow out of the frame or to a place marked on the inside of the frame (will not get wet because of the plastic sheet is between the frame and the water). The total volume or weight placed in the frame is the critical factor. Make careful note of the volume or weight of the water placed in the frame. It is easy to lose track of either the volume or weight.

5: Remove the water from the frame being VERY careful not to disturb the frame.

6: Remove the substrate sample by digging within the frame and continuing to be very careful not to disturb the frame. Retain the material removed for analysis. The hole should be as smooth sided as possible.

7: Place the plastic back on the surface and fill to the hole and frame to the same level as the first volume measurement. The volume or weight of the water placed in the hole and frame must be determined during the process of filling.

8: Dry and measure the weight of the substrate material removed from the hole.

9: If the porosity is the be determined, measure the specific gravity of the substrate sample. It is recommended that the specific gravity not be assumed - it should be measured.

10. Sieve the sample and determine the size distribution curve.

The specific weight of the substrate is the ratio between the dry weight and the volume of the hole. The volume of the hole is the difference between the volume of water placed in the frame before sampling the volume placed in the frame after sampling. If weight of the water placed in frame was determined the volume of the water placed in the frame is calculated from the weight.

MEDIAN SIZE OF THE ARMOUR

At least two procedures are in general use to determine the grain size distribution of the armour of a gravel-bed river. These are 1) the Wolman procedure with size analysis by number; and 2) the area-by-weight procedure with removal of a sample of the armour and size analysis by weight. There are a number of variations of each procedure. The two procedures can result in significant differences in the median size.

Wolman (1954) presented a procedure where the size of the particles at points on a line are determined, the sizes are then ordered in descending order of size, and a particle size distribution curve calculated. The Wolman procedure gives no information on the size of bed material below the armour (the substrate in Figure 1) but may give some information on the fines on the surface. The sampling is sometimes made on a grid instead of a line (see Wohl et al, 1996, for three alternative 'Wolman' procedures).

In the area-by-weight procedure the armour sample is obtained by removing all of the particles in an area of the stream bed and analyzing the sample by weight where the order is by weight of the particles instead of number as used in the Wolman procedure. A third procedure is a variation of the area-by-weight approach where the particles are counted instead of weight. The armour curve in Figure 1 is equivalent to an area-by-weight particle size distribution curve.

An example of the difference in the particle size distribution of the armour obtained using the three procedures is illustrated in Figure 3. Each distributions is representative of the particle size distribution of the armour. In fact, the data for the weight and number curves are for exactly the same sample - the rocks weighted ('weight' curve) were also counted ('number' curve). The curve labeled 'Wolman' is a different distribution in the same area as the weight/number sample.

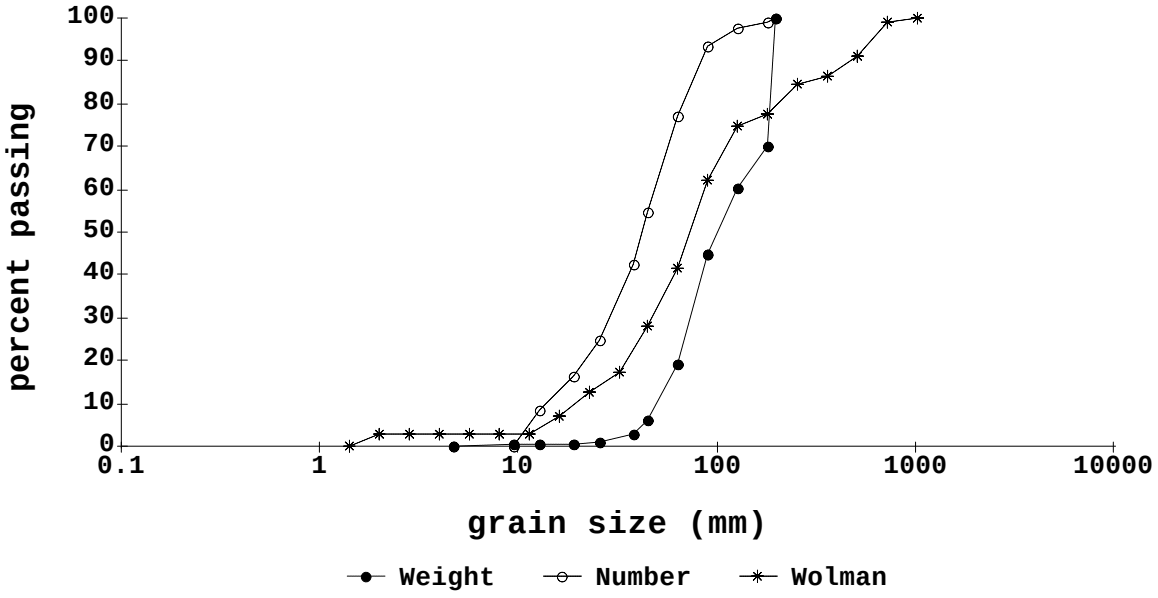

Figure 3. Alternative particle size distributions of the armour of Little Boulder Creek near Boulder, Montana.

Kellerhals and Bray (1971) reviewed sampling and sample analysis procedures for sampling the bed material of gravel and cobble bed rivers. A major point of their paper is that the method of analysis and sampling should be consistent with the way the results are used. Their major example is that if the analyst is mixing sand bed data and gravel bed river data the sample labeled 'Wolman' is the size distribution curve to use in the analysis. The reader should refer to the Kellerhals and Bray paper for an argument about why the 'Wolman' procedure should be used.

The size distributions may be converted from one type to another using the weighting factors in Table 2. The bulk sample is the same as sampling a stream where the material below the armour is the same as the armour, as is the case for most sand bed rivers, but not the case for most gravel and cobble bed rivers with a surface courser than the substrate below. The results of converting the two area curves in Figure 3 to the equivalent Wolman curves are presented in Figure 4. The area curves represent a point in the stream of about 5 square feet and the Wolman curve represents a reach of stream about 100 feet long. The reader should refer to the Kellerhals and Bray paper for specifics on how to make the conversion.

Table 2. Weighting Factors for Conversion of Sample Types. (Modified from Kellerhals and Bray, 1971.)

Conversion from	Conversion to Bulk	Wolman	Area by Weight	Area by Number
Bulk	1	1	D	$1/D^2$
Wolman	1	1	D	$1/D^2$
Area by weight	1/D	1/D	1	$1/D^3$
Area by number	D^2	D^2	D^3	1

The median size of the armour determined by the five procedures are given in Table 3. The measured values are as obtained by the techniques in the first column. The transformed case is where the area data is transformed to an equivalent Wolman sample.

Table 3. The median size (in millimeters) of the armour based on five methods of measurement and analysis. The transformed samples are the equivalent of Wolman samples.

Technique	Measured	Transformed
Area-by-weight	102.5	75.0
Area-by-number	42.4	76.1
Wolman	74.7	74.7

The advantage of an area sample is that it effectively represents a point in the stream that may be in the center of the stream as well as on bars. This is in contrast to the typical Wolman count which represents a bar or some other longitudinal feature above the water. The Wolman

technique can give a composite size distribution and median size for a total reach (as is the case in Figures 3 and 4). This is good if one is interested in the reach average values but not all that good if one is interested in the stream bed characteristics on the scale of the fish in the river.

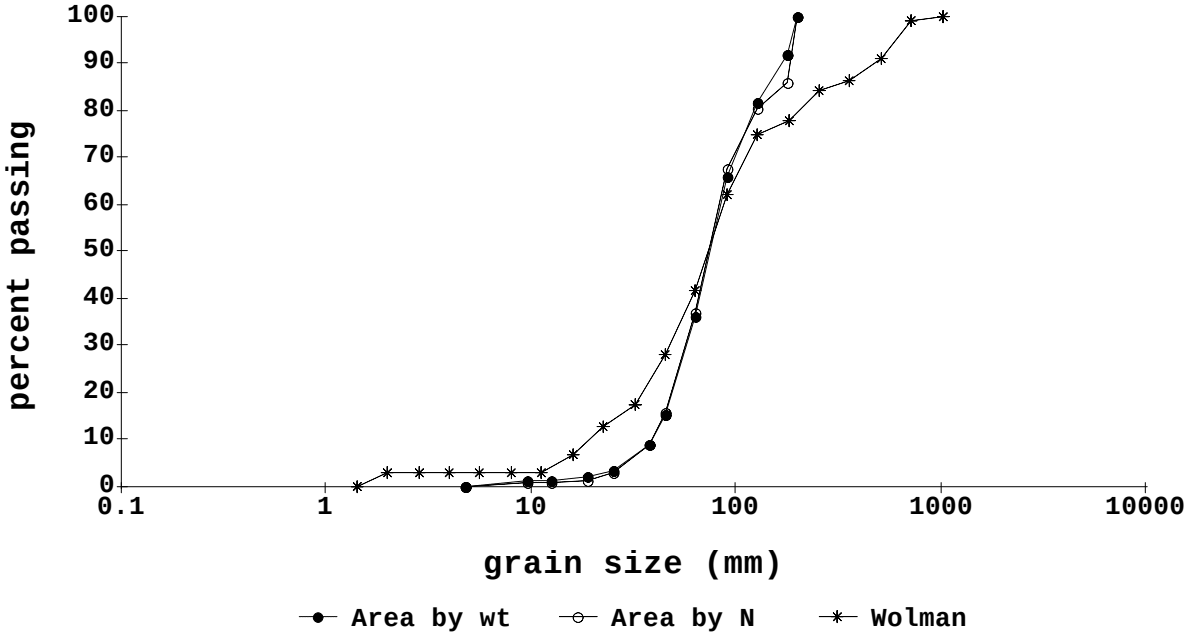

Figure 4. The size distributions equivalent to the Wolman procedure obtained by transforming area-by-number and area-by-weight distributions shown on Figure 3 and the Wolman distribution also shown on Figure 3. Little Boulder Creek near Boulder, Montana.

DISCUSSION

In this paper two characteristics of importance for understanding the ecological and sediment transport process in gravel bed rivers have been presented. The first is about the specific weight (and the porosity) of the bed material in a gravel bed river. The range of specific weight (105-151 lbs/cubic foot) and porosity (0.04-0.41) is relatively large and not completely related to the median size (d50) of the bed material. The technique used to measure the specific weight is volume replacement where the volume of sediment removed from the stream bed is replaced by an measured volume of water.

This paper shows there is a significant range in the specific weights and porosity of gravel/cobble river substrate. It is not demonstrated the importance of differences but does suggest the differences may be important. A procedure for bulk density measurement is outlined. River investigators should make additional measurements of the specific weight and compare these results to other processes occurring in the rivers.

The median size of the armour is important to know in order to understand both ecological processes and sediment transport in a gravel bed river. The median size can have a significant range just because of the way the sample of the armour is obtained and analyzed. The paper shows that it is important to select the appropriate representation of the particle size distribution

used to determine the median size. The type of particle size distribution analysis must be clearly presented in any report or paper containing a particle size distribution curve or median size.

Many people have used Oak Creek bed load transport data. One sample of the armour was reported at the time of the study as having a median size of 66 mm. This median size is based on area-by-weight sampling and analysis. The same data transformed to a equivalent to the Wolman procedure would yield a median size of 44 mm. A value of the dimensionless shear stress of 0.021 has been used in flushing flow studies (Milhous, 1998) and was calculated using area-by-weight analysis of the armour. If the results of the Oak Creek study are used along with data from other studies where the median bed material size was obtained using the Wolman procedure the dimensionless shear stress should be 0.030. This is a significant difference.

REFERENCES

Kellerhals, Rolf and D.I Bray. 1971. Sampling Procedures for Course Fluvial Sediments. Journal of the Hydraulics Division. ASCE. Vol.97, no. HY8, August,1971. pp 1165-1180.

Komura, S. 1963. Discussion of "Sediment Transportation Mechanics: Introduction and Properties of Sediment". Progress Report by the Task Committee on the Preparation of Sedimentation Manual of the Committee on Sedimentation of the Hydraulics Division, Vito A. Vanoni, Chairman. Journal of the Hydraulic Division. ASCE. Vol 89, no. HY1, Paper 3405, Jan. 1963, pp 263-266.

Milhous, R.T. 1998. Modeling of Instream Flow Needs: The Link Between Sediment and Aquatic Habitat. Regulated Rivers: Research and Management Volume 14: 79-94.

Vanoni, V.A. (editor) 1975. Sedimentation Engineering. ASCE Manuals and Reports on Engineering Practice No. 54. American Society of Civil Engineers. New York, NY. pp 745.

Wohl, Ellen E., D.J. Anthony, S.W. Madsen, and D.M. Thompson. 1996. A Comparison of Surface Sampling Methods for Course Fluvial Sediments. Water Resources Research. Vol 32, no. 10, October 1996. pp 3219-3226.

Wolman, M. Gordon. 1954. A Method of Sampling Course River-Bed Material. Transactions, American Geophysical Union. Vol. 35, no 6, December 1954. pp 951-956.

THE EVOLUTION OF CLUSTERS IN GRAVEL BED STREAMS

By A. N. Papanicolaou, Assist. Professor, Dept. of Civil Eng., Washington State University, Pullman, WA 99164-2910; A. Schuyler, ENSR, 9521 Willows Road NE Redmond, WA 98052

INTRODUCTION

Cluster-structures form in gravel-bed streams under various flow conditions and sediment availability. Understanding the flow mechanisms (e.g. turbulence) and sediment parameters (e.g. size and specific gravity) affecting clusters is important for the stability and ecology of natural gravel-bed streams. Clusters work as barriers to the exposure of contaminated beds and keep fine particles from suffocating salmon spawning beds by entrapping them in the wake and stoss regions of the cluster-structure. Biggs et al. (1997) showed that cluster-structures provide refuge for benthos. In areas where cluster-structures were present 50% on the benthic population was reduced after a high flow event, whereas greater than 95% was reduced where no clustering was present.

A typical cluster-structure consists of an obstacle clast (grain of sediment), against which a stoss of imbricate or overlapping clasts develop, and behind which a wake tail grows (Figure 1). For a cluster-structure to form, it is necessary that two or more particles group together (Reid et al., 1992). Cluster-structures form a protruded, but usually streamlined element of the armor layer (Reid et al., 1992)—this makes their presence a major part of the changing streambed. Cluster-structures have been found to occupy 4% to 90% of a streambed (Biggs et al., 1997; Reid et al., 1992). The variation in sediment availability also plays a role in the percent of area covered by the cluster-structures.

Cluster size depends on the bed surface packing density, bed topography, flow intensity, and sediment material properties (Diplas et al., 1998). The aforementioned term, surface packing density, denotes the inter-particle distance and is defined as the ratio between the projected plan area of a particle to the total area of a bed section in which the particle is located (Schlichting, 1968). Cluster-structures are reported widely as characteristics of gravel riverbeds and are known to influence the initial entrainment of bed load (Biggs et al., 1997). According to Hassan and Reid (1990), the spacing and concentration of pebble cluster-structures are regulated by sediment availability and transport rates. These characteristics reach an equilibrium value when maximum flow resistance occurs.

There are several factors affecting the stability of cluster-structures—grain-grain contact, sediment protrusion, flow intensity, and sediment specific gravity (Diplas et al., 1998; Reid et al.; 1992, and James, 1992). While the former three factors have received considerable attention, the role of sediment specific gravity on cluster-structure stability has not been examined thoroughly.

Gravel-bed streams are composed of sediment with different specific gravity, therefore, understanding the role of specific gravity on cluster formation and stability will provide new information on the formation of bed microforms in natural gravel-bed streams.

Subsequently, the focus of the present article is the role that sediment specific gravity plays on the clustering process. For this purpose, tests are performed in a tilting flume for a fixed slope and packing density by using three different types of spherical particles of the same size but of different specific gravity. This is to isolate the role of sediment specific gravity on cluster formation throughout the tests. State-of-the-art image analysis tools allow for a quantitative analysis of the effects of particle specific gravity on the clustering process and monitor the changes occurring on the flume bed.

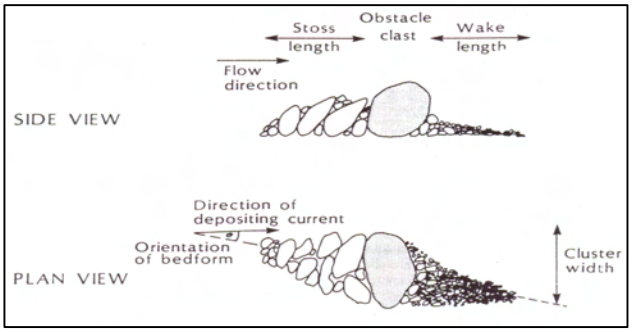

Figure 1: Elements of a typical cluster (Reid et al., 1992)

EXPERIMENTAL SETUP

The experiments in the present study were conducted in a tilting laboratory flume that is 22.86 m long, 0.89 m wide, and 0.21 m deep. Its useful length is 21.00 m. The test section was located 16.8 m from the flume entrance to ensure fully developed, turbulent flow conditions during the experiments. The length of the test section was 4.2 m and its width was approximately 0.40 m. The test bed consisted of 8 mm diameter, colorless, glass beads with a specific gravity (s.g.) of 2.58, laid in four well-packed layers. The porosity of the test bed was approximately 26%. Atop the test section 8 mm spheres, made of clear glass (s.g. = 2.58) and Teflon (s.g. = 2.12) were placed (Figure 2). The clear glass beads were painted green to allow for their detection by the image analysis software. The different specific gravity materials were chosen to simulate the variance in sediment specific gravities in a natural streambed. The clustering of these bead configurations under incipient and twice incipient flow conditions was investigated.

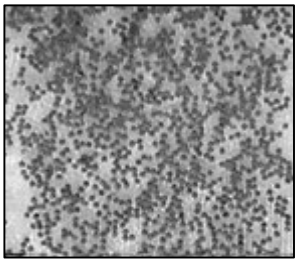

Test 35A: Green Glass.

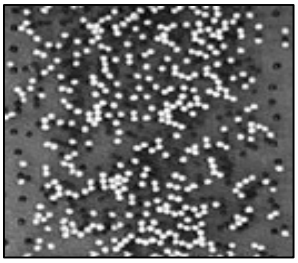

Test 35B: Teflon and

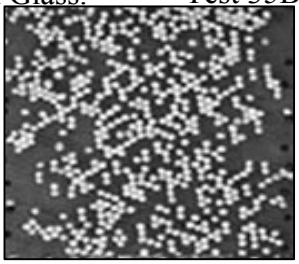

Test 35C: Teflon

Figure 2: Plan view of the test section at t = 0 min.

From the entrance of the flume to the beginning of the test section (16.8 m), naturally worn gravel was placed in a layer approximately the same thickness of the clear glass beads in the test section. A video camera was positioned above the flume to provide a plan view of the test section. The area of view captured by the camera was 30 cm long by 40 cm wide. The length was sufficient for monitoring the particle motion since the average displacement of the spheres is typically on the order of several bead diameters (Sekine and Kikkawa, 1992).

A videocassette recorder was used to digitize the movies. The recorder was connected to a personal computer that allowed the capturing of the movie. Asymetrix Video Capture 4.0 was used to digitize the movies. Individual images were captured at 0, 0.5, 1, 1.5, 2, 5, 10, 15, 20, 25, and 30 minutes. The close spacing of the images in the first five minutes was because a substantial portion of the motion occurred during this time. These frames were then imported into Global Lab Image software for post-processing image analysis. Figure 3 provides a schematic view of the experimental setup.

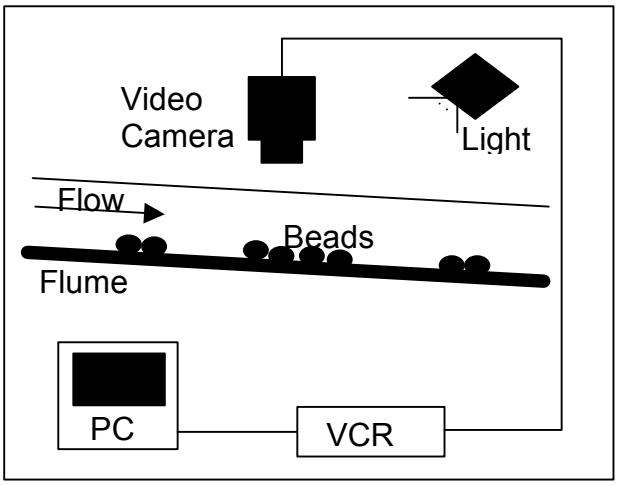

Figure 3: Sketch of Experimental Setup

EXPERIMENTAL CONDITIONS

Six experiments were conducted during the course of this study: the all glass bead test, the all Teflon and then an equal combination of the green glass and Teflon for both incipient and twice incipient conditions. The beads were distributed atop the flat porous test bed with an inter-particle spacing of approximately one ball diameter. Based on the flow-roughness classification of Morris (1955), the above tests correspond to the wake-interference flow regime. The size and specific gravity of the spheres was determined so that the requirement set by Vanoni (1964) would be satisfied:

$$\frac{d}{n}\sqrt{0.1Rgd} \geq 500 \qquad (1)$$

Where R is the particle submerged weight and is equal to $\rho_s/\rho - 1$, where ρ_s is the density of the bead, ρ is the density of water, d is the particle diameter, ν is the kinematic viscosity of water, and g is the acceleration of gravity. This requirement ensures that the dimensionless,

$$t^*_{cr} = \frac{HS}{Rd} \qquad (2)$$

critical shear stress, τ_{cr}^{*} (equation (2)), is independent of the particles Reynolds number (equation (3)):

Where H is the flow depth, S is the flume slope, and $u_?$ is the friction velocity, which is equal to $(gHS)^{1/2}$. The choice of size and specific gravity of the glass beads was also based on the consideration that no suspension motion should occur during the tests. To satisfy this condition, the dimensionless number, $z = \omega/\kappa u_*$, (ω is the terminal velocity, and $\kappa = 0.4$ is the Von Karman constant) must be greater than five (Chang, 1988). For these tests, it was also important that two-dimensional flow existed. To ensure this, the ratio of the top width to the average flow depth, B/H, must be greater than five (Song et al., 1994). The ratio of the average flow depth to the particle diameter, H/d, needed to be greater than 3, so that surface tension had no effect on the particles (Bettess, 1984). Table 1 lists all of the aforementioned parameters as well as other hydraulic parameters related to the tests.

Table 1: Flow Conditions During the Experiments

Test	Slope, *S* (%)	Depth, *H* (m)	Depth Average Velocity, *U* (m/s)	Aspect Ratio, B/H *B* (m) = 0.895	Relative Depth Ratio, H/d *d* (m) = 0.008	Dimen-sionless Critical Stress, τ^{*}_{cr}	$\frac{d}{\nu}\sqrt{0.1Rgd}$	Reynolds Number, $R = \frac{4HU}{\nu}$	Reynolds Number, $R = u_* d/\nu$	Froude Number, $F = U/(gH)^{0.5}$	Rouse Number, *z*
(1)	(2)	(3)	(4)	(6)	(7)	(8)	(9)	(10)	(11)	(12)	(13)
35A	0.8	0.057	0.58	16	7.13	0.037	810	120218	487	0.78	32
35B	0.8	0.039	0.48	23	4.88	0.035	682	68073	400	0.78	40
35C	0.8	0.039	0.48	23	4.88	0.035	682	68073	400	0.78	40
35E	1.6	0.057	0.87	16	7.13	0.074	810	180327	691	1.16	32
35F	1.6	0.039	0.70	23	4.88	0.070	682	99273	567	1.13	40
35G	1.6	0.039	0.70	23	4.88	0.070	682	99273	567	1.13	40

METHODOLOGY

The goal of the present study was to develop a non-intrusive and less subjective procedure in order to monitor the cluster evolution process (i.e., disintegration and integration) in gravel bed streams. This was accomplished by developing an image analysis procedure to obtain for the first time, quantitative information about the size of clusters, the cluster's composition and stability of a large sediment population. This technique, although academic at this stage of the investigation, should be capable of extension to real cases of detecting cluster formation in natural streams.

The digitized images were imported into Adobe Photoshop 4.0 and converted from colored bitmap images to grayscale TIFF (tagged-image file format) images. The images were then imported into Global Lab Image for their image processing and analysis. The steps involved in this analysis are as follows: choosing the region of interest (ROI), setting grayscale threshold values, defining the area boundary conditions, and then counting the number of clusters. The ROI is the region in the image that contains the green glass and/or Teflon beads. The grayscale

$$\mathrm{Re}_P = \frac{u_* d}{n} \qquad (3)$$

threshold values (0 for pure black and 255 for pure white) were then chosen by clicking on the lightest and darkest areas of the particles. Once thresholds were established, the average pixel area of one particle was determined. This was done by selecting ROI's for 20 individual

particles and using the average as the particle size in pixels. The next step was to set the smallest area boundary condition to just less than 2 particles. The upper limit was set to 500,000 pixels to ensure that all clusters would be accounted for. Global Lab Image allows the user to determine what characteristics will be calculated. For this study, individual cluster areas were calculated, from which the minimum, maximum and average cluster sizes were derived. Figure 4 illustrates these steps.

While the image analysis program performed adequately for the 35A and 35C tests, for the 35B case, where both the green and white beads were present in the ROI, limitations of the program were confronted. Because of the large grayscale threshold range between the white and green (obsidian in grayscale) particles, the program also detected the background particles. Due to this limitation, the analysis procedure for 35B varied from that of tests 35A and 35C. In this case, the images were converted to grayscale TIFF format using Adobe Photoshop 4.0. In Photoshop, the background of these images was removed and the particles of interest were changed to all black. This new image was then imported into Global Lab Image where the procedure was as previously mentioned. To ensure accuracy, images were randomly chosen, printed out and then the beads in the ROI were counted by hand. Errors ranged from less than 1% up to 4%.

For tests 35E, 35F, and 35G, no analysis procedure was necessary because the bed became completely mobilized.

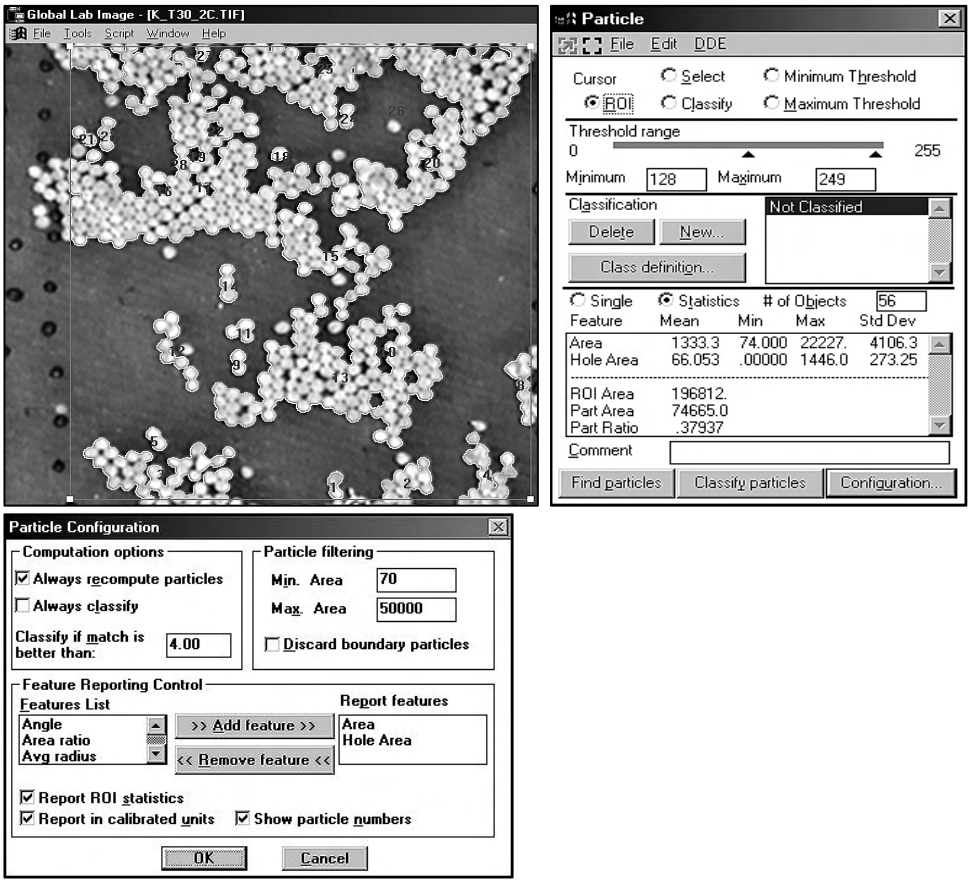

Figure 4: Steps of image processing for test 35C

RESULTS AND CONCLUSIONS

The results of this study show that the size of clusters increases with time and subsequently the number of clusters found within the area of view decreases (Figure 5A-5C). This is due to the smaller clusters disintegrating and then being incorporated into larger clusters. Moreover, it was shown that the lesser the particle specific gravity, the smaller size clusters are formed. Having particles of different specific gravity yielded the largest size clusters and the widest range of cluster sizes (Figure 5A-5C). The fluctuations in tests 35A and 35B show that when heavier particles are present, the evolution of the clusters seems more dynamic. Test 35C illustrates that with a smaller specific gravity, there is a constant "build-up" of the cluster size (within the 0-200 particle size range), showing that the bed tends to be more stable.

Figure 5A-5C reveals that for the three experimental conditions examined here, clusters are the most prevalent structures on the bed, accounting for over 90% of the bed material and that with time the bed reaches an equilibrium condition, as shown by the flattening of the data points.

Finally, the experiments show that when the flow is at twice-incipient motion conditions, the bed is completely mobilized, which agrees with Church and Hassan (1992).

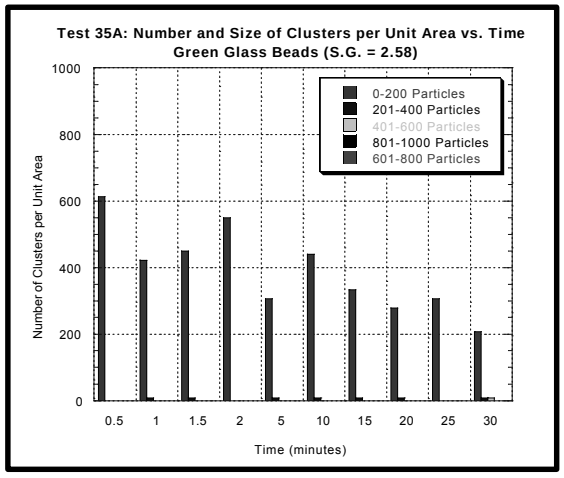

Figure 5a: Variation of the number and size of clusters with time, test 35A

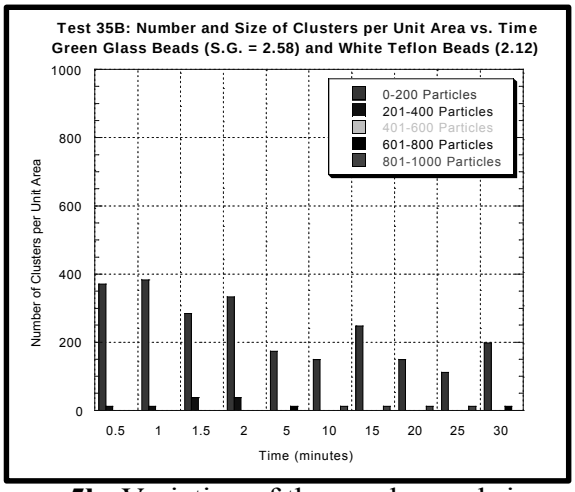

Figure 5b: Variation of the number and size of clusters with time, test 35B

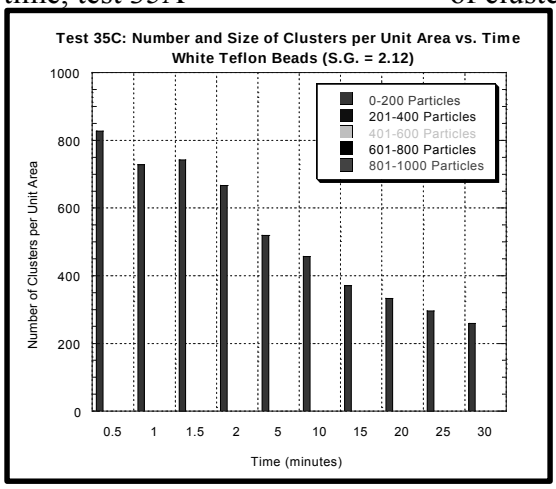

Figure 5c: Variation of the number and size of clusters with time, test 35C

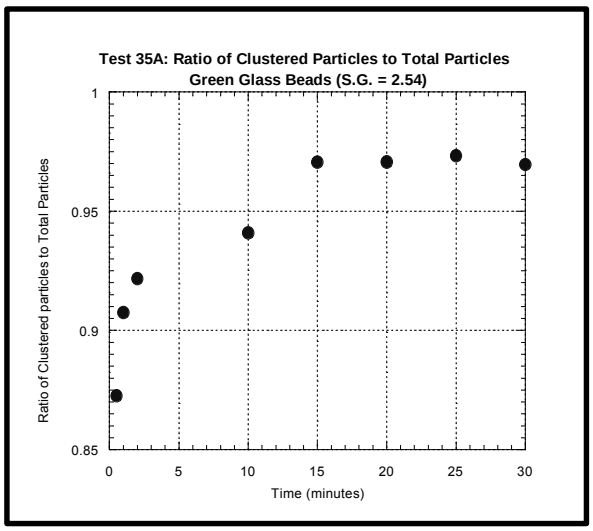

Figure 6a: Ratio of number of particles clustered to total number of particles in viewing area, test 35A

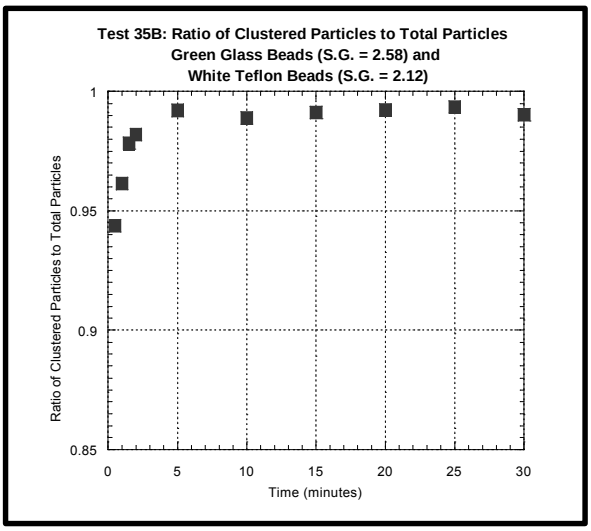

Figure 6b: Ratio of number of particles clustered to total number of particles in viewing area, test 35B

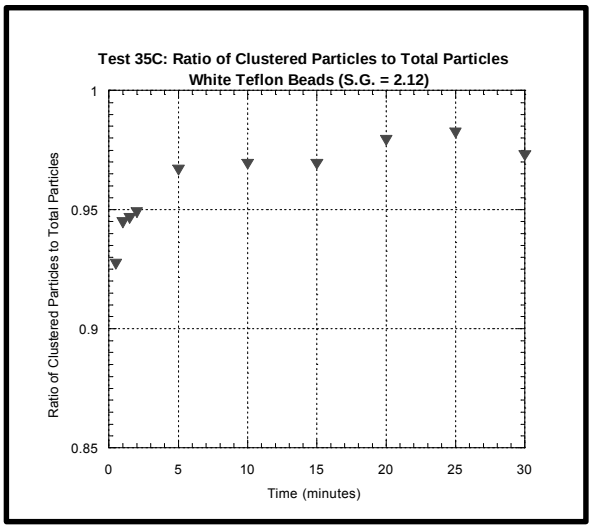

Figure 6c: Ratio of number of particles clustered to total number of particles in viewing area, test 35C

ACKNOWLEDGEMENTS

The authors would like to thank the Department of Civil Engineering at WSU and the Washington Technology Center (Grant #3815-4324) for providing partial financial assistance to the investigators of this study.

REFERENCES

Bettess, K. (1984). "Initiation of Sediment Transport in Gravel Streams." *Proceedings of the Institution of the Civil Engineers*, Part 2, March, 79-88.

Biggs, Barry J.F., Duncan, Maurice J., Francoeur, Steven N., and Meyer, William D. (1997). "Physical characterization of microform bed cluster refugia in 12 headwater streams, New Zealand." *New Zealand Journal of Marine and Freshwater Research*, 31, 413-422.

Chang, H. H. (1992). Fluvial Processes in River Engineering, Reprint Edition, John Wiley and Sons, 146-149.

Church, Michael and Hassan, Marwan A. (1992). "Stabilizing self-organized structures in gravel-bed stream channels: Field and experimental observations." *Water Resources Research*, 34, 11, 3169-3179.

Diplas, P., Papanicolaou, A. N., Dancey, C. L., and Balakrishnan (1998). "The Role of Clusters in the Entrainment of Sediment". *Accepted for publication at the International KRIKOS Conference, Protection and Restoration of the Environment IV.*

Hassan, Marwan A., and Reid, Ian (1990). "The influence of microform bed roughness elements on flow and sediment transport in gravel bed rivers". *Earth Surface Processes and Landforms*, 15, 739-750.

James, C. S. (1992). "Entrainment of spheres-an experimental study of relative size and clustering effects". *unpublished.*

Morris, H.M., (1955). "Flow in rough conditions." *Transactions American Society of Civil Engineers*, 120, 373-398.

Reid, I., Frostick, L. E., and Brayshaw, A. C. (1992). "Microform roughness elements and the selective entrainment and entrapment of particles in gravel-bed rivers". Dynamics of Gravel-bed Rivers, John Wiley and Sons Ltd., 253-275.

Schlichting, H. (1968). Boundary Layer Theory, 6th Edition, McGraw-Hill, New York, 1968.

Sekine, M. and Kikkawa, H. (1992). "Mechanics of Saltating Grains II." *Journal of Hydraulic Engineering*, 118, 4, 536-558.

Song, T., W. H. Graf, and U. Lemmin (1994). "Uniform Flow in Open Channels with Movable Gravel Bed." *Journal of Hydraulic Research*, 32, 6, 861-876.

Vanoni, V. A. (1964). "Measurements of Critical Shear Stress for Entraining Fine Sediments in a Boundary Layer." *Report KH-R-7, W. M. Keck Laboratory of Hydraulic and Water Resources*, California Institute of Technology.

Author contact point

Dr. Thanos (A.N.) Papanicolaou
Dept. of Civil and Env. Engineering
Washington State University
Pullman, WA 99164-2910
E-mail: apapanic@wsu.edu
Phone: 5-09-335-2144

DENSIMETRIC MONITORING OF SUSPENDED-SEDIMENT CONCENTRATIONS, NORTHEASTERN GEORGIA

Daniel L. Calhoun, Hydrologist, U.S. Geological Survey, Atlanta, GA
Todd C. Rasmussen, Associate Professor, The University of Georgia, Athens, GA

Abstract

Differential pressure transducers can be used to monitor the suspended-sediment concentration in a water column. Suspended sediments with densities greater than water increase the fluid density, which is determined by measuring the fluid pressure change between two depths. Lewis and Rasmussen (1999) used a densimetric technique under controlled conditions to determine suspended-sediment concentrations and particle-size distributions. Results from a study that used similar laboratory techniques and newly developed *in situ* methods are summarized herein and condensed from Calhoun (2000). Applications on two tributaries to the South Fork of the Broad River in northeastern Georgia demonstrate that stormflow suspended-sediment concentrations induce large temporal changes in fluid density. The influence of bedload sediment transport also is demonstrated by placing the deeper port in a position that tracks fluid density changes in the mobile bed zone.

INTRODUCTION

Various densimetric approaches to the measurement of suspended sediment have been employed in fluvial sediment studies as alternatives to traditional techniques such as the collection of depth and width-integrated samples in the river cross section. Densimetric techniques rely on the measurement of variations in fluid density that result from changes in the temperature of water, along with changes in the concentration of dissolved and suspended solids and the presence of gases (Skinner and Beverage, 1982; Lewis and Rasmussen, 1999). The suspended sediment in a column of water can be detected using methods that account for thermal variations and dissolved-solids concentrations in the water column.

Skinner and Beverage (1982) utilized an early densimetric instrument to measure suspended-sediment concentrations. The oscillatory period of a cantilevered vibrating U-tube increased with the density of the fluid. Clay concentrations greater than 500 milligrams per liter (mg L^{-1}) were measured to within three percent accuracy and concentrations of coarse sands to within twelve percent accuracy. Standard errors of the estimate for concentrations less than 500 mg L^{-1} were 15 and 25 mg L^{-1} for clay and sand, respectively. Sediment concentrations as much as 97 grams per liter (g L^{-1}) were tested. Skinner and Beverage (1982) reported that organic material would not provide a measurable densimetric response because of the close similarity to the density of water. Challenges identified by Skinner and Beverage (1982) included the need to monitor and correct for changes in fluid temperature (1°C was equivalent to a change in the measured response of 160 mg L^{-1}). At temperatures less than 9°C, the instrument did not function, presumed by the researchers to be the result of condensation on the outside of the tube that altered the oscillatory period. Air bubbles were removed by deaeration and the pumped flow rate of the fluid was tightly regulated to estimate the volume of water passing through the device. Substantial instrument drift occurred due to sediment and biologic material adhering to the inside of the tube, which resulted in an increased apparent concentration and necessitated regular cleaning. Subsequent research on the methodology included improving the error correction process and the development of more applicable *in situ* instrumentation (Skinner and others, 1986; Skinner, 1989).

Early work in 1980 used pressure measurements to estimate bedload sediment transport with the Birkbeck pit sampler (Reid and others, 1980). This work verified the ability to produce a continuous record of bedload transport using fluid-filled pressure pillows placed at the bottom of a pit excavated in a streambed. The types of stream and transport regimes in which the sampler could be used were the only limiting factors for the method. Later work by Lewis (1991) modified the original design by using a differential pressure transducer connected to a datalogger and using a stilling well as a reference column. Difficulties with the method included air entering the system under negative pressure as a result of the transducer being placed above the water surface, ruptured pillows, overpressure damaging the transducer membrane, problems maintaining instrument calibrations, temperature effects on the ambient water density, and removal of sediment that filled the pits during storms. Many of the challenges posed through the use of a densimetric technique were deemed insurmountable and the experiment was altered to use a load cell, similar to a weighing lysimeter, to successfully obtain a continuous record of bedload sediment transport.

Lewis and Rasmussen (1999) demonstrated the use of precision pressure transducers to measure fluid density, which was then used to estimate suspended-sediment concentration and particle-size distributions. Their study focused on the temporal variations in measured fluid pressures that are attributable to factors that alter fluid density and total head. Lewis and Rasmussen (1999) derived a relation between fluid density and the mass concentration of suspended sediments, C_s , in kilograms per cubic meter (kg m^{-3}), based on Bernoulli's equation,

$$C_s = r_s\, C_v = -\frac{\frac{1}{g}\frac{dp}{dz} + r_w}{1 - \frac{r_w}{r_s}} \qquad (1)$$

where $C_v = \frac{V_s}{V_t} = \frac{r_f - r_w}{r_s - r_w}$ $\qquad$ $r_f = -\frac{1}{g}\frac{dp}{dz}$

and C_v is the volumetric concentration of suspended sediments (m^3 m^{-3}), V_s is the volume of suspended sediments (m^3), V_t is the total volume of suspended sediments and clear water (m^3), r_f is the density of the fluid column (kg m^{-3}), r_w is the density of clear water (kg m^{-3}), r_s is the density of the suspended sediments (kg m^{-3}), p is the fluid pressure in hectopascals (hPa), z is the depth (m), and g is the gravitational constant (m s^{-2}). Equation (1) can be tailored to fit the specific instrument design. For example, a differential pressure transducer can be used to eliminate the fluid density term in the numerator. Also, the sign of the numerator becomes positive when the arbitrary datum is placed lower than the elevation reference point, z.

Sediment concentrations were determined to within ninety-nine percent accuracy for three particle size classes; 106 - 150, 180 - 250, and 300 - 425 µm (Lewis and Rasmussen, 1999). The size classes were estimated using equations derived from Stokes' Law. Particle sizes were determined to within ninety-five percent accuracy for the smallest size class analyzed (106-150 µm). The largest size class (300 - 425 µm) was determined with less accuracy, attributed to possible limitations in the application of Stokes' Law. The authors identified the challenges likely to be encountered under field conditions. These challenges include temperature, velocity, and particle-density variability.

LABORATORY STUDY

The investigation summarized herein (Calhoun, 2000), involved trials conducted under ideal, laboratory conditions using [1]Druck LPM 9381, high-accuracy, differential pressure transducers with a maximum pressure range of 1 hectopascal (hPa) (1 hPa ≈ 1 cm of water). Swagelok stainless-steel tubing and pipefittings were attached to the transducers to establish measuring points at depth intervals of 50 and 100 cm in a column of deionized water. Glass microspheres with a diameter of 360 ± 60 µm and a range of concentrations were released into the water column. The microspheres created an increase in differential pressure that was measured by the pressure transducer and translated into an analog signal. The signal was monitored and recorded by a Campbell Scientific CR23X datalogger, and the final data interpretation and analysis was performed on a desktop computer.

The differential pressure transducer response derived from the addition of 0.3 gram of 360-µm glass microspheres is illustrated in Figure 1. The suspended-sediment concentration, calculated from the mass of microspheres within the water column between the two pressure measurement points, was 38.0 mg L^{-1} for the 1-m distance of observation. The maximum response of the instrument to the applied glass microspheres resulted in a measured concentration of 37.8 mg L^{-1}, which is an error of 1 percent. The time lag corresponded to the published fall velocities of like-sized quartzite spheres (Chang, 1988). Both the sensitivity of the instrument to pressure variances and the overall sensitivity of the instrument are both apparent in the instability of the readings. Additional tests over a range of suspended-sediment concentrations indicated that optimal results were obtained for concentrations between 10 mg L^{-1} and 1,000 mg L^{-1}. The sampling error exceeded 15 percent when the concentration was outside this range. Additional tests conducted over a 50-cm sampling distance yielded similar results, although the measurement error doubled when the length of the column was halved.

Tests using differential transducers (Druck PMP 4130) with a larger pressure range of 69 hPa indicated that these sensors were not able to differentiate the change in pressure at low concentrations, but were more appropriate when the suspended-sediment concentration exceeded 1 g L^{-1}. The pressure response to 50 grams of the 360-µm glass microspheres using the 69-hPa sensor is illustrated in Figure 2. The expected concentration was 6.37 g L^{-1}, and the densimetric prediction was 6.24 g L^{-1}, yielding an error of approximately 2 percent.

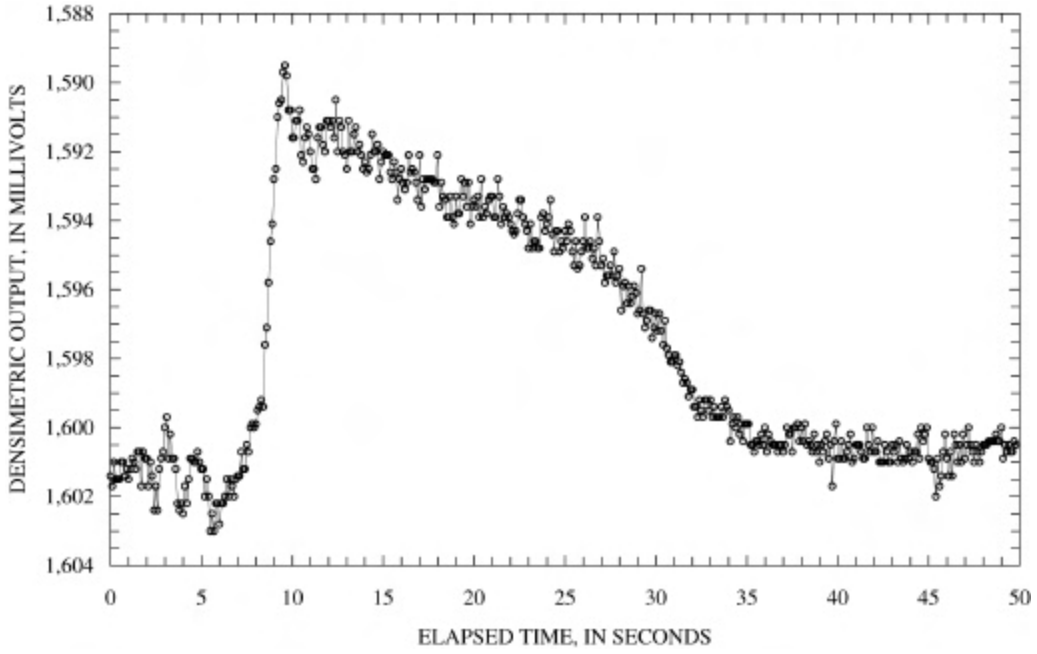

Figure 1. Densimetric response to 0.3 gram of 360-µm glass microspheres using a 1-hPa transducer.

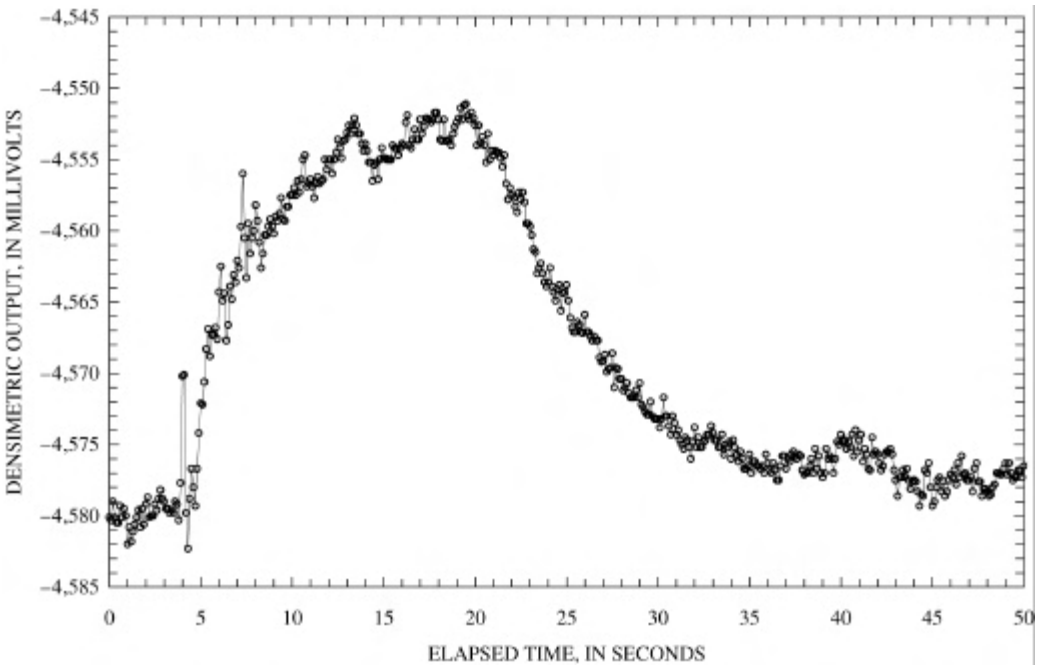

Figure 2. Densimetric response to 50 grams of 360-µm glass microspheres using a 69-hPa transducer.

The results described above indicate that the determination of suspended-sediment concentrations using the densimetric approach can be replicated under ideal, laboratory conditions. The observed error can be reduced through refinements of the procedure, such as deaeration methods to ensure that bubbles of air are excluded within the device that dampens the response of the transducer. Also, methods should be implemented to ensure absolute seals in the fittings and tube connections to reduce the possibility of pressure leaks.

FIELD STUDY

Two stream sites within the South Fork of the Broad River watershed in northeastern Georgia (Figure 3) were used to evaluate the densimetric measurement of suspended-sediment concentrations under field conditions. The sites were selected to be consistent with an ongoing U.S. Environmental Protection Agency (USEPA) National Exposure Research Laboratory (NREL) study within the watershed, the intention of which is to quantify and model nonpoint-source pollutant loads and load responses to watershed characteristics and management strategies.

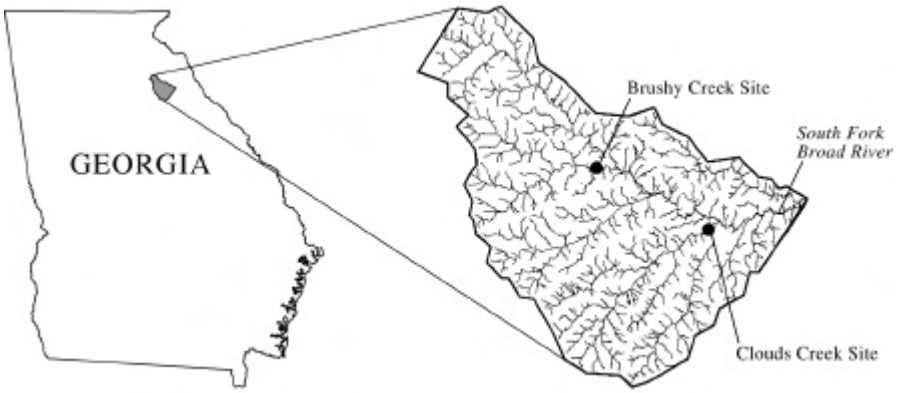

Figure 3. Location of study sites within the South Fork of the Broad River watershed, northeastern Georgia.

The first site, on Brushy Creek (Figure 3), was instrumented with a densimeter constructed from a 1-hPa range differential transducer with measurement points 50 cm apart. The densimeter was mounted on an instream platform constructed from an upright galvanized steel signpost bolted to an angled signpost. Both of these posts were driven approximately 1 to 1.5 m into the streambed and shielded by a 30-cm diameter PVC pipe cut in half and bolted to the posts. Additional doppler water velocity, stream stage, water temperature, specific conductance, and turbidity sensors were attached to the PVC shield and placed within and on the side of a slotted 5-cm diameter PVC pipe. Cabling from the platform to the CR23X datalogger within the instrument shelter ran through a 5-cm PVC pipe. The power supply for the instruments consisted of a 12-volt DC battery charged by a 200-watt solar panel.

A four-month continuous record of the densimeter output and stream stage from December 20, 1999, to April 5, 2000, at the Brushy Creek site is shown in Figure 4. Note that the output from the densimeter, given in millivolts, increases during stormflow periods and tends to mirror changes in stream stage, qualitatively suggesting a linkage of the densimetric output to periods indicative of sediment transport. Note also the existence of a substantial temporal drift in the sensor output during baseflow periods. The specific conductance (not shown) fluctuated from 30 to 80 microSiemens per centimeter at 25°C ($\mu S\ cm^{-1}$) during the four-month period, but such a fluctuation does not explain the observed densimetric response. The water temperature (not shown) fluctuated from 5 to 19°C during the period, but this also does not explain the observed densimetric response.

The largest storm event during the monitoring period occurred from March 20 to 23, 2000. Approximately 5 cm of rain resulted in a stage increase of 60 cm. The data recorded for the densimeter during this event are displayed in Figure 5. Data were stored as 30-minute averages of 5-second measurements. Multiple peaks are evident in the densimetric response. After correction for velocity ($0.4\ m\ s^{-1}$ gradient), temperature, and conductance, the maximum densimetric response converts to approximately $14\ g\ L^{-1}$ suspended sediment. The total potential error associated with the measured parameters influence on total head was estimated to range from 1 to 10 percent during the storm event, reaching the maximum during the densimetric peaks. The majority of this error was associated with the

estimated velocity differential. One explanation for the occurrence of multiple peaks in the densimetric response is that multiple upstream sources of sediment inputs are present, each delayed according to time of travel to the monitoring location.

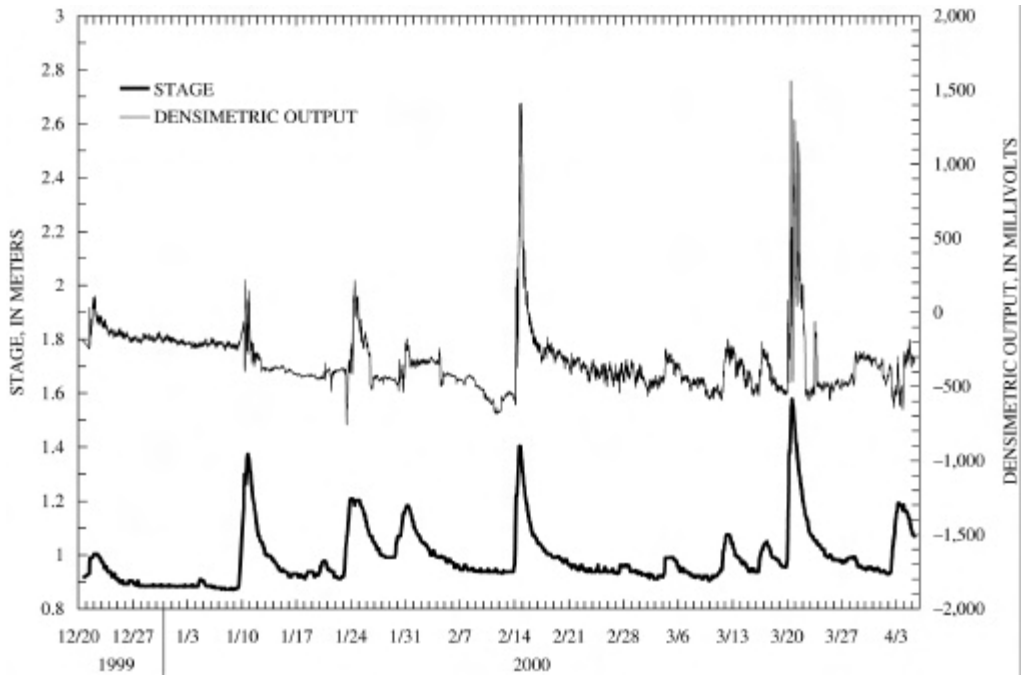

Figure 4. Densimetric response from *in situ* water column measurements at Brushy Creek, December 20, 1999, to April 5, 2000.

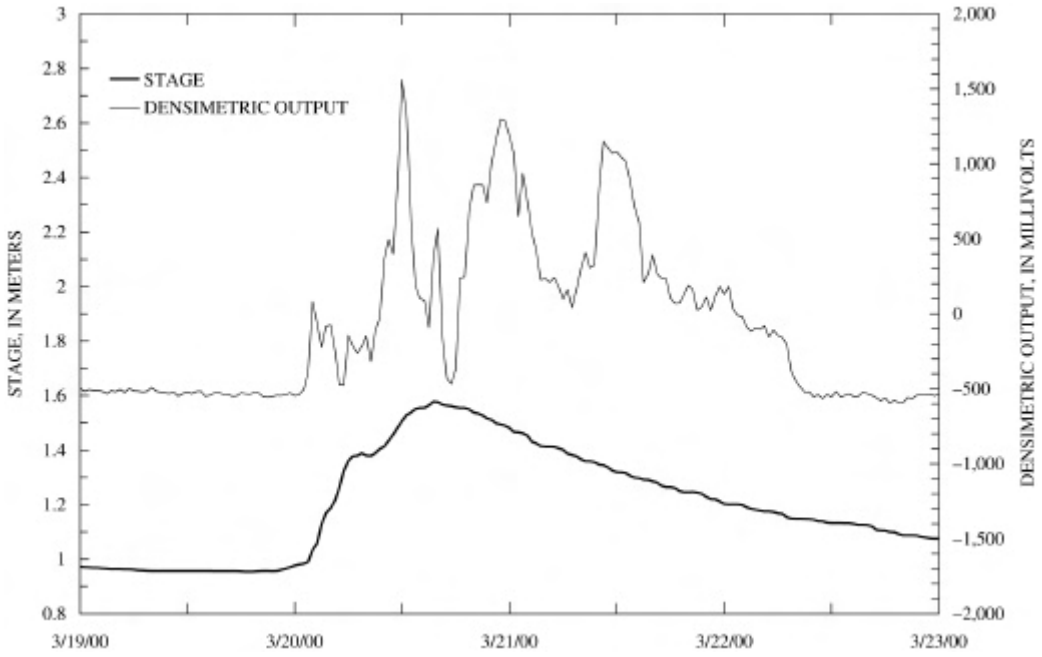

Figure 5. Densimetric response from *in situ* water column measurements at Brushy Creek for the March 20 to March 23, 2000, runoff event

Suspended-sediment samples were manually collected during a storm on September 20, 1999, using a DH-48 handheld sampler. The samples were depth-integrated from the water surface and between the sampling ports for a range of stages. Approximately 25 mm of rain fell during the 4-hour event, with a 10-minute maximum intensity of 13 mm hr^{-1} at 1500 hours. *In situ* measurements were recorded by the datalogger every 10 minutes and were based on the averages of one-second readings. The millivolt response of the densimeter was determined using Equation (1). *In situ* turbidity meter readings were entirely out of range in comparison to all other turbidity measurements collected during storm events and the results are not included herein. The densimetric response to this storm event, along with manually collected suspended-sediment concentrations and the stream stage record, are presented in Figure 6.

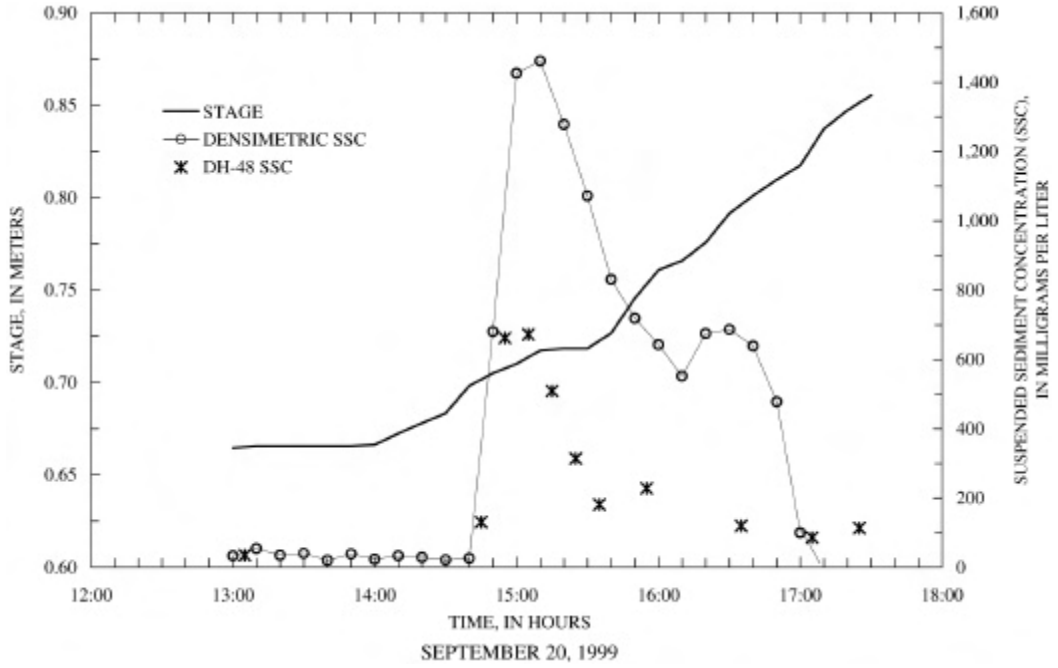

Figure 6. *In situ* water column measurements at Brushy Creek for the September 20, 2000, runoff event. Also shown are manually collected suspended-sediment concentrations from a DH-48 hand-held sampler.

The timing of the densimetric response corresponded with the timing of the fluctuations in sediment concentrations in the manually collected samples. However, the differences between suspended-sediment concentrations based on the manually collected samples and those concentrations estimated from the densimetric output are substantial. Densimetric estimates of suspended-sediment concentrations for this storm event overestimate the DH-48 samples by a factor of three, and the magnitude of the error increases with increasing densimetric output and suspended-sediment concentration. Possible reasons for the differences include:

1. A water temperature decrease of 0.6°C during the event. This change would have affected the fluid density, causing the sensor to record a larger pressure difference. The magnitude of the temperature change is insufficient to account for the difference and was responsible for less than 1 percent of the variance.
2. A decrease in specific conductance of 4 µS cm^{-1} during the event. A decrease of this magnitude can only account for a change of 2.6 mg L^{-1} in the suspended-sediment concentration, which is insufficient to account for the difference.
3. A total head or velocity difference between the two pressure measurement ports may cause a systemic bias in the measurement. A maximum velocity bias of 0.2 m s^{-1}, estimated from velocity measurements, is insufficient to account for the difference.
4. The manual collection using the DH-48 was not ideally performed. It is possible that the DH-48 did not account for the spatial and temporal heterogeneity of suspended sediments within the water column by sampling the distances above the upper port and below the lower port. A series of point measurements may be required to more effectively estimate the depth-integrated suspended-sediment concentration.

The second site, Clouds Creek (Figure 3) (located within Watson's Mill State Park), was instrumented in such a way that the sensor spanned both the water column and a portion of the streambed that is readily mobilized by streamflow. Measurements at the Clouds Creek site employed the 69-hPa range transducer attached to a rebar rod driven into the streambed and stabilized above the water surface. The measurement interval was 1 m, with the lower port installed approximately 30 cm into the sandy bed, leaving approximately 70 cm exposed above the channel bottom. Stream stage, temperature, and specific conductance sensors also were installed.

A 1.5-month record of the Clouds Creek data is shown in Figure 7. The March 20, 2000, event at Clouds Creek was the only substantial storm measured, resulting in an increase in stream stage of approximately 50 cm. The densimetric response for this event yielded a peak total sediment concentration (including bedload) of approximately 20 g L^{-1}; however, before results from this method can be relied upon, additional efforts are needed to obtain actual bedload and suspended-sediment concentration measurements to verify the *in situ* densimetric response and to measure water velocities to fully quantify possible sources of error.

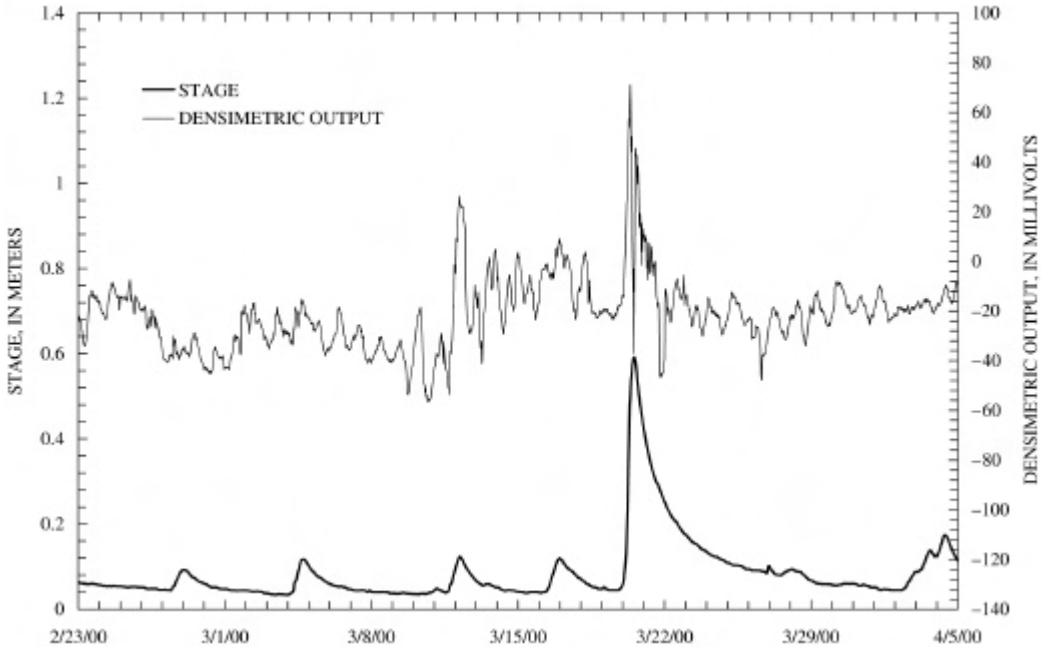

Figure 7. Densimetric response from *in situ* water column and bedload measurements at Clouds Creek for the period February 23, 2000, to April 5, 2000.

SUMMARY AND CONCLUSIONS

Success was achieved in the design and installation of an instrument to continuously measure the fluid density of a water column *in situ*. Responses of the instrument corresponded to increases in stream stage for both suspended sediment increases during two storm events and for suspected lifting and transport of the mobile bed. A method was developed to correct the raw millivolt pressure output of the instrument for errors associated with flow velocity, stream temperature, and specific conductance.

This study established that fluid density could be measured in the laboratory with field-ready devices and in typical alluvial streams using precision *in situ* pressure transducers. Initial manual sampling at Brushy Creek indicated that differential pressure measurements can be related to suspended sediments; however, additional work is needed to develop continuous corrections for variations in flow velocity, stream temperature, dissolved solids, and baseline output of the densimeter during quiescent periods. Instrument optimization is necessary to broaden the range of applicability. Measurements at Clouds Creek indicate that bedload and total load characterizations also are feasible.

Although not fully conclusive, the densimetric analysis of *in situ* suspended-sediment concentrations does hold promise to increase the knowledge of this important area of environmental science. A reliance on traditional methods for determination of sediment concentrations in water can be problematic. Sediment sampling and gravimetric analysis is time consuming and must be timed to coincide with the hydrologic events during which transport occurs. Optical sampling is spatially limited to point measurements that do not represent the entire water column and can be confounded by multiple factors. Other methods exist that are not universally applicable or affordable. The development of sensors that can accurately determine sediment concentrations therefore is essential for the characterization of sediment and sediment-bound contaminants present in fluvial systems and to assess the success of mitigation efforts.

This work reported herein also has revealed that many challenges remain. The field experiment component of this research was not as conclusive as the laboratory component. The need is evident for design improvements involving the deaeration of the system, a more user-friendly in-stream installation process, a reliable regulated power supply, and sealing of the internal system from the sampled water. It also is essential to consider the site and the intended range of measurement of suspended-sediment concentration before selecting a transducer. Laboratory tests indicate that the 1-hPa range is effective for 10 to 1,000 mg L^{-1} concentrations. Smaller range transducers are available that should be tested to improve the detection of sediment concentrations near or below 10 mg L^{-1}. The high-end detection, especially for bedload, could potentially be improved by using a transducer with a range between the 1 and 69 hPa sensors tested in this study. These steps would ensure reliable, remote, and *in situ* estimations of the concentration of suspended sediments in a body of water. Improved estimates of sediment load can then be made that reflect the spatial and temporal character of sediment flux.

REFERENCES

Calhoun, D.L., 2000, *In situ* monitoring of suspended sediments: Development of a densimetric instrument: unpublished Master's Thesis, The University of Georgia, 73 p.

Chang, H.H., 1988, Fluvial Processes in River Engineering: J. Wiley and Sons, Inc., New York, 432 p.

Lewis, A.J., and Rasmussen, T.C., 1999, Determination of suspended sediment concentrations and particle size distributions using pressure measurements: Journal of Environmental Quality, v. 28, no. 5, p. 1490-1496.

Lewis, J, 1991, An improved bedload sampler: *In* Fan, S. and Y.H. Kuo, eds., Proceedings of the Fifth Federal Interagency Sedimentation Conference, Las Vegas, NV, p. 18-21.

Reid, I., Layman, J.R., and Frostick, L.E., 1980, The continuous measurement of bedload discharge: Journal of Hydraulic Research, v. 18, n. 3, p. 243-249.

Skinner, J.V, 1989, Model-B sediment-concentration gage: Factors influencing its readings and a formula for correcting its errors, A study of methods used in measurement and analysis of sediment loads in streams: Federal Interagency Sedimentation Project Report JJ, US Army Corps of Engineers, 34 p.

Skinner, J.V. and Beverage, J.P., 1982, A fluid-density gage for measuring suspended sediment concentration. A study of methods used in measurement and analysis of sediment loads in streams: Federal Interagency Sedimentation Project Report X, US Army Corps of Engineers, 125 p.

Skinner, J.V., Beverage, J.P., and Goddard, G.L., 1986, Continuous measurement of suspended sediment concentration: *In* Proceedings of the Fourth Federal Interagency Sedimentation Conference, Las Vegas, Nev., p. 29-39.

Contact Information

Daniel L. Calhoun, Hydrologist, U.S. Geological Survey, 3039 Amwiler Road, Suite 130, Atlanta GA 30360-2824, dcalhoun@usgs.gov, 770.903.9144, 770.903.9199 (fax).

Todd C. Rasmussen, Associate Professor of Hydrology, Warnell School of Forest Resources, Athens GA, 30602-2152, trasmuss@smokey.forestry.uga.edu, 706.542.4300, 706.542.8356 (fax).

[1] The use of firm, trade, or brand names is for identification purposes only and does not constitute endorsement by the U.S. Geological Survey or by the University of Georgia.

CONTINUOUS TURBIDITY MONITORING AND REGRESSION ANALYSIS TO ESTIMATE TOTAL SUSPENDED SOLIDS AND FECAL COLIFORM BACTERIA LOADS IN REAL TIME

By Victoria G. Christensen, Andrew C. Ziegler, and Xiaodong Jian
Hydrologists, U.S. Geological Survey, 4821 Quail Crest Place, Lawrence, KS 66049

Abstract: *To obtain timely and continuous water-quality information, the U.S. Geological Survey, in cooperation with State and other Federal agencies, has been using an innovative real-time monitoring approach for several Kansas streams. Continuously recorded data and data from periodic collection of water-quality samples are being used to develop surrogate relations between turbidity and constituents of concern. Regression equations were developed to estimate total suspended solids and fecal coliform bacteria from continuous turbidity measurements collected from 1995 through 1998 on the Little Arkansas River in south-central Kansas. The equations were applied to data collected in 1999 to estimate constituent loads. Estimated total suspended solids loads were 460 and 613 million pounds per year for the two sites in the study. Estimated fecal coliform bacteria loads were 30,000,000 and 32,000,000 billions of colonies per year. Despite some large differences between instantaneous measured and regression-estimated loads, continuous monitoring of turbidity in streams may increase the accuracy of load estimates that may be useful for calculating total maximum daily loads (TMDL's). The availability of this data in real time also may be useful for considering whole-body contact and recreation criteria, for adjusting water-treatment strategies, and for preventing adverse effects on fish or other aquatic life.*

INTRODUCTION

Historically, the U.S. Geological Survey's (USGS) stream-gaging network has provided timely water-quantity information to resource managers and others to make informed decisions about floods and water availability. It has not been possible, however, to provide water-quality information in the same timely manner. Timely water-quality information is useful for many reasons, including assessment of the effects of urbanization and agriculture on a water supply.

Nationally, the U.S. Environmental Protection Agency (USEPA) lists both suspended solids and bacteria as primary water-quality concerns. Suspended solids can cause problems for fish by clogging gills and for aquatic plants by reducing light penetration and thus limiting growth. In addition, suspended solids provide a medium for the accumulation and transport of other constituents such as phosphorus and bacteria. The presence of fecal coliform bacteria in surface water indicates fecal contamination and possibly the presence of other organisms that could cause disease.

In the past, to determine concentrations of total suspended solids and fecal coliform bacteria in a stream, it was necessary to manually collect samples and send them to a laboratory for analysis. This procedure took time, and when human health is a concern, immediate information is necessary. In addition, because manually collected samples did not provide continuous data, constituent loads during peak flows often were missed, making accurate load estimates difficult. Load estimates are important to the establishment and monitoring of total maximum daily loads (TMDL's) mandated by the Clean Water Act of 1972.

In response to the need for timely and continuous water-quality information, the USGS, in cooperation with State and other Federal agencies, has been using an innovative continuous, real-time monitoring approach for several Kansas streams. This paper describes results of a study to provide continuous estimates of real-time total suspended solids and fecal coliform bacteria loads for the Little Arkansas River, which is used as a source water for artificial recharge of the *Equus* Beds aquifer. The *Equus* Beds aquifer provides approximately 50 percent of the drinking water for the city of Wichita in south-central Kansas.

METHODS

To assess the quality of the Little Arkansas River, in-stream water-quality monitors were installed in 1998 at two U.S. Geological Survey stream-gaging stations near Halstead and Sedgwick, Kansas (fig. 1), to provide continuous, real-time measurement of turbidity and other physical properties of water. Periodic water samples were collected manually from 1995 through 1998 at the two gaging stations and analyzed for selected constituents and physical properties including turbidity, total suspended solids (TSS), and fecal coliform bacteria.

The manual samples were collected throughout the year and throughout 95 percent of the stream's typical flow duration to describe a wide range of seasonal and hydrologic conditions. Sampling techniques are described in Ziegler and Combs (1997). Linear regression equations were developed using the least-squares method.

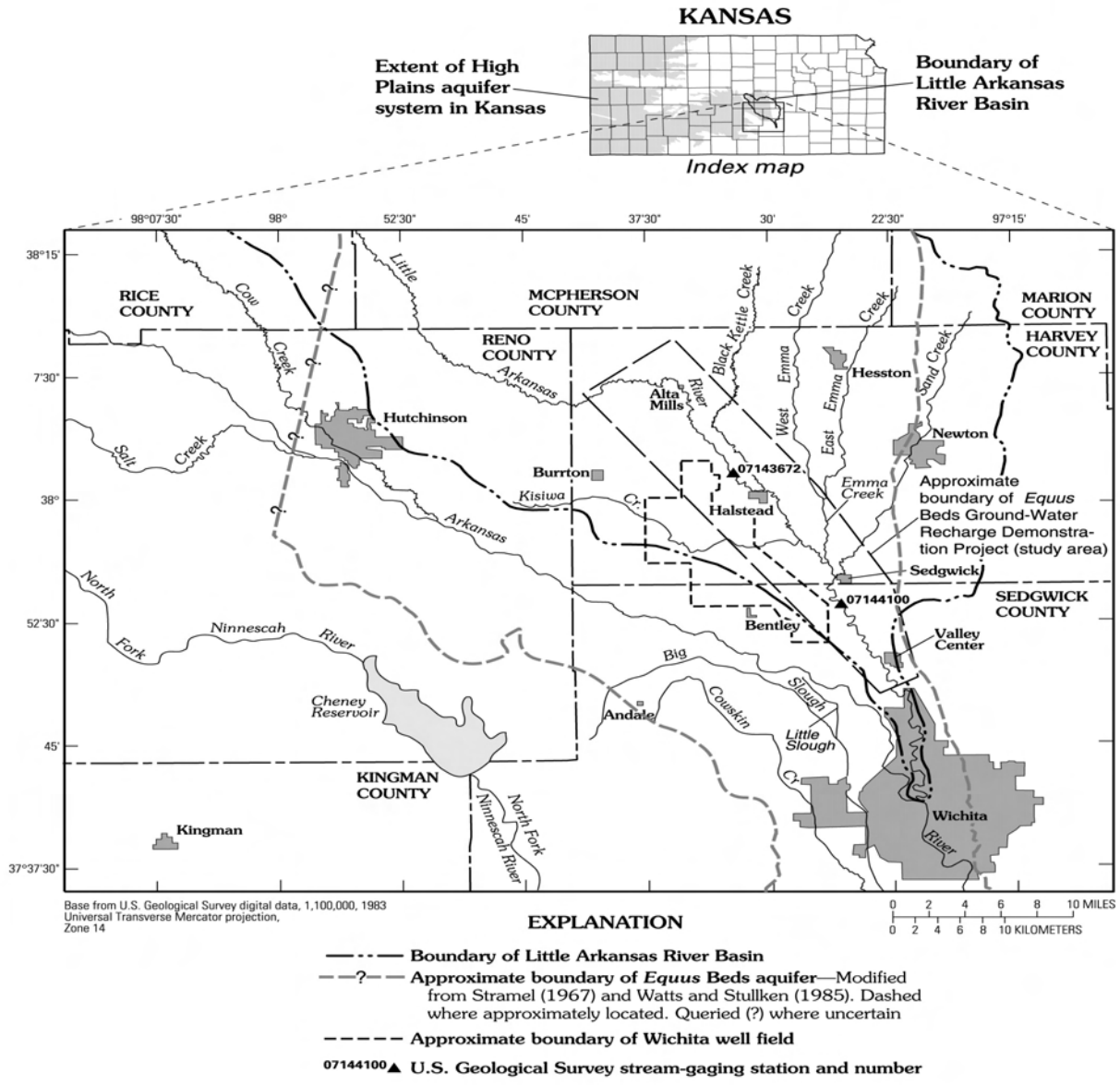

Figure 1. Location of study area in south-central Kansas

To test the regression equations developed from the first 3 years of data collection (1995-98), the equations were applied to the fourth year of data collection (1999) to calculate estimated instantaneous constituent loads and errors associated with these loads. Additional information on methods related to this study can be found in Ziegler and Combs (1997), Ziegler and others (1999), and Christensen and others (2000). Current information on continuous, real-time water quality in Kansas may be accessed through the World Wide Web at http://ks.water.usgs.gov/Kansas/qw.

RESULTS

Turbidity Measurement: Turbidity can be an indicator of the amount of sediment and related constituents transported by a stream. Turbidity and streamflow are related (fig. 2) because streamflow can affect suspension of the sediment and related constituents. Continuous and periodic monitoring enable identification of seasonal trends and effects of extreme hydrologic conditions on turbidity, TSS, and fecal coliform bacteria and estimation of chemical loads transported in the Little Arkansas River. High flows have a significant effect on chemical loads, and concentration data from manual samples often are not available. Therefore, continuous monitoring of turbidity for the estimation of TSS and fecal coliform bacteria in streamflow may increase the accuracy of load estimates. Manual samples were collected using depth- and width-integrating techniques, and because a real-time water-quality monitor

measures the turbidity at a single point in the stream, there was some difference between turbidity of water samples collected manually across the width and depth of the stream and turbidity from the real-time water-quality monitor. Turbidity measurements were not adjusted to account for this small difference.

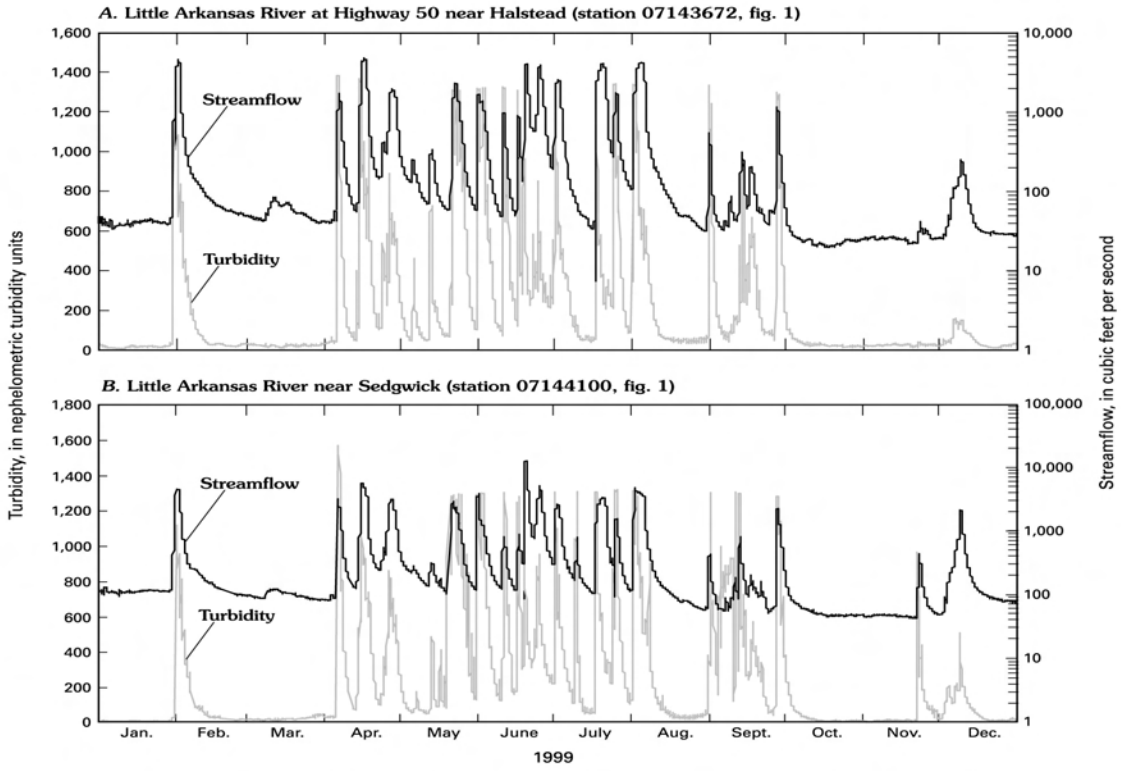

Figure 2. Comparison of turbidity and streamflow for Little Arkansas River (A) at Highway 50 near Halstead and (B) near Sedgwick, Kansas, 1999.

Total Suspended Solids: Total suspended solids (TSS) include both suspended sediment and organic material collected with the water sample. The significance of organic material with respect to the determination of sediment concentration is minimal in most drainage basins (Guy, 1969). In this study, analysis for suspended sediment began in January 1999 and was not used to develop the regression equations. However, regression analysis of samples collected in 1999 indicate that the relation between *TSS* and total suspended sediment is highly correlated (V. Christensen, USGS, written commun., 2000).

At the Halstead gaging station there is a linear relation between TSS and turbidity after logarithmic transformation. Graphic plots of this relation indicate that there are two outliers (the minimum and maximum turbidity values of 0.3 and 1,780 nephelometric turbidity unit (NTU), respectively). To decrease the effects of these outliers, these two points were not used in the regression equation. The range in turbidity values used to develop the equation for the Halstead gaging station was 4.69 to 1,150 NTU. The final linear regression equation for Halstead is:

$$log_{10}(TSS) = 0.920 log_{10}(Turb) + 0.243, \quad (1)$$

where *TSS* is estimated total suspended solids, in milligrams per liter, and *Turb* is turbidity, in nephelometric turbidity units. The mean square error (MSE) for the equation is 0.193, and the coefficient of determination (R^2) is 0.911.

At the Sedgwick gaging station there were three outliers with turbidity values of 3.99, 5.01, and 1.44 NTU. The range in turbidity values used to develop the equation was 3.63 to 1,030 NTU. The final linear regression equation after logarithmic transformation for Sedgwick is:

$$log_{10}(TSS) = 0.878 log_{10}(Turb) + 0.300, \quad (2)$$

where *TSS* is estimated total suspended solids, in milligrams per liter, and *Turb* is turbidity, in nephelometric turbidity units. The MSE for the Sedgwick equation is 0.209, and the R^2 is 0.889.

The relation between TSS and turbidity is similar for the Halstead and Sedgwick gaging stations. In addition, it appears there is very little improvement to the relation with the addition of samples. For example, 19 samples collected throughout the range in hydrologic conditions may be sufficient to define the relation between TSS and turbidity (table 1). Changes in TSS load generally are affected by changes in streamflow (Topping and others, 2000), and thus, load shows a seasonal fluctuation (fig. 3).

Table 1. Sample-size effect on improving sum of squares of error (SSE) for the surrogate-based total suspended solids equation

[R^2, coefficient of determination; SSE, sum of the squares of error; %, percent; --, not determined]

Calendar year	Little Arkansas River at Highway 50 near Halstead (station 07143672, fig. 1)				Little Arkansas River near Sedgwick (station 07144100, fig. 1)			
	Total number of samples	R2	SSE	Change in SSE (%)	Total number of samples	R2	SSE	Change in SSE (%)
1995	19	0.907	2.79	--	19	0.881	3.24	--
1996	41	.908	2.78	-0.36	35	.879	3.28	1.23
1997	58	.909	2.75	-1.08	51	.885	3.12	-4.88
1998	74	.911	2.69	-2.18	71	.889	3.01	-3.53

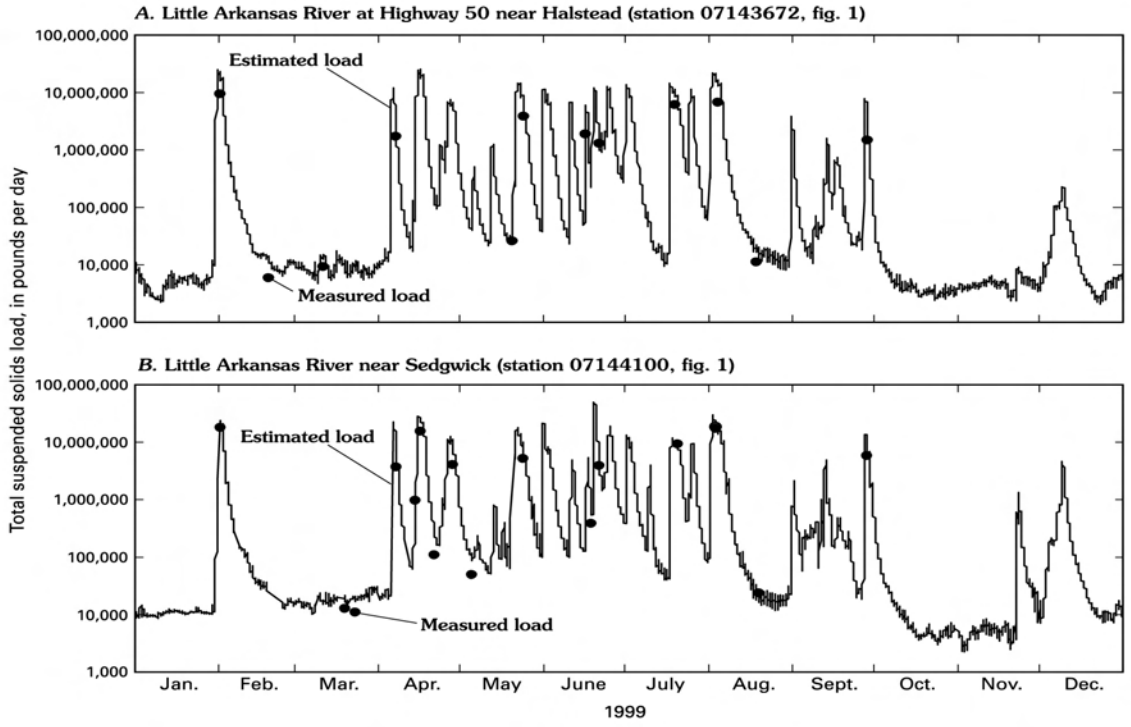

Figure 3. Comparison of measured and estimated total suspended solids load for Little Arkansas River (A) at Highway 50 near Halstead and (B) near Sedgwick, Kansas, 1999.

The median relative percentage differences between measured (calculated from manual samples) and estimated TSS loads were 66.4 and 34.0 percent at the Halstead and Sedgwick gaging stations, respectively (Christensen and others, 2000). There was a large difference between estimated TSS loads at the upstream (Halstead) and downstream (Sedgwick) gaging stations (460 million and 613 million pounds in 1999, respectively) as expected. Turbidity and TSS may be altered significantly between the Halstead and Sedgwick gaging stations due to inflow of intervening drainages, Kisiwa, Emma, and Sand Creeks (fig. 1). Although the 1999 estimated TSS load was larger at the Sedgwick gaging station, the Halstead gaging station had the larger estimated TSS yield (1,050 pounds per acre compared to 826 pounds per acre). The relatively small load contribution of the intervening drainage area (fig. 4)

may be because of storage of solids and sediment in the streambed between the Halstead and Sedgwick gaging stations or because the inflow of Kisiwa, Emma, and Sand Creeks may have a dilution effect on TSS at the Sedgwick gaging station.

Fecal Coliform Bacteria: Total coliform bacteria was identified by Ziegler and others (1999) as a constituent of concern in the Little Arkansas River during high flows. The equations in this paper are based on fecal coliform bacteria, one of the bacteria included in a total coliform analysis. Fecal coliform bacteria analyses were chosen for inclusion in this paper because current (2000) State of Kansas water-quality criteria [2,000 col/100 mL (colonies per 100 milliliters of water) for noncontact recreation, 200 col/100 mL for whole-body contact recreation, and less than 1 col/100 mL for drinking water] are based on fecal coliform bacteria densities (Kansas Department of Health and Environment, 1999). Because runoff from a watershed may transport fecal coliform bacteria to streams, there may be a relation between bacteria densities and streamflow or possibly to time of year because runoff characteristics may vary with season. However, only month (time) and turbidity were found to be significantly related to fecal coliform bacteria.

The range in turbidity values used in the development of the equation for fecal coliform bacteria at the Halstead gaging station was 0.3 to 1,780 NTU. The multiple regression equation with logarithmic transformation for Halstead is:

$$\log_{10}(Bact) = 0.490\ \cos(2p(\frac{month + 2.06}{8.76})) + 0.00106\ Turb + 0.417\ \log_{10}(Turb) + 1.65 \quad (3)$$

where *Bact* is fecal coliform bacteria density, in colonies per 100 milliliters of water; *month* is a number from 1 to 12; and *Turb* is turbidity, in nephelometric turbidity units. This equation has an MSE of 0.609 and R^2 of 0.620.

For the Little Arkansas River near Sedgwick, the range in turbidity values used in the development of the regression equation for fecal coliform bacteria was 1.44 to 1,030 NTU, The final multiple regression equation for fecal coliform bacteria with logarithmic transformation for Sedgwick is:

$$\log_{10}(Bact) = -0.286\ \cos(2p(\frac{month - 29.4}{-6.8})) - 0.000422\ (Turb) + 1.26\ \log_{10}(Turb) + 0.519 \quad (4)$$

where *Bact* is fecal coliform bacteria density, in colonies per 100 milliliters of water; *month* is a number from 1 to 12; and *Turb* is turbidity, in nephelometric turbidity units. This equation has an MSE of 0.784 and R^2 of 0.556.

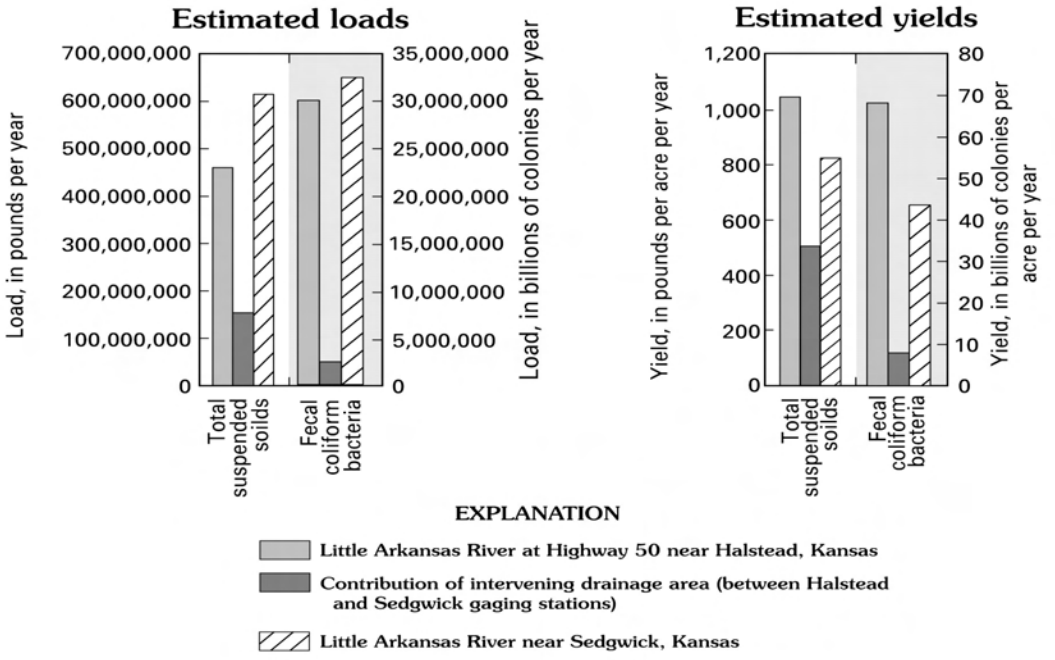

Figure 4. Comparison of estimated loads and yields for total suspended solids and fecal coliform bacteria for Little Arkansas River at Highway 50 near Halstead and near Sedgwick, Kansas, 1999.

The periodic cosine function is used in the bacteria equations for both stations with the period equal to 8.76 and 6.8 months, respectively. The physical basis for this period or cycle is related to the seasonal variability of fecal coliform bacteria in streams. Cattle are one of the sources of fecal coliform bacteria in the Little Arkansas River Basin. High fecal coliform bacteria densities occur at least twice during the year. During the spring when there is considerable rainfall, runoff from cattle-producing areas may result in large amounts of fecal coliform bacteria reaching streams. At the other end of the seasonal cycle, fecal coliform bacteria densities can be high in the dry, late fall and winter months when the cattle congregate near streams.

For both the Halstead and Sedgwick gaging stations, the second year of data collection offered a significant improvement in the sum of squares of error (SSE). The SSE did not improve significantly for either gaging station after 1996 (table 2). Although 2 years of data were sufficient to define this relation at these two gaging stations, this does not mean that 2 years of data collection would be sufficient to define this relation at other sites.

The regression equation for fecal coliform bacteria cannot estimate extreme fecal coliform bacteria densities that sometimes occur as a result of spills or point-source contamination. The estimates from the regression equation are similar to measured densities for smaller bacteria values that may occur as a result of nonpoint-source contamination, such as livestock production. However, if a spill, such as a breached waste lagoon, contributes to the bacteria density, the regression equation cannot estimate this accurately.

Relative percentage differences between measured and estimated loads were 242 percent at the Halstead gaging station and 83.7 percent at the Sedgwick gaging station (Christensen and others, 2000). These large differences are due not only to error in the regression, but also to the amount of error involved in the laboratory analysis of fecal coliform bacteria. Standard methods for analyzing bacteria can have several substantial sources of error such as the length of time before sample analysis, exposure to direct sunlight, temperature during storage, presence of different types of bacteria, and errors in the enumeration of colonies.

Estimated fecal coliform bacteria loads were slightly larger for the Sedgwick gaging station than for the Halstead station (32,400,000 and 30,000,000 billion colonies per year, respectively), and estimated yields were larger for the Halstead station than for the Sedgwick station (68.3 and 43.7 billions of colonies per acre per year, respectively) (fig. 4).

Although samples were collected during a wide range of streamflows, some of the differences between the measured (calculated from manually collected samples) and estimated bacteria loads (fig. 5) could be due to factors other than turbidity. Examples of such factors include manure application, feedlot runoff, sewage-treatment-plant discharges, precipitation characteristics, soil characteristics, and topography.

The dependent variables in equations 1 through 4 were transformed; therefore, consideration must be given to retransformation bias when interpreting the results of the regression analysis. The retransformation has no effect on the form of the equations or on the error associated with the equations. However, retransformation can cause an underestimation of TSS and fecal coliform bacteria loads when adding individual load estimates over a long period of time. Cohn and others (1989), Gilroy and others (1990), and Hirsch and others (1993) provide additional information on the interpreting the results of regression-based load estimates.

Table 2. Sample-size effect on improving sum of squares of error (SSE) for surrogate-based fecal coliform bacteria equation

[R^2, coefficient of determination; SSE, sum of the squares of error;%, percent; --, not determined]

	Little Arkansas River at Highway 50 near Halstead (station 07143671)				Little Arkansas River near Sedgwick (station 07144100, fig. 1)			
Calendar year	Total number of samples	R^2	SSE	Change in SSE (%)	Total number of samples	R^2	SSE	Change in SSE (%)
1995	20	-0.574	75.5	--	18	0.043	94.1	--
1996	42	.578	30.1	-60.1	36	.567	42.6	-54.7
1997	58	.606	28.1	-6.64	50	.593	40.0	-6.10
1998	75	.620	27.1	-3.56	73	.556	43.6	9.00

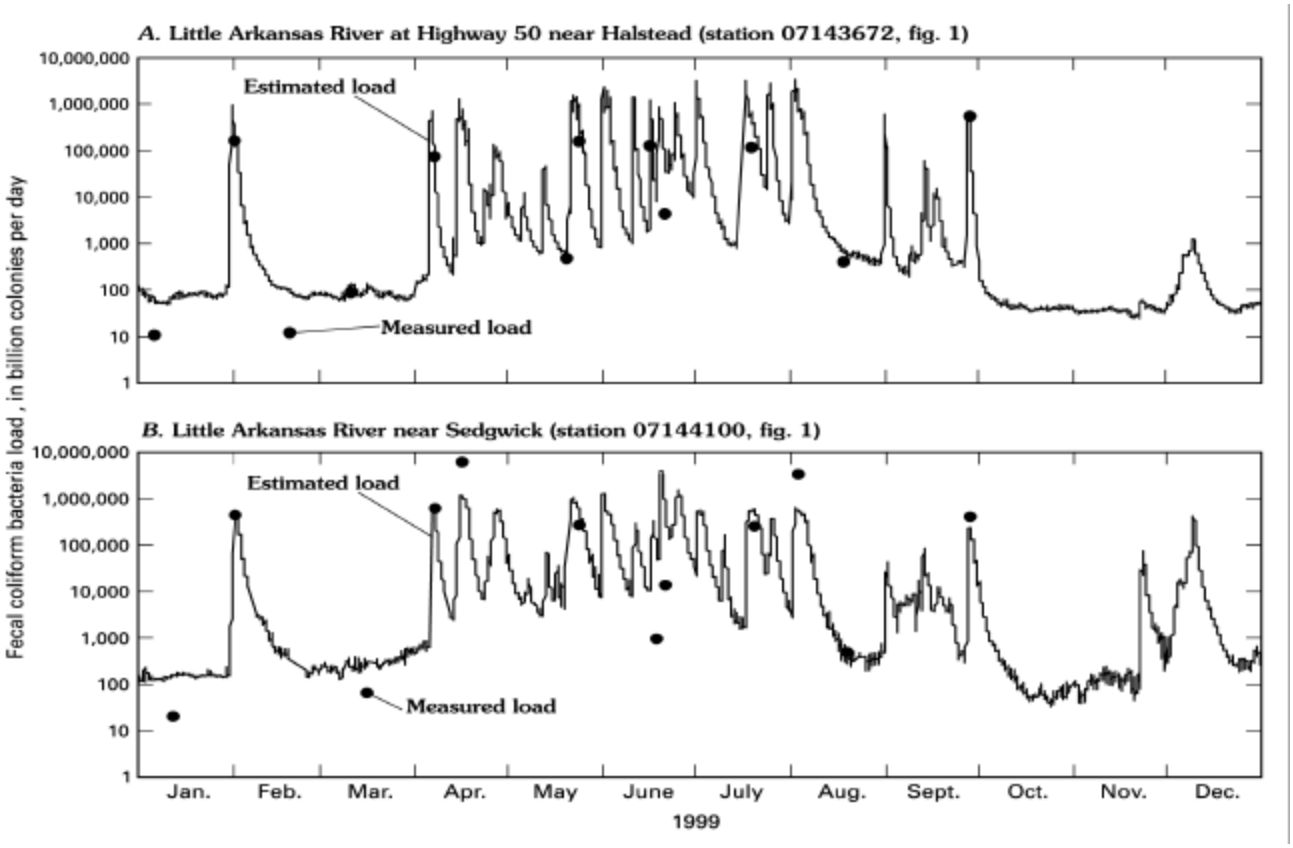

Figure 5. Comparison of measured and estimated fecal coliform bacteria loads for Little Arkansas River (A) at Highway 50 near Halstead and (B) near Sedgwick, Kansas, 1999.

DISCUSSION AND CONCLUSIONS

Continuous and periodic monitoring have allowed the identification of trends in turbidity, TSS, and fecal coliform bacteria and the estimation of chemical load transported in the Little Arkansas River. Varying chemical concentrations during high flows have a substantial effect on calculated chemical loads, and concentration data from manual samples often are not available for these conditions. Therefore, continuous monitoring of turbidity for the estimation of TSS and fecal coliform bacteria in streamflow may increase the acuracy of load estimates.

The regression-estimated mean daily loads of TSS and fecal coliform bacteria may be more reflective of actual loads than the calculated loads from periodic manually collected data because of the continual nature of the in-stream data. There are few or no gaps in the real-time monitoring of turbidity, except in the case of water-quality monitor malfunction. On the other hand, TSS and bacteria calculated loads from manually collected samples are based on approximately 10 to 15 discrete samples collected throughout the year, and peaks in bacteria densities may have been missed.

In addition to the utility of the regression equations to the city of Wichita for recharge purposes, they also may be useful for calculating total maximum daily loads (TMDL's), which the State of Kansas is mandated to establish for stream segments that have been identified by section 303 (d) of the 1972 Clean Water Act as limited for specific uses because of water-quality concerns. With the development of surrogate relations between continuous turbidity measurements and periodic collection of samples for analysis of TSS and fecal coliform bacteria, a more accurate representation of actual daily loads is probable.

Information on loads and yields may be an indication of which subbasin in which to concentrate efforts with regard to land-resource best-management practices (BMP's). Estimated TSS loads were 460 and 613 million pounds per year for the Halstead and Sedgwick gaging stations, respectively. Estimated fecal coliform bacteria loads were 30,000,000 and 32,000,000 billions of colonies per year. Constituent loads alone are more substantial at the

Sedgwick gaging station due to its downstream location and thus higher streamflows. However, when estimated yields are compared, the Halstead subbasin has much higher yields for both constituents. This information can be used by resource managers to prioritize implementation of BMP's.

In addition to the continuous nature of the turbidity data, the data also are available in real time. The timely availability of TSS and fecal coliform bacteria data may be important when considering whole-body contact and recreation criteria for a water body; water suppliers would have timely information to use in adjusting water-treatment strategies; and environmental effects could be assessed in time to prevent adverse effects on fish or other aquatic life.

REFERENCES

Christensen, V.G., Jian, Xiaodong, and Ziegler, A.C., 2000, Regression Analysis and Real-Time Water-Quality Monitoring to Estimate Constituent Loads and Yields in the Little Arkansas River, South-Central Kansas, 1995–99. U.S. Geological Survey Water Resources Investigations Report 00–4126, 36 p.

Cohn, T.A., DeLong, L.L., Gilroy, E.J., Hirsch, R.M., and Wells, D., 1989, Estimating Constituent Loads. Water Resources Research, v. 25, no. 5, p. 937–942.

Gilroy, E.J., Hirsch, R.M., and Cohn, T.A., 1990, Mean Square Error of Regression-Based Constituent Transport Estimates. Water Resources Research, v. 26, no. 9, p. 2069–2077.

Guy, H.P., 1969, Laboratory Theory and Methods for Sediment Analysis. U.S. Geological Survey Techniques of Water-Resources Investigations, book 5, chap. C1, 58 p.

Hirsch, R.M., Helsel, D.R., Cohn, T.A., and Gilroy, E.J., 1993, Statistical Analysis of Hydrologic Data, *in* Maidment, D.R., ed., Handbook of Hydrology. New York, McGraw-Hill, Inc., p. 17.1–17.55.

Kansas Department of Health and Environment, 1999, List of Water Quality Limited Stream Segments Impacted Predominantly by Nonpoint and Point Sources. accessed March 2, 2000, at URL http://www.kdhe.state.ks.us/befs/303d/table1.htm

Stramel, G.J., 1967, Progress Report on the Ground-Water Hydrology of the Equus Beds Area, Kansas, 1966. Kansas Geological Survey Bulletin 187, part 2, 27 p.

Topping, D.J., Rubin, D.M., Nelson, J.M., Kinzel, P.J., III, and Corson, I.C., 2000, Colorado River Sediment Transport, Part 2. Systematic Bed-Elevation and Grain-Size Effects of Sandy Supply Limitation. Water Resources Research, February 2000, v. 36, no. 2, p. 543.

Watts, K.R., and Stullken, L.E., 1985, Generalized Configuration of the Base of the High Plains Aquifer in Kansas. U.S. Geological Survey Open-File Report 81–344, 1 sheet, scale 1:500,000.

Ziegler, A.C., Christensen, V.G., and Ross, H.C., 1999, Preliminary Effects of Artificial Recharge on Ground-Water Quality, 1995–98—*Equus* Beds Ground-Water Recharge Demonstration Project, South-Central Kansas. U.S. Geological Survey Water-Resources Investigations Report 99–4250, 74 p.

Ziegler, A.C., and Combs, L.J., 1997, Baseline Data-Collection and Quality-Control Protocols and Procedures for the *Equus* Beds Ground-Water Recharge Demonstration Project near Wichita, Kansas, 1995–96. U.S. Geological Survey Open-File Report 97–235, 57 p.

CONTINUOUS AUTOMATED SENSING OF STREAMFLOW DENSITY AS A SURROGATE FOR SUSPENDED-SEDIMENT CONCENTRATION SAMPLING

Matthew C. Larsen[1], Hydrologist, Carlos Figueroa Alamo[1], Hydrologist, John R. Gray[2], Hydrologist, and William Fletcher[3], Engineer
[1]U.S. Geological Survey, GSA Center, Guaynabo, PR, 00965, mclarsen@usgs.gov,
[2] U.S. Geological Survey, Reston, VA, 20192
[3]Design Analysis Associates, Inc., Logan, UT, 84321

Abstract A newly refined technique for continuously and automatically sensing the density of a water-sediment mixture is being tested at a U.S. Geological Survey streamflow-gaging station in Puerto Rico. Originally developed to measure crude oil density, the double bubbler instrument measures fluid density by means of pressure transducers at two elevations in a vertical water column. By subtracting the density of water from the value measured for the density of the water-sediment mixture, the concentration of suspended sediment can be estimated. Preliminary tests of the double bubbler instrument show promise but are not yet conclusive.

INTRODUCTION

Suspended sediment is the most common contaminant of surface water in the world. Sediment particles can reduce the quality of potable water supplies; increase filtration and treatment costs for drinking water; damage hydroelectric turbines; degrade fluvial, lacustrine, estuarine, and marine habitats; and serve as a transport mechanism for a variety of trace elements, herbicides, insecticides, and other toxic substances (Douglas, 1990). Concentrations of suspended sediment in fluvial systems tend to be relatively large in settings with extensive loess deposits, semi-arid environments with little vegetation, and steeply sloping areas of the humid tropics. Many of the world' s highest sediment yields, however, are recorded in human-disturbed regions (Milliman and Meade, 1983). As human populations exploit increasingly fragile environments, the problems associated with fluvial-sediment transport and deposition have worsened.

Monitoring daily and annual suspended-sediment yield is costly and time consuming. For example, the current annual (2000) cost for the U.S. Geological Survey (USGS) to collect and publish daily stream flow and suspended-sediment data at a station is rarely less than $20,000, and in some cases can be nearly triple that, depending on such factors as site location, types and frequency of data collection, size distribution of suspended sediments, and hydraulic characteristics of the reach. The standard monitoring procedure requires frequent manual and (or) automated sampling, particularly during high flows, followed by laboratory processing and subsequent analysis of large data sets. Less costly, safer, and more accurate techniques for measuring sediment discharges in streams are being conceived and developed. Although several techniques show considerable promise (Wren and others, 2000), none is certified by the Federal Interagency Sedimentation Project (U.S. Geological Survey, 2000) as an adequate replacement for conventional sampling methods, nor is deployed as part of a large operational network in the United States.

A newly refined instrument for continuously and automatically measuring the density of the water-sediment mixture as a surrogate for suspended-sediment concentration, referred to as a

double bubbler instrument by the manufacturer, is being tested at a USGS streamflow-gaging station in Puerto Rico. This paper describes a double bubbler instrument for measuring suspended-sediment concentrations for use in sediment-discharge estimates and provides preliminary results from field tests of the instrument that began in October 1999.

RIO CAGUITAS, PUERTO RICO

The Río Caguitas (USGS ID 50055225) sampling site has a 30.3-km^2 drainage area, and land cover is predominately urban and secondary forest (fig 1). The watershed is a sub-basin of the Río Grande de Loíza watershed, which contains the Loíza reservoir. This reservoir supplies about one half of the water supply for the San Juan metropolitan area, with a population of about one million (Molina-Rivera, 1998). Mean annual runoff for the period 1990 - 99 in the Río Caguitas watershed is 1,080 mm, and the flood of record had a peak discharge of 708 cubic meters per second (Díaz and others, 1999). Periods of substantial sediment-transport are frequent and can occur in any month of the year (fig. 2). Most of the annual sediment discharge occurs in runoff from a few storms when concentrations of suspended sediment exceed about 500 mg/L (fig. 3). Mean suspended-sediment yield for the period 1992-99 was about 1,340 tonnes/km^2-yr. To-date, the maximum suspended-sediment concentration measured at the site using conventional techniques is 17,700 mg/L.

DOUBLE BUBBLER INSTRUMENT

The double bubbler instrument measures the weight density, ?, of water by means of two immersed pressure-transducer orifices separated by 304.8 mm (12 in.) in a vertical column of water (fig. 4). Because the density of water increases with increased suspended-sediment concentration, the density data can be used as a relatively inexpensive and continuously measured surrogate for suspended-sediment concentrations obtained from analyses of water samples.

A constant mass flow of gas (dry air or nitrogen) to the two orifices submerged in the measurement fluid (water) is provided by a gas supply system (fig. 5). A water-temperature probe is placed near the bubble discharge orifices to provide the requisite data to correct for the effect of temperature on the density of pure water. The precision differential pressure measurement system developed by Design Analysis Associates, Logan, Utah[1] measures the pressure difference sensed at the two bubbler line orifices. Two solenoid valves feeding the differential unit are used to obtain offset and atmospheric correction for the actual pressure-sensing element. The pressure-sensing element produces a voltage value directly proportional to the pressure difference sensed at the orifices. Once ? has been evaluated, a reference density value (pure water, or stream water with a dissolved solids concentration typical of sediment-transporting runoff) is subtracted to calculate the weight density (concentration) of suspended sediment.

[1] Use of firm names in this report is for identification purposes only and does not constitute endorsement by the U.S. Geological Survey.

Differential hydrostatic pressure is recorded by a data logger at regular intervals and can be downloaded periodically or transmitted via satellite (fig. 5). The differential pressure values are converted to water-density values. Samples from which comparative suspended-sediment concentrations are determined by laboratory analysis are collected with a US DH-48 wading sampler during low stage and a US DH-59, US DH-77, or automatic pump sampler during high stage, based on methods described by Edwards and Glysson (1999). The suspended-sediment concentration data from samples are used to compare to density values computed from double bubbler instrument data. Laboratory testing of the double bubbler instrument was performed by the manufacturer using salt solutions with concentration in excess of 1,000 mg/L.

FIELD TRIALS

Initial double-bubbler-instrument data collected during October-December 1999, contain a large amount of signal noise that makes interpretation difficult. The data collected on 5-minute intervals were smoothed by stepwise averaging of 6 data points by using a 30-minute moving mean. Although this increased the serial correlation somewhat, a more sophisticated method for data analysis, not yet tested, is required and should include determination of minimum and maximum thresholds so that outliers can be discarded from the data set. To calculate the weight density of suspended sediment and dissolved solids, the weight density of pure water at 27 degrees C (996.515925 kg/m^3) was subtracted from the smoothed data value. Data collected after installation of a thermistor for temperature compensation in summer 2000 (several months after the initial installation) will be corrected for pure-water densities that are computed by using the recorded water-temperature values.

The first tests of the correspondence between discharge, suspended-sediment concentration, and water density, showed little agreement (fig. 6). A series of measurements made during a 3-month period in 1999 show that the double bubbler instrument values generally track substantial variations in suspended-sediment concentrations, but a large amount of signal noise remains.

A complicating factor for this method is turbulence in the water column, which introduces noise about equal to the signal of interest, particularly during high discharges when the largest sediment concentrations occur. Additionally, diurnal and storm-related fluctuations in water temperature must be accounted for by using a continuously logging temperature sensor. Differences of diurnal extremes in water temperatures measured at the Río Caguitas test site are as much as 10 degrees C. The high relative-humidity characteristic of this humid-tropical site may also complicate the use of the bubbler because of the sensitivity of the narrow diameter bubbler gas lines to moisture.

CONCLUSIONS

Initial testing of a double bubbler instrument for continuous automated sampling of streamflow density as a surrogate for suspended-sediment concentration sampling has proven to be a challenging task. Although some correspondence between double bubbler instrument data and measurements of discharge and suspended-sediment concentration is evident, additional field trials are needed. If adequate results can be achieved, substantial cost reduction in sediment monitoring programs can be realized.

REFERENCES

Díaz, Pedro L., Aquino, Zaida, Figueroa-Alamo, Carlos, Vachier, R.J., and Sanchez, A.V., 1999, Water Resources Data Puerto Rico and the U. S. Virgin Islands, Water Year 1999: U.S. Geological Survey Water-Data Report PR 99-1, 599 p.

Douglas, Ian, 1990, Sediment transfer and siltation in Turner, B.L., Clark, W.C., Kates, R.W., Richards, J.F., Mathews, J.T., and Meyer, W.B., The Earth as transformed by human action-- global and regional changes in the biosphere over the past 300 years: Cambridge University Press, New York, p. 215-234.

Edwards, T.K., and Glysson, G.D., 1999, Field methods for measurement of fluvial sediment: U.S. Geological Survey Techniques of Water-Resources Investigations Book 3, Chapter C2, 89 p.

Milliman, J.D., and Meade, R.H., 1983, World-wide delivery of river sediment to the oceans: Journal of Geology, v. 91, p. 1-21.

Molina-Rivera, W.L., 1998, Estimated water use in Puerto Rico, 1995: U.S. Geological Survey Open-file report 98-276, 28 p.

U.S. Geological Survey, 2000, Federal Interagency Sedimentation Project: Accessed August 16, 2000, at http://fisp.wes.army.mil/ .

Wren, D.G., Barkdoll, B.D., Kuhnle, R.A., and Derrow, R.W., 2000, Field techniques for suspended-sediment measurement: American Society of Civil Engineers, Journal of Hydraulic Engineering, Vol. 126, No. 2, pp. 97-104.

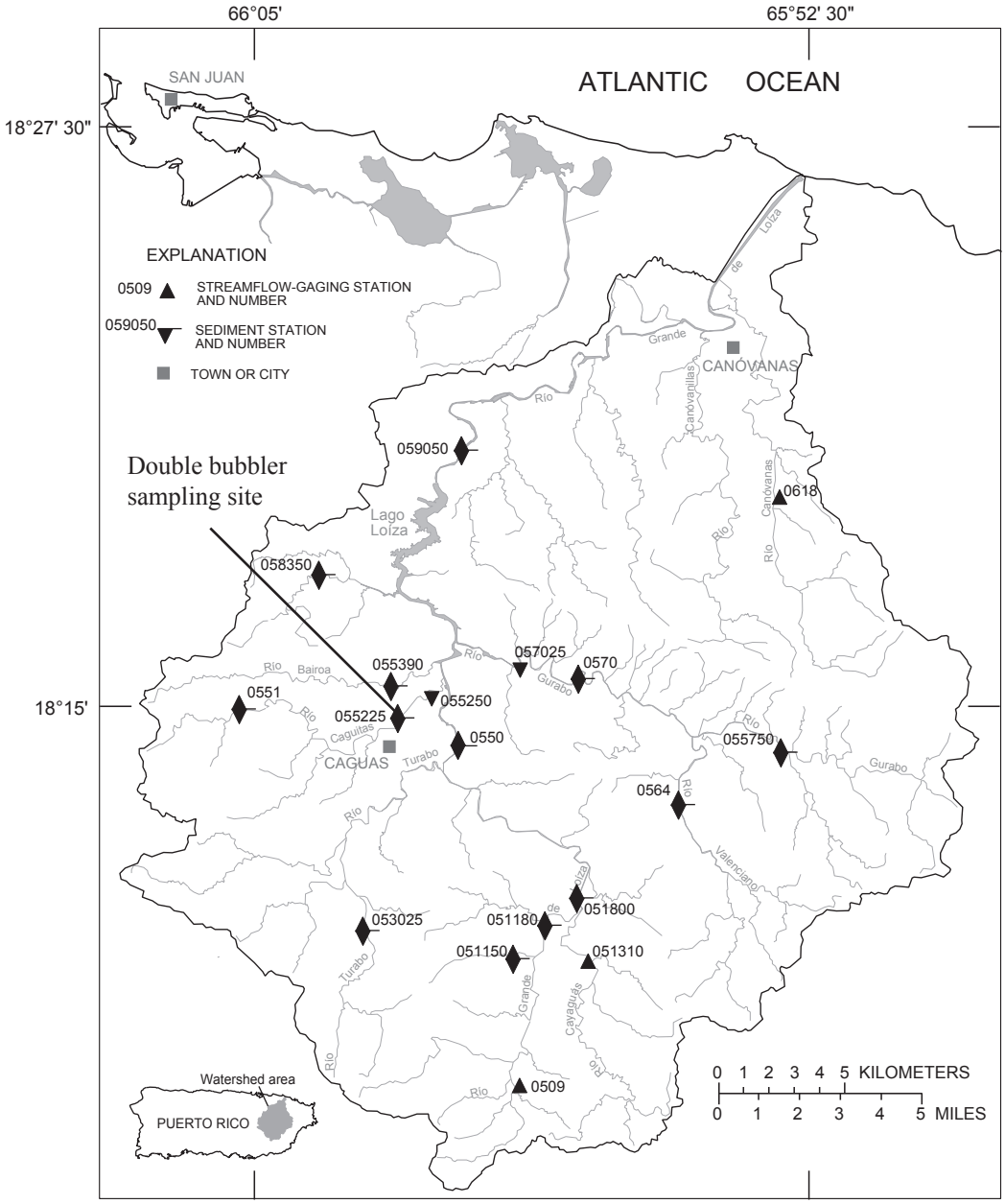

Figure 1. Location of the Río Caguitas (50055225) and other streamflow-gaging stations in the Río Grande de Loíza watershed, eastern Puerto Rico.

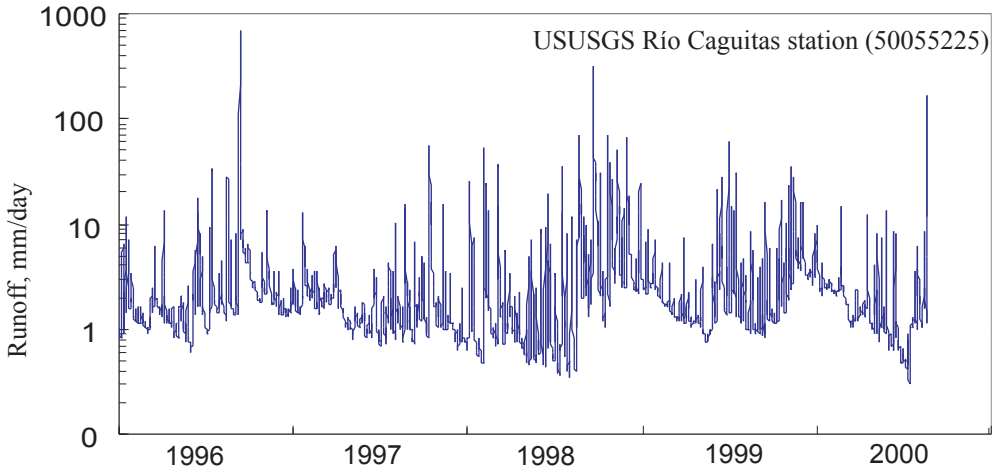

Figure 2. Daily mean runoff at Rio Caguitas, showing hight frequency and seasonal/inter-annual variability of streamflow events. Mean for period of record, 1990-99, equals 2.96 mm/day (1,080 mm/yr) (Diaz and others, 1999).

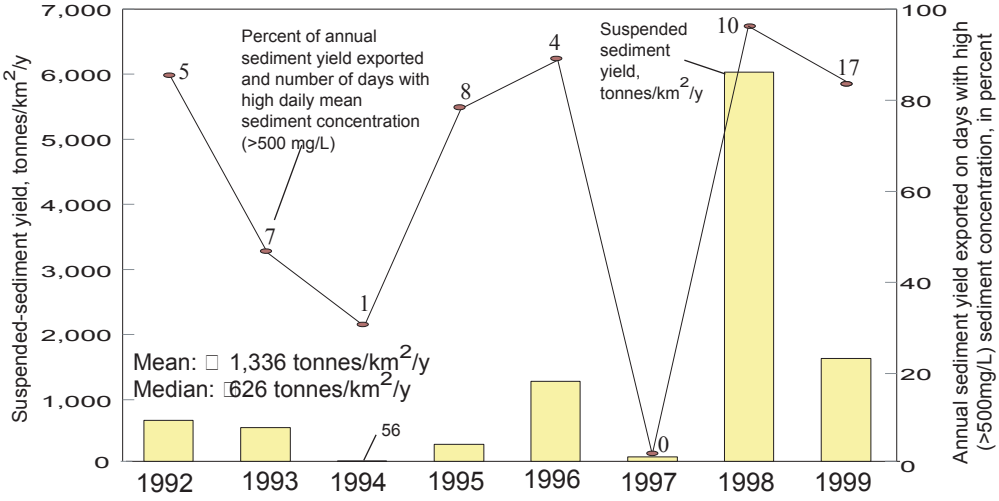

Figure 3. AAnnual suspended-sediment yield at Río Caguitas, USGS station 50055225, 1992-1999. IIn 6 of the 88years, about half or more of the suspended-sediment yield was exported on 2 to 5 percent of the days. The large yield in 1998 resulted from runoff associated with Hurricane Georges.

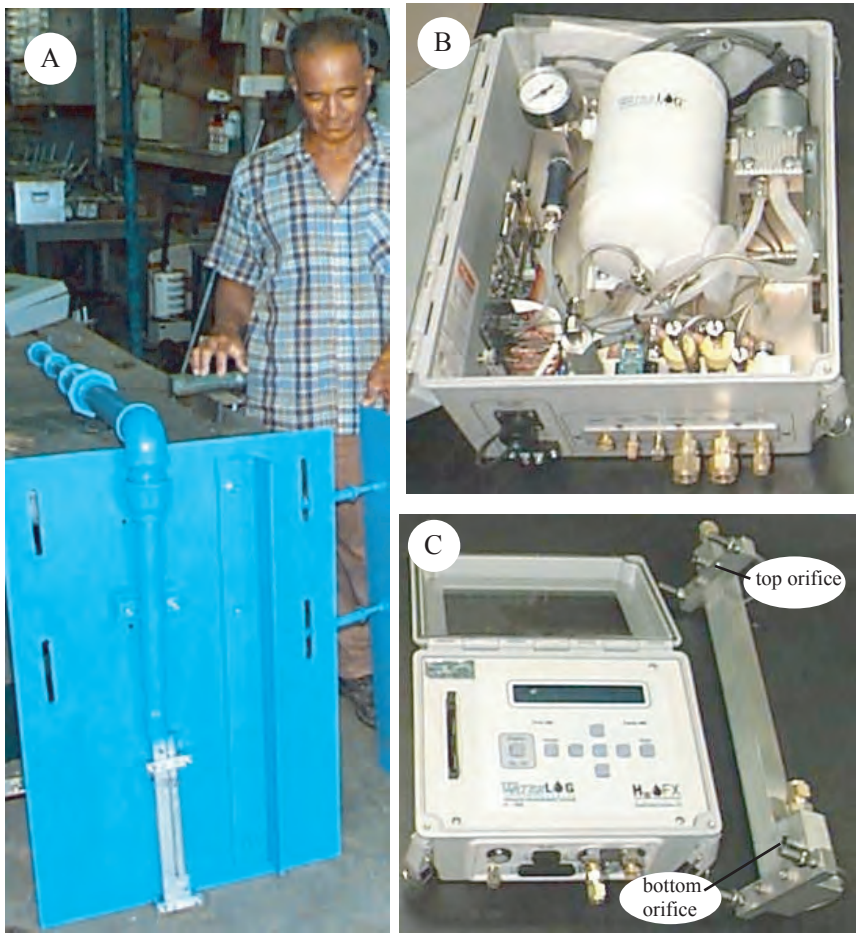

Figure 4. AA. Double bubbler and mounting plate. Angle iron on right protects instrument from transported debris. BB. Air compressor and hardware for generating bubbles. C. Data logger on left, double bubbler on right. Orifices are 3304.8 mm (12 in.) apart.

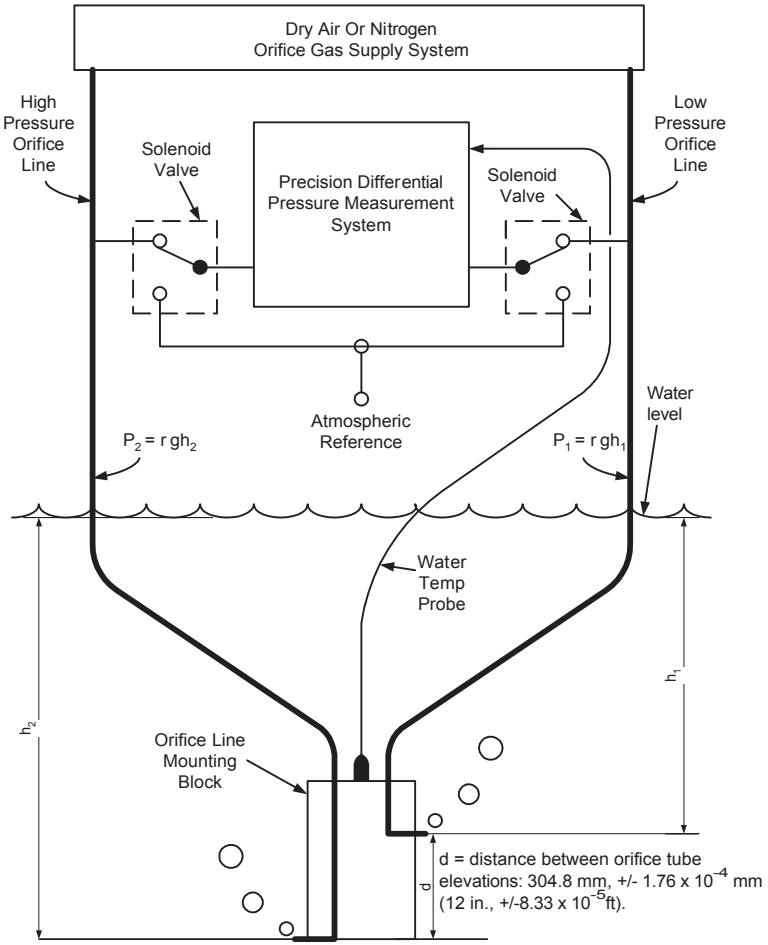

Figure 5. MModel of a double bubbler media determination system.

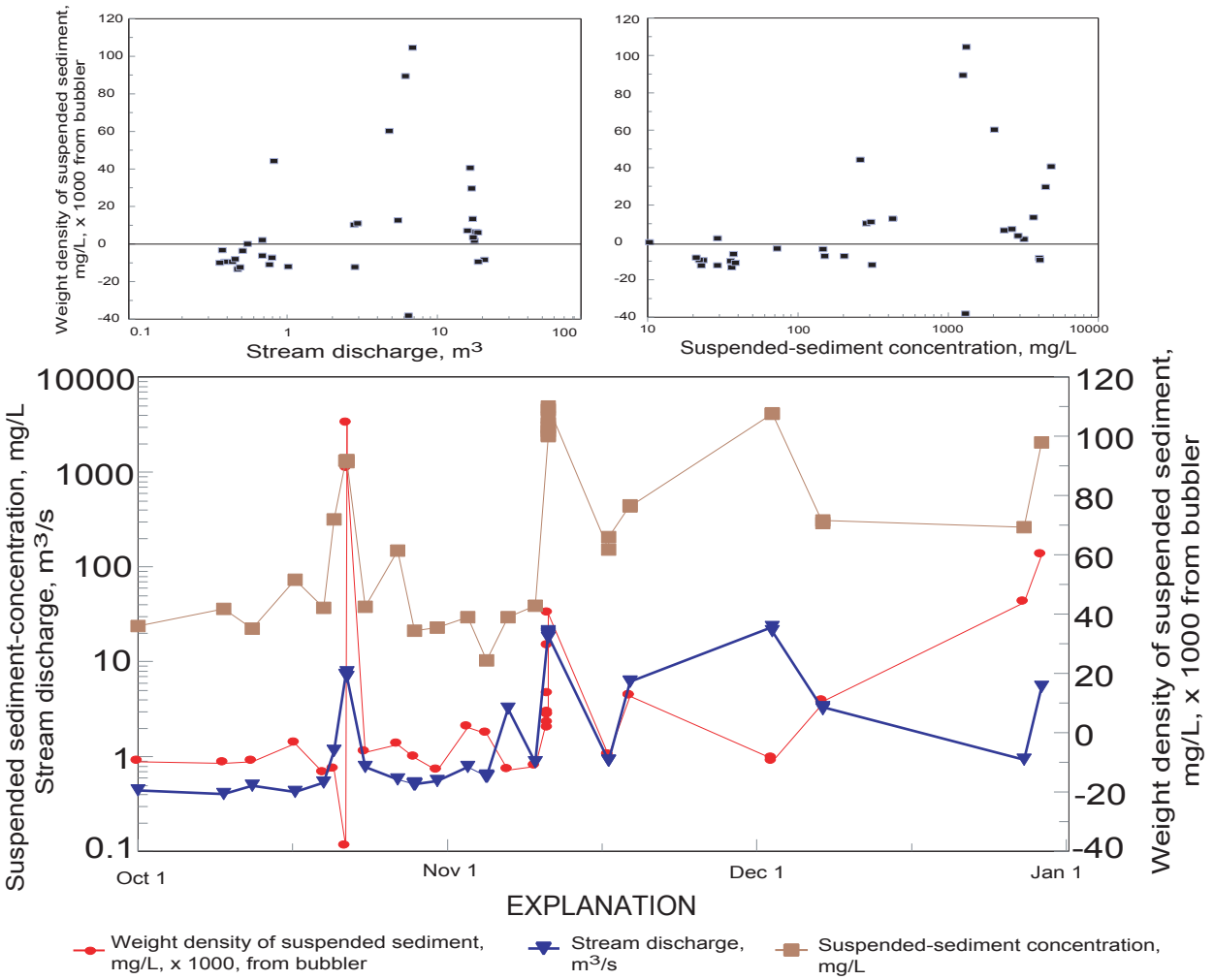

Figure 6. SScatter plots and time series of stream discharge, suspended-sediment concentration, and weight density of suspended sediment and dissolved solids measured with double bubbler, October 1, 19999to January1, 2000. Discharge and sediment data are instantaneous samples, double bubbler weight density value is 30-minute mean of measurements made at 5-minute intevals.

TURBIDITY THRESHOLD SAMPLING FOR SUSPENDED SEDIMENT LOAD ESTIMATION

Jack Lewis, Mathematical Statistician, Pacific Southwest Research Station, Arcata, California
Rand Eads, Hydrologic Instrumentation Specialist, Pacific Southwest Research Station, Arcata, California

Abstract: The paper discusses an automated procedure for measuring turbidity and sampling suspended sediment. The basic equipment consists of a programmable data logger, an in situ turbidimeter, a pumping sampler, and a stage-measuring device. The data logger program employs turbidity to govern sample collection during each transport event. Mounting configurations and housings for the turbidimeters have been prototyped and tested or deployed at 16 gaging sites in northwestern California. Operational data are presented with examples illustrating storm load estimation.

INTRODUCTION

The utility of information about suspended sediment transport is dependent on the timing and frequency of data collection. Even in seasonally snow-dominated watersheds, most of the annual suspended sediment is usually transported during a few, large rainstorm events. Automated data collection is essential to effectively capture such events. Although it is possible to rely solely on manual measurements, important storm flows are infrequent and difficult to predict, and when they do occur, trained personnel may not be available to collect the required information.

As of yet, there is no reliable method to directly measure total suspended sediment concentration (SSC) in the field. Pumped or manual samples must be transported to a laboratory for analysis. However, a number of manufacturers now offer turbidity sensors that can be deployed on a continuous basis in streams. While turbidity cannot replace SSC, it can be a tremendous asset as an auxiliary measurement. Turbidity can be used, along with discharge, in an automated system to make real-time sampling decisions linking turbidity to concentration. And the continuous turbidity record can reveal sediment pulses unrelated to discharge, providing information about the timing and magnitude of landslides or stream bank failures upstream.

METHODS

Sampling: The turbidity threshold sampling (TTS) method distributes sample collection over the range of rising and falling turbidity values and attempts to sample all significant turbidity peaks. A data logger records discharge and turbidity at frequent time intervals (10 or 15 minutes at current installations) and activates a pumping sampler when specified turbidity conditions are met. Discharge information is used to disable sampling when either the turbidity sensor or pumping sampler intake is not adequately submerged. The resulting set of TTS samples can be used to accurately determine suspended sediment loads by establishing a relation between sediment concentration and turbidity for any sampled period with significant sediment transport. The relation is then applied to the nearly continuous turbidity data.

Turbidity thresholds for sampling are based on the expected turbidity range for a given stream and the number of desired physical samples. The TTS method is designed to permit estimation of sediment loads for individual storm events that vary greatly in size. Thresholds are chosen such that their square-roots are evenly spaced (Lewis, 1996) to ensure the collection of samples during small events while holding the number of samples collected in large events within practical limits. Different sets of thresholds are used when turbidity is rising and falling, with more thresholds required during the lengthier falling period. To avoid oversampling due to transient turbidity spikes, each threshold condition must be met for two intervals before sampling is initiated and a minimum user-specified period of time must elapse before a sampled threshold can be re-utilized.

Reversals in turbidity are detected when the turbidity falls 20% below the previous maximum or 10% above the previous minimum, as long as the change is at least 5 NTU (nephelometric turbidity units). To avoid sampling during ephemeral turbidity reversals, the new direction must be maintained for at least two intervals. Upon reversal detection, a sample is collected if a threshold was passed between the actual time of the reversal and its detection. A pumped sample is collected when sampling is first enabled if the lowest turbidity threshold is exceeded, and pumped

samples are collected at fixed intervals when the turbidity exceeds the upper limit of the turbidity sensor. In addition, field personnel can collect pumped samples, under program control, to pair with depth-integrated samples or to augment the number of threshold samples at any desired interval. A program is available from the authors to implement the sampling logic on Campbell data loggers. (The use of trade names is for information only and does not constitute endorsement by the U.S Department of Agriculture.) All of the numeric values in the algorithm are parameters that the user can easily change.

Suspended Sediment Load Estimation: Suspended sediment loads are ideally estimated for each storm using a turbidity sediment rating curve or *TTS rating curve*, which is a simple linear regression of SSC versus turbidity, based on the samples collected during the event being estimated. In a series of simulations (Lewis, 1996), the best or near-optimal results were obtained without data transformations or polynomial terms. The simulations were based on 10-minute records of turbidity and SSC that had been collected from five storm events at Caspar Creek in northwestern California. In some cases, more accurate estimates were obtained using quadratic regression, or separate regressions for periods of rising and falling turbidity. But the advantages were not large, and complex fitting procedures are best avoided, particularly with small samples, to limit extrapolation errors. Applying simple linear regressions resulted in root mean square errors between 1.9 and 7.7% for the five storms, with mean sample sizes between 4 and 11. These are very small errors by conventional standards of sediment load estimation.

The uncertainty of the load estimated from a TTS rating curve can be quantified using standard theory (Lewis, 1996). However, with small samples, the variance estimates themselves are subject to great uncertainty. In addition, if the model does not fit the population from which the data were sampled (difficult to assess from a small sample), the variance estimates can be very biased as well. In simulations where linear models were applied to nearly linear data with log-linear error distributions (Lewis, 1996), estimated standard errors of the load estimates exhibited root mean square errors from 38 to 72% of their true values, with bias up to 49%. Fortunately, the load estimates themselves exhibited root mean square errors of only 5.6 to 8.3% with a maximum bias of 4.0%.

At some gaging stations, we have found that there are often periods when the recorded turbidity is invalid, typically when the turbidimeter is not fully submerged or because debris or sediment are covering the sensor's optical window. Such conditions typically result in erratic turbidity readings that cause the algorithm to collect extra samples. If that is the case, it is usually not difficult to estimate the sediment load for the period of invalid turbidity using either time-interpolation or a sediment rating curve constructed from the extra samples. However, sometimes the pumping sampler's capacity (usually 24 bottles) is exceeded during a period of optical fouling, resulting in an un-sampled period. In these cases, unless the un-sampled period is very brief, the concentrations must be estimated using a sediment-rating curve constructed from a nearby period of time that covers the appropriate discharge range. The use of multiple estimation methods can result in discontinuities of the estimated concentration versus time. Sometimes discontinuities can be avoided by a judicious choice of methods or transition times between methods. The uncertainty can be judged in part by the amount that the load estimates change when different choices are made.

Equipment: The TTS method requires a data logger, a stage measurement device, a pumping sampler, a turbidimeter, a housing and mounting hardware for the turbidimeter, and a pumping sampler intake.

Data logger: The data logger records the stage and turbidity and signals a pumping sampler to collect a sample based on the TTS algorithm. The lack of a commercially available data logger, programmable in a high-level language, and available with the appropriate hardware interface to connect external devices, has been an impediment to the adoption of the TTS method. During water years 1996-1999, we utilized a TTS program written in TXBASIC, a dialect of the BASIC programming language that runs on ONSET Tattletale data loggers The practitioner must fabricate these data loggers from a single-board computer, a user-built interface board, and a memory board. Their fabrication and assembly proved to be an obstacle to the transfer of the TTS technology to practicing hydrologists. Therefore, in water year 2000 we converted the TXBASIC code to the widely available Campbell CR510 and CR10X programmable data loggers. The programming language and its capabilities are primitive but adequate and do permit us to distribute code that can immediately be used by hydrologists wanting to employ TTS.

Stage measurement: A device is needed that can provide the data logger with an electronic output linearly related to stage height. We have used pressure transducers at all our installations. The TTS program records the mean of 150 stage readings during each interval to increase the measurement precision.

Turbidimeter: Our first experiments were with the Analite 190 turbidimeter (McVan Instruments, Co.). Subsequently all of our gaging sites have deployed the OBS-3 turbidimeter (D&A Instruments, Co.). Both of these sensors are nephelometers that measure the scattering of infrared light and have a standard operating range of 0-2000 NTU. The TTS program records the median of 61 turbidity readings during a 30-second period to reduce the influence of outlier values.

Housing: Erroneous (usually inflated) turbidity readings can be caused by organics trapped on or near the sensor, entrainment of air bubbles, fine sediment or biological colonization of the optical window, or the proximity of the sensor to the water surface or channel bottom. Some turbidity sensors have been designed with electronically activated mechanical wipers or other devices to keep the optical window clean, but these have not gained wide acceptance due to reliability issues. In our experience, the most effective control of biofouling is through regular cleaning of the optical window, especially during periods of elevated stream temperature and solar input. But a properly designed sensor housing can limit most of the problems listed above as well as protecting the sensor from physical damage from large organic debris.

The sensor housing design is naturally dependent on the device being used. The OBS-3 that we have used at our gaging stations is cylindrically shaped and its optical window is positioned near the end and at a right angle to the probe's axis. We have found that enclosing the sensor in black ABS pipe, screened on the upstream end, created problems by reducing the velocity through the pipe, leading to regular coating of the optical window and pipe wall with a film of fine sediment during storm recessions. The most effective design we have tried to date encloses the sensor in a section of aluminum square tubing that is cut at a shallow angle on the downstream end to expose the optical window to the flow (Plate 1a). The sensor is oriented parallel to the flow with the optical window aimed sideways. In shallow streams, a solar visor is added above the optical window to reduce infrared saturation. This design effectively limits trapped organics and exposure of the detector to sun or water surface. And we have not experienced problems with fine sediment or air bubbles with this housing.

Mounting hardware: It is essential to mount the turbidity sensor and housing in such a way that it can be accessed at any time for cleaning. The mounting hardware should shed debris and keep the sensor above the bed load transport zone and below the water surface. In forested watersheds, it needs to protect the sensor from the impacts of large woody debris. Mounting configurations are very site specific. In the smallest channels, where flow depths rarely exceed 30 cm, we have mounted the turbidimeters on fixed brackets that are bolted to a plywood base staked into the channel. Brackets are drilled to mount the sensors at one of three heights. In channels that can be waded with flow depths up to 60 cm, we have mounted the turbidimeters on bottom-mounted floating booms (Plate 1b) or overhead suspension booms. On bottom-mounted booms the upstream end is hinged to the bed and the downstream end is fitted with a float, thus maintaining the turbidimeter at a depth proportional to the stage (Eads and Thomas, 1983). In larger channels, we have utilized bridge- or bank-mounted overhead booms (Plates 1c and 1d) that allow access to the sensor at any flow. Overhead booms are suspended vertically from a pivoting horizontal arm and typically are positioned and retrieved with a cable and winch system. The vertical arm is jointed to swing both downstream and sideways to shed large woody debris and to reduce stresses from changing flow lines.

Each of the boom configurations has advantages and disadvantages. Booms on fixed brackets are the simplest to build, but are suitable only for very small channels, where it may be impossible to keep the sensor submerged at all times. If the sensor is mounted too close to the bottom, bed load can bury the sensor or otherwise interfere with measurements during high flows. In small channels, the most promising approach seems to be overhead mounting in natural or artificially created pools. Booms hinged on the streambed have the advantage of keeping the sampling point at a constant proportion of the depth, but it is usually difficult to access the sensor for cleaning during high flows. In addition, bottom-mounted equipment is much more vulnerable than overhead-mounted equipment to damage by bed load. Overhead-mounted booms are the most difficult to build and install, but they allow access to the sensor at any flow. Their main disadvantage is that it is difficult to control the sampling depth. As flow increases the boom and sensor rise in the water column. Counter-weights are added to keep the sensor submerged at high flows, but the sensor's exact depth depends on frictional forces and is thus difficult to control.

Pumping sampler: At our gaging sites we have deployed ISCO pumping samplers, model 2700 or 3700, operated in a flow mode and activated by a signal from the data logger. The intake line from the sampler to the stream is

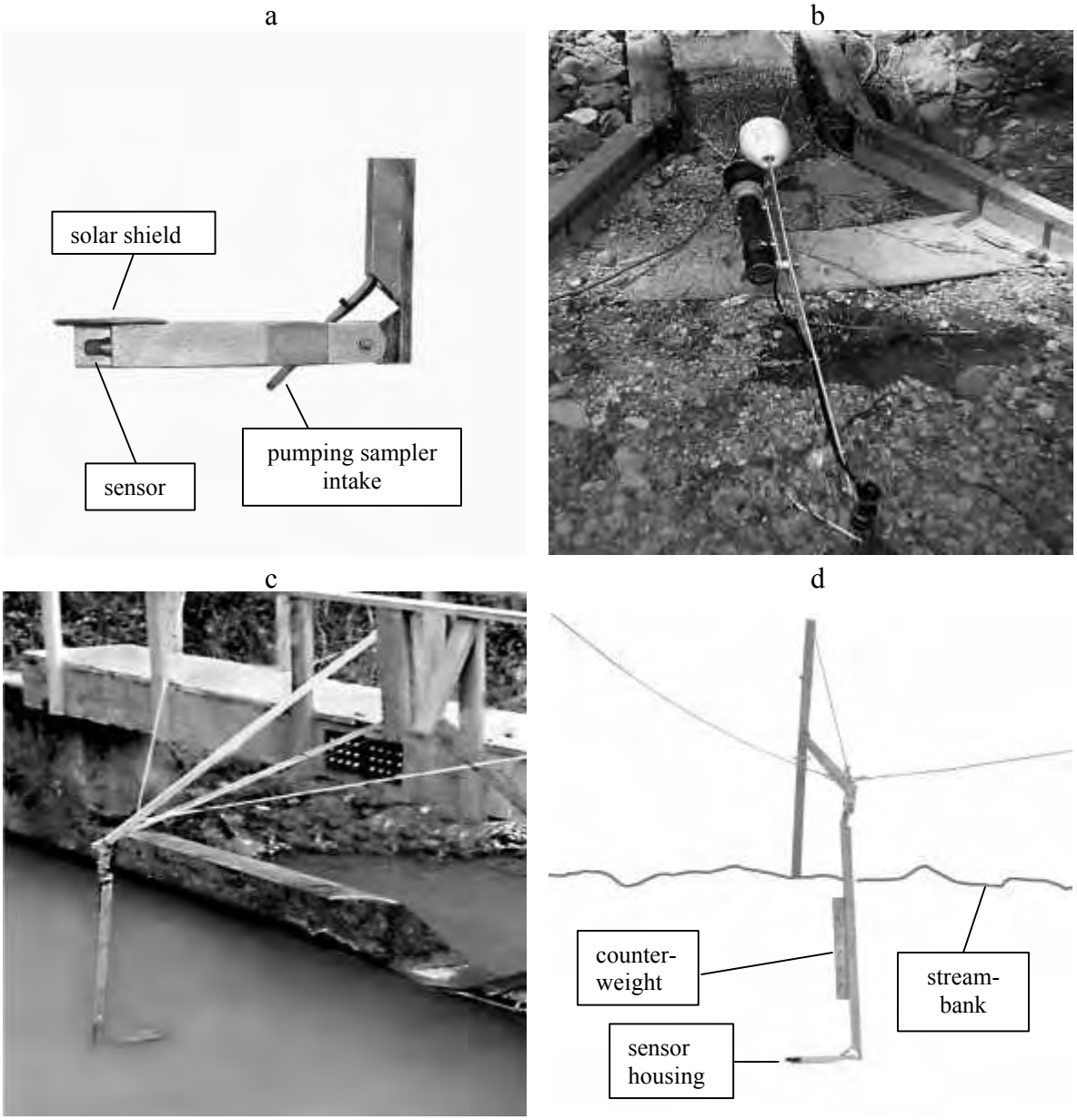

Plate 1. (a) Turbidity sensor in aluminum housing with solar shield, (b) bottom-mounted pivoting boom and sensor in ABS housing, (c) retractable bridge-mounted boom stabilized by lateral cables, and (d) retractable bank-mounted boom.

positioned so that it slopes continuously down to the intake nozzle, thus reducing the opportunity for sediment to fall out of suspension and become trapped. We use 0.635 cm inside diameter intake line to increase line velocity while ensuring representative sampling (standard line diameter is 0.953 cm). The intake is a stainless steel tube, of the same diameter as the intake line, and is often mounted on the boom in close proximity to the sensor. At some sites, the intake is mounted in a fixed position in the channel, at a height of 7.6 cm above the bed. In both mounting configurations the intake is positioned in the thalweg, pointing downstream (Winterstein, 1986).

Gaging sites: We have deployed in situ turbidimeters at 16 gaging stations in northwestern California. Some were used temporarily for testing purposes only. At three stations, both turbidity and SSC were collected at 10 or 15-minute intervals for pilot testing. One station was used briefly to test a new mounting configuration. The TTS

program has been used to control sampling for at least one complete winter at 10 gaging stations. Twelve new gaging stations will be operational during the winter of 2000-2001.

Caspar Creek: Pilot testing was conducted in water years 1994 and 1995 at the 3.8-km^2 Arfstein station in the Caspar Creek Experimental Watershed near Fort Bragg, California. Caspar Creek is a sedimentary basin that produces mostly fine sediments. Turbidity and SSC were collected at 10-min intervals during 7 storm events. The data were subsequently used in sampling simulations to test the accuracy of TTS for estimating sediment loads (Lewis, 1996). Since water year 1996, the TTS method has been running on ONSET data loggers at 8 Caspar Creek gaging stations draining watersheds between 0.2 and 4.7 km^2. These stations are operated as part of a long-term research project focused on the hydrologic effects of forest practices (USDA Forest Service, 1998).

The two original Caspar Creek gaging stations are compound V-notch weirs. At these sites, the turbidity sensors are suspended in aluminum housings on retractable overhead booms mounted on bridges above the weir faces (Plate 1c). Another site has a bank-mounted overhead boom (Plate 1d) and one site has its boom suspended from a cable running across the channel. There are two sites with bottom-mounted pivoting booms (Plate 1b) and three sites have fixed mounts on the channel bed. In the winter of 2000-01, as part of a new study of third-growth logging, ten new gaging stations will utilize TTS in the 4.2-km^2 South Fork of Caspar Creek and its tributaries.

Other gaging sites: Turbidity and suspended sediment were collected at 15-minute intervals for two storms on Mill Creek, a boulder-bedded stream draining 63 km^2 of mostly dioritic terrain in the Hoopa Valley Indian Reservation. The bottom-mounted boom was destroyed and the turbidimeter lost when the streambed was entrained in a moderately high flow.

Our first experiment with an overhead boom (bank-mounted) was at Grass Valley Creek (80 km^2), which transports an abundance of coarse sandy material derived from decomposed granitic rocks. This location was a severe test for our equipment because of its coarse load, high velocities, woody debris loading, and freezing temperatures.

Upper Prairie Creek in Prairie Creek Redwoods State Park near Orick was an experimental site where a prototype bridge-mounted boom was deployed for one season. Bank-mounted booms have also been installed at Freshwater Creek (34 km^2), Little Jones Creek (71 km^2), Godwood Creek (4.4 km^2), and Horse Linto Creek (99 km^2) in Humboldt and Del Norte Counties. Freshwater Creek was the first site where TTS was implemented on a Campbell data logger. The program has been running for two winters there, and for a partial season at Little Jones Creek. Godwood Creek and Horse Linto Creek have no pumping samplers and are collecting only turbidity data.

RESULTS AND DISCUSSION

The most successful installations have been at sites with overhead booms using the aluminum housing design. At these sites, the sensor is continually submerged, interference from debris is minimized, and the sensor can be accessed at any time for cleaning.

Two examples from Caspar Creek (Figure 1a, b) demonstrate the utility of TTS in situations where discharge-sediment rating curves would have failed to adequately describe supply-limited sediment transport. The first case, from the South Fork weir, was a double-peaked storm in which the second discharge peak was higher than the first, while the relative magnitudes of the turbidity peaks were reversed. The second case, from the Dollard tributary, shows two sediment peaks completely unrelated to discharge. We know the sediment originated from the channel in the 600-meter reach between Dollard and the upstream Eagle gaging station because (1) no turbidity spikes occurred at Eagle, and (2) the only active erosion sources in that reach are the channel banks and bed. In both examples, there was a tidy linear relation between laboratory SSC and field turbidity, dispelling any doubt that might exist about the veracity of the turbidity spikes. The coefficients of variation (standard error divided by estimated suspended load) in these two examples were 2.3% and 10.2%, respectively.

A single TTS rating curve is not always entirely satisfactory for defining the sediment transport during a storm event. The predicted concentrations at low turbidities during the storm recession are commonly too low or even negative. In a typical example from Freshwater Creek (Figure 1c), this was easily remedied by applying a second

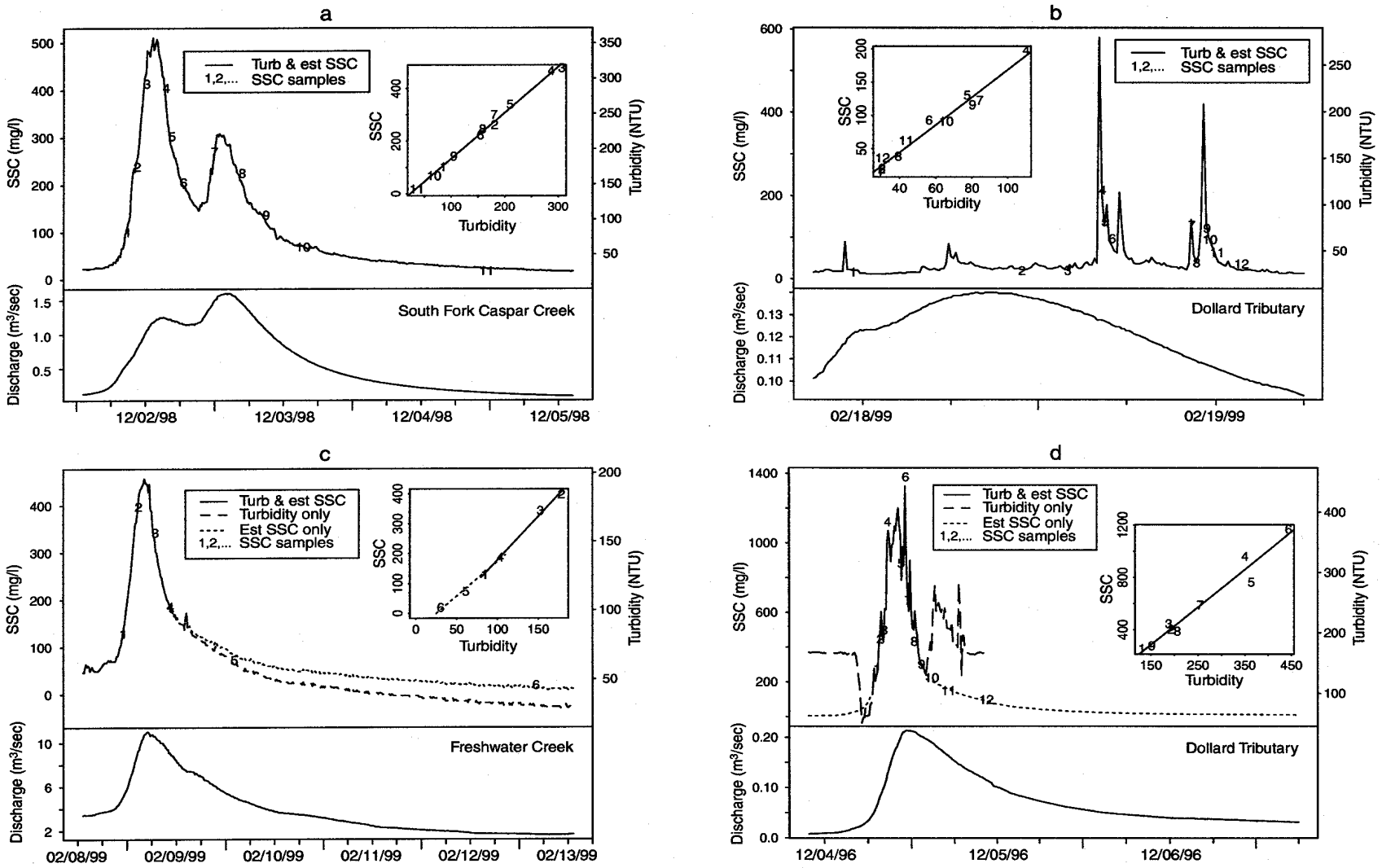

Figure 1. Suspended sediment concentration (SSC), turbidity, and discharge in four storm events. Inset graphs show TTS rating curves used to estimate SSC. Plotted numbers represent measured SSC. Solid lines in upper frames of (a), (b), (c), and (d) represent both turbidity and SSC estimated from TTS rating curve. Left-hand SSC axis is scaled to right-hand turbidity axis through the TTS rating curve. Dashed lines in (c) and (d) represent turbidity only. Dotted lines show SSC estimated from a second TTS rating curve (c) or from discharge-based rating curves (d).

TTS rating curve, based on the last three samples, for the recession period. The load estimated from the two rating curves, each based on three samples, is only 2% greater than that from a single rating curve (replacing negative predictions with zeroes), but the predictions from the second rating curve are clearly more realistic for the recession.

Negative predictions on storm recessions might in some cases result from using 1-micron filters in the laboratory. In 1-micron filtrate from 65 samples collected at 8 of the Caspar Creek gaging stations, an average of 15.5 mg/l was measured on 0.22-micron membrane filters. Assuming the relation between total SSC and turbidity passes through the origin, the effect of disregarding the finest particles is to shift the TTS rating curve downward, creating a negative y-intercept. Extrapolations at the low end of the regression thus can result in negative predictions of concentration.

Various problems often preclude using a TTS rating curve for much of the storm. Figure 1d shows a storm at the Dollard station in 1996, before the turbidimeter was relocated to a pool. In the first part of the storm, the turbidimeter was not submerged because the water was too shallow. Beginning early on Dec. 5, the sensor became fouled with debris. Several hours later, the field crew removed the debris, but made an error that resulted in no electronic data or samples being collected for the remainder of the storm. The discharge for the missing period was later reconstructed from the Eagle station upstream and SSC was estimated for the start and end of the storm using two sediment rating curves. The relation of SSC to discharge formed a wide hysteresis loop, but the first four samples and final three samples of the loop defined more-or-less linear relationships. Therefore separate sediment rating curves were computed from these two subsamples and applied to the periods of invalid or missing turbidity at each end of the storm.

Sometimes when the sensor is fouled, fluctuations in turbidity are produced that result in collection of enough additional samples to adequately define the temporal trend in SSC without resorting to a sediment-rating curve. In these circumstances, linear interpolation between the measured values of SSC is all that is necessary to reliably estimate the load during the period of missing turbidity.

Sampling at Mill Creek and Grass Valley Creek was conducted in order to investigate the feasibility of the TTS method where suspended particles are mostly sand. In the storms sampled at Mill Creek, about half the load consisted of sand, but most was fine sand less than 0.5mm. The TTS rating curve for the larger of the two storms (Figure 2) suggests that the TTS method should work fine in this stream. Whereas the bottom-mounted boom was destroyed at Mill Creek, the prototype overhead boom at Grass Valley Creek was able to withstand impacts from

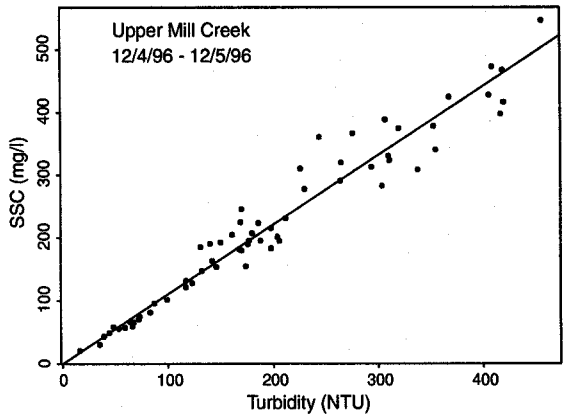

Figure 2. TTS rating curve (regression line) based on a fixed 15-minute sampling interval at Upper Mill Creek

large woody debris transported at velocities as high as 15 ft s^{-1}. However, at Grass Valley Creek, the load was so coarse and the velocities often so great that in one storm the concentration of particles larger than 0.5mm in pumped samples averaged just 4% of that in simultaneous depth-integrated samples (n=8). The relations between SSC from pumped and depth-integrated samples (composited from multiple verticals) are shown in Figure 3. These relations indicate that, unless a pumping sampler becomes available that can efficiently sample sand-size particles at both high velocities and moderate head heights, the TTS methodology can be effective at estimating only the finest part

of the load in streams such as Grass Valley Creek. Unless a tight and reliable relationship could be established between pumped and manual SSC, manual samples would be required throughout high transport events to reliably estimate the total suspended load.

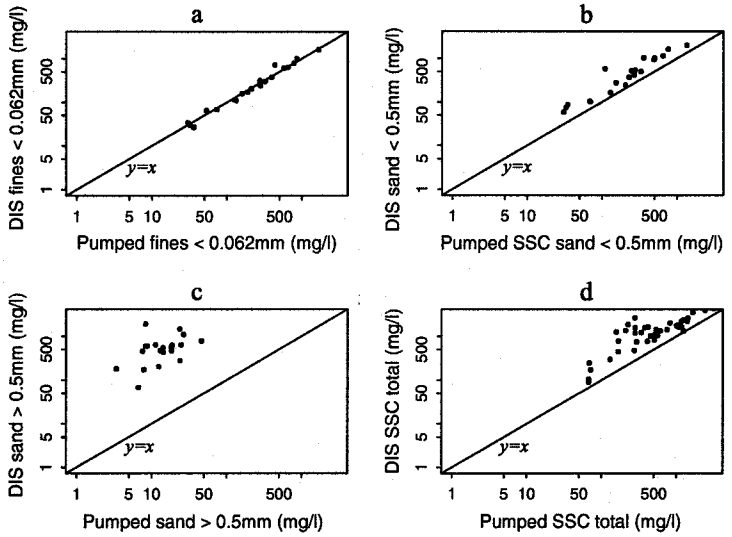

Figure 3. Comparison of SSC in 1998 at Grass Valley Creek from depth-integrated D-49 samples and simultaneous pumped samples for (a) fines < 0.062mm, (b) fine sand < 0.5mm, (c) coarse sand > 0.5mm, and (d) all particles.

The TTS method can also be used to estimate seasonal or annual sediment loads, either by summing storm event loads or by applying seasonal or annual TTS rating curves. However, since TTS samples every significant sediment pulse, it probably collects more samples than necessary for the task. A more suitable approach, when event loads are not of interest, might be random sampling stratified by turbidity. Such a design should be an improvement upon the similar flow-stratified sampling method, which Thomas and Lewis (1995) recommended for estimating seasonal and annual loads.

CONCLUSIONS

Turbidity Threshold Sampling is a proven method for accurately measuring suspended sediment loads at stream gaging stations on a storm event basis. If turbidimeters are properly installed and maintained, the sampling algorithm distributes samples over the entire turbidity range during each transport event. However, in streams with very coarse suspended loads, accuracy is limited by the ability of pumping samplers to collect representative samples.

REFERENCES

Eads, R. E., Thomas, R. B., 1983, Evaluation of a depth proportional intake device for automatic pumping samplers. Water Resources Bulletin 19(2), 289-292.

Lewis, J., 1996, Turbidity-controlled suspended sediment sampling for runoff-event load estimation. Water Resources Research 32(7), 2299-2310.

Thomas, R. B., and Lewis, J., 1995, An evaluation of flow-stratified sampling for estimating suspended sediment loads. Journal of Hydrology 170, 27-45.

USDA Forest Service, 1998, Proceedings of the conference on coastal watersheds: the Caspar Creek story. General Tech. Rep. PSW GTR-168, 149 pp.

Winterstein, T. A., 1986, Effects of nozzle orientation on sediment sampling. *In* Proceedings of the Fourth Federal Interagency Sedimentation Conference, Las Vegas, Nevada, Subcommittee on Sedimentation of the Interagency Advisory Committee on Water Data, Vol. 1, 20-28.

THE PROMISES AND PITFALLS OF ESTIMATING TOTAL SUSPENDED SOLIDS BASED ON BACKSCATTER INTENSITY FROM ACOUSTIC DOPPLER CURRENT PROFILER

Jeffrey W. Gartner and Ralph T. Cheng
U.S. Geological Survey, Water Resources Division, Menlo Park, CA, USA

Abstract

Mass concentration of suspended solids is one of the properties needed to understand characteristics of sediment transport in bays and estuaries. Meaningful estimates of total suspended solids concentrations are particularly difficult to obtain because common methods require collection of numerous water samples that tend to under sample the highly variable characteristics of suspended solids. If optical sensors are used they often become useless because of biological fouling after short periods of time in highly productive water bodies. Acoustic sensors that are routinely used to measure water velocity hold promise as a means of quantitatively estimating total suspended solids from acoustic backscatter intensity, a by-product used in measurement of velocity. A field experiment was designed and carried out in San Francisco Bay, California in October 1998 to investigate the possibility of estimating total suspended solids concentration from backscatter intensity measured by acoustic Doppler current profilers. Results of estimates from two acoustic Doppler current profilers (1200 kHz and 2400 kHz) deployed at two sites in South San Francisco Bay are described in this paper. Estimated total suspended solids concentrations are found to agree within about 15 percent (of total range of concentration) of values estimated by optical backscatterance sensors. Success of these estimates provides promise that this technique might be appropriate for determining total suspended solids concentration from commercially available acoustic Doppler current profilers. Some potential pitfalls and limitations of this approach that stem from theoretical limitations of attenuation properties of acoustic waves are discussed.

INTRODUCTION

Transport, deposition, and suspension of sediments in bays and estuaries are of critical importance to understanding overall condition and health of complex marine systems. Sediments are a source of nutrients or potentially toxic materials; transport of sediments has the potential to re-distribute these materials along with the sediments within the system. High concentration of suspended materials may limit light transmission and thus photosynthesis. In addition, deposition of suspended sediments in shipping channels requires periodic dredging to maintain navigable waterways. Knowledge of total suspended solids concentration (TSSC) is needed to begin to understand these processes; however, meaningful measurement of this highly variable property is difficult. Use of in-situ instruments such as optical backscatterance sensors (OBS) and transmissometers for estimate of TSSC addresses some measurement issues but these sensors are subject to biological fouling after short periods of time in highly productive waters. Collection of water samples does not have the problem of biological fouling but is extremely labor intensive and tends to under sample because of the variable nature of suspended material.

Widespread use of acoustic instruments to measure current velocity has led to interest in the possibility of using the acoustic sensors to estimate TSSC from acoustic backscatter intensity

(ABS) measurements which are much less susceptible to biological fouling and which provide concurrent velocity measurements and TSSC estimates. Initial studies conducted provided qualitative results, for example, Schott and Johns (1987); Flagg and Smith (1989); and Heywood et al (1991). Later work attempted to quantify TSSC estimates through laboratory or field calibration. Laboratory experiments designed to calibrate ABS to sand concentration were conducted by Thorne et al (1991) and Lohrmann and Huhta (1994). Hanes et al (1988) used a 3 mHz acoustic source to estimate suspended sand concentration near Prince Edward Island and Thevenot et al (1992) developed calibration parameters as part of a study to monitor dredged material near Tylers Beach, Virginia using Broadband-ADCPs (BB-ADCPs). Hamilton et al (1998) provide an excellent comparison of optical and acoustic methods in a study describing measurements of cohesive sediments using an acoustic suspended sediment monitor and Thevenot and Kraus (1993) compared optical and acoustic methods using a 2400 kHz BB-ADCP in the Chesapeake Estuary. The references listed here provide only a partial list of research in this field; however, in general, previous studies have been qualitative in nature or limited to large (sand-size) particles. Some studies used non-commercial, special designed acoustic sensors. Many required extensive laboratory calibrations, were short duration (hours), and did not account for acoustic losses in the near field of the acoustic transducer.

This paper describes results of a field experiment in which time series of TSSC were estimated at multiple levels from profiles of ABS measured by an RD Instruments[†] 1200 kHz BB-ADCP and 2400 kHz BB-ADCP. Theoretical background of the technique and an approach for correction of transmission loss in the transducer near field are reviewed. Practical application of using an ADCP for concurrent flow and TSSC measurements is described. Finally some limitations of the methodology are described.

ACOUSTIC METHOD

The method of estimating $TSSC_{(est)}$ from ABS is to use a formula based on the sonar equation for sound scattering (reverberation) from small particles. In exponential form, the equation is

$$TSSC_{(est)}=10^{(A+B*RB)}. \tag{1}$$

The exponent of Eq. (1) contains a term for the measured (for example by ADCP) relative acoustic backscatter, RB, as well as terms for an intercept, A and slope, B that are determined by regression of concurrent ABS with known mass concentration measurements on a semi-log plane in the form of $log(TSSC_{meas})=A+B*RB$.

In its simplified form for reverberation, the sonar equation (Urick, 1975) can be written as

$$RL=SL-2TL+S_v+10log(V_e) \tag{2}$$

where RL is reverberation level (ADCP ABS, in dB), V_e is the ensonified volume, in m^3; and S_v is the volume scattering strength, in dB; S_v is a function of particle shape, diameter, density, rigidity, compressibility, and acoustic wavelength. Volume scattering strength is defined as S_v =

[†] Use of trade, product, or firm name is for descriptive purposes only and does not imply endorsement by the U.S. Geological Survey.

$10log(I_r/I_i)$ where I_r is intensity of reflected signal, in W/m^2, and I_i is intensity of incident signal, in W/m^2. In terms of ADCP parameters, $RL=K_c(E-E_r)$ where E is ADCP echo intensity recorded in counts, E_r is ADCP received signal strength indicator (RSSI) reference level (the echo baseline), in counts, and K_c is the RSSI scale factor used to convert counts to dB. K_c varies among instruments and transducers and has a value of 0.35 to 0.55 (Deines, 1999). SL is the source level in dB, which is the intensity of emitted signal that is known or measurable. $2TL$ is the two-way transmission loss, in dB defined as

$$2TL=20log(R)+2\alpha R \tag{3}$$

where R is range to the ensonified volume, in meters, α is absorption coefficient, in dB/m. $20log(R)$ is the term for loss due to spreading and $2\alpha R$ is the term for loss due to absorption. Attenuation due to sediment is not accounted for because it can be shown to be insignificant at ranges (<2m) and levels (<≈300 mg/l) generally encountered in this study. The absorption coefficient for water is a function of acoustic frequency, salinity, temperature, and pressure. Using equations from Schulkin and Marsh (1962) the absorption coefficient, α was found to be 0.41 dB/m and 1.45 dB/m for 1200 kHz and 2400 kHz respectively. The spreading loss is different in near and far transducer fields. The transition between near and far transducer fields is called the critical range, $R_{critical}$. $R_{critical}=\pi a_t/\lambda$ where a_t is the transducer radius, in cm, and λ is acoustic wavelength. The near field correction, Υ, for spreading loss is calculated from the formula in Downing et al (1995) as

$$\Upsilon = [1+1.35Z+(2.5Z)^{3.2}]/[1.35Z+(2.5Z)^{3.2}] \tag{4}$$

where Z is $R/R_{critical}$. $R_{critical}$ is 167cm for a 1200kHz ADCP with a 5.1cm transducer and 80cm for a 2400kHz ADCP with a 2.5cm transducer.

From a practical standpoint, it is not possible to measure all the characteristics of the suspended material and the acoustic source that are required to directly model TSSC from ADCP ABS. The approach described here involves relating the TSSC to a relative backscatter utilizing calibration parameters. Following the technique of Thevenot et al (1992) relative backscatter, RB, is defined as $RB=RL+2TL$ and the parameters K_1 and K_2 are defined as $K_1=SL+10log(V_e)$ and $K_2=K_1+10log(V_e/M)+TS$ respectively. Substituting RB, K_1, and the definition of S_v in Eq. (2) gives

$$RB= K_1+10log(I_r/I_i). \tag{5}$$

With the assumption of single particle theory (no multiple scattering), $I_r/I_i=N(IS_r/IS_i)$ where N is the number of (uniform mass, M) particles in the sample volume V_e of mass concentration, $TSSC$. Thus $N=(TSSC*V_e)/M$. The parameter IS_r is intensity of (single particle) reflected signal, and IS_i is intensity of (single particle) incident signal. Target strength, TS of any single particle is equal to $10log(IS_r/IS_i)$. After making appropriate substitutions

$$RB=10log(TSSC)+10log(V_e/M)+K_1+TS \tag{6}$$

Substituting the parameter K_2 and rewriting Eq. 6 results in $RB=K_2+10log(TSSC)$ which can be rewritten in the same form as Eq. 1 in which $A=-0.1K_2$ and B=0.1. The theoretical parameters $A=-0.1K_2$ and $B=0.1$ are appropriate for a concentration of uniform particles of the same mass and other properties. For a distribution of particles in the field, these parameters are determined experimentally by regression of RB with measured estimate of total suspended solids concentration at the same location. Thus Eq. (1) can be used to estimate time series of TSSC from ADCP ABS at any distance from the acoustic transducer where valid backscatter data are available.

Application of Acoustic Method: The procedures to estimate a time series or profile of TSSC from a time series or profile of ADCP ABS are summarized below.

1. Determine ADCP received strength signal indicator (RSSI) reference level, E_r, as a function of power and individual instrument.
2. Determine absorption coefficient, a, as a function of salinity, temperature, pressure, and ADCP frequency.
3. Calculate the critical range of near/far field transition for the ADCP transducer, $R_{critical}$, as a function of ADCP frequency and transducer diameter.
4. Determine slant range to each ADCP bin as a function of sound speed, transducer angle, and values determined by the ADCP setup such as ADCP blanking distance, bin size, and transmit pulse length.
5. Calculate the transmission loss from spreading and absorption at each bin as a function of range and the absorption coefficient including the near field transducer correction for spreading loss.
6. Determine relative backscatter, RB (in dB) at each bin by removing the RSSI reference level, correcting for transmission loss and converting backscatter units to dB utilizing an RSSI scale factor (≈0.45 dB/count).
7. Calculate the log of the OBS measured estimate of mass concentration, $TSSC_{meas}$.
8. Finally, determine the slope, B, and intercept, A, for a regression between $log(TSSC_{meas})$ and relative backscatter, RB (at the same location) such that $log(TSSC_{meas})=A+B*RB$.
9. Determine the profile of $TSSC_{est}$ from Eq. (1) using A, B, and the value of RB at each bin.

Limitations of Acoustic Methods: There are two practical limitations to the method of predicting TSSC from ABS using Eq. 1. The first is a common limitation of any single frequency (optical or acoustical) instrument. Since single frequency instruments cannot differentiate between changes in concentration and changes in particle size distribution, a change in size distribution will be interpreted as a change in concentration unless independent particle size distribution measurements indicate need for additional calibrations. In addition, acoustic and optical methods respond differently to particle size with acoustic sensors more sensitive to large particles (proportional to volume) and optical sensors more sensitive to small particles (proportional to cross sectional area).

The second limitation is associated with the relation between instrument frequency and particle size distribution. The theoretical basis for the present analysis is the Rayleigh (long wavelength) scattering model which is restricted to particles whose ratio of circumference to wavelength is less than unity or, ($2\pi a/\lambda<1$) where a is particle radius, λ is acoustic wavelength. Since wave number $k=2\pi/\lambda$, then this restriction can be rewritten as $ka<1$, where ka is non-dimensional frequency. For a fixed frequency acoustic instrument, this condition restricts the maximum particle size for which the method is appropriate and beyond which estimates of TSSC can be

expected to have increasing errors. In addition, attenuation falls off significantly below *ka* values near 0.01-0.1. This condition limits the theory to particle sizes greater than a lower bound beyond which estimates of TSSC would also be expected to display increasing errors. Thus, there are both upper and lower particle size limits (in addition to effects from changes in particle size distribution) in the acoustic method for estimating TSSC. For a 1200 kHz acoustic source, particle diameters corresponding to *ka* values of 1.00, 0.10, and 0.01 are 400 μm, 40 μm, and 4 μm respectively; the acoustic method is most appropriate for particle size distributions between about 10 μm and 400 μm. If frequency is doubled (2400 kHz), the applicability of the acoustic instrument would correspond to particle diameters one half the values of those at 1200 kHz.

FIELD APPLICATIONS OF THE ACOUSTIC TECHNIQUE IN SAN FRANCISCO BAY

A suite of instruments including a 1200 kHz ADCP and a 2400 kHz ADCP was deployed in the shipping channel north of the San Mateo Bridge (SMB) between October 19 and 23, 1998 (fig. 1). Instruments were moved to the shipping channel south of the Dumbarton Bridge (DB) between October 23 and 29, 1998. In addition to ADCPs, there were four conductivity-temperature-depth (CTD) data loggers, and four OBS sensors. The ADCPs were oriented facing down; bin 1 of the 1200 kHz ADCP was at 118 cm and bin 1 of the 2400 kHz ADCP was at 141 cm above bed. The 1200 kHz unit used a 25cm bin size and the 2400 kHz unit used a 10cm bin size. Thus, most of the measured profiles fell within the near field of both ADCP transducers. Both ADCPs were setup utilizing RD Instruments water sample Mode-1 with 175 pings per ensemble and a 15-minute sample interval between ensembles. It took approximately 16-17 seconds for the ADCP ensemble measurements.

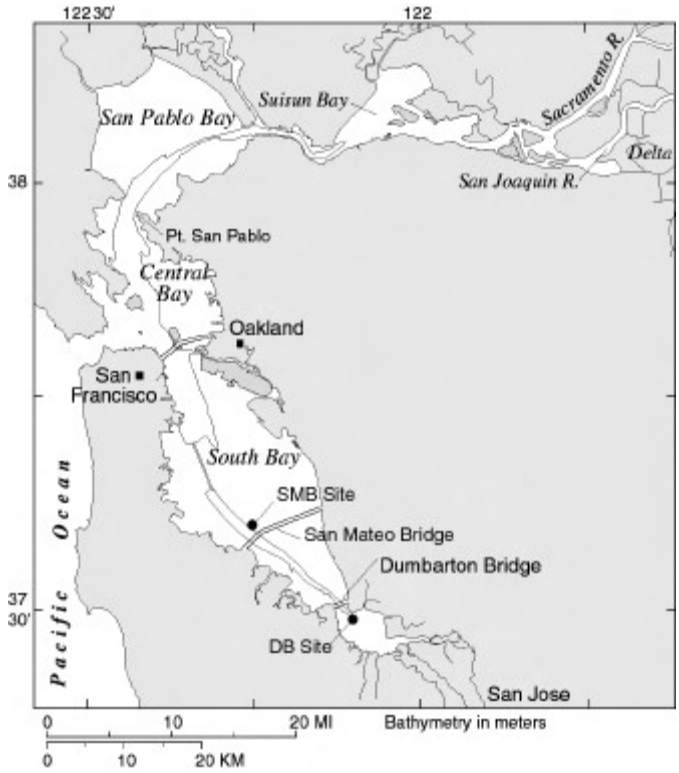

Figure 1. Map of San Francisco Bay estuarine system showing study sites at San Mateo and Dumbarton Bridges.

Time-series plots of TSSC estimated from ADCP ABS and from OBS measurements at the SMB site are shown in figure 2. Results at the DB site are similar and are not shown here. Time series for the lower OBS at 33 cm is not compared with 1200 kHz ADCP data since the corresponding ADCP bin was in the area of acoustic side lobe interference and was thus invalid. In evaluating these results it is important to understand that OBS estimates of TSSC may be inaccurate because they are also made from single frequency instruments that are subject to calibration errors.

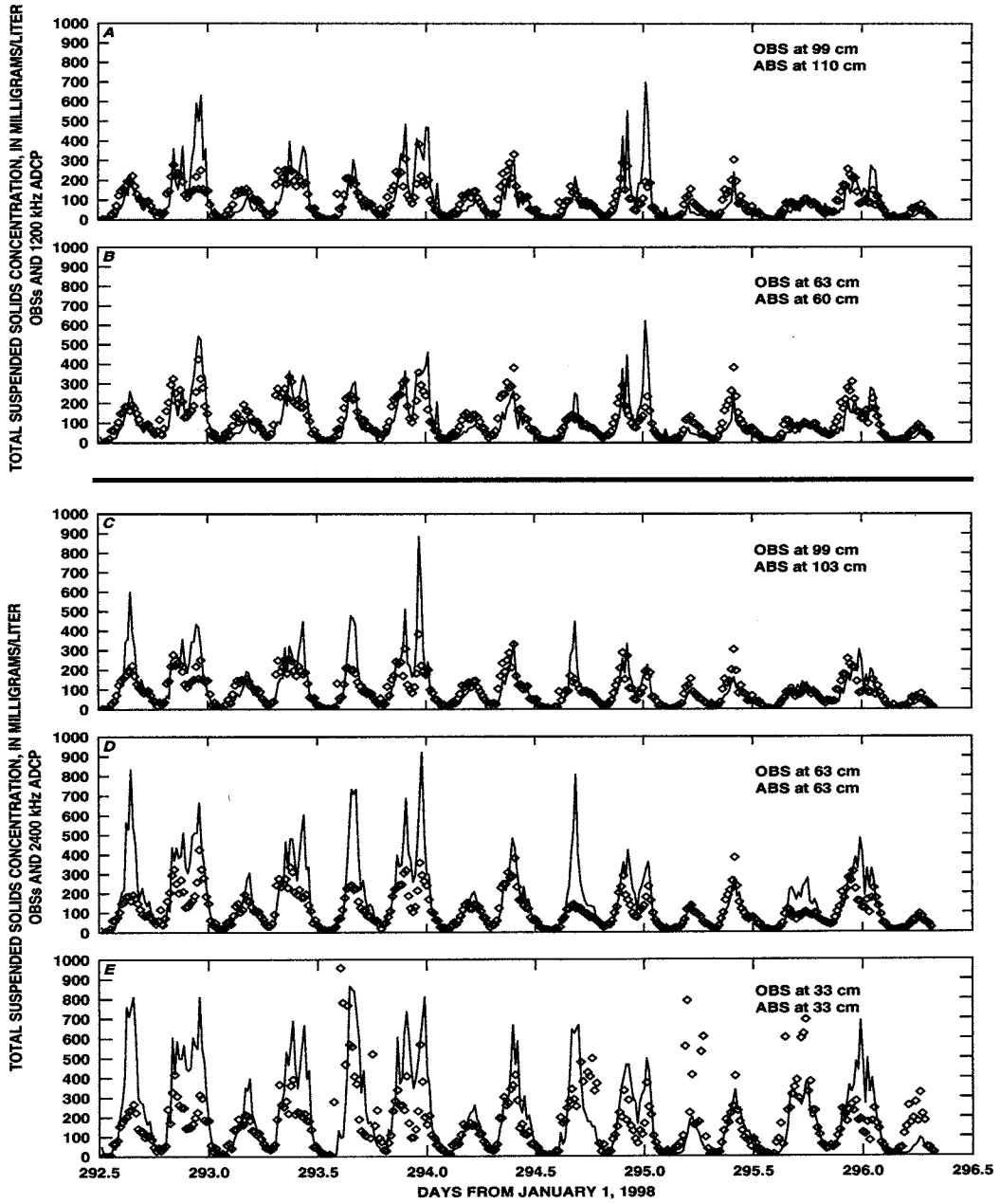

Figure 2. Time-series plots of comparisons between TSSC estimated by OBS (open diamond) and TSSC estimated by acoustic backscatter (solid line) from the 1200 kHz ADCP at bin 2 (A) and bin 4 (B) and from the 2400 kHz ADCP at bin 6 (C), bin 10 (D), and bin 13 (E) at the San Mateo Bridge site.

Results of the acoustic method show generally good qualitative agreement between OBS and ADCP backscatter estimates of TSSC (fig. 2). In order to quantify these comparisons, results of statistical analyses at levels where regressions were performed are shown in table 1. Prediction error (column 5) is defined as the difference (in mg/l) between estimates of TSSC by OBS and by ADCP ABS. In order to provide some meaning to these errors they are shown as a percent relative to the OBS estimated range (column 7) and the OBS estimated mean (column 9) concentrations in mg/l. Also shown in table 1 are the slopes and intercepts determined from regressions and which were used in the predictions using Eq. (1).

Agreement between OBS and ADCP ABS estimates of TSSC appears to slightly worsen as distance from transducer (regression point) increases (fig. 2). There are several possible factors for this which include: 1) an error in the RSSI scale factor used to convert ADCP ABS to dB; 2) differences in particle size distribution at different levels of the profile from those used for calibration of OBSs; 3) errors in calculation of transmission losses at different distances from the transducers, including possible attenuation losses at high levels of suspended sediments; 4) errors in calculation of correction for the transducer near field spreading losses; 5) differences in sample interval for the OBS and ADCP: and 6) changes to ADCP transmit power voltage over the deployment period. Nevertheless, the method provides estimates of TSSC that are in good agreement with those estimated by OBS under conditions encountered during this field test.

Table 1. Estimation statistics for bin where regression was performed to determine slope and intercept values used in Eq. 1. Error is difference in mg/l between OBS and ADCP estimates. Errors are shown as percent relative to the OBS range (column 7) and OBS mean (column 9) of TSSC.

STATION	ADCP FREQUENCY (kHz)	SLOPE	INTERCEPT	PREDICTION ERROR (MG/L)	OBS RANGE (MG/L)	ERROR TO RANGE (%)	OBS MEAN (MG/L)	ERROR TO MEAN (%)
SMB98B	1200	0.129	-7.419	53	383	14	93	55
SMB98B	2400	0.125	-5.624	41	383	11	93	44
DB98B	1200	0.095	-4.541	17	272	6	49	35
DB98B	2400	0.092	-3.428	16	272	6	49	31

SUMMARY

The technique of using ABS measured by commercially available Doppler velocity sensors is shown to provide reasonably accurate estimates of mass concentration of total suspended solids at two test sites in San Francisco Bay. The method suffers from the same limitation as any other single frequency sensor as far as being unable to differentiate between changes in size distribution and concentration. Although optical and acoustical instruments react differently to grain size, the acoustic method provides TSSC estimates concurrent with velocity measurements without the use of an additional sensor. It overcomes the problem of biological fouling, a major limitation of optical instruments. Another significant improvement over single point instruments such as OBSs is that estimates of TSSC are in the form of profiles rather than single point measurements. This method will prove an extremely useful research tool if additional testing shows it to consistently provide reasonably accurate results (within theoretical limitations), in spite of some minor changes in particle size distribution.

REFERENCES

Deines, K. L., 1999. Backscatter estimation using broadband acoustic Doppler current profilers, Proceedings of the IEEE Sixth Working Conference on Current Measurement, San Diego, CA, March 11-13, 1999, pp. 249-253.

Downing, Andrew, Thorne, P. D., Vincent, C. E., 1995. Backscattering from a suspension in the near field of a piston transducer, J. Acoustical Society of America, 97 (3), pp. 1614-1620.

Flagg, C. N., Smith, S. L., 1989. On the use of the acoustic Doppler current profiler to measure zooplankton abundance, Deep-Sea Research, Vol 36, No. 3, pp. 455-474.

Hamilton, L. J., Shi, Z., Zhang, S. Y., 1998. Acoustic backscatter measurements of estuarine suspended cohesive sediment concentration profiles, Journal of Coastal Research 14(4), pp. 1213-1224.

Hanes, D. M., Vincent, C. E., Huntley, D. A., Clarke, T. L., 1988. Acoustic measurements of suspended sand concentration in the C2S2 experiment at Stanhope Lane, Prince Edward Island, Marine Geology, Elsevier Science Publishers, Amsterdam, pp. 185-196.

Heywood, K. J., Scrope-Howe, S, Barton, E. D., 1991. Estimation of zooplankton abundance from shipborne ADCP backscatter, Deep-Sea Research, Vol 38. No. 6 pp. 677-691.

Lohrman, Atle, Huhta, Craig, 1994. Plume measurement system (Plumes) calibration experiment, dredging Research program, Technical Report DRP-94-3, US Army Corps of Engineers, Washington, D.C, 152 p.

Schott, Friedrich, Johns, William, 1987. Half-year-long measurements with a buoy-mounted acoustic Doppler current profiler in the Somali Current, Journal of Geophysical Research, Vol 92, No. C5, pp. 5169-5176.

Schulkin, M., Marsh, H. W., 1962. Sound absorption in seawater, J. Acoustical Society of America, 34 (6), pp. 864-865.

Thevenot, M. M., Prickett, T. L., Kraus, N. C., 1992. Tylers Beach, Virginia, dredged material plume monitoring project 27 September to 4 October 1991, Dredging Research Program Technical Report DRP-92-7, US Army Corps of Engineers, Washington, D.C, 204 p.

Thevenot, M. M., and Nicholas C. Kraus, 1993: Comparison of acoustical and optical measurements of suspended material in the Chesapeake Estuary, *J. Marine Env. Eng.*, Vol. 1, Gordon and Breach Science Publishers, pp. 65-79.

Thorne, P. D., Vincent, C. E., Harcastle, P. J., Rehman, S., Pearson, N., 1991. Measuring suspended sediment concentrations using acoustic backscatter devices, Marine Geology, 98, Elsevier Science Publishers, Amsterdam, pp. 7-16.

Urick, R. J., 1975. Principles of Underwater Sound, 2nd ed., McGraw Hill, N. Y., 384 p.

ACOUSTIC MEASUREMENT OF SEDIMENT FLUX IN RIVERS AND NEAR-SHORE WATERS

By: J. M. Land, Director, Dredging Research Ltd, Godalming GU7 1LG, United Kingdom
P. D. Jones, Senior Scientist, Environment Agency, Warrington WA4 1HG, United Kingdom

Abstract: Procedures for data collection, calibration, processing and analysis have been developed for use with RDI's Acoustic Doppler Current Profilers. They permit the derivation of reliable solids concentrations from acoustic backscatter data. The procedures have been used mainly for monitoring sediment release and plume decay during dredging and dredged material disposal operations but, in combination with the current data, are now being applied to measurement of sediment flux in rivers and estuaries.

Many of the perceived problems with acoustic measurement can be overcome and, subject to certain limitations, flux estimates can now be obtained which are at least as accurate as those derived using conventional techniques. An example of work undertaken in the estuary of the River Mersey in the UK is presented together with calibration data from other locations. These illustrate how problems with high concentrations, periodic flocculation of fine sediments and variable temperature and salinity profiles can be overcome to produce reliable flux estimates.

INTRODUCTION

RD Instruments' Acoustic Doppler Current Profiler (ADCP) was initially developed as a powerful method for the measurement of water velocities and water fluxes in oceanographic research. The applicability of the original narrowband devices was extended for work in estuaries and rivers, by the development of broadband instruments. The use of ADCPs for discharge measurement in rivers and estuaries has been researched in detail. Gordon (1991,1992) reported on evaluations of the ADCP on the Rivers Danube and Mississippi where the discharges measured by the ADCP were compared with stage discharge relationships. Differences of 1.5% (Danube at 2084 m^3 s^{-1}) and 3% (Mississippi at 14000-16000 m^3 s^{-1}) were noted. Pollard (1992) reported on discharge measurements on the Willamette River, comparing an RDI ADCP with an Acoustic Velocity Meter operated by the U.S. Geological Survey. Discharges measured by the two methods differed by less than 1% at a mean flow of505 m^3 s^{-1}. Evaluation of performance in several shallower UK rivers has shown that the ADCP measurement of flow compares well with that of multipath ultrasonic flow gauges (Jarvis et al. 1995, 1997). Repeatability of the ADCP has been summarised by Gordon (1992) using data from eight sites on European and American rivers. The tests were carried out under steady state flow conditions with flows varying from 711 m^3 s^{-1} to 16100 m^3 s^{-1}. The recorded repeatability of tests at individual sites varied between ± 0.3% and ± 2.0% of the mean value.

Although ADCPs are now routinely used to measure discharge, only limited work has been directed at using them for measurement of sediment flux. The Sediview Method, an integrated approach to ADCP data collection, calibration, processing and analysis, has been developed to derive suspended solids concentrations from ADCP relative backscatter data. The method was originally developed to monitor the effects of dredging and dredged material disposal operations and has been used for that purpose in Hong Kong, USA, Germany and the UK. However, in recent years, it has become increasingly used for measurement of sediment flux in rivers and estuaries including the River Mersey in the UK, the Rhine and Elbe in Germany and the Scheldt in Belgium.

THE SEDIVIEW METHOD

General Approach: The relevant acoustic theory has been developed by a number of workers, e.g.Thorne et al. (1991), Sheng and Hay (1988), and Richards et al. (1996). Until recently, the majority of successful applications have used relatively short-range, bed-mounted devices for detailed studies of near-bed sediment transport processes. The Sediview Method has been developed, using a simplified theoretical approach provided by Thorne (1993), for vessel-mounted, longer-range applications (up to 100 metres and more) using ADCPs for the study of large-scale sediment transport processes in which the minimisation of range-dependent errors becomes critical. Successful application of the Method is dependent on the following:

1) knowledge of the temperature and salinity profile at the measurement site;
2) detailed knowledge of the performance characteristics of the ADCP (in particular, the relationship between the received signal strength and decibels) and the manner in which the performance can change with time;

3) mounting of the ADCP to avoid air bubbles created by the passage of the survey boat and ensuring that the sailing speed is less than that which gives rise to noise caused by water passing over the transducers; interfering noise caused by other equipment (e.g. echo sounders, sonars) must also be investigated and eliminated;
4) acquisition of calibration data (preferably water samples) at intervals appropriate to the site conditions followed by thorough analysis of that data to identify and define temporal and/or spatial trends in the sediment regime, e.g. variation of particle size with depth, or periodic flocculation and deflocculation of fine sediments.

A simplified overview of the approach is shown in Figure 1.

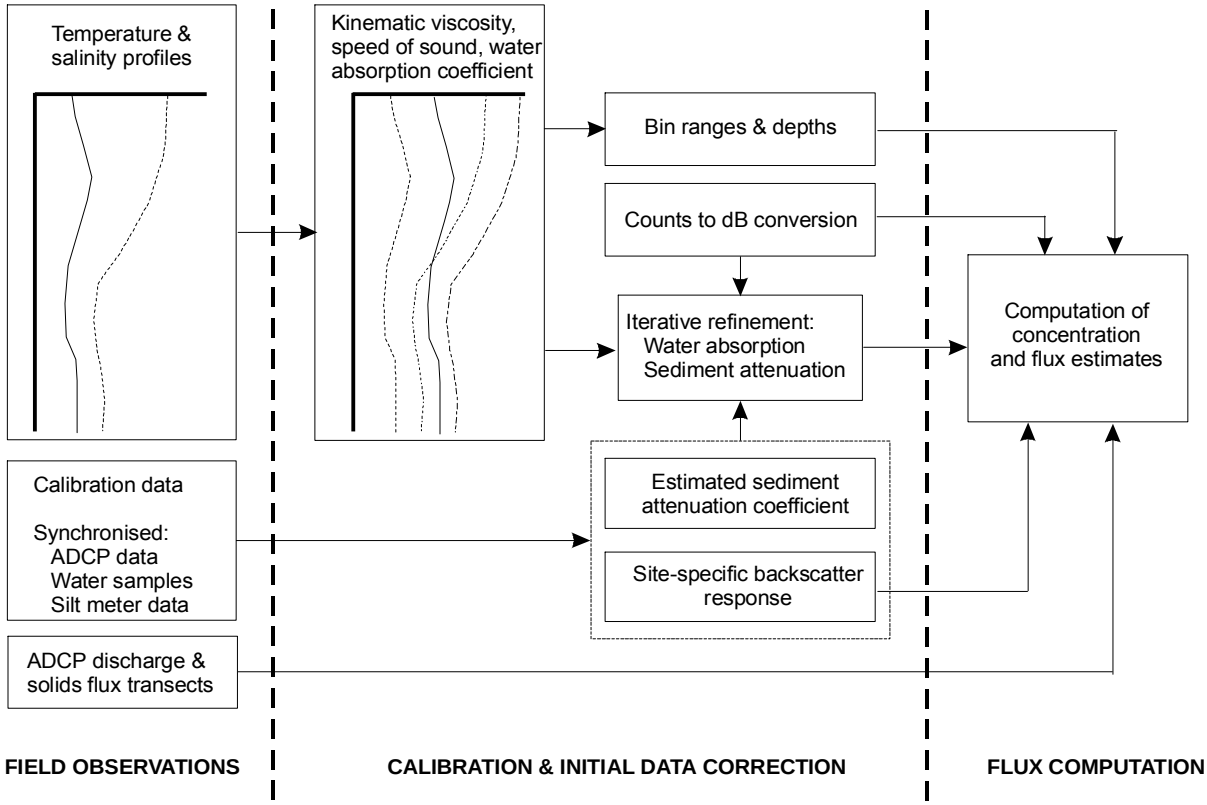

Figure 1. Simplified overview of the Sediview Method of solids flux measurement.

Computation of Concentration Estimates: In order to convert observed relative backscatter intensity into estimates of concentration, it is necessary to correct the data to account for attenuation due to beam spreading, water absorption, and scattering and absorption by the suspended load. In addition, it is necessary to derive the site-specific (and often time- and depth-dependent) relationship between corrected backscatter intensity and unit solids concentration. A software package has been developed to undertake the complex computations involved in the derivation of concentration and to perform a variety of data analysis and presentation routines.

The correction for beam spreading is a function of range. In the existing version of the software, a single function is applied over the full profiling range but a two-stage correction will be incorporated in the next version to account for differences between near-field and far-field spreading (Downing *et al*, 1995). The water absorption and sediment attenuation coefficients are initially derived using theoretical expressions and refined, in an iterative calibration process, to develop reliable, site-specific values. The site-specific relationship between backscatter intensity and solids concentration is derived using field calibration data obtained with water samplers and turbidity (silt) meters. The computation of the concentration estimates commences in the measurement cell closest to the transducers with an initial estimate of the solids concentration without application of any correction for signal attenuation due to the sediment. The computation is then iterated, using the sediment attenuation coefficient, and progressively refined until the concentration estimate does not change. This process is repeated step-wise through all cells in turn.

Field Calibration: Field calibration data are obtained using both silt meters and water samplers. The calibration is site-specific and will change if the characteristics of the suspended solids vary during the course of the work. Particle size is the most important sediment characteristic which influences backscatter but shape and mineralogy (and consequential variations of compressibility and density) are also important. It may therefore be necessary on some sites to collect calibration data at frequent intervals (e.g. 10-30 minutes). Single water samples and silt meter observations can easily be obtained from shallow depths while the vessel is underway in order to monitor and quantify such variation. More detailed data to establish depth-related calibration parameters can be obtained at less frequent intervals by stopping the boat and obtaining profiles of data through the entire water column.

Accuracy: The absolute accuracy of a calibration, and of the concentration estimates derived using the calibration, is always difficult to determine, largely because much of the calibration is based on data which is itself subject to inaccuracy (eg. laboratory determinations of solids content). Broadband ADCPs are able to measure relative backscatter intensity to provide concentration estimates which are theoretically accurate to within about ±2% for a 4-ping data ensemble. Narrowband instruments are less accurate and concentration estimates based on a single 4-ping ensemble are unlikely to be better than about ±25%. These errors are truly random and the large data sets used to measure sediment flux (which will contain hundreds or thousands of individual measurements) should not be systematically biased by them.

Systematic and potentially large errors may be encountered due to variations of the environment in which the measurements are made, ie. variations of water temperature and salinity (leading to variation of the water absorption coefficient) and variations of sediment particle size (leading to variations of backscatter response and acoustic attenuation). These can largely be avoided by frequent sampling and measurement of water temperature and salinity during the survey. The required frequency will depend on the characteristics of the site and the magnitude of the changes which can be expected during the course of the survey. The greatest errors result from inadequate calibration procedures. In particular, the derivation of the correct conversion from instrument 'counts' to dB is critical; errors arising from the use of the wrong conversion can, in theory, approach an order of magnitude.

Overall, it has been found that with broadband instruments and with careful data collection and analysis, individual concentration estimates can be derived which are generally within about ±25% of the concentrations measured on contemporaneous water samples. Over the course of seven years fieldwork, the overwhelming impression gained has been that the majority of such 'residual errors' are, in fact, largely due to the inevitable impossibility of achieving perfect temporal and spatial synchronisation of measurements made using two or more different methods, ie. they are not errors but differences between measurements obtained by different techniques (each of which suffer from varying degrees of inherent inaccuracy) using different sample volumes and at slightly different times. In recognition of this unavoidable problem, a calibration is deemed to be satisfactory when the concentrations derived using Sediview and those from water samples or (calibrated) turbidity meters are generally within 25%, the basic population statistics (eg. mean, standard deviation etc) are similar and there is no indication of any systematic variation of error magnitude in response to absolute concentration, measurement range or time.

More detailed accounts of the use of ADCPs to obtain concentration data are provided by Land and Bray (1998), Land et al (1997), Ogushwitz (1994) and Thevenot and Kraus (1993).

POTENTIAL PROBLEMS WORKING IN RIVERS AND COASTAL WATERS

There are numerous problems which may be encountered when attempting to measure sediment flux in rivers and coastal waters. These are briefly reviewed below.

Particle size variations: Variation of particle size will affect accuracy if ignored. A particular problem arises in estuaries at the interface between fresh and saline waters where flocculation of fine sediment can give rise to substantial particle size variation. This can usually be overcome with careful treatment of the data and the use of time- or distance-variable calibrations. Elsewhere, it is often found that particle size increases with concentration and/or with depth. Concentration-related increases can be accommodated by adjusting the site-specific backscatter relationship while depth-related increases can be accommodated (adopting a pragmatic approach) by adjustments to the counts-to-dB conversion and/or water absorption coefficient.

ADCP measurement range: Near-bed concentrations cannot be measured reliably by the ADCP due to the corruption of the backscatter data by side lobe echoes (Figure 2). When ADCPs with a 20° beam angle are used, approximately 6% of the water column is 'lost' due to this limitation.

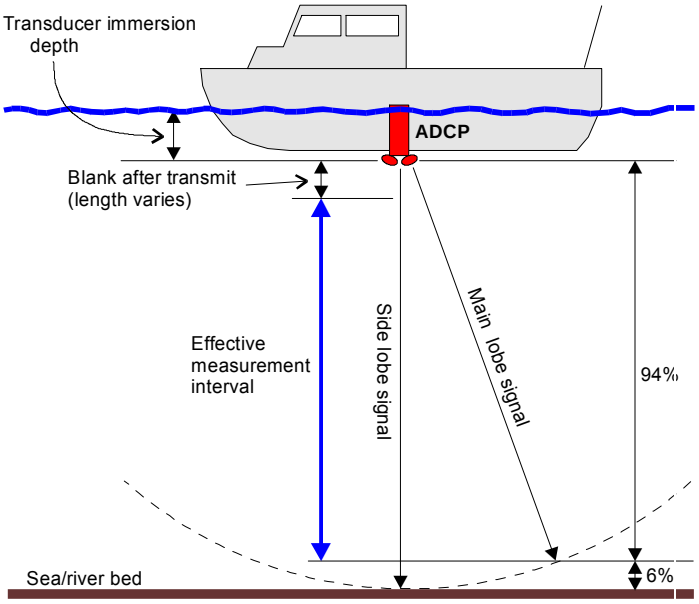

Figure 2 Limits of ADCP measurement interval

In order to overcome this problem, a profiling silt meter can be used to measure the near-bed concentration gradient. If there is a degree of consistency, the form of the concentration profile can be input to the Sediview software which will compute an estimate of the near-bed solids flux. Of course, these estimates must be treated with caution.

Data cannot be obtained in the near-surface zone because the transducers must be immersed and because of the blank-after-transmit requirement. This area can be treated in a manner similar to the near-bed zone but the estimated solids flux is generally fairly reliable as concentration gradients in the near-surface zone are usually modest. The limitations of measurement interval are most pronounced when working in very shallow water where the near-surface 'blank' zone may account for a significant proportion of the overall water depth.

Sea conditions: During storms in coastal waters and estuaries, air bubbles may be formed in the near-surface zone which may take several hours to dissipate. It may also be difficult to obtain reliable data when using ADCPs in rough weather.

Rapid currents: Fast water currents may make it difficult to sail the survey boat along the transect at a speed (through the water) which is sufficiently slow to avoid water noise. They also make it difficult to obtain ADCP data and water samples which are spatially matched. This can only be overcome by increasing the number of calibration samples which are taken and relying on the power of statistics to develop the calibration.

Loss of bottom track: Bottom track may be lost in areas where there are very high near-bed solids concentrations. Use of differential GPS overcomes the problems of positioning but the depth to the bed still needs to be known. Echo-sounders can be interfaced with the ADCP to provide bed level data or the bed can be reconstructed manually using the backscatter data. Several features are incorporated in the Sediview software to assist with this problem.

Stratification: Significant temperature and salinity stratification is most commonly encountered when working in estuaries. It is important that the temperature and salinity profiles are accurately defined so that the correct water absorption coefficient profiles are applied during data processing. In some situations, this may lead to a requirement to obtain temperature and salinity profile data at frequent intervals during a survey.

Steep concentration gradients: Very steep concentration gradients hinder calibration of the ADCP because of spatial mismatching of ADCP data and water samples (or silt meter observations).

Mobile beds: In some rivers, the bed sediments may move at high current speeds. This can lead to significant bottom-track errors and resulting errors in the determination of both currents and the dimensions of measurement cells. In such situations, it is essential to interface the ADCP with a differential GPS system.

Outfalls: Particulate matter discharged from outfalls will be detected by the ADCP and will add to the total estimate of solids flux.

Shipping movements: Shipping movements give rise to air bubbles which corrupt the ADCP backscatter data.

CASE STUDY: MEASUREMENT OF NET SOLIDS TRANSPORT THROUGH THE MERSEY ESTUARY

In order to test the ability of an ADCP and the Sediview software to determine net solids flux, two surveys covering a spring and neap tidal cycle were undertaken by the UK Environment Agency in the Mersey Estuary during the winter of 1995/6 (Dredging Research Ltd.1996, Wither et al, 1998). A 614 KHz broadband ADCP was used, controlled using 'Transect' software and interfaced with a differential GPS system. A rapid-drop profiling silt meter was used to obtain data on the concentration profile close to the bed where side-lobe interference corrupts ADCP data. It also provided concentration profiles to check ADCP output. A pumped water sampler was used to provide samples for calibration of the ADCP and silt meter.

Difficulties were initially encountered during calibration of the ADCP. These were due mainly to flocculation of the sediments predominantly during slack water periods. As the current speed increased after slack water, the weak flocs were broken apart. After elimination of corrupted or otherwise suspect data, large calibration errors remained which, when plotted against time, were seen to be closely related to the tidal state. Figure 3 shows these errors plotted against time for the neap tide survey.

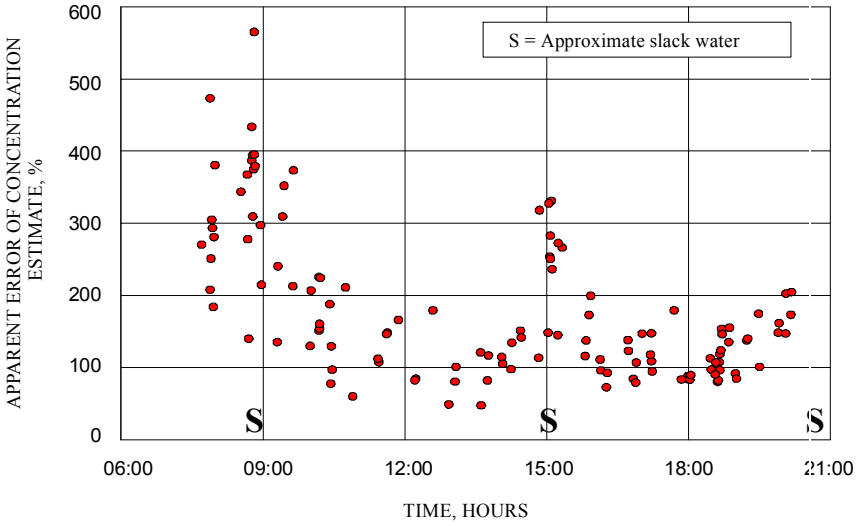

Figure 3.
Errors of concentration estimates obtained using a non-variable calibration in sediments which flocculate at slack water.

In addition, there was a general underlying tendency for the average particle size to increase with increasing concentration. The next stage of the calibration was to devise a non-linear, time-variable calibration which would account for these effects. This was done by varying the calibration constant C_2 in the basic calibration equation [dB = C_2 * log[mg/l] + C_1] until a best fit was obtained. In an ideal, non-variable suspension, C_2 should have a value of 10 but values of up to 20 were applied to data obtained during slack water to account for the flocculation. A minimum value of about 14 was required to account for the underlying tendency for the particle size to increase with increasing concentration. A minor adjustment of the water absorption coefficient was found to be adequate to compensate for the tendency for particle size to increase with depth.

Figure 4 shows the comparison between the estimated concentrations and the water sample concentration for the neap tide surveys after application on the time-variable calibration. The data were obtained over a range of depths up to 22 metres. It is considered that a large part of the 'residual' errors are due to lack of spatial synchronisation of the water samples due to the fast water currents during most of the survey periods. These made it impossible to maintain the sampler at the required depth and directly under the survey boat. The calculated discharge and solids flux data are summarised in Table 1. Figure 5 shows neap and spring tidal variations in solids flux.

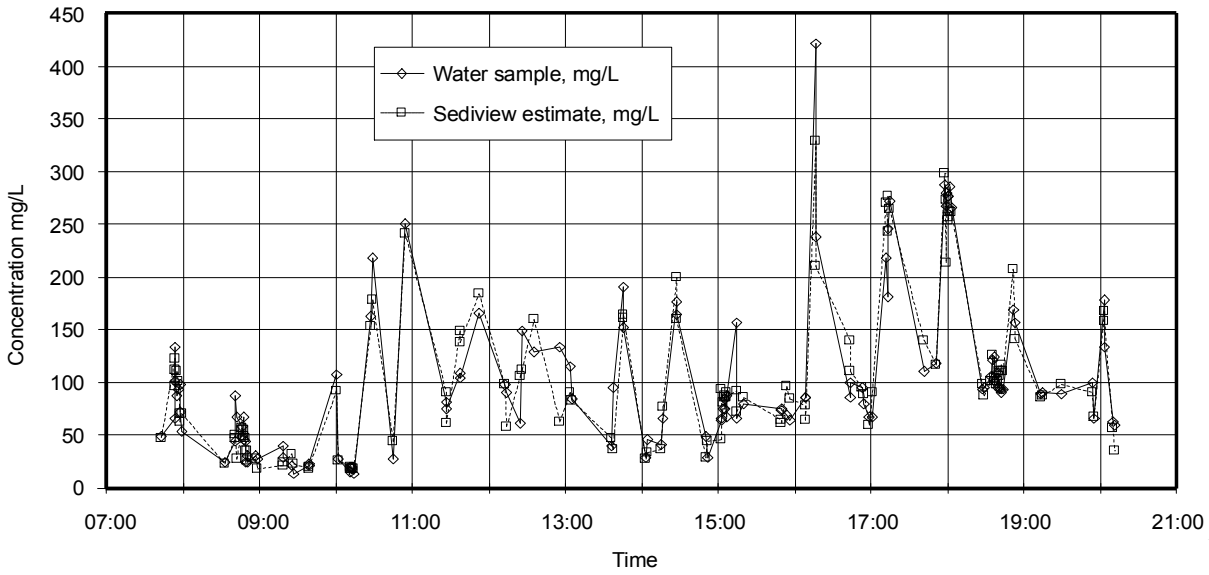

Figure 4. Time-series comparison of Sediview concentration estimates and water sample concentrations.

Tide	Discharge, m^3*10^6	Solids flux, tonnes
Spring Flood	390.8	73,228
Spring Ebb	429.9	81,166
Neap Flood	334.6	36,143
Neap Ebb	342.9	35,008

Table 1. Calculated fluxes - November 1995 & January 1996

The spur to use ADCP-based methods was the unreliability of existing measurements. Consequently there are no reliable data with which to cross check the ADCP-derived flux. All that can be said is that the results are consistent with the Environment Agency's understanding of the estuary, and it is believed that these currently represent the best estimates of the net solids transport.

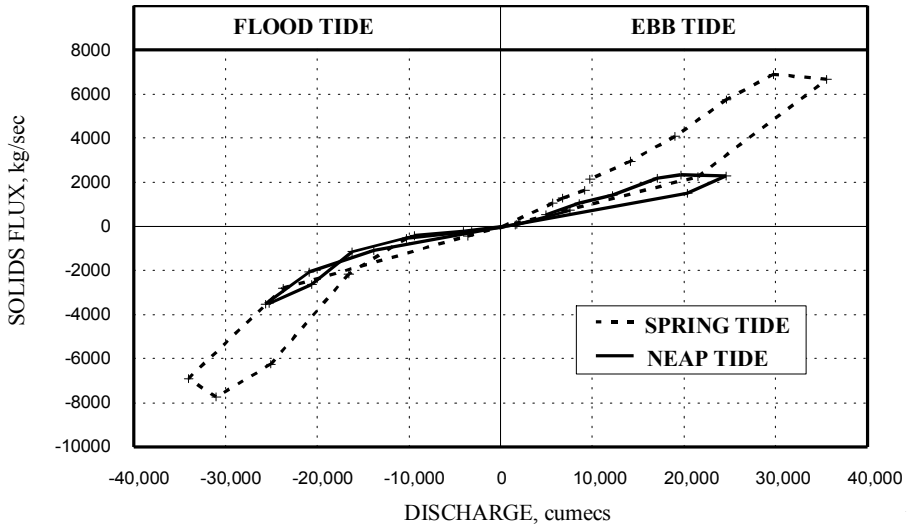

Figure 5. Measured variation of solids flux with discharge.

OTHER CALIBRATION EXAMPLES

Two examples of calibrations obtained in other rivers are briefly presented here. Figure 6 shows a preliminary calibration derived from a very limited number of water samples from a major South American river system. The data were obtained at ranges of between 10 and 50 metres. It is interesting to note that some of the ADCP data points had to be rejected because they were corrupted by backscattering from large animals and submerged tree trunks.

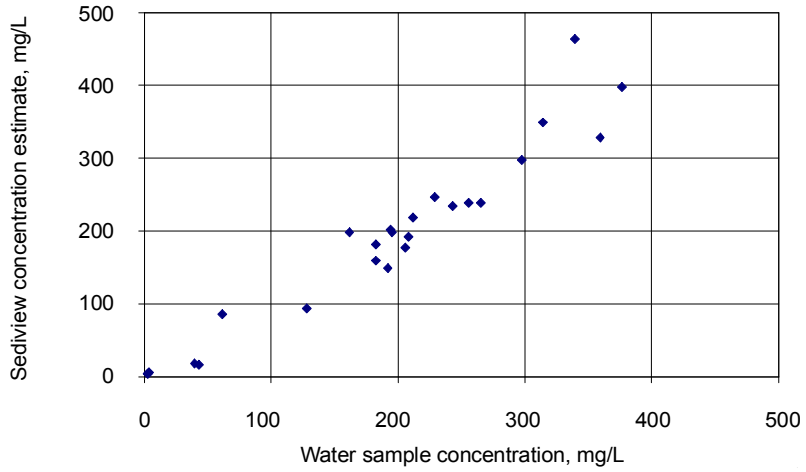

Figure 6. Preliminary calibration – South American rivers.

Figure 7 shows a quasi-time series of calibration data obtained in the Elbe River in Hamburg, Germany. The data were obtained over ranges of 2 to 18 metres in the main river and in harbour basins in both natural suspensions and those created during water injection dredging. Steep concentration gradients were observed through the survey which made accurate spatial synchronisation of water sampling and ADCP data difficult.

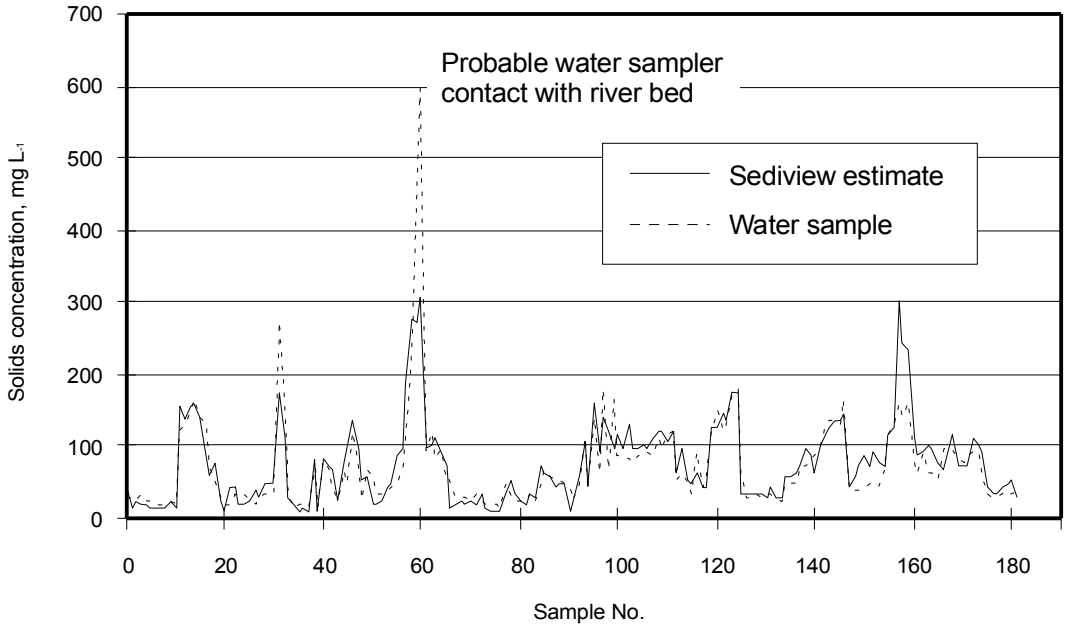

Figure 7. Quasi-time series of calibration data obtained in the Elbe River, Germany

CONCLUSIONS

There are many problems which may arise when measuring sediment flux using ADCPs. However, most can be overcome by careful data collection, processing and analysis. Accurate measurement of solids flux is heavily dependent on the quality of the calibration. We believe the work described in this paper shows that good calibration is possible using the methods developed. However it must be stressed that each calibration is site- and event-specific.

REFERENCES

Downing, A., Thorne, P.D., and Vincent, C.E., 1995, Backscattering from a suspension in the near field of a piston transducer. J. Acoust. Soc. Am., 97 (3), March 1995, pp1614-1620.

Dredging Research Ltd., 1996, Acoustic measurements of sediment flux through the Mersey Narrows. The Environment Agency, Bristol, UK.

Gordon R.L., 1991, Flow Velocity structure and discharge measurement in the Danube River. RD Instruments, San Diego.

Gordon R.L., 1992, Flow Velocity structure and discharge measurement in the Mississippi River. RD Instruments, San Diego.

Jarvis C.C. Adams J.RW, and Waters J.S., 1995, Preliminary investigations to determine the potential of ADCP for river flow measurement. BHS 5th National Hydrology Symposium, Edinburgh.

Jarvis C.C., 1997, The evaluation of Acoustic Doppler Current Profiler equipment. R & D note W71. The Environment Agency Bristol U.K.

Land, J.M., and Bray, R.N., 1998, Acoustic measurement of suspended solids for monitoring of dredging and dredged material disposal. Proc. 15th World Dredging Congress, Las Vegas.

Land, J.M., R. Kirby and J.B. Massey., 1997, Developments in the combined use of acoustic Doppler current profilers and profiling siltmeters for suspended solids monitoring. In: Cohesive Sediments. Proceedings 4th Nearshore and Estuarine Cohesive Sediment Transport Conference, INTERCOH '94. John Wiley and Sons.

Ogushwitz, P.R., 1994, Measurements of acoustical scattering from plumes of sediment suspended in open waters. Journal of Marine Environmental Engineering, **1**, pp119-130.

Perillo G.M.E. and Piccolo M.C., 1998, Importance of grid-cell area in the estimation of estuarine residual fluxes. Estuaries **21** No1 14-28.

Pollard T.G., 1992, Discharge measurements on the Willamette River. RD Instruments San Diego USA.

Richards S.D., A.D. Heathershaw and P.D. Thorne., 1996, The effect of suspended particulate matter on sound attenuation in seawater. J. Acoustical Soc. Am., 100 (3), pp1447-1450.

Sheng, J. and Hay, A.E., 1988, An examination of the spherical backscatter approximation in aqueous suspensions of sand. Journal of the Acoustical Society of America, 83, pp598-610.

Thevenot, M.M. and N.C. Kraus, 1993, Comparison of acoustical and optical measurements of suspended material in the Chesapeake Estuary. Journal of Marine Environmental Engineering, **1**, pp65-79.

Thorne, P.D., Vincent, C.E., Hardcastle, P.J., and Pearson, N., 1991, Measuring suspended sediment concentration using acoustic backscatter devices. Marine Geology, **98**, pp7-16.

Thorne, P.D., 1993, Measuring suspended sediments using acoustics: theory and practice. Proudman Ocenographic Laboratory Report to Dredging Research Ltd

Wither, A.W., Land, J., Jarvis, C.C, and Jones, P.D., 1998, A new technique for contaminant flux measurement in estuaries. Conference on Estuarine Research and Management in Developed and Developing Countries. Organised by Centre for Estuarine Research and Management (RSA) & Estuarine and Coastal Sciences Association (UK). University of Port Elizabeth, South Africa, July 1998.

FEASIBILITY OF USING ACOUSTIC AND OPTICAL BACKSCATTER INSTRUMENTS FOR ESTIMATING TOTAL SUSPENDED SOLIDS CONCENTRATIONS IN ESTUARINE ENVIRONMENTS.

Michael J. Byrne, Hydrologist and Eduardo Patiño, Hydrologist,
U. S. Geological Survey, Ft. Myers, FL.
Michael J Byrne 3745 Broadway Suite 301, Ft. Myers, FL 33901. (Phone 941-275-8448; Fax (941) 275-6820; Email: mbyrne@usgs.gov).

Abstract

To determine the feasibility of using acoustic and optical backscatter instruments for estimating total suspended solids (TSS) in estuarine environments, acoustic Doppler and water quality instruments were installed and water samples collected at three estuarine sites in the St. Lucie River Estuary, Florida (fig. 1). At each site, the Doppler instrument measures an index of the mean velocity of water at the monitoring section and the intensity of the return signal (acoustic backscatter) received by the sensor. Two water quality instruments (near the water surface and channel bottom) measure salinity, temperature and optical backscatter (turbidity) at two depths in the water column. Water samples were collected using a depth integrating sampler and a point sampler at a location near the water-quality and Doppler instruments. These samples were analyzed for TSS and volatile suspended solids (VSS).

These sites (North Fork, Roosevelt Bridge, and Evans Crary Bridge) exhibit different flow, water quality, and channel cross-sectional characteristics. Flow velocities vary between –2 and +2 feet per second during normal tidal cycles; salinity varies from fresh to brackish (less than 1 to 30 parts per thousand); temperature ranges seasonally from 15 to 30 degrees Celsius;

and TSS concentrations range from 3 to 37 milligrams per liter; with organic content ranging between 50 and 70 percent, depending on the location. Water quality is affected by tidal exchange, urban and agricultural runoff, and releases from Lake Okeechobee (west of the study area) through the St. Lucie Canal.

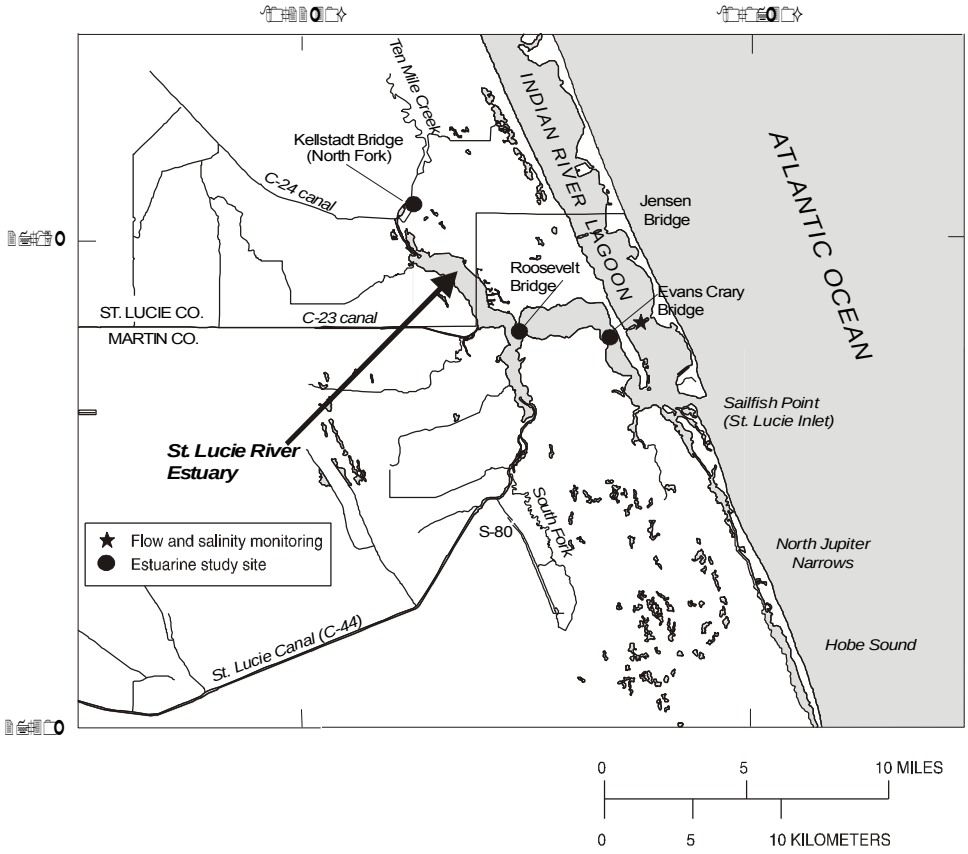

Figure 1. Study area.

Because the instruments at the Evans Crary Bridge site had to be relocated during the study, there was insufficient acoustic and optical data for analysis. However, sufficient data were available for analysis at the North Fork and Roosevelt Bridge Sites. The equation developed using acoustic backscatter data also includes the use of salinity and temperature data to compensate for daily and seasonal variability in water density (TSS= 10^[(ABS 0.0623) + (0.0012 Log Sal) – (0.0221 Log T) – 1.3232] R^2 = 0.87). The strongest acoustic backscatter to TSS relation has been found for the North Fork site (fig. 2), which has relatively stable hydraulic

characteristics. These characteristics include a straight reach, low velocity, and salinity ranging from 1 to 12 parts per thousand. A weaker correlation between acoustic backscatter data and

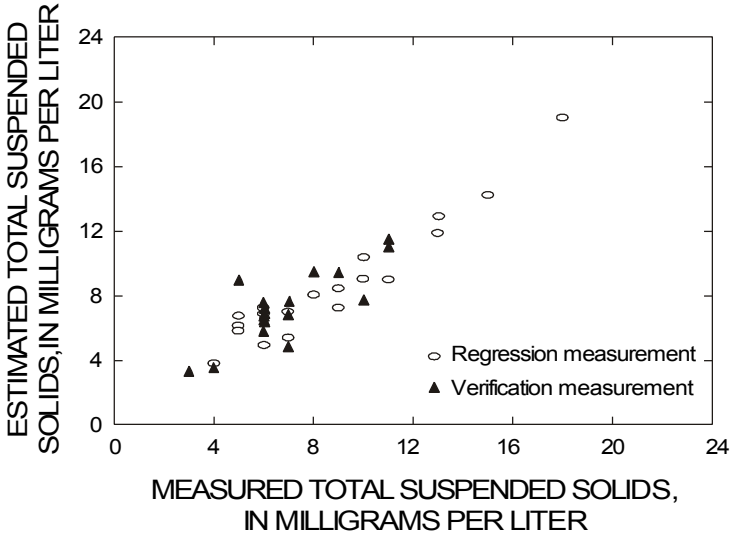

Figure 2. Relation between estimated and measured total suspended solids (TSS) concentrations for the North Fork site. TSS estimates computed using acoustic backscatter (ABS), salinity, and temperature data. Correlation coefficient is 0.87.

measured TSS at the Roosevelt Bridge site is believed to be the result of unstable hydraulic characteristics. There is turbulent flow at the monitoring section causing errors (spikes) in the data. On the other hand, the strongest correlation between optical backscatter (turbidity) and measured TSS was at the Roosevelt Bridge site (fig. 3), which has a 1,000 foot wide cross section, a main navigational channel where the instruments are located, turbulent flow due to the number and design of bridge pilings and footings, and salinity varying from 1 to 25 parts per thousand (depending on releases from Lake Okeechobee). The correlation was much weaker between optical backscatter and measured TSS at the North Fork site, possibly due to a smaller range of measured TSS concentrations (3 to 13 milligrams per liter).

Preliminary results indicate that acoustic and optical backscatter data can be used to estimate TSS concentrations. The strongest correlation for acoustic backscatter has been found at the site with the most stable hydraulic characteristics. The strongest correlation for optical backscatter was found at the site with the greatest range of TSS. However, one significant complication with the use of optical backscatter sensors in highly organic and biologically active environments, such as the St. Lucie River Estuary, is the excessive field maintenance and data quality assurance time required by the optical sensors in comparison to the acoustic Doppler instruments.

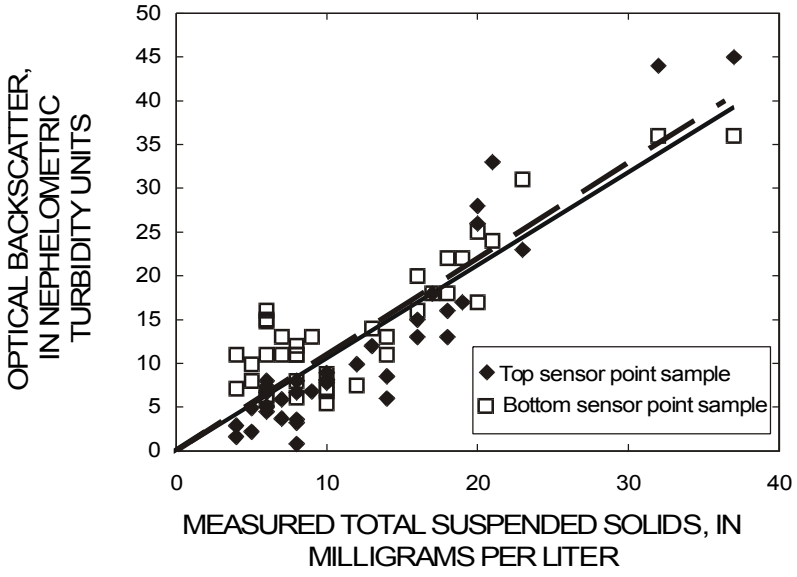

Figure 3. Relation between optical backscatter and total suspended solids in point samples for the Roosevelt Bridge site. Regression lines are for top sensor (dashed) and bottom sensor (solid) point samples. Equation for top sensor is y = 1.06x (correlation coefficient is 0.83); bottom sensor is y = 1.10x (correlation coefficient is 0.73).

USE OF ROTATING SIDE-SCAN SONAR TO MEASURE BEDLOAD

D. M. Rubin, Geologist, U.S. Geological Survey, Santa Cruz, California;
G. B. Tate, Geologist, U.S. Geological Survey[1], Menlo Park, California;
D. J. Topping, Hydrologist, U.S. Geological Survey, Reston, Virginia; and
R. A. Anima, Geologist, U.S. Geological Survey, Menlo Park, California
[1] Present address, Woods Hole Group, Redwood City, California

Abstract: Experiments in the 1960's demonstrated that the rate of sediment transport represented by migrating bedforms gives a more accurate measure of bedload transport than rates predicted from flow measurements. Rotating side-scan sonar can be used in the field to measure the rate of bedform migration and to calculate bedload transport rates. A rotating side-scan sonar system was deployed in the Colorado River in Grand Canyon for this purpose. For two sites where total load was measured using a depth-integrating sampler, approximately 5% and 0.3% of the sand transport was bedload involved in bedform migration; the other 95-99.7% occurred as suspended load that bypassed the bedforms.

INTRODUCTION

In deep marine flows and in rivers with soft, sandy beds, measurements of bedload transport are difficult to obtain using standard sampling techniques. Standard bedload samplers (such as Helley-Smith, BL-84, or BLH-84 samplers) tend to dig into sandy beds and thus can yield overly high measurements of bedload transport. This sampling problem illustrates the need to develop a method for measuring bedload transport that does not involve direct contact with the bed. One such method is to employ rotating side-scan sonar to measure the rate of bedload transport represented by migrating bedforms.

Simons et al. (1965) tested a variety of bedload transport equations using experimental flume data. They found that the rate of sediment transport represented by migrating bedforms gives a more accurate measure of bedload transport than rates predicted from flow measurements. The rate of sediment transport per unit width represented by a migrating bedform, called the "bedform transport rate" by Rubin and Hunter (1982), is equal to the product of three terms: bedform height, bedform migration speed, and a dimensionless shape factor (equal to 1/2 for bedforms whose cross-section approximates triangles touching end-to-end). These values can be measured relatively easily in the lab, but are difficult to measure in the field where bedforms are larger and the water is usually deeper and more opaque. The bedload transport rates calculated using this approach are mean rates for the area over which bedform heights and migration rates are sampled. In contrast, rates measured with a bedload sampler at a point on the bed are local rates, which can be expected to vary from approximately zero in a dune trough to twice the mean at a dune crest (Rubin and Hunter, 1982).

ROTATING SIDE-SCAN SONAR TECHNOLOGY

Hardware: Rotating side-scan sonar is well suited for field observations of bedform migration. It scans circular areas of the bed and has a range of tens of meters and a resolution of a few cm; it works in turbid water; and it can record sequential observations from a single point over time intervals of many hours. The first bed-deployed rotating sonar was an analog system that weighed several hundred pounds (Rubin et al., 1983). Modern commercially available systems are digital and weigh just a few pounds.

The system that we tested operates at 675 kHz and records up to 2000 acoustic pixels per acoustic ping. The transducer is mounted approximately 1 m above the bed. At a range of 10 m, it records 1000 pixels per ping (1 per cm) and takes 1-2 minutes to complete each circular scan. A typical deployment recorded several hundred complete scans over a duration of 10-20 hours.

Data processing: Sequential images at a site were converted into digital movies and displayed frame by frame on a computer screen. Individual dunes were tracked, and their migration speeds determined from the observed migration distances and times. Dune height was determined from fathometer profiles collected when the rotating side-scan sonar was deployed or by calculations from dune wavelength and assuming a height/wavelength ratio of 1/15. A preferable option would be to use a rotating interferometric or multibeam system to record 3-dimensional topography, rather than the 2-dimensional planform images recorded by standard rotating side-scan sonar.

EXAMPLE

The rotating side-scan sonar was deployed at approximately 20 locations in the Colorado River in Grand Canyon. Figure 1. shows two images and bedform-migration vectors at one of these sites.

A.

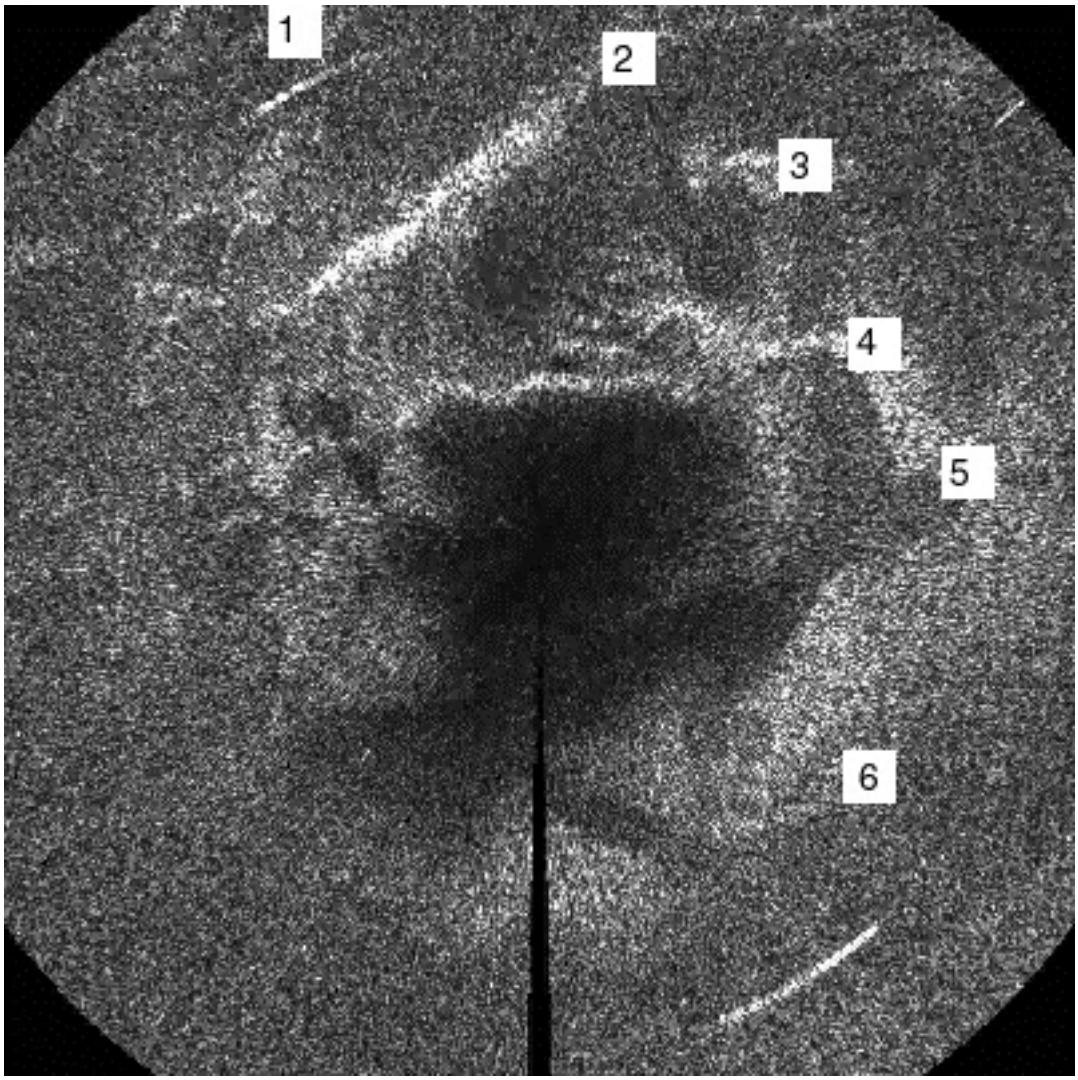

Figure 1. Rotating sonar images from the Colorado River at the Grand Canyon gage cableway. Flow is approximately from top of the image to the bottom. Bright areas on the image are strong acoustic reflections, indicating slopes that are facing toward the centrally located sonar transducer. The diameter of the circular part of the image is 20 m. Numbers identify 6 specific locations on 6 dunes. **A**. Image at initial time of bedform migration measurements. **B**. Same area of river bed after 2.5 hours of dune migration. **C**. Initial image with dune migration vectors superimposed. To track individual dunes requires viewing the intervening frames. The mean dune migration distance during the observation period was 2 m, and the migration speed was 0.02 cm/s.

B.

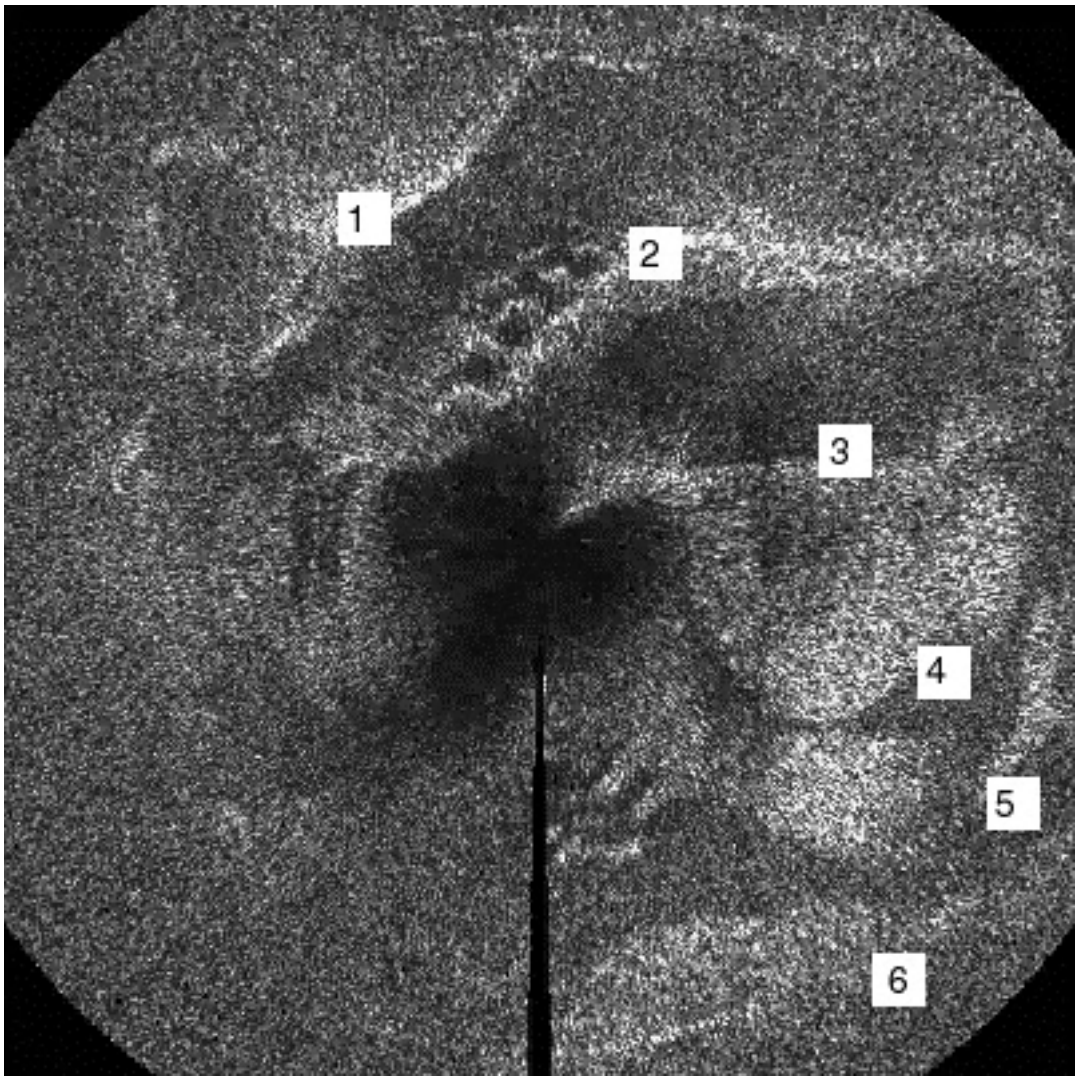

C.

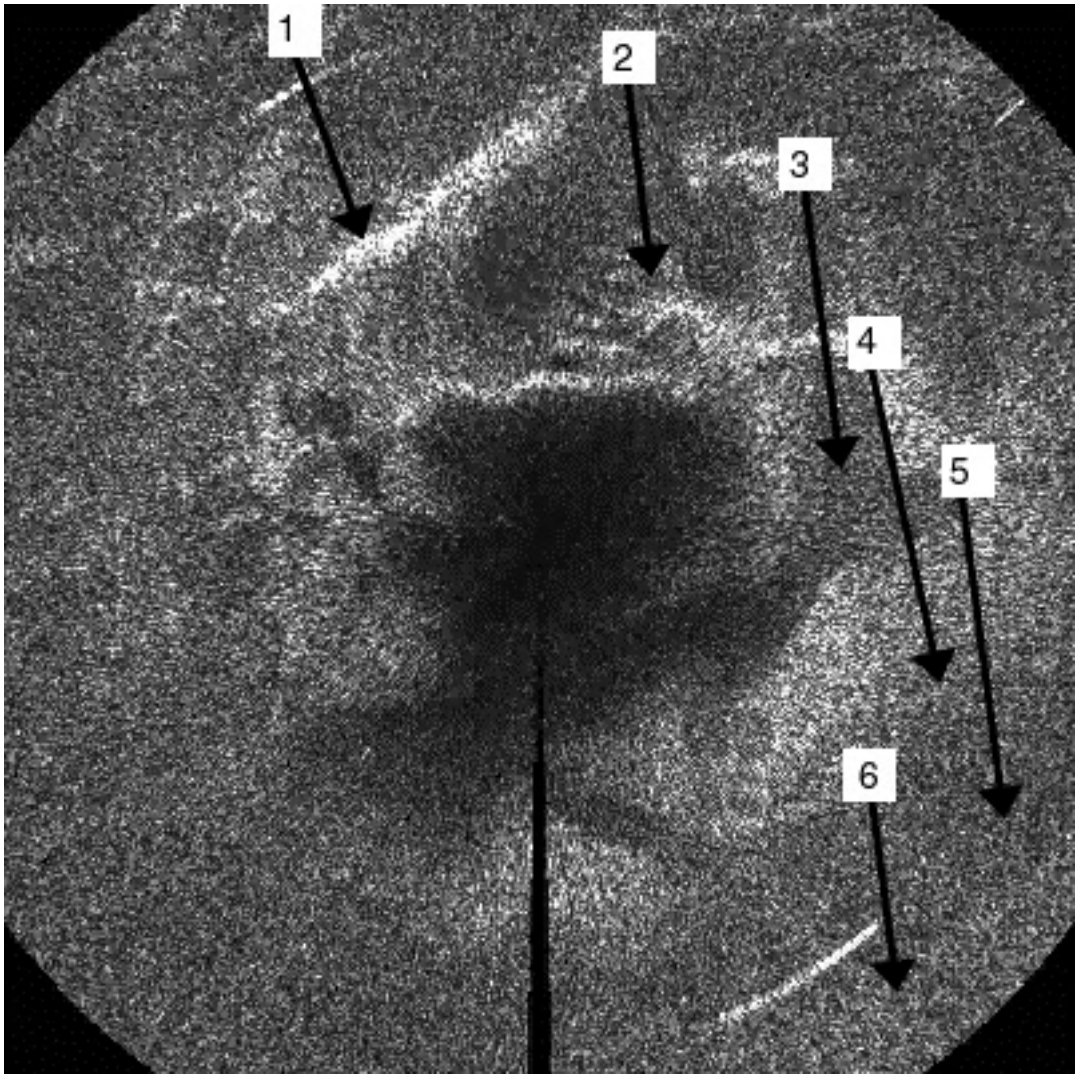

APPLICATION OF THE METHOD

Comparison of bedload and suspended-load transport: To determine the relative importance of bedload and suspended-load transport in the Colorado River in Grand Canyon, measurements of suspended load were made at 2 locations using a P-61 point-integrating sampler during the interval of rotating side-scan sonar observations. These measurement locations were at 2 USGS gaging stations: (1) the Colorado River above Little Colorado River near Desert View (station # 09383100) and the Colorado River near Grand Canyon (station # 09402500). These gages are informally known as the Lower Marble Canyon gage and Grand Canyon gage, respectively. The discharge of water and the grain size of the bed sand at each location were comparable during the measurements. At the Lower Marble Canyon gage, the discharge of water during the measurement period was approximately 550 m^3/s [19,300 cfs] and the median size of the bed

sand was 0.45 mm (as measured with a pipe dredge). At the Grand Canyon gage, the discharge of water during the measurement period was approximately 595 m^3/s [20,800 cfs] and the median size of the bed sand was 0.42 mm. At the Lower Marble Canyon gage, bedload involved in bedform migration was only 0.3% of the total sand load; at the Grand Canyon gage, bedload was approximately 5% of the total sand load.

Other observations: In addition to allowing accurate measurements of bedload transport, rotating side-scan sonar provides information about dune orientation relative to flow; cross-channel differences or similarities in transport rate; cross-channel differences in bedform size, migration speed, and migration direction; migration of superimposed dunes over larger bedforms; changes through time in bedforms and sediment transport; and bedform interactions such as splitting and merging. Rotating sonar is also useful in detecting starved bedforms migrating over a cobble bed: individual cobbles appear and disappear as they are exposed and then buried by troughs and crests of the migrating dunes.

REFERENCES

Rubin, D. M., and Hunter, R.E., 1982, Bedform climbing in theory and nature. Sedimentology 29, 121-138.

Rubin, D. M., McCulloch, D. S., and Hill, H. R., 1983, Sea-floor-mounted rotating side-scan sonar for making time-lapse sonographs. Continental Shelf Research 1, 295-301.

Simons, D. B., Richardson, E.V., and Nordin, C.F., Jr., 1965, Bedload equations for ripples and dunes. U.S. Geological Survey Professional Paper 462-H, 9 p.

Contact:
David M. Rubin
Coastal and Marine Geology
USGS Pacific Science Center
University of California at Santa Cruz
1156 High Street
Santa Cruz, CA 95064
831-459-3156
drubin@usgs.gov
http://walrus.wr.usgs.gov/seds/

LASER SENSORS FOR MONITORING SEDIMENTS: CAPABILITIES AND LIMITATIONS, A SURVEY

Yogesh C. Agrawal, President; Henry C. Pottsmith, V.P. Technology;
Sequoia Scientific, Inc., Redmond, Washington

WestPark Technical Center, 15317, NE 90th St., Redmond, WA 98052; (425)867-2464; fax: (425)867-5506; yogi@sequoiasci.com, pottsmith@sequoiasci.com

Abstract *:* This paper reviews current methods for monitoring sediments, comments on methods based on optical transmission or backscatter, and acoustic backscatter with regard to measurement physics and accuracy, and presents the performance of new sensors developed at this company under sponsorship of the Office of Naval Research. We note that fundamental physics stand in the way of accurate sediment measurement with earlier technologies, and that our LISST series of sensors deliver the most accurate measurement of suspended sediment. We describe the principles of operation, provide examples of field data, and discuss strengths and limitations of the LISST technology with regard to the interests of the Federal Government and other organizations interested in suspended sediment measurements.

INTRODUCTION

Natural Sediments: Natural marine sediments represent a vast diversity of compositions, shapes, points of origin, and environmental activity. In this survey, we shall disregard chemical aspects, instead focusing on physical measures of size, concentration, and in a limited way shapes. From the transport standpoint, 3 parameters may be considered to be most important: the volumetric concentration C_n, the size-dependent settling velocity distribution $w_{f,n}$, and a mean diameter, say D_{50} that separates the concentration equally on either side of the size range (Agrawal and Pottsmith 2000). An important parameter, relatively newly being recognized is the fractal dimension of these sediments, n_f. The fractal dimension, which relates volume d^{nf} to a characteristic diameter via d is 3 for Euclidean particles (i.e. particles that are solid), and lower values imply particles that become increasingly less dense as their size increases. Data on the magnitude of the fractal dimension is represented by the work of (Risovic 1996). When information on particle size and settling velocity is simultaneously available, as with the LISST-ST instrument to be described briefly here, an estimate of the fractal dimension n_f is possible.

Prior Technology: There are two classes of sensors in use : optical and acoustic. The most commonly used optical sensor is the OBS (Downing, Sternberg et al. 1981). It is an elegant and simple device. A light source produces an expanding beam that is projected into water. Light backscattered from particles is sensed by a photosensor. The calibration of the sensor is performed purely empirically, and is widely known to be size-dependent. A strong attraction of the OBS sensors is their potentially wide dynamic range; particularly, their ability to function in extreme turbidity. Within the same general category is the equally widely used beam transmissometer. In this case, the measurement is the attenuation of a fairly well collimated beam of light that is produced by a light-emitting-diode (LED). Again, it is well-known that the transmissometer calibration is size-dependent (Moody, Butman et al. 1987). Similar results for optical backscatterance sensors are presented by (Maa, Xu et al. 1992).

The size-dependence of optical transmission or back-scatterance sensors is simply a consequence of the fundamental physics of light scattering by particles. The optical scattering cross-section of a particle is very nearly exactly proportional to its geomterical cross-section. This is amply described in basic texts on the subject (e.g. (Hulst 1981)). For particles larger than about 0.1 micron, the extinction cross-section (i.e. the light removed by a particle from the incident beam) is proportional to the geometrical cross-section, with an order-one variability. Consequently, when a polydisperse suspension exists, as in nature, one measures the total particle area concentration, not volume. Only when particles are much smaller

than the wavelength of light, this proportionality is violated, being replaced by a volume-squared dependence. Such situations concern particles smaller than 0.1 micron. Fortunately, the sediment load in the marine environment is dominated by larger particles, except perhaps in extremely clear waters.

Acoustic methods hold the additional attraction of range-gated line-of-sight measures of sediment cross-section. This attraction is strong enough that the strong size-dependence of acoustic scattering is often overlooked in interpreting 'calibrated' measurements. A series of papers by Thorne and colleagues (e.g. (Thorne, Hardcastle et al. 1993),(Holdaway 1999),(Thorne 1997)) represent progress with this method. The multi-frequency method has been employed by these investigators and others ((Hay and Sheng 1992)) as well. Although development of ideas continues, fundamental physics make progress difficult.

The challenge of acoustics is the following. Even if one makes an assumption of the form of particle size-distribution in water – as was done by all workers cited in the preceding paragraph – a minimum of 3 parameters are needed to estimate concentration: for example, with an assumed log-normal size-distribution, the mean size, size-spread, and the magnitude of the peak are 3 unknowns that need to be estimated. This requires 3 independent measurements. Hence the 3-frequency method. Furthermore, in order to assure independence of the 3 measurements, all frequencies must be high enough that the scattering is not in the Rayleigh regime ($2\pi a/\lambda < 1$, a being radius of particle, λ being acoustic wavelength). In practical terms, this forces the use of MHz acoustics, with the consequent reduction in range of penetration due to water absorption. Even these methods require serious calibration, frequently done with optical transmission/scatterance sensors which themselves have problems as already noted. It is for these reasons that the present sensors were developed with support of US Office of Naval Research.

LASER DIFFRACTION INSTRUMENTS

Principles of Laser Diffraction and the LISST Instruments: In contrast to the 3 frequencies needed for acoustics, optical methods employ measurements of scattering at multiple *angles*. These methods are called multi-angle scattering, low-angle scattering (when scattering at small forward-angles alone is employed) and also, most commonly, laser diffraction. This technique is now described in an ISO standard, ISO-13220. A critical advantage of the method is that small-angle scattering is dominated by diffraction *around* the particle, so that particle composition is irrelevant. This makes the method widely applicable.

LISST-100 Instrument: In Figure 1, we show the basics of the LISST-100 series laser diffraction instruments. The scattered optical power sensed by the 32-ring-detectors is described by a 32-element vector $\underline{E}$:

$$\underline{E} = \exp\{-c\,l\}\,[\mathbf{K}\,\underline{N}_A + \underline{E}_{zscat}]. \qquad \text{(i)}$$

where:

c	represents beam attenuation coefficient, a variable depending on particle size-distribution;
l	is the path length of laser in water (5 cm standard, smaller available)
$\mathbf{K}$	kernel matrix, scattering on 32 ring-detectors by 32 size classes, based on Mie theory
$\underline{N}_A$	is area distribution, i.e. $n(a)a^2$ where $n(a)$ is number of particles of size a to $a+da$
$\underline{E}_{zscat}$	is the background light on detector rings from optical surfaces, in absence of particles.

The attenuation, $\exp\{-c\,l\}$ is measured with the photodiode placed behind a hole in the center of the ring-detectors; the background $\underline{E}_{zscat}$ is recorded with clean, particle-free water (Figure 1).

The inversion of equation (i) is carried out using methods described by us elsewhere. Once the area distribution has been constructed, the volume distribution $C_{n,}$, ie. volume concentration in size class n, is

quite simply estimated from a product of the mean size in the size class, say a_n, and the area in the size class, $\underline{N}_{A,n}$:

$$C_n = \mathbf{C}\, a_n\, \underline{N}_{A,n} \qquad \text{(ii)}$$

where **C** is an instrument specific calibration constant, and the total volume is quite simply $S_1^{32}\, C_n$.

The size-range measured by these instruments is defined by the minimum and maximum anglesθ at which scattering is observed; if f is receiving lens focal length and r is radius of a detector ring:

$$a_{max,min} = \lambda/[\pi\, \theta_{min,max}]; \quad \theta_{max,min} = \text{atan}(r_{max,min}/f). \qquad \text{(iii)}$$

It follows that for a given detector (which is a specially made silicon circuit), adjusting f permits adjustment of the range of observable particle sizes. The dynamic range of sizes examined is similarly:

$$a_{max}/a_{min} = r_{max}/r_{min}\ . \qquad \text{(iv)}$$

The LISST instruments have a dynamic range of 200:1 covering 1.25 to 250 microns,or 2.5 to 500 μm.

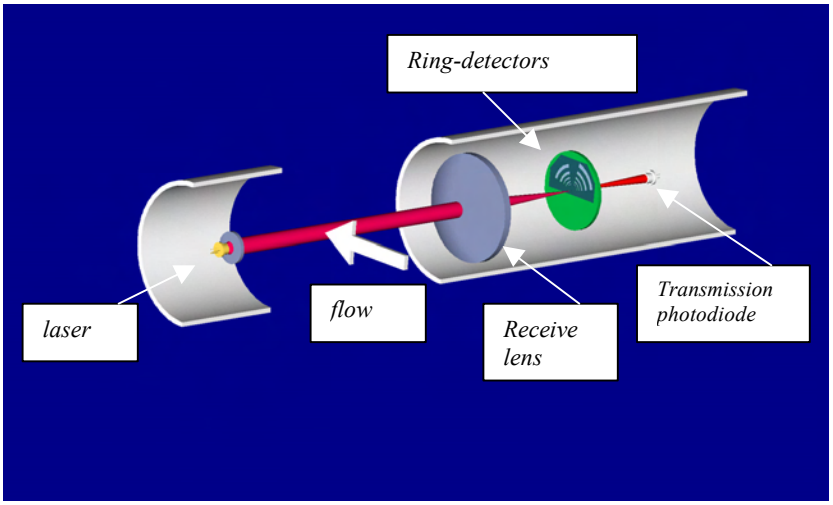

Figure 1: Laser diffraction principles – a cut away view of the basic LISST-100 instrument. A collimated laser beam illuminates particles (left to right). Multi-angle scattering is sensed by a specially constructed photo-diode array placed in the focal plane of the receiving lens. The array detector has 32 concentric rings, placed in alternate quadrants. A hole in the center passes the attenuated beam for measurement of optical transmission.

Calibrations of these instruments are performed as follows. The size range is dictated strictly by the physics and geometry. Thus only a verification is involved. The verification is performed using particle standards traceable to the National Institute of Standards and Technology of the US (NIST). We employ NIST's own glass sphere standards, as well as single-size particles obtained from Duke Scientific Co. in Palo Alto, California. Calibrations for mass concentration is done by a black box test, i.e. by finding a factor relating instrument-specific measured concentration against the known, weighed concentration of a sample. Further details are included in (Agrawal and Pottsmith 2000).

For the present work, we display size-distributions of two riverine samples. The first is a sample of river bank sediment taken off northern bank under a rather canonized bridge on highway 99; the bridge spans across the Toutle River which drains Mt. Saint Helens (Washington State, US). The second sample is obtained from the Yangtze river of China.

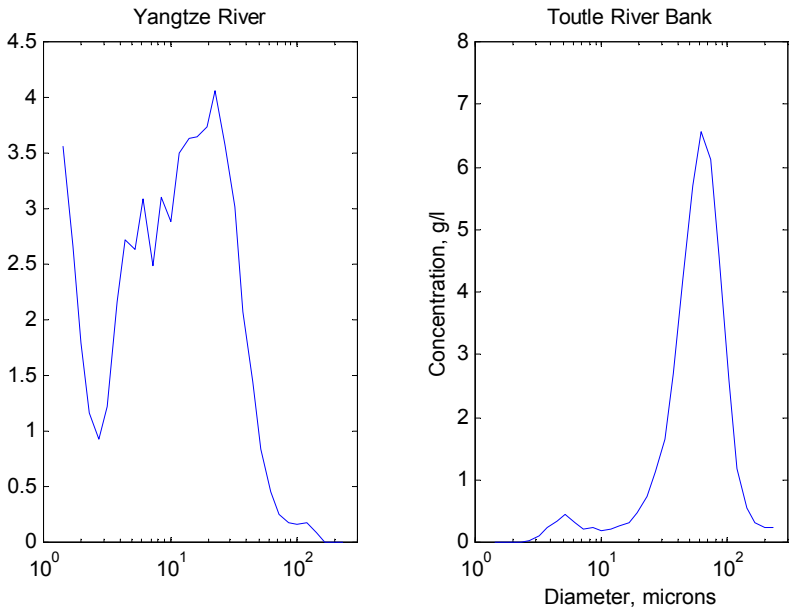

Figure 2: The size-distribution measurements of two types of sediments: a water sample of the Yangtze river, China, and a sample of sediment from the deposits on the northern bank of Toutle river, Washington.

LISST-25 Instrument: In contrast to the LISST-100, this instrument provides not the full size-distribution, but a mean size, and the total suspended sediment concentration (SSC). Its particular values is in that the concentration calibration is unaffected by changes in particle size over a 200:1 size range – over which prior technology sensors would have a roughly 20,000% variation in calibration. In this manner, this sensor marks a quantum leap in technology for measuring suspended sediment concentration. The underlying principle is as follows. The scattered optical power in the focal plane can be written, analogous to (i) as:

$$\underline{E} = \exp\{-c\,l\}\,[\mathbf{K}_V\,\underline{N}_V + \underline{E}_{zscat}]. \qquad (v)$$

where we use the subscript v is used on the kernel matrix and size-distribution. Here the matrix is constructed on a per-unit-particle-volume basis. One now simply asks a question if there exist a set of weights, $\underline{T}_v$, such the the scalar product of $\underline{E}$ and $\underline{T}_v$ is linearly proportional to the total volume concentration, i.e. the scalar product $\underline{N}_V\,\underline{U}$ where $\underline{U}$ is a unit vector. In other words, one seeks a $\underline{T}$ such that:

$$\underline{T}_v \bullet \underline{E} = \underline{N}_V \bullet \underline{U}$$

It follows that

$$\underline{T}_v = \mathbf{K}_V^{-1}\,\underline{U} \qquad (vi)$$

This is the essential solution. The result is physically interpreted as follows: if the outputs of the ring vector $\underline{E}$ are summed in accordance with the weights $\underline{T}$, then *the summation represents a linear measure of suspended volume concentration, valid for any size*. Now, the weighted sum can be accomplishing by adjusting the azimuthal coverage of the rings in proportion to the weight functions and then combining them to form a single silicon chip. This produces a comet shaped detector.

An identical solution for weights applies to considerations of particle area concentration. In this case:

$$\underline{T}_A = \mathbf{K}^{-1}\,\underline{U} \qquad \text{(vii)}$$

and one has a detector shaped a bit like a dumbbell. Thus two slices of silicon, one shaped like a comet and the other like a dumbbell report the volume and area concentrations of particles. The ratio, with factors of π, yields a Sauter Mean Diameter (SMD). The LISST-25 sensor system, in this manner, relies on specially shaped photo-detectors replacing the ring-detectors of Figure 1. The correction for attenuation is applied as usual via a measure of beam attenuation. A photodiode is placed behind the hole at center of the comet-dumbbell detector, for the attenuation measurement.

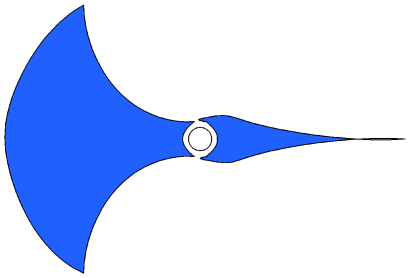

Figure 3: A pair of specially conFigured focal plane detectors replace the ring-detector of Figure 1, and sense the volume (right) and area concentration (left) of particles, separately. The ratio produces a mean diameter. These detectors substitute the rings of Figure 1 to form the LISST-25 sensor. A hole at center, similar to Figure 1, is used for optical transmission measurement.

An extensive test of the weight functions $\underline{T}$ is carried out via simluations. For this purpose, simulated particle distributions of Gaussian form, with equi-phi spaced mean sizes x and equi-phi spread s, are employed. The scattering signature is predicted using Mie theory, to construct the vectors E. The scalar product $\underline{T}\bullet\underline{E}$ is then constructed and compared against the input to the simulation. The results are presented in Figure 4 below. It is seen that but for one corner of the x-s space, the concentration and mean size are recovered correctly.

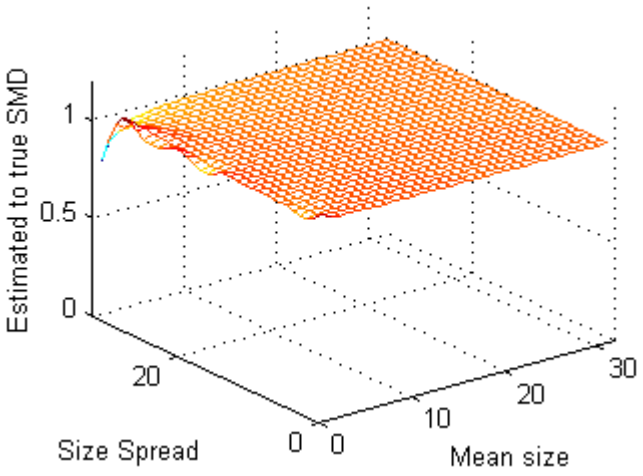

Figure 4: The estimated vs. true Sauter Mean Diameter of sediment particles with The LISST-25 method. The estimate of volume concentration obtained with the comet detector of Figure 3 parallel this same form. Note: the size and size spread represent the size-class and number of size classes in a log-spaced size-class set that increase by a factor of 1.18, from 1.25 to 250 microns in 32 size classes.

In the remaining of this section, we discuss questions on performance usually asked of a new sensor.

Concentration limits: The operating limits of such devices are determined by signal-to-noise considerations in extreme of clear water; or with optical transmission for extremely turbid waters. In clean waters, the scattering from particles is weak due to the small concentration, but also, it is noisier due to small-number statistics. The small-number statistics arise as the sample volume of the instrument is typically 6 mm in diameter, and 5 cm long (clear water instruments are also made in 20 cm path length). Thus the illuminated volume is merely 1.4 cm^3 (or 5.6 cm^3 for the 20 cm path). The weak and noisy signals require additional time spent in averaging (effectively, increasing the illuminated volume). Thus, averaging can continue to extend operating range into increasingly clearer waters.

The upper turbidity limit of operation is set by constraints on single scattering. At high concentrations, a significant fraction of light scattered once can be rescattered into the field of view. This alters the scattering matrix **K** in equation (i) and requires different inversion algorithms. The optical scattering literature notes that multiple-scattering can be identified directly based on the optical attenuation. For this reason, the optical transmission is the defining parameter which determines if multiple scattering is a concern. There is no sudden onset of multi-scattering. We specify transmission of ~30% as the lower limit for operation. When data in lower transmission conditions are obtained, the resulting inversion will bias the measurements to smaller sizes as multiple scattering robs small-angle scattered energy and puts it at larger angles.

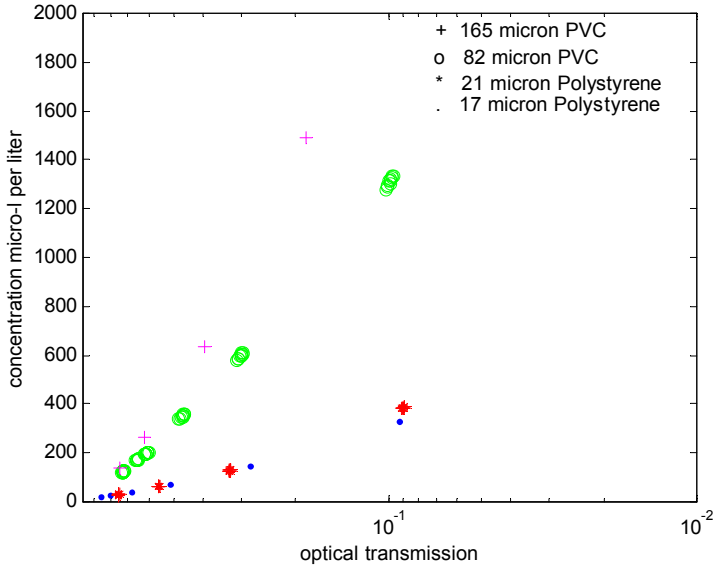

Figure 5: Optical transmission (reversed scale) and concentration estimated after inversion of scattering data. Note first, that any estimate of concentration from transmission depends on size of particles. Similar results apply for optical scatterance sensors. Second, note that when transmission is as low as 10% or less, i.e. even when multiple scattering is significant, the linearity for each size is maintained.

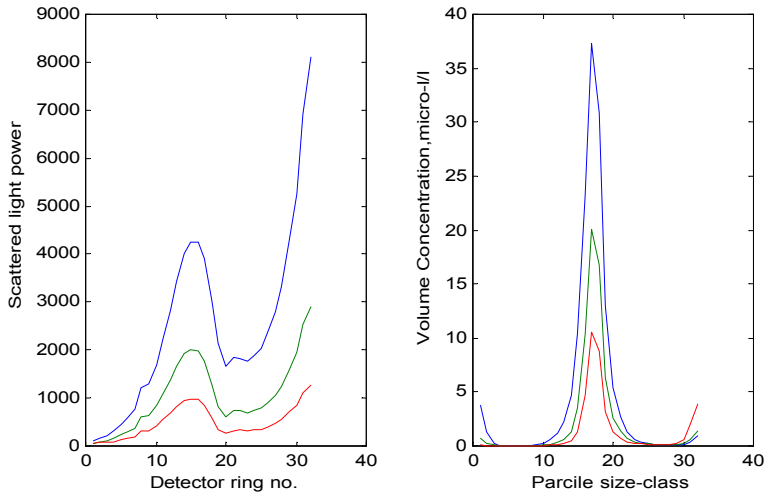

Figure 6: The scattering signature (left panel) and size-distribution (right) for 3 concentrations of 17 µm particle data. The scattering curves show a disproportionately strong increase in scattering at the outer rings (left) due to multiple-scattering. This corresponds to an apparent concentration of small sizes in the size-distribution (right). The small peaks at the largest sizes (right) are believed to be caused by bubbles, and are not significant.

The simplest means of extending the operating range of these instruments into extreme turbidity is to shorten the optical path. This simply reduces the exponential factor preceding the matrix product in

equation (i). Significantly, a halving of the pathlength l increases the transmission to a square-root of the original. For example, a 10% situation changes to 32% by just one halving. For still higher concentrations, a $1/4^{th}$ path length would similarly extend a 1% situation to 32%.

The influence of high concentration is examined next for possible departure from linearity of estimates of the volume distribution. First, with reference to Figure 5, Beer's law suggests that a linear relation should exist between concentration and the negative logarithm of optical transmission. This is clearly verified. Significantly, even when the transmission drops below 10%, linearity is maintained. Also clearly visible is the size dependene of calibration for optical transmission – a widely known fact.

We now consider the influence of multiple scattering on estimates of size-distribution. In Figure 6, the scattering signatures (left) and the volume distributions (right) are shown for 17 micron PVC spheres, at concentrations decreasing from 509 µl/l, halved twice to 127 µl/l. It is evident that multiple-scattering produces a more-than-linear increase in light on the outer detector rings (left panel). The consequence is the appearance of a weak concentration of fine particles on the small size end (right panel). Again, note that the total concentration estimates shown in Figure 5, which are derived from inversion of the scattering, remain quite linear.

To summarize, first, multiple-scattering has the effect of producing small particles at very low optical transmission, although the estimate of concentration is relatively unaffected. Further, for extreme conditions of clarity or turbidity, useful concentration limits can be extended by adjustment of the optical path length of the scattering volume.

Velocity limits: The measurements of scattering in this method are insensitive to fluid velocity. Fast flow-through is helpful in smoothing the scattering signatures. Extremely slow flows get in the way of obtaining statistically independent scattering signatures when such samples are desired for averaging. For the 6 mm diameter beam and 0.2 second data capture time, velocities less than 3 cm/sec will cause samples to be overlapping, requiring more averaging.

Out-of-size-range particles: It is easy to understand the effect of particles that are either too large or too small. In this case, one can rewrite equation (i) for contributions from those particles in range, and those out of range, as:

$$\underline{E} = \exp\{-(c_1+c_2)\, l\}\, [\mathbf{K}\, \underline{N}_A + \mathbf{K_2}\, \underline{N}_{A,2} + \underline{E}_{zscat}].$$

Where the attenuation term in curly brackets is explicitly separated into its two components, and the scattering terms are explicitly shown as two matrix products. Since attenuation is measured, there is no uncertainty resulting from it. The additional scattering due to $\mathbf{K_2}\, \underline{N}_{A,2}$ does not fall on the detector rings (or, at worst, is weak for particles just out of range). This was verified in a simple experiment where very fine particles were added to a lab mixture. Thus the size-distribution and concentration of in-range particles is correctly recovered.

Fractal Effects: We note that the preceding work is based on Euclidian ideas, or a fractal dimension of 3. If the fractal dimension is smaller than 3, corrections can be applied in the case of the LISST-100 by converting the area distribution to volume distribution by multiplying the area in each size class by d^{nf-2}. This is straight-forward. In the case of the LISST-25, entirely new vectors $\underline{T}$ will need to be employed.

Other Factors: One of the most obvious question concerns shape of particles. It is not possible to cover this topic in a short survey; however, a brief mention of scattering by flocs is necessary (also, see

Agrawal and Pottsimth, 2000). To our knowledge, a generalized theory for scattering by flocs – which is needed to build the matrix **K**, is not now available. In general, it is empirically known that natural particles that are not fibrous, tend to behave rather like absorbing spheres. This , in effect, parallels the discussion of composition. In both cases, the refractive index is the essential variable. Since the small-angle scattering method depends primarily on diffraction (i.e. blockage) *around* particles, refractive index is a secondary factor. Its effect is to alter estimates of fines. The explanation is as follows: the tail of scattering at the outer rings sees light *transmitted* by the larger particles, in addition to the light diffracted by fines. The transmitted component depends on composition (refractive index). Hence the diffraction signature is contaminated by a transmitted component. The most effective solution is to calibrate the sensor with the actual particles, wherever possible.

Acknowledgements: We are grateful to Dr. Joseph Kravitz of ONR for supporting the development of these sensors over a period of several years.

REFERENCES

Agrawal, Y. C. and H. C. Pottsmith (2000). "Instruments for Particle Size and Settling Velocity Observations in Sediment Transport." Marine Geology **168**(1-4): 89-114.

Downing, J. P., R. W. Sternberg, et al. (1981). "New Instrumentation for the Investigation of Sediment Suspension Processes in the Shallow Marine Environment." Marine Geology **42**: 19-34.

Hay, A. E. and J. Sheng (1992). "Vertical Profiles of Suspended Sand Concentration and Size from Multifrequency Acoustic Backscatter." Journal of Geophysical Research **97**(No. C10): 15,661-15,677.

Holdaway, G. P., Thorne,P.D., Flatt,D.,Jones,S.E.,Prandle,D. (1999). "Comparison between ADCP and transmissometer measurements of suspended sediment concentration." Continental Shelf Research **19**: 421-441.

Hulst, H. C. V. d. (1981). Light scattering by small particles. New York, Dover Publications Inc.

Maa, J., J. Xu, et al. (1992). "Notes on the Performance of an Optical Backscatter Sensor for Cohesive Sediments." Marine Geology **104**: 215-218.

Moody, J. A., B. Butman, et al. (1987). "Near-Bottom Suspended Matter Concentration on the Continental Shelf During Storms: Estimates Based on In-Situ Observations of Light Transmission and a Particle Size dependent transmissometer claibration." Contiental Shelf Research **7**(6): 609-628.

Risovic, D. M., M. (1996). "Fractal dimensions of suspended particles in seawater." Journal of Colloid and Interface Science **182**: 199-203.

Thorne, P. D., P. J. Hardcastle, et al. (1993). "Analysis of Acoustic Measurements of Suspended Sediments." J. Geophys. Res. **98**(C1): 899-910.

Thorne, P. D., Hardcastle, P.J. (1997). "Acoustic measurements of suspended sediments in turbulent currents and comparison with in-situ samples." J. Acoustical Society of America **101**(5): 2603-2614.

AUTOMATED SEDIMENT SIZE DISCRIMINATOR

by: Seth M. Dabney, Research Agronomist; Robert F. Cullum, Agricultural Engineer; and Sammie Smith, Jr., Research Chemist,
USDA-ARS National Sedimentation Laboratory, Oxford, MS

Abstract: Agriculture is increasingly being suggested as a major source of non-point source pollutants. Many upland water quality Best Management Practices (BMPs), such as detention ponds and filter strips, rely on the settling of sediment and adsorbed pollutants to improve water quality. The effectiveness of such practices depends strongly on particle settling velocity. There is, therefore, a need to assess the settling velocity characteristics of sediment leaving agricultural fields. Because much agricultural sediment is transported in the form of aggregates of primary particles that may be altered during storage or transport to a laboratory, we developed and tested an automated settling tube apparatus suitable for installation at remote sites. Sediment is separated into five size fractions with fall velocities similar to that of quartz sand falling in water at 25°C: >250 μm, 125 to 250 μm, 62.5 to 125 μm, 31 to 62.5 μm, and <32 μm. This device should be of value in many water quality studies because it provides an assessment of the quantity of sediment fractions that can be easily trapped by BMPs, and provide samples of those fractions so that their quality, such as their pollutant content or contaminant adsorption capacity, can be assessed in later laboratory analyses.

INTRODUCTION

Interest in understanding and quantifying diffuse non-point sources of pollutants in surface runoff will increase as Total Maximum Daily Loads (TMDLs) are promulgated. Many Best Management Practices (BMPs) rely on settling to remove contaminants (buffers, detention basins). The settling velocity of sediment particles is a critical parameter controlling the efficiency of these BMPs. Although several erosion and water quality models track sediment size classes (Knisel, 1980; Flanagan and Nearing, 1995, Renard *et al.*, 1997; Cronshey and Theurer, 1998; Muñoz-Carpena *et al.*, 1999), relatively little data is available to validate their predictions (Beuselinck *et al.*, 1999).

Unlike streambed and marine sediments, much sediment in runoff from agricultural lands occurs in the form of aggregates of primary particles (Swanson and Dedrick, 1967; Mutchler and Murphree 1988; Meyer *et al.*, 1992). The specific gravity of eroded aggregates is approximately 2.0 (Rhoton *et al.*, 1983). The size distribution of eroded sediment cannot be directly calculated from soil texture, but clay soils generally erode with a higher fraction of aggregates than soils high in silt or sand. Silty soils generally have a larger fraction of sediment particles finer than 125 μm than do coarser or finer textured soils (Meyer *et al.*, 1992). The size distribution of sediment eroded from simulated rainstorms has been empirically determined to be similar to that resulting from slowly prewetting a dry soil sample followed by stirring for 5 to 45 minutes (Rhoton *et al.*, 1982; Meyer *et al.*, 1983).

Eroded aggregates have similar or higher clay percentages than the bulk soil (Swanson and Dedrick, 1967; Meyer *et al.*, 1992). Therefore, trapping these aggregates can have a profound impact on transport of contaminants from agricultural fields. Meyer *et al.* (1995) found that when simulated concentrated flow on a 5% slope was retarded by an narrow strip of erect grass, nearly all sediment coarser than 125 μm was trapped regardless of flow rate while trapping of 32 to 125 μm sediment was reduced 80% to 40% as specific discharges increased from 0.008 to 0.045 m^2s^{-1}. Because of the sensitivity of results to sediment sizes in the range between 32 and 250 μm, Dabney *et al.* (1995) recommended characterization of three sediment size fractions within this range in future modeling and validation studies.

Aggregates can break down to form smaller and more stable aggregates over time. Generally, the smaller aggregates eroded by raindrop impact are more stable than larger aggregates eroded by concentrated runoff (Meyer *et al.*, 1992). To avoid risks of aggregate breakdown or coagulation after sample collection or during storage or transport to a laboratory, Meyer and Scott (1983) developed a field laboratory procedure to evaluate sediment size shortly after sample collection during rainfall simulator studies. However, a field laboratory is of little value when studying natural rainfall runoff processes because personnel are seldom on site during storm events. We therefore developed an automated sediment particle size discriminator that can be deployed at remote field sites to separate sediment samples based on effective fall velocity.

METHODS

The approach taken was a modification of the Griffith Tube (Hairsine and McTainsh, 1986). The Griffith Tube consists of three parts: (1) a sediment introduction device, (2) a 2-m long settling tube, and (3) a turntable on which settled sediment samples are collected. The bottom of the settling tube is submerged in water filling the turntable pan, while its top is sealed to prevent air from entering and water from escaping the settling tube. Sediment is collected in 20 discrete sub-sampling trays placed around the perimeter of the turntable pan. An operator rotates the pan at specified intervals.

We felt that a similar device might be constructed that would quantitatively divide a flow-weighted composite sample into effective size classes in close to real time and provide a sample of each size fraction for sediment quality analysis.

The apparatus was developed with the following performance and design criteria:

1) Separate five sediment size fractions including three between 250 and 32 μm;
2) Capable of remote operation, powered by 12 VDC, controlled by and/or compatible with commercially available flow meters and sediment samplers; and
3) Cost less than $2000.

Figure 1 is a schematic diagram of the sediment particle size discriminator (SPSD). Pipe sizes indicated are nominal U.S standard sizes. The 5-cm (2-in) ball valves employed were Model MVE22CF full port valves manufactured by Banjo Corporation[1], Crawfordsville, IN. They had a stainless steel ball, teflon seats, and viton seals and performed satisfactorily in testing to date. To reduce void space where sediment could be lost within the valves, we poured melted paraffin between the stainless steel balls and the valve housings. The 1-cm (3/8-in) valves were model 5750 water timers manufactured by L.R. Nelson Co., Peoria, IL. The connections of these small valves were terminated inside the mixing chamber with inverted elbows to minimize sediment deposition inside the tubing. Collection jars were 500 ml straight-sided wide-mouth jars (8 cm diameter X 9 cm high) with teflon-lined screw caps. Five jars were arranged in a positioning rack contained in a 26-cm diameter 1200 ml plastic bucket keyed to a turntable and stepper motor (EAD Motors, Dover, NH, Model LH1713-12). The makeup water reservoir was operated as a Marriot bottle to ensure the mixing chamber always filled completely. The top funnel diameter (Figure 1) was compatible with the pump head of a model 3700 ISCO peristaltic pump sampler.

The SPSD tests reported were conducted with manual operation of the turntable and valves. The microprocessor control circuit to enable remote operation is still being constructed. A separate flow meter will trigger sample collection at a frequency proportional to the runoff rate so a flow-weighted composite sample will be obtained. A microprocessor (Parallax Inc., Rocklin, CA) will track the number of times that samples have been successfully collected. When sufficient sample volume (~500 ml) has been pumped to fill the mixing chamber, the microprocessor will activate the valves and stepper motor to initiate the size separation sequence described below and tested manually to date. Sample acquisition will continue independently of the separation sequence while a flag is set to prevent reinitiation of the separation sequence until the turntable has returned to the fifth jar (home) position. The separation sequence will be repeated as often as necessary until the total sample from a storm has been processed. During each cycle, additional sediment of a given fall velocity class will be composited in the same five jars. If no sample has been pumped within 6 hours, the storm will be considered completed and the device will cycle twice more using makeup water to flush residual sediment from the funnel and valve.

Device operation: Prior to sample separation, the settling tube is full of water, the mixing chamber is drained, the raw sample is contained in the sheet metal funnel, the turntable is in the home position, and all valves are closed. To initiate sample separation, the turntable is rotated so that the jar that will contain the coarsest fraction (> 250 μm, jar 1 is positioned under the settling tube. The top ball valve is then opened and closed, processes that each require about 1.25 s. The large air bubble escaping from the mixing chamber creates turbulence that mixes the sample

[1] Names are necessary to report factually on available data; however, the USDA neither guarantees nor warrants the standard of the product, and the use of the name by USDA implies no approval of the product to the exclusion of others that may also be suitable.

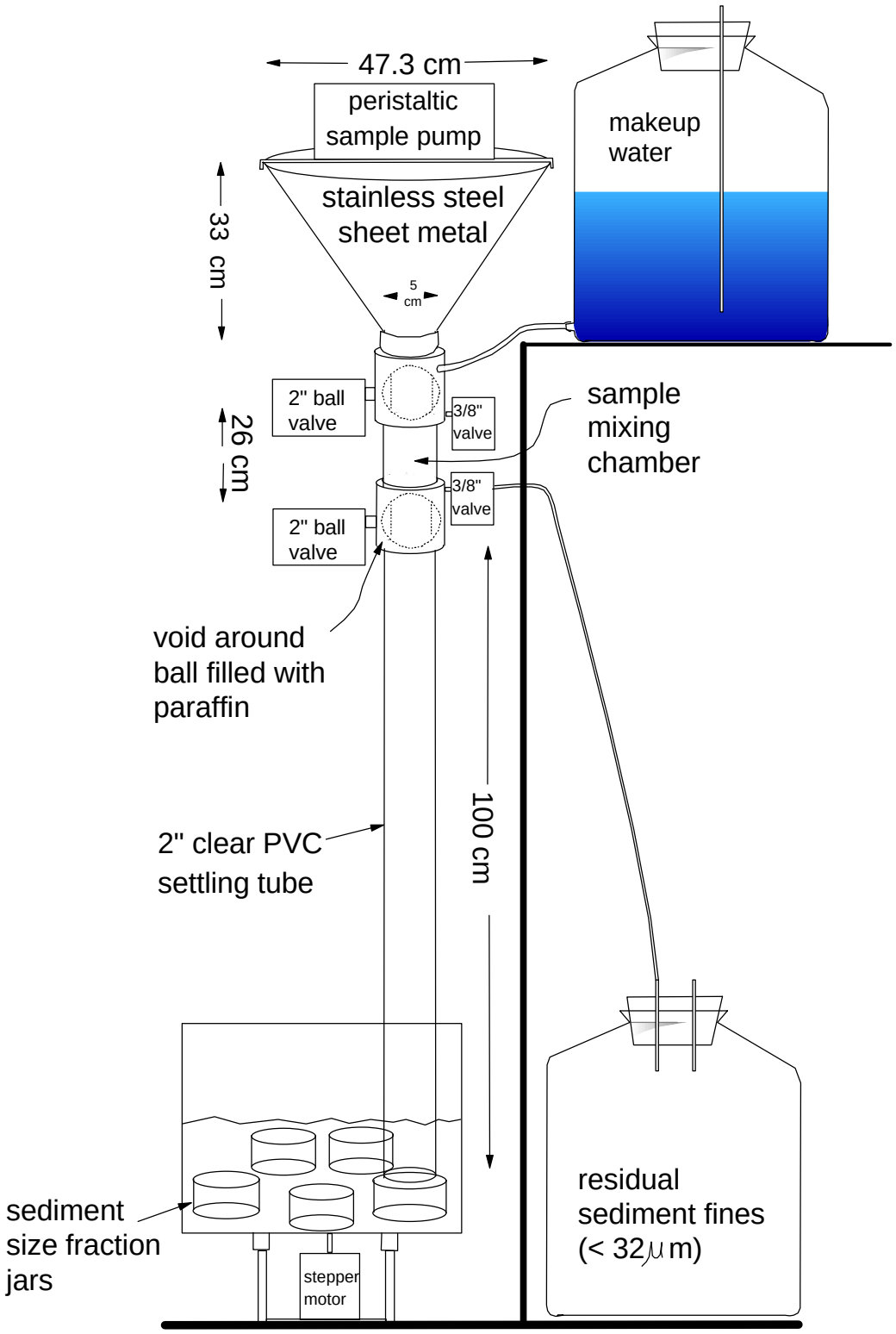

Figure 1. Schematic illustration of the sediment size discriminator showing sample collection funnel, 4 electronically controlled ball valves, a 1-m settling tube, and a collection bucket containing 5 sample jars mounted on a turntable connected to a stepper motor.

throughout the mixing chamber. The bottom valve is then opened and the microprocessor begins a timing sequence. At programmed intervals, the turntable is rotated so that progressively finer sediment is sequentially collected in the remanding four jars. Rotation of the turntable from one position to the next takes less than 1 s. After sufficient time has elapsed for sediment > 32 µm to have fallen through the 26 cm mixing chamber (~5 min), the lower ball valve is closed and the water in the mixing chamber is drained into the residual fine sediment container by opening the two 3/8-inch ball valves for 2 min. After the final (forth) sample fraction is collected, the turntable is rotated to position the fifth jar under the settling tube where it remains until another separation sequence is initiated. This jar collects some portion of the sediment finer than 32 µm and its contents are added to that of the residual fines prior to analysis.

Performance Testing: Device performance was evaluated under laboratory conditions at 25 to 26 °C using fine quartz sand comprised mainly of 64 to 250 µm size particles. Sand samples of 2.5, 5, or 25 g were wetted and washed into the apparatus with a total volume of 500 ml of water. Two alternative sediment introduction sequences were compared: (1) a 1-min delay between closing the top and opening the bottom 2-inch ball valve or (2) no delay between the close of the top valve and initiation of the sediment sequence by opening the bottom valve. The quantity of sand collected in sample jars was determined either with an Imhoff Cone (Sojka *et al.*, 1992), by drying and weighing, or both. We also determined the dry sieve-size distribution of samples collected from separation of four of the 25 g samples. Turntable rotation times were: 31 s for jar 1 (nominal >250 µm), 71 s for jar 2 (250 to125 µm), 285 s for jar 3 (125 to 62 µm), and 1140 s for jar 4 (62.5 to 31 µm sized sediment). These sedimentation times reflect fall velocities similar to those reported for settling of quartz spheres or sand at 20 to 25°C (Inter-Agency Committee on Water Resources, 1957; Gibbs *et al.*, 1971) and a sediment to fall distance of 1.0 m in the sedimentation tube plus 0.06 m in the lower ball valve and flange. To test these times, additional tests were made with the no-delay procedure using 10 g samples of two sand fractions separated by dry sieveing. Samples were obtained at 15 s intervals for the 125 to 250 µm sieve fraction and at 30 s intervals for the 62.5 to 125 µm fraction.

RESULTS

Volumes of sand in Imhoff cones were well correlated with the dry weights of the same samples. The regression line was: weight (g) = 0.3 + 1.56 (volume (ml)), $R^2 = 0.994$, n=6. This calibration included samples from all four jar fractions. Imhoff cone analysis was much faster than drying and weighing samples, but was limited to volumes greater than about 0.5 ml. In the following, weight and volume analyses have been combined.

The cumulative sediment size distribution based on sieve analysis and SPSD separations with both sediment introduction techniques are illustrated in Fig. 2. Data from all sediment concentrations are plotted, but lines connect p oints only for the 25 g samples. A 1 min delay between closing the upper valve and opening the bottom valve, "settled," resulted in more rapid sediment deposition and a coarser apparent particle size distribution than no delay operation, "mixed," in which the sediment was still well mixed within the sample chamber when the bottom valve was opened. Operation with "mixed" sample introduction resulted in a size distribution closer to the sieve distribution than did "settled" introduction. Fall velocity increased slightly with increasing sediment sample concentration, but a

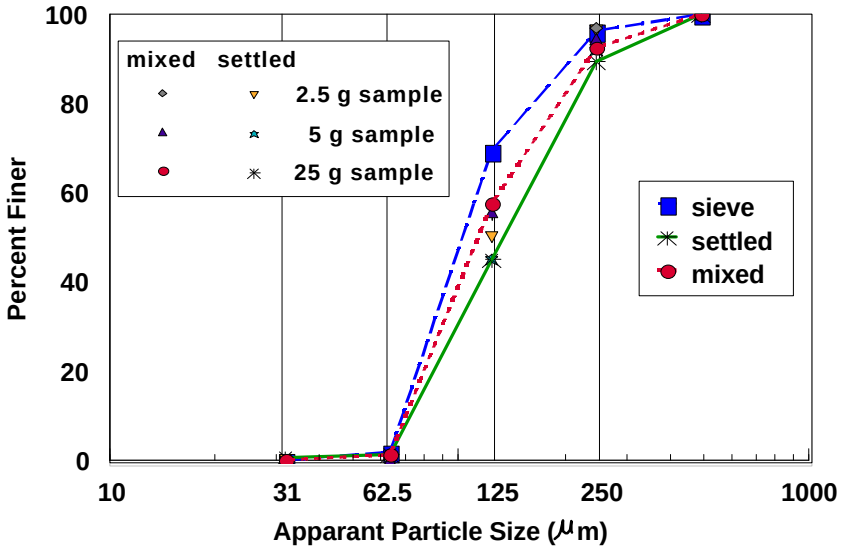

Figure 2. Sediment size distribution was closer to sieve data when SPSD separation began immediately after sample introduction ("mixed") compared to after allowing the sample to settle and rest on the lower ball valve ("settled").

Table 1. Size distribution fractions (mean±standard deviation) of three 25 g sand samples separated by the SPSD were finer and less variable using "mixed" compared to "settled" sample introduction.

Nominal Size	"Mixed" No Delay	"Settled" 1-min Delay
>250 µm (jar 1)	7.0±0.42	10.3±2.61†
125 to 250 µm (jar 2)	35.1±0.52	44.4±3.67**
62.5 to 125 µm (jar 3)	56.5±1.20	43.8±3.80**
31 to 62.5 µm (jar 4)	0.87±0.23	0.87±0.06

† row means different at P=0.07; ** row means different at P < 0.01

10-fold change in concentration effected size distribution less than the 1 min delay between valve operations. Size fraction data were less variable for mixed sample introduction compared to settled introduction (Table 1), a finding similar to that reported by the Inter-Agency Committee on Water Resources (1957) for sediment introduction into a visual accumulation tube.

Dry sieving (Figure 3) was used to determine the size distribution of the sediment fractions collected from the 25 g samples (Table 1). Because little sediment was collected in jars 1 and 4 (Table 1), attention is directed toward jars 2 and 3. Jar 2 nominally contained 125 and 250 µm sand. However, about half of it was actually 62.5 to 125 µm sand (Fig 3), indicating that this sediment fell faster than expected with both sediment introduction techniques. In contrast, the jar 3 was composed 80 to 90% of its nominal fraction with the balance being coarser sediment. Thus the performance trends were opposite in jars 2 and 3.

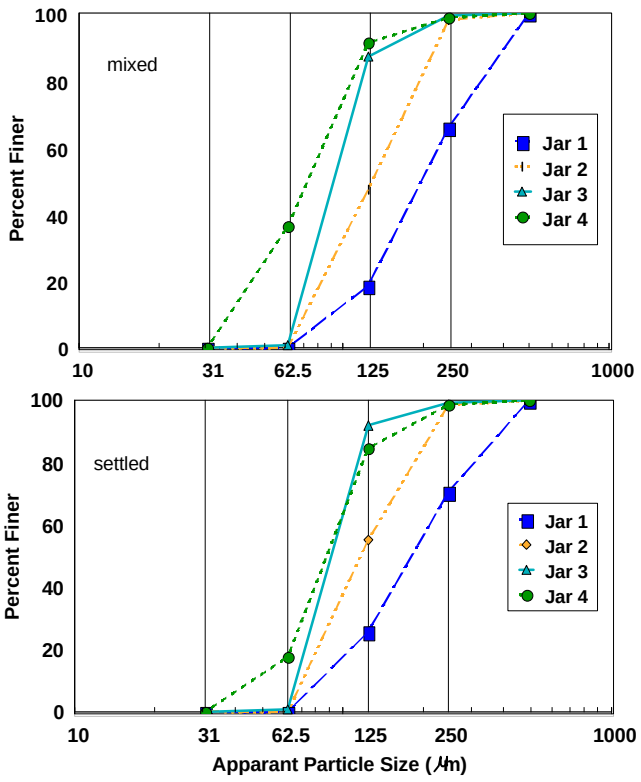

Figure 3. Dry sieve analysis of the samples collected from SPSD separation of 25 g samples (Figure 2, Table 1) show that coarser fractions included sediment finer than their nominal size and that there was some overlap between fractions.

The nature of this difference was clarified when sieved fractions of the sand were passed through the SPSD (Fig. 4). The results indicate that the fall times for the two fractions were spread out and overlapped but that the majority of each fraction was collected within the expected time frame.

We think that two opposing trends account for the results obtained. First, fall velocity may be increased due to "group settling" or "density currents" in which sediment raises the local density of a suspension and the denser suspension moves through the surrounding fluid with little size sorting. Fine sediment may also be transported by "drafting" within fluid shells surrounding coarser sediment particles (Lovell and Rose, 1991). Dilute suspensions minimize these problems, and the "mixed" sediment introduction procedure reduced local concentrations. However, when sediment is mixed, actual fall distances can vary from 106 to 132 cm because of a random position of individual particles within the 26-cm mixing chamber. Longer fall distances result in longer fall times so coarser sediment than expected may be collected in a fraction. Results in Fig 2, 3, and 4 suggest that accelerated settling processes dominate for particles coarser than 62 µm while longer fall distances control and retard particles finer than 62 µm.

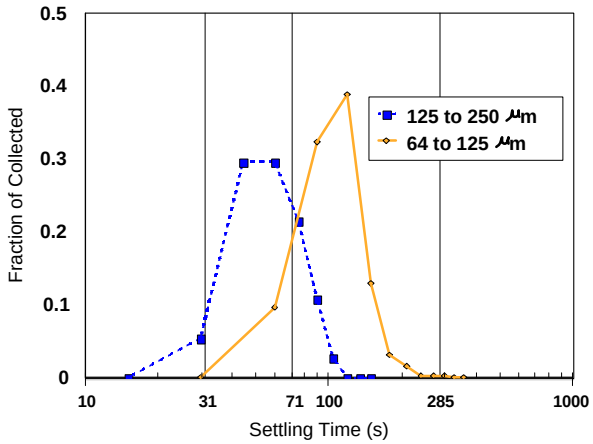

Figure 4. Fall times following "mixed" sample introduction of 10 g of sieved sand size fractions illustrate expected overlap of adjacent fractions due to varying fall distances within the mixing chamber.

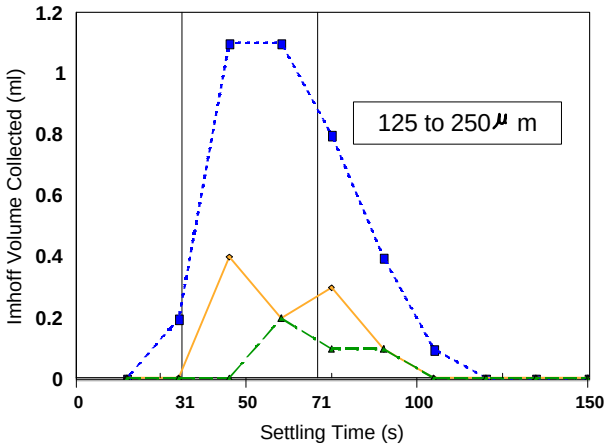

Figure 5. Sequential operation of SPSD after addition of a single 10 g sample of 125 to 250 μm sand illustrates progressive recovery of sediment retained in top ball valve or funnel.

If a mixture of the two sediments in Fig. 4 fell as the summation of the individual curves, a 71 second rotation time would result in about 20% of the coarser sediment being recovered in jar 3 and a similar fraction of the finer sediment being recovered in jar 2. Comparison with the "mixed" part of Fig. 3 shows that this describes the composition of jar 3 quite well, but that the amount of fine sediment in jar 2 is larger than predicted, reinforcing the idea that sediment size mixtures may fall faster than uniform-size groups (Emery, 1938; Schlee, 1966).

Another feature of the SPSD was an incomplete recovery of introduced sediment. Turbulence created by sediment introduction resulted in some sediment being retained in the upper ball valve and in the funnel above it. Repeated cycling of the device using makeup water recovered most of this material (Fig. 5). Some sediment was also lost between the jars during rotation of the turntable, and this could not be recovered.

DISCUSSION

We refer to the separates collected as standard sediment size equivalents because the sediment fractions fall similarly to that of various sizes of uniform quartz sand in water at standard temperatures. It would be difficult to calibrate natural runoff samples with sieve data since particle fall velocities are affected by variation in particle shape and density, mixture concentration and size distribution, and water temperature and chemistry. Nevertheless, sediment sample separation based on fall velocity is most suitable for our purpose of quantifying and sampling sediment that could be trapped by deposition processes using flow retarding BMPs. Changes in ambient conditions would alter our separation and BMP effectiveness in similar ways. For example, varying ambient temperatures would change the size of material in each sediment fraction, but would not alter our interpretation about that fraction' s potential to be removed by a BMP. Thus, temperature compensation of rotation times in not planned or desirable.

One limitation of the SPSD involves the time required to process each sample compared to the frequency with which samples are expected to be collected. The device can process 500 ml every 20 min. In a typical agricultural runoff monitoring scheme a 150 ml sample aliquot may be obtained for every 0.5 mm of runoff. One liter of runoff usually contains from 0.01 to 10 g of sediment, and may occasionally contain as much as 100 g (Meyer *et al.*, 1999). During intense runoff, samples will be obtained faster than they can be processed by the SPSD. The extra sample volume will be retained in the top funnel, which has a capacity of approximately 12 L. Since sediment will collect at the bottom of the funnel, concentration in the mixing chamber may be greater than ambient. The Inter-Agency Committee on Water Resources (1957) gave an upper limit of 15 g sand to be dispersed in 100 ml in a 20 cm-long mixing chamber for analysis with a 50 mm diameter visual accumulation tube. This corresponds to a maximum sample concentration of 150 g L^{-1}. Our tests compared sediment concentrations ranging from 5 to 50 g L^{-1} and found satisfactory performance. We therefore believe the device will operate at most concentrations likely to be encountered in practice. However, further research is needed on the impact of higher concentrations and of

significant amounts of organic matter or of particles < 32 μm on the separation of coarser sediment fractions since several authors indicate possible interferences (Emery, 1938; Inter-Agency Committee on Water Resources, 1957; Schlee, 1966). These tests may best be conducted by determining the effect of adding known quantities of dispersed silt and clay on analyses of the fine sand characterized in this report.

If it proves desirable to reduce the length of the sedimentation tube in order to increase sample throughput, this could be easily accomplished by adjusting the rotation times in the microprocessor program. However, there is always a compromise between precision of separation and ability to process samples rapidly. As the ratio length of the settling tube to that of the mixing chamber is reduced, overlap of sediment fractions will increase.

CONCLUSIONS

The SPSD appears to meet the performance criteria established. Electronic parts, valves, and stepper motor have a combined cost less than $1000. Labor to fabricate and program the device should not cost more if design and testing times are not considered. The SPSD separates sediment samples into five size fractions including three between 31 and 250 μm. Although the SPSD is not as accurate or precise in estimating particle size distributions as laboratory settling tube methods (Inter-Agency Committee on Water Resources, 1957; Schlee, 1966; Hairsine and McTainsh, 1986), it gives a meaningful estimate of the quantity of sediment in several important size fractions. Further, the SPSD provides samples of each size fraction so that their quality (texture, organic matter) and contaminant content or adsorption capacity can be assessed. We feel some sacrifice in precision is acceptable because of the benefits of unmanned, remote, "real-time" operation combined with the acquisition of size fractionated samples for sediment quality analyses.

ACKNOWLEDGEMENTS

We would like to thank Mike Williams for his excellent work in the construction and testing of the SPSD.

REFERENCES

Beuselinck, L., Govers, G., Steegen, A., Hairsine, P.B., and Poesen, J. 1999. Evaluation of the simple settling theory and predicting sediment deposition by overland flow. Earth Surf. Process. Landforms 24:993-1007.

Cronshey, R. G. and Theurer, F. G. 1998. AnnAGNPS-Non Point Pollutant Loading Model. In Proceedings First Federal Interagency Hydrologic Modeling Conference. 19-23 April 1998, Las Vegas, NV(on CD).

Dabney, S. M, Meyer, L. D., Harmon, W. C., Alonso, C. V., Foster, G. R. 1995. Depositional patterns of sediment trapped by grass hedges. Transactions of ASAE 38:1719-1729.

Emery, K.O. 1938. Rapid method of mechanical analysis of sands. J. Sed. Petrol. 8:105-111.

Flanagan, D.C. and Nearing, M.A., (eds.). 1995. *USDA-Water Erosion Prediction Project: Hillslope Profile and Watershed Model Documentation*. NSERL Report No. 10. West Lafayette, IN: USDA-ARS National Soil Erosion Research Laboratory.

Gibbs, R.J., Matthews, M.D., and Link, D.A. 1971. the relationship between sphere size and settling velocity. J. Sed. Petrol. 41:7-18.

Hairsine, P. and McTainsh, G. 1986. The Griffith Tube: a simple settling tube for the measurement of settling velocity of aggregates. AES Working Paper 3/86. School of Australian Environmental Studies. Griffith University, Australia.

Inter-Agency Committee on Water Resources, Subcommittee on Sedimentation. 1957. The development and calibration of the visual-accumulation tube. Report No. 11 in the series: A Study of Methods used in Measurement and Analysis of Sediment Loads in Streams. St. Anthony Falls Hydraulic Laboratory, Minneapolis, MN. 109 pp.

Knisel, W.G.(editor). 1980. CREAMS: A Field-Scale Model for Chemicals, Runoff, and Erosion from Agricultural Management Systems. U.S. Dept. Agric. Conservation Research Report 26.

Lovell, C.J. and Rose, C.W. 1991. Wake-capture effects observed in a comparison of methods to measure particle settling velocity beyond Stokes' range. J.Sed. Petrol., 61:575-582.

Meyer, L.D., Dabney, S.M., and Harmon,W.C. 1995. Sediment-trapping effectiveness of stiff-grass hedges. Transactions of ASAE 38:809-815.

Meyer, L.D., Dabney, S.M., Murphree, C.E., Harmon, W.C., and Grissinger, E.H. 1999. Crop production systems to control erosion and reduce runoff from upland silty soils. Transactions of ASAE 42:1645-1652.

Meyer, L.D., Line D.E., and Harmon, W.C. 1992. Size characteristics of sediment from agricultural soils. J. Soil and Water Cons. 47:107-111.

Meyer, L.D., and Scott, S.H. 1983. Possible errors during evaluations of sediment size distributions. Transactions of ASAE 26:481-485 & 490.

Meyer, L.D., Willoughby, W.E., Whisler, F.D., and Rhoton, F.E. 1983. Predicting size distributions of sediment eroded from aggregated soils. Transactions of ASAE 26:486-490.

Muñoz-Carpena, R., Parsons, J.E., and Gilliam, J. W. 1999. Modeling hydrology and sediment transport in vegetative filter strips. J. of Hydrology 214:111-129.

Mutchler, C.K. and Murphree, C.E. Jr. 1988. Tillage effects on erosion and sediment sizes. Transactions of the ASAE 31:402-407.

Renard, K.G., G.R. Foster, G.A. Weesies, D.K. McCool, and D.C. Yoder (coordinators). 1997. *Predicting Soil Erosion by Water: A Guide to Conservation Planning with the Revised Universal Soil Loss Equation (RUSLE).* U.S. Dept. Agric. Handbook 703. USDA, Washington, D.C.

Rhoton, F.E., Meyer, L.D., and Whisler, F.D. 1983. Densities of wet aggregated sediment from Different textured soils. Soil Sci. Soc. Am. J. 47:576-578.

Rhoton, F.E., Meyer, L.D., and Whisler, F.D. 1982. A laboratory method for predicting the size distribution of sediment eroded from surface soils. Soil Sci. Soc. Am. J. 46:1259-1263.

Schlee, J. 1966. A modified Woods Hole rapid sediment analyzer. J. Sed. Petrol. 36:403-413.

Sojka, R.E., Carter, D.L., and Brown, M.J. 1992. Imhoff cone determination of sediment in irrigation runoff. Soil Sci. Soc. Am. J. 56:884-890.

Swanson, N.P. and A.R. Dedrick. 1967. Soil particles and aggregates transported in water runoff under various slope conditions using simulated rainfall. Transactions of the ASAE 10:246-247.

CONTINUOUS MONITORING OF SUSPENDED SEDIMENT IN RIVERS BY USE OF OPTICAL SENSORS

David H. Schoellhamer, Research Hydrologist, U.S. Geological Survey, Sacramento, California

Placer Hall, 6000 J Street, Sacramento, California 95819, dschoell@usgs.gov

Abstract: Optical sensors have been used to measure turbidity and suspended-sediment concentration by many marine and estuarine studies, and optical sensors can provide automated, continuous time series of suspended-sediment concentration and discharge in rivers. Two potential problems are particle size effects and biological fouling. Output from an optical sensor at Freeport on the Sacramento River was successfully calibrated to discharge-weighted cross-sectionally averaged suspended-sediment concentration, despite varying particle size whereas the calibration of an optical sensor used at Cisco on the Colorado River was affected by particle size variability. The optical sensor time series at Freeport was used to calculate hourly suspended-sediment discharge that compared well with daily values from a sediment station at Freeport.

INTRODUCTION

Marine and estuarine studies of sediment transport have benefited from the use of optical sensors to measure turbidity and suspended-sediment concentration (SSC). Optical sensors transmit a pulse of infrared light through an optical window (Downing and others 1981). The light is scattered, or reflected, by particles in front of the window to a distance of about 4 - 8 inches at angles of as much as 165°. Some of this scattered, or reflected, light is returned to the optical window where a receiver converts the backscattered light to a voltage output. The voltage output is proportional to SSC if the particle size and optical properties of the sediment remain fairly constant. Calibration of the sensor output voltage to SSC will vary according to the size and optical properties of the suspended sediment; therefore, the sensors must be calibrated either in the field or a laboratory using suspended material from the field. If the optical window is fouled by biological growth or debris, the sensor output is invalid.

Compared to conventional water sampling, the primary advantage of using optical sensors is that they can provide automated continuous time series of SSC. This is essential for studies

- at inaccessible locations, such as the continental shelf (Cacchione and others 1995),
- during hazardous conditions, such as a tropical storm (Schoellhamer 1995),
- of environments with rapidly changing SSC, such as tidally affected water bodies (Uncles and others 1994, Schoellhamer 1996b, Christiansen and others 2000, Dyer and others 2000),
- requiring instantaneous vertical profiles of SSC (Edmunds and others 1997),
- of irregular resuspension, such as by trawlers and vessel wakes (Schoellhamer 1996a).

The disadvantages of using optical sensors are that changing particle size can confound calibration and fouling by biological growth and debris can invalidate data. The slope of the calibration curve, which is approximately equal to the ratio of concentration to output voltage,

increases with the particle size. Conner and DeVisser (1992) recommended that optical sensors not be used for particle sizes less than 100 μm because of the sensors' increased sensitivity to changes in particle size. Ludwig and Hanes (1990) recommended that optical sensors not be used for sand/mud mixtures. Biological growth on the optical window and biota or debris in front of the optical window can increase sensor output and invalidate data (Schoellhamer 1993). Despite these potential problems, many marine and estuarine studies have successfully used optical sensors to acquire accurate continuous SSC data.

The purpose of this paper is to demonstrate that optical sensors can successfully monitor suspended sediment in rivers if the effects of particle size do not preclude sensor calibration. The issue of the effects of particle size on optical sensors is addressed first followed by an example calculation of suspended-sediment discharge with an optical sensor.

PARTICLE SIZE EFFECTS

The relationship between SSC and sensor output is dependent on particle size, which can confound calibration of a sensor. In estuaries like San Francisco Bay, particle size is fairly constant and sensor calibrations are remarkably invariant with time (Buchanan and Ruhl 2000). In channels with a variable suspended particle size, however, sensor output depends on particle size and SSC. Finer sediment has more reflective surfaces per unit mass, so, for constant SSC, sensor output increases as the suspended sediment becomes finer. Particle size effects on optical sensors were absent in the Sacramento River at Freeport, California, but were present in the Colorado River at Cisco, Utah.

Freeport: Flow at Freeport is unidirectional but is affected by tidal backwater during low discharge. An optical sensor was installed to measure the effect of tidal fluctuations and flood pulses on suspended-sediment discharge and, therefore, sensor output was calibrated to discharge-weighted cross-sectionally averaged SSC. Optical sensor measurements were continuously collected near the right bank of the river every 15 minutes at 3 feet above the bed beginning in July 1998. The sensor was cleaned every 1-2 months. Twenty concurrent suspended-sediment samples and optical sensor measurements are available from July 1998 to September 1999. The discharge-weighted cross-sectionally averaged samples were analyzed for SSC and percent fines (fraction of mass less than 63 μm in diameter). The median SSC was 44 mg/L and the range was from 14 to 148 mg/L. For most sets of samples the right bank SSC is close to the average SSC and any discrepancy between the right bank and cross-sectional average would increase the scatter of the calibration.

The linear equation for SSC as a function of sensor output (fig. 1) was determined using the robust, nonparametric, repeated median method (Buchanan and Ruhl 2000). Optical sensor calibration data typically do not have residuals with constant variance, which is required when using ordinary least squares to obtain the best linear unbiased estimator of SSC. Robust regression also minimizes the influence of high leverage points.

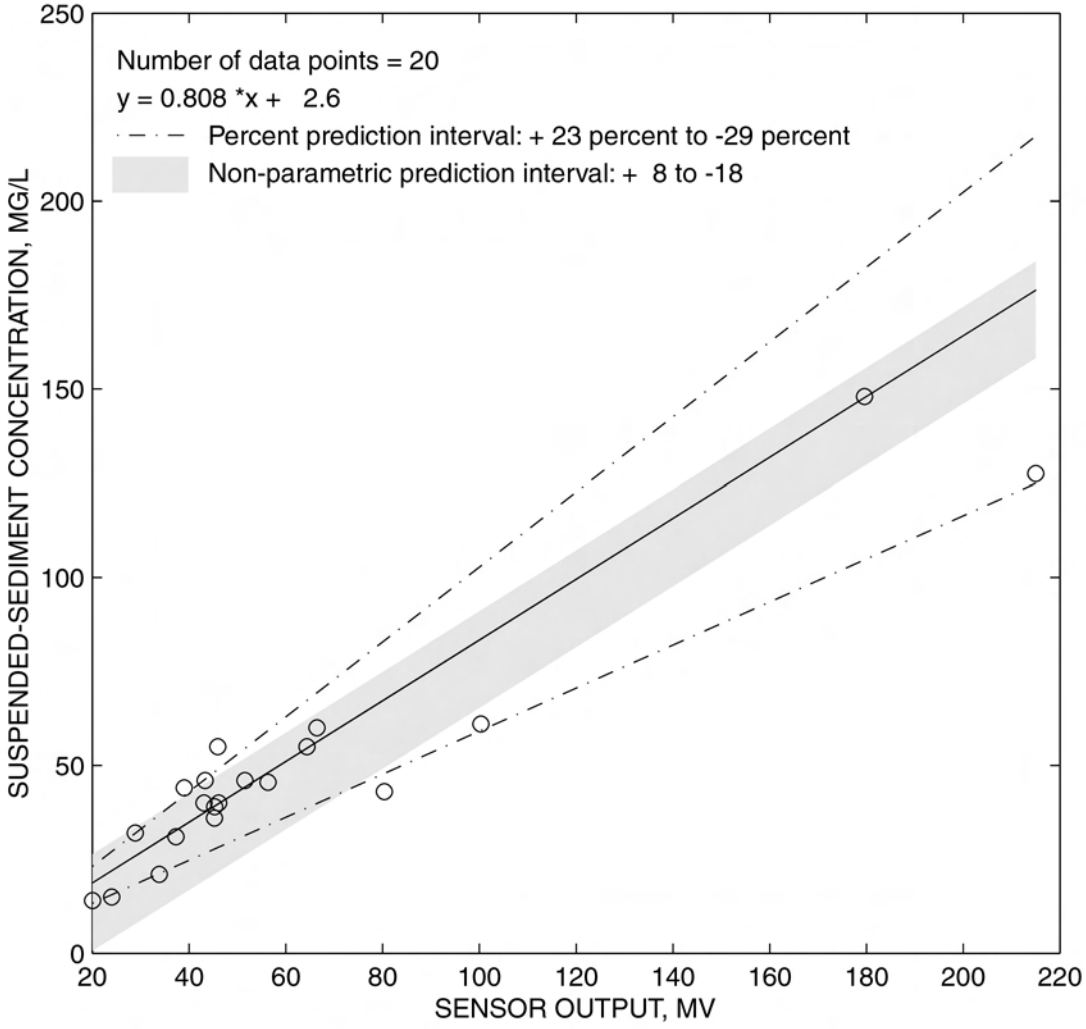

Figure 1. Calibration of an optical sensor at Freeport, Sacramento River, California, July 1998 – September 1999.

Particle size variations did not affect the calibration of the optical sensor at Freeport. The output of optical sensors is virtually zero when SSC is zero, so the ratio of concentration to voltage (C/V) for any data point is approximately equal to the slope of a calibration line through that point. At Freeport, the fraction of fine sediment ranged from 46 to 94 percent but C/V remained constant with some scatter (fig. 2).

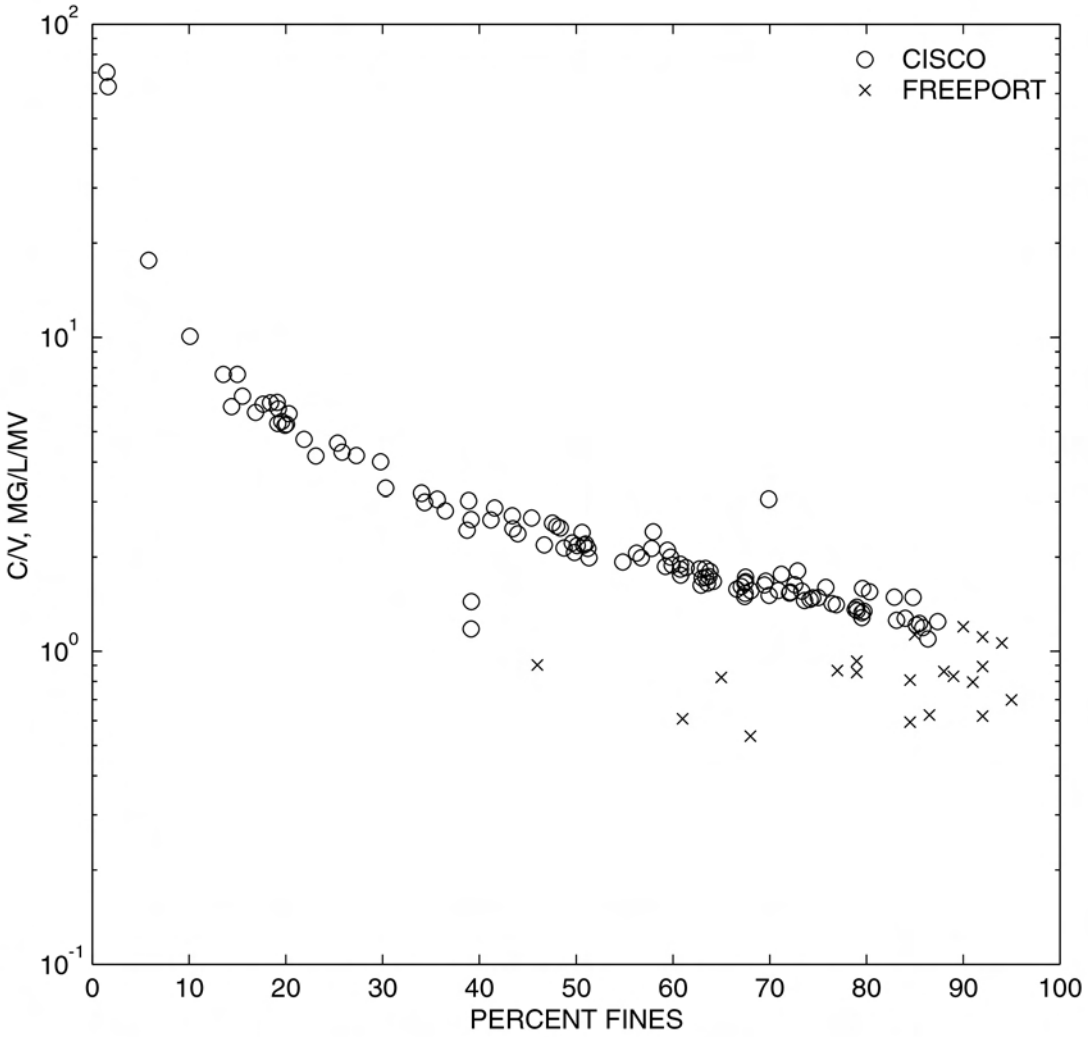

Figure 2. Ratio of suspended-sediment concentration to voltage (C/V) as a function of the fraction of fine sediment, at Freeport on the Sacramento River and Cisco on the Colorado River. C/V for any data point is approximately equal to the slope of a calibration line through that point. A different sensor was used at each site and each sensor has slightly different optical characteristics, so the difference in the trend of C/V should be compared between the two sites, not the absolute value of C/V.

Cisco: Vertical profiles of optical sensor measurements and suspended sediment were collected from the Colorado River near Cisco, Utah, from May 10-12, 1995. While measuring vertical profiles at 3 stations, 118 pairs of optical sensor measurements and suspended-sediment samples were collected from near the bed to near the water surface with an optical sensor attached to the side of a US P61 suspended-sediment sampler (Edwards and Glysson 1999) behind the nozzle. The optical sensor was much smaller than the sampler and probably had negligible effect on the isokinetic properties of the sampler. Optical sensor measurements were averaged while the

nozzle of the sampler was open. Water samples were analyzed for SSC and percent fines. Near the bed, almost all of the suspended sediment was sand, and near the surface there was very little suspended sand. SSC was greater at Cisco than at Freeport, with a median of 849 mg/L and a range of 476 to 40,300 mg/L.

Particle size variation precluded successful calibration of the optical sensor at Cisco. As the fraction of fine sediment increased from 1 to 87 percent, C/V decreased exponentially by almost two orders of magnitude (fig. 2). The Cisco data have less scatter than the Freeport data because the Cisco optical sensor was very close to the nozzle of the sampler, whereas the Freeport optical sensor was near the right bank and the samples were collected over the entire cross section.

In summary, optical sensor calibration was satisfactory at Freeport but not at Cisco. Therefore, successful application of optical sensors depends on local conditions, and the effect of particle size variation on optical sensors should not be presumed.

.

CALCULATION OF SUSPENDED-SEDIMENT DISCHARGE WITH AN OPTICAL SENSOR

The calibrated optical sensor on the Sacramento River at Freeport has been used to successfully measure suspended-sediment discharge. Output from the sensor was converted to a time series of discharge-weighted cross-sectionally averaged SSC and the calibration line is shown in figure 1. This concentration is multiplied by the water discharge measured by a calibrated ultrasonic velocity meter every hour (Webster and others 2000) to calculate the suspended-sediment discharge.

The hourly suspended-sediment discharge from the optical sensor compares well with daily suspended-sediment discharge from a sediment station operated by the U.S. Geological Survey at Freeport (fig. 3, Webster and others 2000). Thus, the output of the optical sensor can be used as an index value that is calibrated to cross-sectionally averaged SSC and multiplied by discharge to determine the suspended-sediment discharge. In this case, the same water discharge time series was used to calculate both time series of suspended-sediment discharge.

Advantages and disadvantages of the optical sensor are demonstrated in this time series. The optical sensor allows identification of two peaks in SSC during a typical flow pulse: an immediate rise to peak, in response to local resuspension, and a smaller, broader peak 4 - 5 days later (Schoellhamer and Dinehart 2000). As flow increases, resuspension decreases the supply of erodible sediment on the bed, therefore, the first peak begins to diminish in 1 - 2 days. Because particle size variations did not adversely affect the sensor calibration, the primary disadvantage of the optical sensor was that only 61 percent of the data were valid, due to fouling. The fouling problem was subsequently reduced by cleaning the sensor weekly.

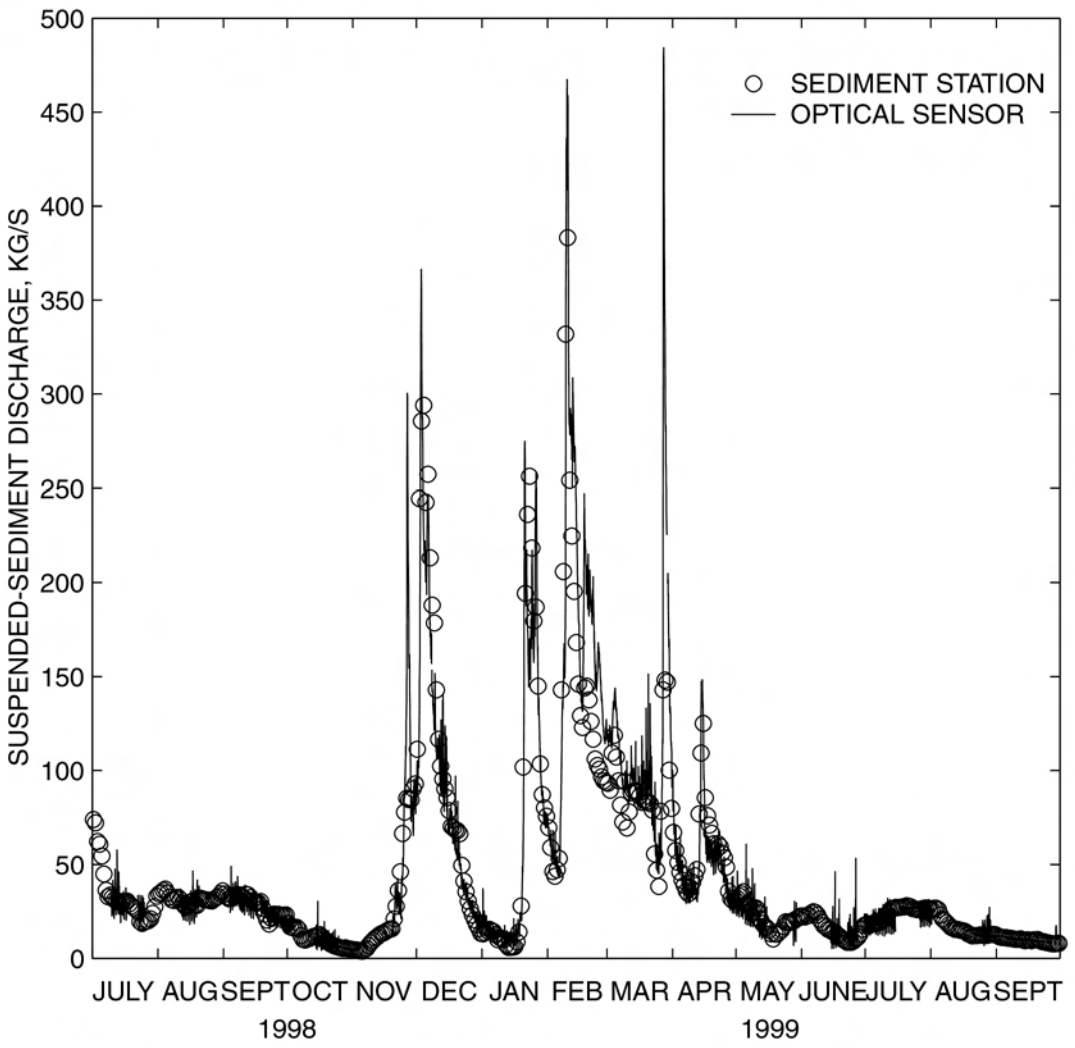

Figure 3. Suspended-sediment discharge at Freeport, Sacramento River, California, July 1998 – September 1999. Sediment station data are daily (Webster and others 2000) and optical sensor data are hourly.

CONCLUSIONS

Optical sensors can successfully monitor suspended sediment in rivers if the effects of particle size do not preclude sensor calibration. In the Colorado River at Cisco, the approximate slope of the calibration line (C/V) varied by two orders of magnitude over the range of particle size, but in the Sacramento River at Freeport C/V did not vary with particle size. The sensor output at Freeport was successfully calibrated to discharge-weighted cross-sectionally averaged suspended-sediment concentration. This concentration was multiplied by water discharge to determine an hourly time series of suspended-sediment discharge that compared well with daily suspended-sediment discharge from a USGS sediment station. The appropriateness of using

optical sensors in rivers should be evaluated on a site-specific basis and the objective of the measurement, potential particle size effects, and potential fouling should be considered.

ACKNOWLEDGEMENTS

I would like to thank Greg Brewster, Paul Buchanan, Rob Sheipline, and Brad Sullivan for installing and operating the optical sensor at Freeport, which was supported by the CALFED Bay-Delta Program. Some of the water samples used for calibration of the sensor were collected by the USGS California District Sacramento Field Office and Sacramento River Basin National Water-Quality Assessment Program. Jon Nelson and several other participants collected the Cisco data as part of a test of suspended-sediment samplers. Denis O'Halloran, Carol Sanchez, and Richard Wagner provided helpful comments on initial drafts of this paper.

REFERENCES

Buchanan, P.A., and Ruhl, C.A., 2000, Summary of suspended-solids concentration data, San Francisco Bay, California, water year 1998: U.S. Geological Survey Open File Report 00-88, 41 p.

Cacchione, D.A., Drake, D.E., Kayen, R.W., Sternberg, R.W., Kineke, G.C., and Tate, G.B., 1995, Measurements in the bottom boundary layer on the Amazon subaqueous delta: Marine Geology, v. 125, p. 235-257.

Christiansen, T., Wiberg, P.L., and Milligan, T.G., 2000, Flow and sediment transport on a tidal salt marsh surface: Estuarine, Coastal and Shelf Science, v. 50, p. 315-331.

Conner, C.S., and DeVisser, A.M., 1992, A laboratory investigation of particle size effects on an optical backscatterance sensors: Marine Geology, v. 108, p. 151-159.

Dyer, K.R., Christie, M.C., Feates, N., Fennessy, M.J., Perjup, M., and van der Lee, W., 2000, An investigation into processes influencing the morphodynamics of an intertidal mudflat, the Dollard Estuary, The Netherlands: I. Hydrodynamics and suspended sediment: Estuarine, Coastal and Shelf Science, v. 50, p. 607-625.

Downing, J.P., Sternburg, R.W., and Lister, C.R.B., 1981, New instrumentation for the investigation of sediment suspension processes in the shallow marine environment: Marine Geology, v. 42, p. 19-34.

Edmunds, J.L., Cole, B.E., Cloern, J.E., and Dufford, R.G, 1997, Studies of the San Francisco Bay, California, Estuarine Ecosystem. Pilot Regional Monitoring Program Results, 1995: U.S. Geological Survey Open-File Report 97-15, 380 p.

Edwards, T.K., and Glysson, G.D., 1999, Field methods for measurement of fluvial sediment: Techniques of Water-Resources Investigations of the U.S. Geological Survey, book 3, chapter A2, 89 p.

Ludwig, K.A., and Hanes, D.M., 1990, A laboratory evaluation of optical backscatterance suspended solids sensors exposed to sand-mud mixtures: Marine Geology, v. 94, p. 173-179.

Schoellhamer, D.H., 1993, Biological interference of optical backscatterance sensors in Tampa Bay, Florida: Marine Geology, v. 110, p. 303-313.

Schoellhamer, D.H. 1995. Sediment resuspension mechanisms in Old Tampa Bay, Florida. Estuarine, Coastal and Shelf Science, v. 40, p. 603-620.

Schoellhamer, D.H., 1996a, Anthropogenic sediment resuspension mechanisms in a shallow microtidal estuary: Estuarine, Coastal and Shelf Science, v. 43, p. 533-548.

Schoellhamer, D.H., 1996b, Factors affecting suspended-solids concentrations in South San Francisco Bay, California: Journal of Geophysical Research, v. 101, no. C5, p. 12087-12095.

Schoellhamer, D.H., and Dinehart, R.L., 2000, Suspended-sediment supply to the Delta from the Sacramento River: Proceedings of the CALFED Bay-Delta Program Science Conference, Sacramento, California, October 3-5, 2000.

Uncles, R.J., Barton, M.L., and Stephens, J.A., 1994, Seasonal variability of fine-sediment concentrations in the turbidity maximum region of the Tamar Estuary: Estuarine, Coastal and Shelf Science, v. 38, no. 1. p. 19-39.

Webster, M.D., Anderson, S.W., Rockwell, G.L., Smithson, J.R., and Friebel, M.F., 2000, Water resources data, California, water year 1999: U.S. Geological Survey Water-Data Report CA-99-4, v. 4. URL http://ca.water.wr.usgs.gov/data/